Identification of Novel Targetable Signaling Pathways in the Inherited Ichthyoses

Dr Priya Dewan

Supervisors: Professor Edel O'Toole & Professor David Kelsell

A thesis submitted for the degree of PhD

Centre for Cell Biology and Cutaneous Research
Blizard Institute, Barts and the London School of Medicine and Dentistry,
Queen Mary University of London

I, Priya Dewan, declare that the work presented in this thesis is my own, unless stated otherwise, and is in accordance with the University of London's regulations for the degree of PhD.

Priya Dewan

Abstract

In this study the non-syndromic ichthyoses were studied to evaluate any genes or biological processes common to them and to identify key genes and pathways pertaining to each ichthyosis individually. This group of monogenic diseases comprises of ichthyosis vulgaris (loss of *FLG*), X-linked ichthyosis (loss of *STS*) lamellar ichthyosis/congenital ichthyosiform erythroderma (due to mutations in *ALOX12B, ICH, ABCA12*) and harlequin ichthyosis (due to *ABCA12*). They all affect terminal differentiation and the cornified layer and manifest as scaly conditions along a spectrum ranging from mild (as in ichthyosis vulgaris) to having a major impact on quality of life (as in lamellar ichthyosis/congenital ichthyosiform erythroderma) to severe (as in harlequin ichthyosis). The aim of this study was to investigate the effect of ichthyosis gene knockdown (*STS, FLG, ABCA12, TGM1, ICH* and *ALOX12B*) using RNAi technology in primary neonatal keratinocytes. 3D *in vitro* cultures using primary keratinocytes for the ichthyosis of interest, from the same genetic background, were developed including a novel model (*STS* knockdown). All the ichthyosis gene knockdowns in this study affected terminal differentiation (change in TGM1 expression) and loss of *ABCA12* altered early differentiation in addition to terminal differentiation. *RNA-Seq* analysis was performed in primary keratinocytes transfected with siRNA. 62 genes were significantly down-regulated and 26 genes were significantly up regulated overlapping in all the ichthyoses models. Altered gene clusters were found for cell cycle, innate immune response, keratin filament/cytoskeleton and metabolism of lipids and lipoproteins. Functional studies showed an altered cytokine profile in unstimulated primary keratinocytes and following stimulation of TLR -2, -3, -5 in all the ichthyoses. The findings suggest that several overlapping genes involved in biological processes, including innate immunity, are altered in this group of non-syndromic, monogenic ichthyoses.

Acknowledgements

I would like to thank my supervisor, Professor Edel O'Toole for her support, guidance and patience throughout my PhD. I am very grateful to my collaborators Dr Anton Enright and Dr Harpreet Saini at European Bioinformatics Institute, Cambridge and to Dr Ute Meier for her advice and discussions related to chapter 7.

I would like to thank the members of my supervisors' group in particular Dr Mat Caley and all my colleagues at the Centre for Cutaneous Research especially Dr Muhammad M Rahman. I would especially like to thank Dr Sofia Sisay without whose enthusiasm, encouragement and sense of humor this work would not have been possible.

I would like to acknowledge the Medical Research Council for funding this research.

Finally, to my family and especially to the many loved ones who strongly supported this piece of work but passed away during its evolution-you will always be my inspiration. I dedicate this thesis to you.

Table of Contents

List of Figures and Tables

Abbreviations

ABCG1	ATP-Binding Cassette, Sub-Family G (WHITE), Member 1
AD	Atopic Dermatitis
ACSVL	very long-chain acyl-CoA synthetase
AMP	Antimicrobial peptides
AP-1	Activator Protein-1
ARCI	Autosomal Recessive Congenital Ichthyosis
CE	Cornified Envelope
CHUK	Conserved Helix-Loop-Helix Ubiquitous Kinase
CI	Common Ichthyosis
CE	Cornified Envelope
CLE	Cornified Lipid Envelope
CRISPR/Cas9	Clustered regularly interspaced short palindromic repeats
CSO_4	Cholesterol Sulfate
CYP4F22	Cytochrome P450, Family 4, Subfamily F, Polypeptide 22
DED	De-epidermalised dermis
DEFB	beta-defensins
DEGs	Differentially expressed genes
DMSO	Dimethyl Sulfoxide
DNA	Deoxyribonucleic acid
dNTP	Deoxynucleotide triphosphate
DOC	Disorders of Cornification
DSC	Desmocollin
dsDNA	Double-stranded DNA
dsRNA	Double-stranded RNA
DSG	desmoglein
FA	fatty acid
FBS	Fetal Bovine Serum
FLG	Filaggrin
GBA	β-glucocerebrosidase
H&E	Haematoxylin and Eosin
HC	High calcium
HI	Harlequin Ichthyosis
IF	Immunofluorescence
IFN	Interferons
IHC	Immunohistochemistry
IKK1	IκB kinase 1
IL	Interleukin
IL6R	Interleukin-6-receptor
IV	Ichthyosis Vulgaris
kDa	Kilodalton
KIFs	Keratin Intermediate Filaments
KLK	Kallikrein
KRT	Keratin
LB	Lamellar Bodies
LC	Low calcium

LEP	Leptin
LI	Lamellar Ichthyosis
LOR	Loricrin
LOX	Lipoxygenases
miRNAs	MicroRNAs
mRNA	Messenger RNA
NBF	Nucleotide Binding Folds
NCIE	Nonbullous Congenital Ichthyosiform Erythroderma
NGS	Next generation sequencing
nHEKs	Normal human epidermal keratinocytes
nt	Nucleotide
o/n	Overnight
PAMPs	Pathogen associated molecular patterns
PBS	Phosphate buffered saline
PFA	Paraformaldehyde
PGN	Peptidoglycan
PKP	plakophilin
Poly I:C	Polyinosinic–polycytidylic acid
PPAR	Peroxisome proliferator-activated receptor
RNA	Ribonucleic acid
RNAi	RNA interference
RNAse	Ribonuclease
RT	Room temperature
RT-PCR	Reverse transcription PCR
RXLI	Recessive X-linked Ichthyosis
SB	Stratum Basale
SC	Stratum Corneum
SG	Stratum Granulosum
sgRNA	single guide RNA
siRNA	Short interfering RNA
shRNA	Short hairpin RNA
SS	Stratum Spinosum
TGF-β	Transforming growth factor-beta
TGM	Transglutaminase
TGs	Transglutaminases
TLR	Toll-like receptors
TMD	Transmembrane Domains
TNF	Tumor necrosis factor
UGCG	UDP-Glucose Ceramide Glucosyltransferase
ULC-FA	ultra long-chain fatty acids
VEGF	Vascular endothelial growth factor
VLC-FA	very long-chain fatty acids

SI units

G	gram
Kb	kilobase
M	molar
mA	milliampere
ml	millilitre
mm	millimetre

mM	millimolar
µg	microgram
µl	microlitre
µm	micrometre
µM	micromolar
ng	nanogram
nm	nanometre
U	units
V	volts

Chapter 1: Introduction

1.1 An Overview Of The Skin

The skin consists of three layers: subcutaneous fat, the dermis and an overlying epidermis.

1.1.1 Subcutanous Fat/Hypodermis

The tissue of the hypodermis is the innermost and thickest layer of the skin that protects vital structures, maintains body heat and acts as an energy reserve (Griffiths et al., 2016). The basic unit of the subcutaneous fat is the microlobule that is composed of collections of adipocytes-cells specialised in accumulating and storing fat. Aggregations of primary microlobules form secondary lobules that are separated by connective tissue septa containing nerves, vessels, and lymphatics (Haake et. al. 2001).

1.1.2 The Dermis

Beneath the epidermis a vascularized dermis provides structural and nutritional support. Its thickness varies from less than 0.5 mm to more than 5 mm (Calonje et al.; 2012). It is composed of two principle types of protein fibres: collagen and elastin. Collagen is the major extracellular matrix protein (comprising 80-85% of the dry weight of the dermis) and provides the skin with its tensile strength. 12 of the known twenty-nine collagens are expressed in the skin; the main interstitial dermal collagens are I and III (Smith et al., 2006). Elastic fibres (~2-4% of the extracellular matrix) play a major role in skin elasticity and resilience (Kielty et al., 2002). The dermis also contains a number of non-collagenous glycoproteins including fibronectin, thrombospondin, laminin, vitronectin, and tenascin that interact with other matrix components via cell surface receptors called integrins and facilitate cell adhesion, migration, morphogenesis and differentiation (Griffiths et al., 2016). Between the dermal collagen and elastic tissue is the ground substance made up of proteoglycans and glycosaminoglycan macromolecules (Haake et. al. 2001). These contribute only 0.1-0.3% of the total dry weight

of the dermis but provide a vital role by maintaining hydration mostly due to the high water-binding capacity of hyaluronic acid (Calonje et al.; 2012). In addition, the dermis accommodates epidermal-derived appendages (hair follicles and sweat glands), the cellular components of the dermis such as fibroblasts (most abundant cells in the dermis and are known to synthesize collagen, elastin, other matrix proteins and enzymes), macrophages and mast cells (Griffiths et al., 2016). It is well vascularised by a deep and superficial vascular plexus.

1.1.3 The Epidermis

The normal epidermis is a terminally differentiated, stratified, squamous epithelium. It is typically 0.05-0.1mm in thickness (Calonje et al., 2012). It has evolved to provide a physical and permeability barrier, which is essential for survival as an adaptation to terrestrial life in mammals. The epidermis is mainly composed of keratinocytes (95% of epidermal cells). Other cells in the epidermis are melanocytes (distribute packages of melanin pigment in melanosomes to surrounding keratinocytes to give skin its colour), Langerhans cells' (antigen-presenting cells and play a key role in adaptive immune responses in the skin) and Merkel cells (serve as mechanosensory receptors in response to touch) (Griffiths et al., 2016).

The keratinocyte moves progressively from the basal layer towards the skin surface, forming several well-defined layers during its transit (Freinkel et al., 2001). Thus on morphological grounds the epidermis can be divided into 4 distinct layers: stratum basale, stratum spinosum, stratum granulosum and stratum corneum.

1.1.3.1 Basal layer/Stratum Basale (SB):

This is a continuous layer that is generally only 1 cell thick. The basal cells are small and cuboidal and have large, dark staining nuclei and ribosome rich cytoplasm. A small number of stem cells are also present in the basal layer, these cells undergo mitotic divisions which results in the continued production of keratinocytes necessary for epithelial homeostasis. Basal keratinocytes are attached to the underlying basement membrane by hemidesmosomes and to the surrounding cells via desmosomes and adherens junctions (Simpson et al., 2011; Walters and Roberts, 2002). The basal layer is typified by the expression of keratins 5 and 14 (Candi et al., 2005).

1.1.3.2 Stratified layer/Stratum Spinosum (SS):

Triggered by poorly understood signals, certain basal keratinocytes migrate from the basal into the spinous layers, lose their mitotic activity, and begin to synthesize a new set of structural proteins and enzymes that are characteristic of cornification (the process by which epidermal cells progressively mature from basal cells with proliferative potential to non-viable corneocytes is called keratinisation or cornification) (Candi et al., 2005; Simpson et al., 2011). The spinous layer is characterised by the expression of differentiation-specific keratins 1 and 10 (Fuchs et. al. 1980, Sun et. al. 1983). Here tightly packed polyhedral shaped keratinocytes are held together by many desmosomes, which help to stabilize adjacent keratinocytes (Calonje et al.; 2012). The name of this layer is derived from the histological appearance of desmosomes that appear as narrow spikes or projections.

1.1.3.3 Granular layer/Stratum Granulosum (SG):

The granular layer can be identified by the presence of basophilic keratohyalin granules. The keratohyalin granules contain profilaggrin the precursor of the interfilamentous protein filaggrin. The cytoplasm of cells of the upper spinous and granular layer also contain

multifunctional, lysosome-like organelles, called lamellar bodies (LB). They discharge their lipid components into the intercellular space playing important roles in barrier function and intercellular cohesion within the SC (Candi et al., 2005; Kalinin et al., 2002; Walters and Roberts, 2002). In addition, they secrete a broad variety of lipid hydrolases, proteases/antiproteases, antimicrobial peptides, apolipoproteins and other proteins, in addition to lipids, into the extracellular spaces (Raymond et al., 2008). The movement of these organelles to the cell periphery in anticipation of secretion is dependant upon a set of colocalised motor and non-motor proteins (Raymond et al., 2008). In the stratum granulosum, keratinocytes are connected among each other by tight junctions (Simpson et al., 2011).

1.1.3.4 Cornified layer /Stratum Corneum (SC)

The outermost layer of the epidermis is the stratum corneum composed of mechanically tough, dead cornified cells (corneocytes), which develop as a result of terminal differentiation (Elias, 2010; Kalinin et al., 2002; Walters and Roberts, 2002) (Figure 1.1). These cells are anucleated and devoid of all organelles. Corneocytes in the cornified layer have a characteristic flattened shape. The shape of the keratinocytes is provided by a cytoskeleton made of keratin intermediate filaments, KIFs. Filaggrin aggregates the KIFs into tight bundles. This promotes the collapse of the cell into the flattened shape. The plasma membrane of the corneocytes is completely replaced and they are encapsulated within a highly specialized structure termed the cornified envelope (CE) formed by cross-linking of a series of structural proteins, involucrin, loricrin, trichohyalin and the small-proline-rich proteins, by specific epidermal transglutaminases that are synthesized in the high SS (Candi et al., 2005). A monomolecular layer of long-chain ceramides (ω-hydroxyceramides) is covalently bound to this protein layer, forming a cornified lipid envelope (CLE) on the surface of each

corneocyte. The cells in the CLE are surrounded by orderly intercellular lipids consisting of a mixture of ceramides, free fatty acids, cholesterol and its esters that are organised into repeating arrays of broad lamellar membranes that completely engorge the extracellular spaces (Candi et al., 2005). These lipids are processed/derived from precursor lipids (glucosylceramides, phospholipids and cholesterol), which were released from the lamellar bodies (LB) at the SG/SC interface, by concurrently released enzymes (Freinkel and Traczyk, 1985). The structural behaviour of the SC is analogized to a brick wall comprising of corneocytes, the “bricks”, provide the mechanical strength and are embedded in the "mortar" lipid lamellae, which represents the permeability barrier (Elias, 1983; Nemes and Steinert, 1999). The composition of the intercellular lipids is important for an intact barrier function (Holleran et al., 2006; Menon et al., 2012). Corneocytes are connected to each other by corneodesmosomes, which derive from desmosomes through morphological changes in the transition zone between SG/SC (Candi et al., 2005; Proksch et al., 2003; Simpson et al., 2011). Proteolysis of corneodesmosomes releases the bonds between corneocytes of the outer cornified layer, leading to desquamation (Elias, 2010; Walters and Roberts, 2002). Under physiological conditions skin surface pH is between 5.0 and 5.5 (Schmid-Wendtner and Korting, 2006), the optimal pH for lipid processing by enzymes and also for limiting the colonization of pathogenic bacteria (Chan and Mauro, 2011; Holleran et al., 2006). One main difference of the intercellular lipid lamellae to other lipid matrices in the human body, is the absence of phospholipids in the stratum corneum (Walters and Roberts, 2002). The lamellar body-derived phospholipids are processed by secretory phospholipase to A_2 ($sPLA_2$) free fatty acids and glycerol. The latter has a strong water-binding capacity and, hence, contributes to SC hydration (Feingold, 2007).

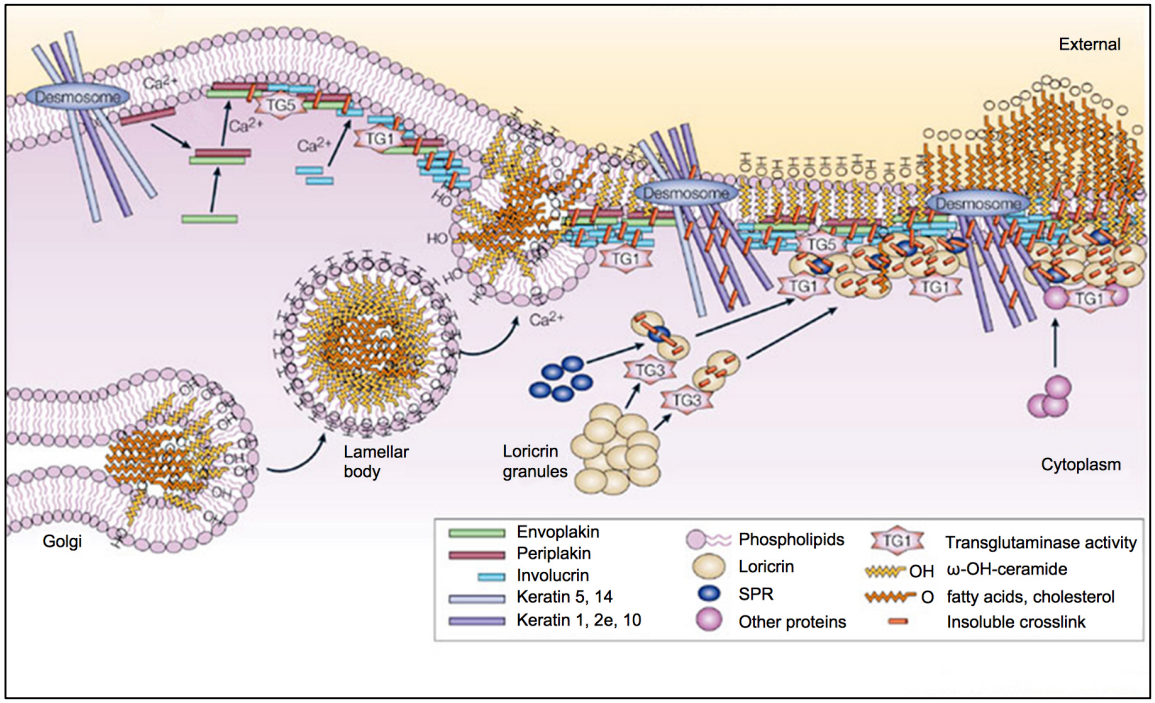

Figure 1.1: Formation of the cornified envelope
This is a complex process that involves the synthesis of cornified envelope proteins (envoplakin, periplakin, loricrin small proline-rich proteins (SPRs), involucrin and loricrin) and cross-linking of these proteins by transglutimases (TGs) to form the cornified envelope. The intercellular lipids (ω-OH-ceramides, fatty acids and cholesterol) are extruded by the lamellar bodies into the extracellular space and are covalently attached to the cornified envelope to form the cornified lipid envelope. Adapted from (Candi et al., 2005).

1.2 Ichthyoses

1.2.1 Classification of the Ichthyoses: disorders of cornification (DOC)

In 2009, the first Ichthyosis Consensus Conference was held to establish a consensus for the nomenclature and classification of inherited ichthyoses, by which an international consensus for the classification of ichthyoses was achieved (Oji et al., 2010). This is a clinically-based classification in which DOC are referenced with their causative gene. Two principal groups are recognised: non-syndromic (limited to the skin without other organ involvement) and syndromic forms (skin and other organ involvement). There are several non-syndromic inherited ichthyoses as follows (Table 1):

Inherited ichthyoses Part A: nonsyndromic forms		
Disease	**Mode of inheritance**	**Gene(s)**
Common ichthyoses*		
IV	**Autosomal semidominant**	**FLG**
RXLI Nonsyndromic presentation	**X-linked recessive**	**STS**
ARCI		
Major types		
HI	**Autosomal recessive**	**ABCA12**
LI°	**Autosomal recessive**	**TGM1/NIPAL4●/ALOXE12B/ABCA12/loci on 12p 11.2-q13**
CIE	**Autosomal recessive**	**ALOXE3/ALOXE12B/ABCA12/CYP4F22/NIPAL4●/TGM1/loci on 12p11.2-q13**
Minor variants		
SHCB	**Autosomal recessive**	**TGM1, ALOXE12B, ALOXE3**
Acral SHCB	**Autosomal recessive**	**TGM1**
BSI	**Autosomal recessive**	**TGM1**
Keratinopathic ichthyosis (KPI)		
Major types		
EI✱	**Autosomal dominant**	**KRT1/KRT10**
SEI	**Autosomal dominant**	**KRT2**
Minor variants		
AEI✱	**Autosomal dominant**	**KRT1/KRT10**
ICM	**Autosomal dominant**	**KRT1**
AREI	**Autosomal recessive**	**KRT10**
Epidermolytic nevi''	**Somatic recessive**	**KRT1/KRT10**
Other forms		
LK	**Autosomal dominant**	**LOR**
EKV>>	**Autosomal dominant**	**GJB3/GJB4**
PSD	**Autosomal recessive**	**Locus unknown**
CRIE	**Autosomal dominant (isolated cases)**	**Locus unknown**
KLICK	**Autosomal recessive**	**POMP**

AEI, Annular epidermolytic ichthyosis; *ARCI*, autosomal recessive congenital ichthyosis; *AREI*, autosomal epidermolytic ichthyosis; *BSI*, bathing suit ichthyosis; *CIE*, congenital ichthyosiform erythroderma; *CRIE*, congenital reticular ichthyosiform erythroderma; EI, epidermolytic ichthyosis, *EKV*, erythrokeratodermia variabilis; *HI*, harlequin ichthyosis; *ICM*, ichthyosis Curth-Macklin; *IV*, ichthyosis vulgaris; *KLICK*, keratosis linearis-ichthyosis congenital-keratoderma; *LI*, lamellar ichthyosis; LK, loricrin keratoderma; *PSD*, peeling skin disease; *RXLI*, recessive X-linked ichthyosis; *SEI*, superficial epidermolytic ichthyosis; *SHCB*, self-healing collodion baby.
*Often delayed onset (in RXLI mild scaling and erythroderma may be present already at birth).
°Few cases of autosomal dominant LI described in literature (locus unknown).
●Also known as ICHTHYIN gene.
✱KRT1 mutations are often associated with palmoplantar involvement.
''May indicate gonadal mosaicism, which can cause generalized EI in offspring generation.
>>Whether progressive symmetric erythrokeratodermia represents distinct mendelian disorders of cornification form is debated.

Table 1: Clinicogenetic classification of inherited non-syndromic ichthyoses.
The phenotype is limited to the skin without other organ involvement. Taken from (Oji et al., 2010).

This study focuses on the monogenic non-syndromic ichthyosis, due to mutations in *STS, FLG, ABCA12, TGM1, ICHTHYIN* and *ALOX12B* which constitute a subgroup within the greater group of DOC.

1.2.2 The non-syndromic monogenic ichthyoses:

Defects in SC lead to a clinically and etiologically heterogenous group of disorders ranging from mild (as in ichthyosis vulgaris MIM 146700) to having a major impact on quality of life (X-linked ichthyosis MIM 308100, lamellar ichthyosis MIM 242300/congenital ichthyosiform erythroderma MIM 242100) to severe cases that can be life-threatening (harlequin ichthyosis MIM 242500). The last 10 years have seen considerable advances in our understanding of the genetic basis of the ichthyoses (Oji et al., 2010) (Figure 1.2).

The pathogenesis of various ichthyoses can be thought to be associated with at least one of components of the epidermal skin barrier (sections 1.4 and 1.5). The known causative molecules underlying ichthyosis include ABCA12, lipoxygenase-3, 12R-lipoxygenase, ichthyin and steroid sulfatase, are thought to be related to the intercellular lipid layers. Transglutaminase1 plays a role in cornified cell envelope formation. Filaggrin is essential for the formation of keratohyalin granules.

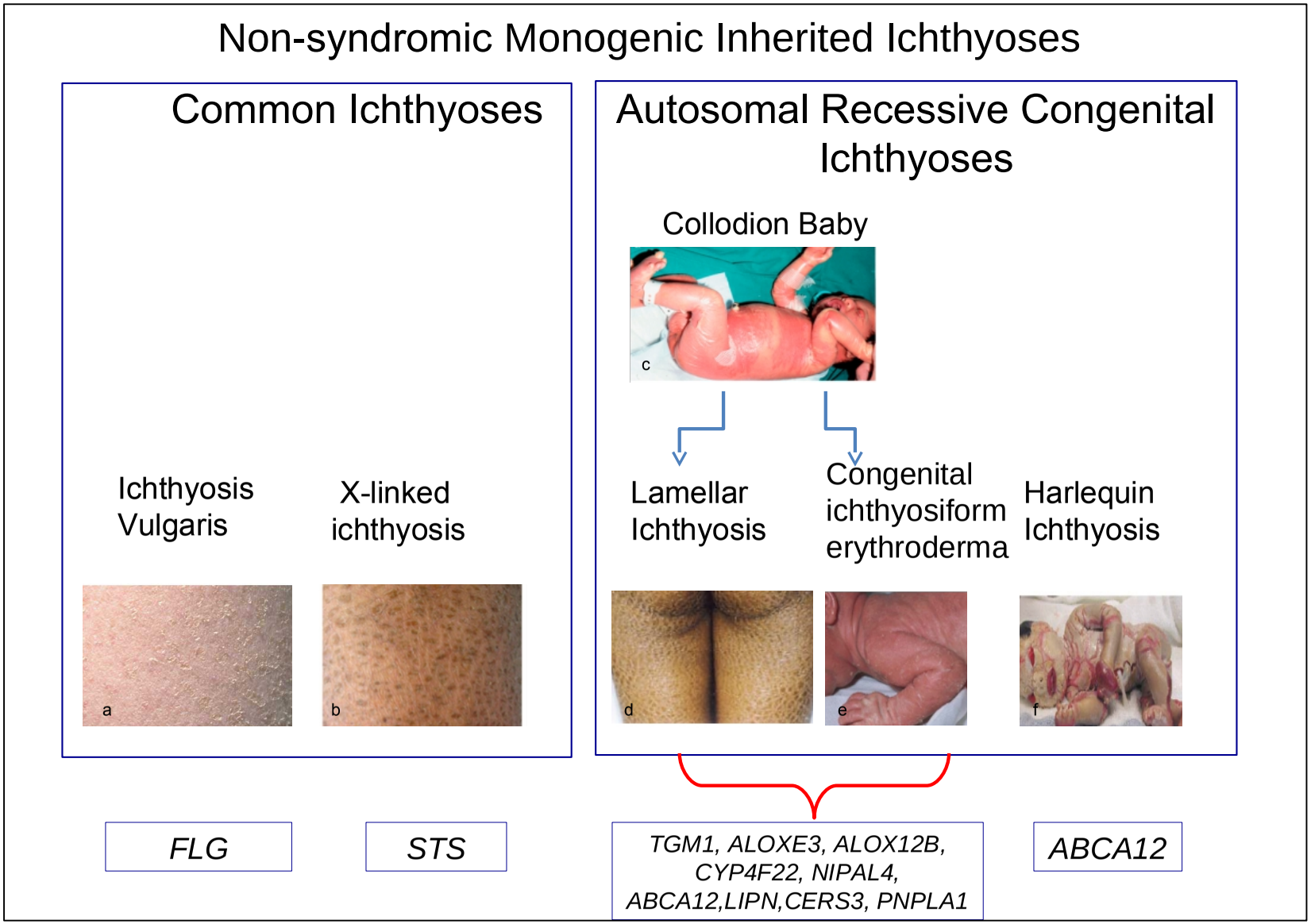

Figure 1.2: The monogenic non-syndromic ichthyoses in this study.
Variety of phenotypical findings in different monogenic non-syndromic ichthyosis: a) Fine scaling phenotype in ichthyosis vulgaris, taken from (Smith et al., 2006) b) Moderate scaling phenotype in recessive X-linked ichthyosis, taken from (Schmuth et al., 2013) c) Parchment like collodian membrane, taken from (Vahlquist et al., 2010) d) Large, brown scaling phenotype in lamellar ichthyosis, taken from (Jobard et al., 2002) e) erythema and small scale of congenital ichthyosiform erythroderma, taken from (Oji and Traupe, 2006) f) Thick scale plates separated by fissures in harlequin ichthyosis, taken from (Kelsell et al., 2005).

1.3 Common Ichthyoses

1.3.1 ICHTHYOSIS VULGARIS (IV) (MIM 308100)

Ichthyosis vulgaris represents the most common disorder of cornification. Its prevalence appears to vary with geographical region ranging from 1 in 100 in British school children (Wells, 1966) to 1:1000 and 2000 in Japan and Mexico (Cuevas-Covarrubias et al., 1999). Varying clinical criteria for the diagnosis and/or geographical variation in the mutation frequency and seasonal variability (improves in the summer months) are thought to account for the discrepant prevalence rates.

The phenotype is rarely evident before 3–6 months after birth, but usually manifests during childhood and becomes more severe with age. Individuals display mild generalized fine scaling most pronounced on the extensor surfaces of extremities with characteristic flexural sparing. Hyperlinearity of palms and soles (linear grooves perpendicular to the thenar and hypothenar eminence) is common as is the association with keratosis pilaris and atopic dermatitis (AD) (Sandilands et al., 2007).

Atopic dermatitis is a chronic relapsing inflammatory skin disease presenting as pruritic, dry, scaly skin with excoriations as well as cutaneous infections and is associated with asthma and/or alleric rhinitis (McGrath and Uitto, 2008, Sidbury et al., 2014, Spergel, 2010). It occurs most commonly during infancy/childhood but can also affect adults (Griffiths et al., 2016).

1.3.1.1 *FLG*: Gene

In 2006, loss of function mutations in the *FLG* gene, located in the epidermal differentiation complex (a region that also harbours genes for several other proteins that are expressed during

terminal differentiation several of which become cross-linked enzymatically into the CE) on chromosome 1q21, resulting in a lack of functional filaggrin were identified in IV patients from Scottish, Irish and European-American populations (Smith et al., 2006). In addition to causing IV, a monogenic genodermatosis, mutations in the *FLG* gene is the major genetic predisposing factor for AD, which is a complex trait, resulting from the interaction of multiple genetic and environmental risk factors (McLean, 2016).

FLG comprises three exons, the initiation codon for translation being located in exon 2, and the bulk of the profilaggrin protein is encoded by exon 3 (Presland et al., 1992). In addition to the two common premature termination causing mutations, p.R501X and c.2282del4 in exon 3, that were initially identified, several other rare or family-specific loss-of-function mutations within FLG exon 3 have been discovered in populations of white European ancestry. Asian populations have been shown to have their own mutation spectra, following detailed study of the Japanese (Osawa et al., Nomura et al., 2009) and Han Chinese (Zhang et al., 2011) and Singaporean Chinese populations (Chen et al., 2011). All mutations are either nonsense or frame-shift mutations in the protein encoding exon.

The prevalent filaggrin mutations are loss-of-function alleles leading to complete or almost complete loss of filaggrin expression (Sandilands et al., 2007, Palmer et al., 2006). There is a dose effect in that heterozygous patients display a mild or no phenotype, while homozygous and compound heterozygous *FLG* genotypes exhibit the full ichthyosis vulgaris phenotype. The same *FLG* mutations have been linked to atopic dermatitis (Palmer et al., 2006, Sandilands et al., 2007) but these are predominantly found in the heterozygous configuration.

1.3.1.2 Pro-Filaggrin and Filaggrin Protein

The initial product of *FLG* translation is Profilaggrin, a 400-kDa protein (Figure 1.3). It is composed of a short N-terminal domain, followed by the 10 to 12 repeats of nearly identical filaggrin that makes up most of the profilaggrin molecule (typically, there are 10 highly homologous and only slightly genetically distinct filaggrin units, although the number of filaggrin repeat units is variable and genetically determined). This means different individuals have 10, 11 or 12 filaggrin repeat units (copy number variants) in total plus a C-terminal domain (Gan et al., 1990). An incremental reduction in the risk of atopic dermatitis with each additional unit of copy number has been noted (Brown et al., 2012) and even a modest 10-20% increase in epidermal filaggrin expression is predicted to be therapeutic for eczema or protective against developing eczema (Brown and McLean, 2012).

Upon terminal differentiation, profilaggrin is proteolytically cleaved into filaggrin peptides of approximately 37 kDa and the N-terminal domain containing an S100-like calcium-binding domain. The N-terminal domain translocates to the nucleus where it possibly plays a role in the enucleation of keratinocytes in the outer stratum corneum (Sandilands et al., 2009). The S100-like calcium binding domain (Markova et al., 1993) may play a role in the regulation of calcium-dependent events during terminal epidermal differentiation (Presland et al., 1992) or conversely, calcium may be involved in the control of profilaggrin processing (Presland et al., 1992, Sandilands et al., 2009). Filaggrin has keratin binding properties. The precise function of the C-terminal domain is not known but it is required for the processing of profilaggrin to filaggrin.

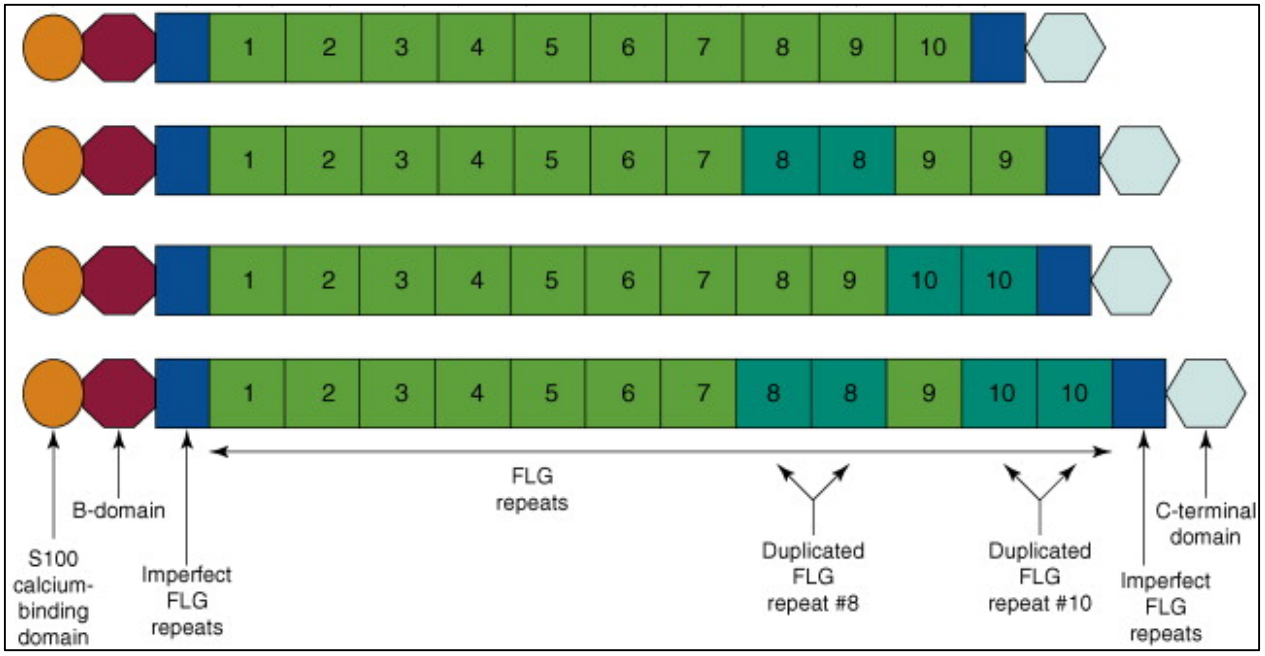

Figure 1.3: Schematic representation of Pro-FLG showing loss of function mutations in the *FLG* gene detected in individuals with IV and eczema.
Profilaggrin is composed of a short N-terminal domain (contains a S100 calcium-binding domain), followed by the 10 nearly identical filaggrin that makes up most of the profilaggrin molecule plus a C-terminal domain. There are polymorphic variations in the number of filaggrin repeats: some individuals have duplication of the 8th or 10th domain or both. The mutations shown in green are common in individuals of European ancestry while those in dark green are common in Oriental populations. The other mutations are rare. Taken from (McGrath and Uitto, 2008).

1.3.1.3 Paucity/loss of keratohyalin granules due to loss-of-function mutations

In the absence of functional protein, as in IV, a reduced or absent granular layer due to paucity of keratohyalin granules and reduced cellular profilaggrin content (profilaggrin is the major component of the keratohyalin granules seen in the SG) is observed (Fleckman and Brumbaugh, 2002). Ultrastructurally, the residual keratohyalin granules are poorly formed ("crumbly") (Anton-Lamprecht and Hofbauer, 1972) or absent (Fleckman and Brumbaugh, 2002). Absence of the granular layer is independent of body site and season of the year, but correlates with severity of the disease (Fleckman and Brumbaugh, 2002), and mutation status. Patients with one mutation (heterozygous) display a reduced granular layer whereas patients with two *FLG* mutations (homozygous or compound heterozygous) in most instances show a virtually complete lack of a granular layer (Smith et al., 2006, Gruber et al., 2007, Nomura et

al., 2007). However in rare cases even patients with two mutations show residual granular cells (Gruber et al., 2007). This persistence of keratohyalin granules appears to depend on the location of the mutation within the gene i.e. more proximal mutations show complete absence of profilaggrin in homozygotes (Smith et al., 2006), whereas more distal mutations show residual, yet greatly reduced, truncated profilaggrin species that are not processed to FLG monomers (Sandilands et al., 2007).

1.3.1.4 Filaggrin: Role in structural integrity of SC

Filaggrin, also known as filament-aggregating protein, aggregates the keratin cytoskeleton, facilitating the collapse and flattening of cells in the outermost stratum corneum to produce flattened anuclear squames (Manabe et al., 1991). Although, this process of cell flattening is seen in the absence of processed filaggrin, on an ultrastructural level disorganized keratin filaments are noted (Gruber et al., 2011). Additionally, impaired lamellar body loading and abnormal architecture of the lamellar bilayer is observed (Gruber et al. 2012). One possible explanation for this may be that filaggrin is a histidine-rich protein (Lynley and Dale, 1983) and histidine is metabolized to *trans*-urocanic acid (*trans*-UCA); pyrrolidone-5-carboxylic acid (PCA) is the other main breakdown product of filaggrin and together these organic acids help to maintain the pH gradient of the epidermis as evidenced by a higher surface pH in FLG null mutation carriers (Jungersted et al., 2010). An acidic pH within the stratum corneum is also important for the functional activity of enzymes involved in ceramide metabolism (Fluhr et al., 2010). Another observation is reduction in corneodesmosome density and tight junction protein expression observed in the skin from ichthyosis vulgaris patients (Gruber et al., 2011). It is unclear as to how these observations may be attributable to filaggrin deficiency and the mechanisms by which profilaggrin and filaggrin, as intercellular proteins contribute to what appears to be a paracellular barrier defect (Gruber et al., 2011)

(Scharschmidt et al., 2009) remain to be defined.

1.3.1.5 Filaggrin: Role in SC hydration

FLG is proteolysed into its constituent amino acids and other small molecules, the so-called 'natural moisturising factor' which contributes to epidermal hydration and barrier function (Presland et al., 2000, Scott et al., 1982, Nachat et al., 2005). *FLG* null mutations are associated with lower levels of hygroscopic amino acids in the SC and there is a concominant increase in transepidermal water loss (Kezic et al., 2008).

1.3.1.6 Filaggrin: In Vitro knockdown models

Several *in vitro* models for filaggrin knockdown and IV have been reported; these models were generated either using siRNA transfected primary keratinocytes grown at air-liquid interface on collagen I (containing fibroblasts) gels and were cultured for 7 (Mildner et al., 2010) and 14 days (Kuchler et al., 2011, Vavrova et al., 2014) or by shRNA interference of primary keratinocytes grown on a polycarbonate filter cultivated for 10 days (Pendaries et al., 2014). Loss of FLG was demonstrated by qPCR, immunofluorescence in all three models and additionally by western blotting by Mildner et al. and Pendaries et al (Mildner et al., 2010, Pendaries et al., 2014). The model generated by Mildner et al. did not demonstrate changes in keratinocyte differentiation and SC morphology but this was in contrast to the other models where alteration in both was noted and this difference was attributed to the longer cultivation time (Kuchler et al., 2011). No difference in intercellular lipid lamellae or total lipid content in the *FLG* knockdown compared to normal construct was found on day 7 (Mildner et al., 2010, Vavrova et al., 2014) but disordered intercellular lipid lamellae accompanied by an almost 2-fold increase in FFA was found on day 14 of cultivation (Vavrova et al., 2014). All the *in vitro* models showed reduced levels of FLG degradation products, urocanic and/or

pyrrolidone carboxylic acid compared to a normal skin model, which is in agreement with *in vivo* findings (Kezic et al., 2008, O'Regan et al., 2010). The skin barrier function was assessed by assessing SC permeability using a dye penetration assay, Lucifer yellow, by Mildner et al. and Pendaries et al (Mildner et al., 2010, Pendaries et al., 2014). In both studies increased permeability was noted; the dye penetrated into the SC and diffused further down to the SB or polycarbonate filter in the *FLG*-deficient skin model whilst in the control it was retained within the SC. This finding was supported by Kuchler et al. who reported higher permeability towards lipophilic testerone but no significant increase in permeability to hydrophilic caffeine in the *FLG* knockdown compare to control was noted. In contrast another *FLG* knock-down model using shRNA transfected NTERTs (on a collagen I scaffold cultivated for 14 days) showed no changes in SC permeability for lipophilic butyl *p*-aminobenzoic acid. In addition there was no effect in SC lipid organisation and composition in the NTERT model in keeping with Mildner et al. (van Drongelen et al., 2013).

1.3.2 RECESSIVE X-LINKED ICHTHYOSIS (RXLI) (MIM 308100)

RXLI is a keratinization disorder and affects roughly 1:2000 to 1:6000 males (Shwayder, 1999) who inherit an X chromosome bearing a mutated steroid sulfatase gene (*STS*) from their asymptomatic carrier mother (Shapiro et al., 1978, Koppe et al., 1978). In 75% of cases scaling is evident within the first week of life but 6% develop scaling after the age of 1 year (D. A. Burns, 2010). The disorder sometimes presents with fine peeling of the entire integument at the age of 1-3 weeks and shows fine scaling in early life. The scaling increases throughout childhood and is polygonal, thick and dark. It is prominent on the posterior and lateral neck, upper, lateral abdominal wall, outer thighs, the lower legs and preauricular facial skin. Extensor surfaces of the upper arms are commonly affected but in contrast to IV, flexures are involved (Hernandez-Martin et al., 1999). Palms and soles are spared. Extra-

cutaneous organ involvement as a result of contiguous gene syndrome has been described. A family history of prolonged labour and consequently perinatal complications may be reported (Hernandez-Martin et al., 1999).

1.3.2.1 *STS*: Gene

STS is located on Xp22.3 and has 10 exons spread over 146 kilo base pairs encoding a 62 kDa polypeptide (Sugawara et al., 2006). *STS* gene deficiencies are heterogeneous and in addition to the more common deletions (80-90% of RXLI) there are several described point mutations; most are missense mutations but non-sense mutations and one splice site mutation has also been reported (Gonzalez-Huerta et al., 2006, Liao et al., 2007). Although the genotypic deficiencies are heterogeneous, they all lead to loss of STS enzyme activity.

1.3.2.2 Steroid sulfatase (SSase): Protein

The *STS* gene encodes steroid sulfatase, a membrane-bound microsomal enzyme that is ubiquitously expressed and hydrolyzes estrone sulfate, dehydroepiandrosterone sulfate, and cholesterol sulfate, CSO_4, (Alperin and Shapiro, 1997). In epidermis, SSase activity is low in the basal and spinous layers, whereas enzyme levels peak in the SG (10–20 times higher) and persist into the SC. In the SG, SSase is concentrated in lamellar granules and then secreted into the intercellular spaces of the SC, along with other lamellar granule-derived lipid hydrolases (Elias et al., 2004) where steroid sulfatase catalyzes the desulfation of CSO_4 generating cholesterol for the barrier (Shapiro et al., 1978, Kubilus et al., 1979). In RXLI, due to absence of the enzyme steroid sulfatase cholesterol sulfate accumulates in the SC (up to 10- to 20-fold increase) [(Williams and Elias, 1981)].

1.3.2.3 Sulfatases: The superfamily

Sulfatases belong to a conserved family of enzymes that are involved in the regulation of cell metabolism and in cell signaling (Mueller et al., 2015). They are hydrolytic enzymes that desulfate esters contained in hormones, proteins, and complex macromolecules. Each sulfatase has its own substrate specificity (Buono and Cosma, 2010). To date, 17 distinct genes that can code for sulfatases in humans have been identified, which have been further divided on the basis of their subcellular localization and their pH-dependent activities. The protein structures are characterized by four domains: A, B and C, highly conserved domains, participate in the formation of N-terminal region with the B domain including the active site while the D domain includes the less conserved C-terminal region. A highly conserved cysteine in their active site is post-translationally converted into formylglycine by the formylglycine-generating enzyme encoded by *SUMF1* (sulfatase modifying factor 1) in all sulfatases leading to protein activation. Disorders due to gene mutations of sulfatases include those resulting from improper catabolism of substrates (*ARSA* gene mutations cause metachromatic leukodystrophy, which is characterized by extensive neuron demyelination in the nervous system due to improper catabolism of the sulfatide, cerebroside-3S, which is one of the major structural components of the myelin sheath) or accumulation of non-catabolised substrates (Louis and Fluharty, 1991; Buono and Cosma, 2010). Mutations in the genes encoding for lysosomal sulfatases such as *ARSB* results in a group of lysosomal storage disorders, mucopolysaccharidoses, that arise following accumulation of non-catabolized substrates which severely impair lysosomal function, resulting in defects in protein, glycoconjugate, lipid, nucleic acid, and phosphate metabolism) (Neufeld EFM, 1999).

1.3.2.4 SSase: Role in Permeability Barrier Function

Ultrastructural images of SC in RXLI show frequent but focal disruption of intercellular lipids (Rehfeld et al., 1988, Zettersten et al., 1998) due to excess CSO_4, and to some extent,

decreased cholesterol (reduced by ~50%) [(Elias et al., 2004)].

1.3.2.5 SSase: Role in desquamation

In normal epidermis, the progressive decline in cholesterol sulfate (~5% of total lipid in the SG, declining to ~1% in the outer SC [(Long et al., 1985, Ranasinghe et al., 1986, Elias et al., 1998)] permits corneodesmosome degradation leading to intact desquamation (Elias et al., 2004) and regulation of permeability barrier homeostasis. Loss of SSase in RXLI leads to persistence of corneodesmosomes. Two key serine proteases, kallikrein (KLK) KLK7 [stratum corneum chymotryptic enzyme (SCCE)] and KLK5 [stratum corneum tryptic enzyme (SCTE)] are thought to mediate desquamation by degrading corneodesmosomes. CSO_4, is a known serine protease inhibitor and accumulation of CSO_4, possibly retards desquamation by inhibiting serine proteases in the SC (Williams, 1991, Elias et al., 2004).

1.3.2.6 SSase: Regulation of differentiation by cholesterol sulfate

CSO_4 is known to stimulate epidermal differentiation by at least two mechanisms; It activates the η isoform of protein kinase C (Denning et al., 1995), which in turn stimulates the phosphorylation of differentiation-linked proteins (Elias et al., 2004). CSO_4 is a transcriptional regulator of TGM1 and involucrin expression, operating through an activator protein-1, AP-1, binding site in the promoter region (Hanley et al., 2001).

1.4 The Autosomal Recessive Congenital Ichthyoses (ARCI)

ARCIs is an umbrella term for the lamellar ichthyosis (LI)/Nonbullous congenital ichthyosiform erythroderma (NCIE) spectrum patients and Harlequin Ichthyosis (Oji et al., 2010). They all share in common an autosomal recessive mode of inheritance and disease presentation at birth, most often with a collodion membrane.

1.4.1 HARLEQUIN ICHTHYOSIS (HI) (MIM 242500):

HI is the most devastating congenital ichthyosis. Affected newborns are encased in an "armour" of thick scale plates separated by deep fissures. There is bilateral ectropion and eclabium. The nose and ears are flattened and appear rudimentary. Digital contractures and autoamputation of digits due to constricting skin bands have been reported. Infants are often born prematurely, and some are stillborn. As the skin barrier is severely compromised, neonates are more prone to sepsis, dehydration, and impaired thermoregulation. Additionally, the constricting scales can impair respiration and/or feeding leading to perinatal mortality. In neonates who survive the perinatal period, the plate-like encasement is shed, and the phenotype shifts to a severe ichthyosiform erythroderma (Williams and Elias, 1993, Akiyama, 1999). The compensatory mechanisms for ABCA12 leading to the milder phenotype are not known. In 2005, mutations in *ABCA12* on chromosome 2q33-5 were reported to underlie HI (Kelsell et al., 2005, Akiyama et al., 2005)

1.4.1.1 *ABCA12*: Other Genotype/Phenotype correlations

Several genotype／phenotype correlations with ABCA12 mutations, other than HI, have also been reported; in 2003 it was reported that combinations of missense mutations (resulting in only one amino acid alteration) underlie the LI phenotype, (Lefevre et al., 2003). Clinically, no distinct characteristic features are known for this type of LI (Parmentier et al., 1999, Parmentier et al., 1996, Lefevre et al., 2003). In addition, two cases of NBCIE were reported to have *ABCA12* missense mutations (Natsuga et al., 2007, Nawaz et al., 2012, Sakai et al., 2009).

1.4.1.2 *ABCA12*: Gene

Thus far the mutations reported in HI are homozygous or compound heterozygous nonsense substitutions, whole exon deletions and insertions or splice site mutations predicted to cause a

truncated protein affecting important nucleotide-binding fold domains and/or transmembrane domains resulting in severe loss of ABCA12 function (although a compound heterozygous mutation with a missense and a premature stop codon has been reported) whereas the *ABCA12* mutations in LI/NCIE reported to date have solely been missense mutations. (Akiyama et al., 2005, Kelsell et al., 2005, Akiyama et al., 2006a, Akiyama et al., 2006b, Thomas et al., 2006, Akiyama et al., 2007b, Akiyama et al., 2007a, Rajpar et al., 2006). Both lamellar ichthyosis and NCIE have a much milder phenotype than HI. ABCA12 mutations in LI have been found exclusively in the first nucleotide-binding fold and in NCIE in the extracellular domain and the nucleotide-binding fold (Rajpopat et al., 2011, Nawaz et al., 2012). Thus, the severity of the disease is thought to be affected by the nature of the *ABCA12* mutation and its location within the protein and mortality is associated with homozygous mutations. Additionally certain mutations are more prevalent in certain populations due to founder effect such as c7322delC in exon 49 in 80% of Pakistani HI patients (Thomas et al., 2008).

1.4.1.3 ABCA12: Protein

ABCA12 is found in 2 isoforms-ABCA12-L (NM_173076) and the shorter ABCA12-S (NM_173076). The former has a calculated molecular weight of 293 kDa and the latter 257 kDa. The full-length expressed protein contains a signal peptide at the N terminus, two transmembrane domains (TMD) and two nucleotide binding folds (NBF) (Figure 1.4). The NBFs bind ATP and the energy released in this process is used to transport lipids across the membrane. In normal skin, ABCA12 is expressed throughout the epidermis with abundant expression in the spinous and granular layers (Sakai et al., 2007) and abnormal LGs are the most obvious characteristic findings in HI lesional epidermis. It serves as a putative transporter for glucosylceramides from the Golgi apparatus (Sakai et al., 2007) into epidermal LB.

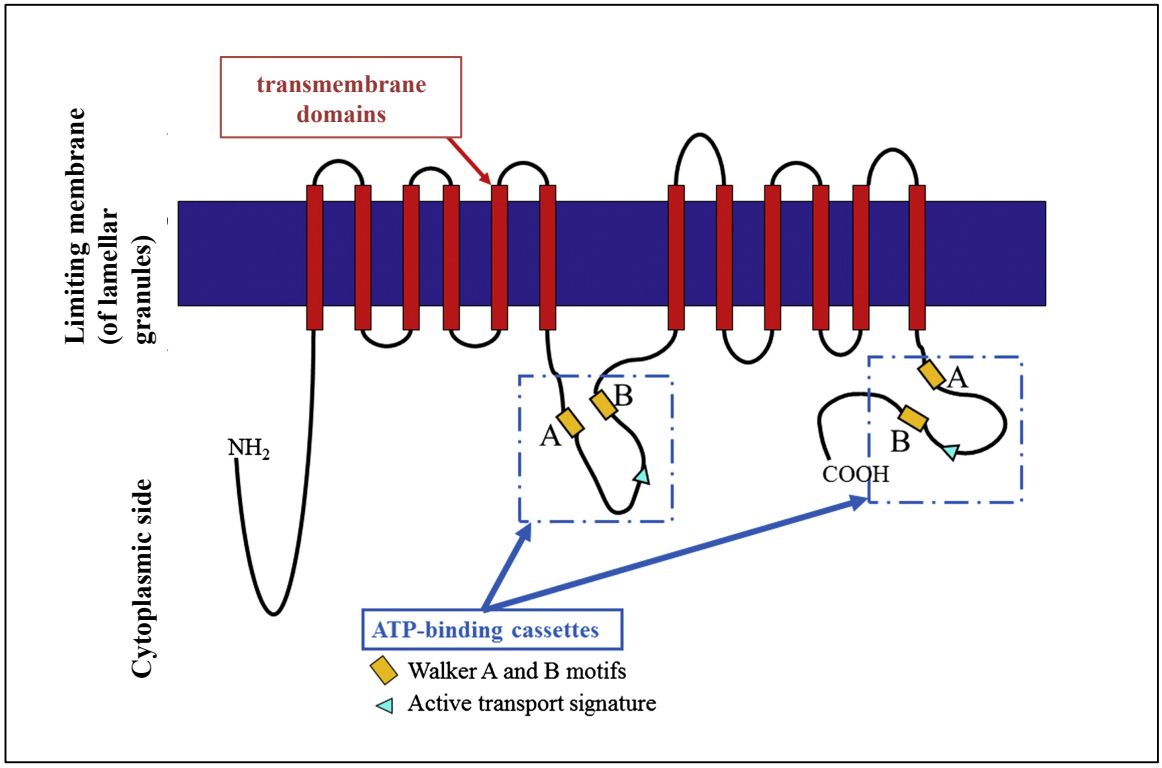

Figure 1.4: Structure of ABCA12 protein:
ABCA12 is a transmembrane protein. It contains a signal peptide at the N terminus, two transmembrane domains (in red) and two nucleotide binding folds. The nucleotide binding folds bind ATP and the energy released in this process is used to transport lipids across the membrane (Akiyama, 2014).

1.4.1.4 ABCA: The transporter superfamily

ABCA12 is a member of a large superfamily of the ATP-binding cassette (ABC) transporters. ABCs are a large group of proteins which bind and hydrolyze ATP to transport various molecules across a limiting membrane or into a vesicle (Borst and Elferink, 2002). To date, 48 ABC genes have been identified, which have been further divided into seven subfamilies organized from A to G, based on the amino acid sequence and the organization of ATP nucleotide binding folds (Akiyama et al., 2005, Borst and Elferink, 2002, Allikmets et al., 1996, Dean et al., 2001). These proteins contain two transmembrane sequences and two ATP binding domains, which undergo conformational changes that facilitate first the binding and then the dissociation of attached lipids (Hollenstein et al., 2007). The transmembrane domains typically contain from six to eleven membrane-spanning alpha-helices and it is this region of the protein that provides the specificity for the substrate. The ABCA subfamily comprises 12

functional transporters that all mediate lipid transport (Jiang et al., 2008), (Peelman et al., 2003) with the exception of one pseudogene (ABCA11). ABCA transporters function as components of highly specialized cellular lipid-transporting organelles in major physiological systems, in which defects cause severe inherited diseases in the cardiovascular, visual, and respiratory systems. Gene mutations in ABCA1 leads to Tangier disease where patients have a greatly reduced ability to transport cholesterol out of their cells, leading to a deficiency of high density lipoproteins in the blood stream and the accumulation of cholesterol in many tissues (Jetten et al., 1989, Jetten et al., 1987). ABCA3 regulates pulmonary surfactant transport/secretion by LB in type II alveolar cells (Yamano et al., 2001, Mulugeta et al., 2002) and pulmonary surfactant deficiency in newborns has been linked to ABCA3 deficiency (Strott and Higashi, 2003).

1.4.1.5 *ABCA12*: Role in lipid delivery and permeability barrier formation

In normal skin, ABCA12 localises to the LB and Golgi apparatus colocalising with glucosylceramide (Sakai et al., 2007). LB are found in the spinous and granular layers and are contiguous with the trans-Golgi network and fusion of LB with the surface of granular cells is observed (Ishida-Yamamoto et al., 2004). These observations imply that ABCA12 serves as a transporter for glucosylceramides from the Golgi apparatus into epidermal LB. The LB fuse with the plasma membrane at the apical surface of the granular keratinocytes secreting glucosylceramides into the extracellular space where they are hydrolysed to ceramides. They contribute both to lamellar extracellular lipids and to form the CLE (Sakai et al., 2007, Akiyama, 2006). In HI, loss of function mutations in *ABCA12* results in several morphological defects in skin. Compared to normal skin, electron microscopy of HI skin has shown absent, abnormally shaped, or reduced number of LB with absence of intercellular lamellae (Dale et al., 1990, Milner et al., 1992, Akiyama et al., 1994, Akiyama et al., 1998).

In HI keratinocytes an aberrant distribution of glucosylceramide immunofluorescent staining is noted, demonstrating defective glucosylceramide transport, but this phenotype is recoverable by *in vitro ABCA12* corrective gene transfer (Akiyama et al., 2005). Furthermore, unlike in normal skin where there are polar and nonpolar lipids in HI skin the majority of the lipids are polar suggesting an absence of nonpolar lipids such as ceramides (Thomas et al., 2009). Mutations in *ABCA12* cause defective lipid accumulation into LB (Akiyama et al., 2005, Yamanaka et al., 2007), resulting in malformation of the intercellular lipid layers of the *stratum corneum* (Akiyama et al., 2005) leading to a profound barrier abnormality (Moskowitz et al., 2004). Despite these findings the nature and scope of ABCA12's involvement in lipid homeostasis remains unclear.

1.4.1.6 *ABCA12*: Role in protease delivery and corneodesmosome retention

Harlequin ichthyosis is characterized by striking hyperkeratosis. Although this is driven, at least in part, by the high transepidermal water loss (Moskowitz et al., 2004) due to the profound barrier abnormality, it is possible that this is also due to a desquamation abnormality, but by an indirect mechanism, since corneodesmosomes are found to persist in the outer SC. An array of LB-derived proteases is required for degradation of corneodesmosomes and normal desquamation (Brattsand et al., 2005, Caubet et al., 2004, Horikoshi et al., 1999). Lipid delivery to LB is required for the subsequent or concurrent importation of these proteases into these organelles (Jobard et al., 2002). Colocalisation of proteases Cathepsin D and KLK5 with ABCA12 in normal keratinocytes and reduction of both in HI skin and a HI organotypic model has been noted (Thomas et al., 2009). Thus a failure of lipid delivery may also impair the delivery of these proteins into LB and consequently to the SC thereby resulting in corneodesmosome retention, explaining (along with the intense hyperplastic response to the barrier abnormality) the extreme hyperkeratosis

in neonates with HI. However the mechanism by which this happens in HI is unknown.

1.4.1.7 *ABCA12*: Role in late epidermal differentiation

Expression of markers of late epidermal differentiation such as filaggrin, TGM1, K10 are highly dysregulated in HI skin leading to premature epidermal differentiation suggesting that ABCA12 may have a key role in keratinocyte differentiation (Thomas et al., 2009, Smyth et al., 2008).

1.4.1.8 *ABCA12*: Gene Regulation

Nuclear hormone receptors peroxisome proliferators-activated receptor, PPAR (gamma and -beta/delta) and liver X receptor, LXR (to a lesser extent than PPAR) upregulate ABCA12 expression in cultured human keratinocytes and improve epidermal permeability barrier homeostasis by stimulating keratinocyte differentiation, lipid synthesis, and increasing LB formation/secretion (Jiang et al., 2008).

1.4.2 LAMELLAR ICHTHYOSIS (LI)/NONBULLOUS CONGENITAL ICHTHYOSIFORM ERYTHRODERMA (NCIE)

The LI/NCIE group is clinically and genetically heterogeneous with LI phenotype at one end of the spectrum and NCIE at the other with many intermediate, overlapping phenotypes (Williams, 1992b, Williams, 1992a). Clinical phenotypes can change over time and in response to treatment e.g. retinoid-treated LI can turn into NCIE. Histological features in this patient group are non-specific but include a compensatory thickening of the SC and epidermal hyperplasia. Mutations in 8 genes have been identified that cause the observed phenotype including *TGM1, ABCA12, Ichthyin* (also known as *NIPAL4*) *CYP4F22* and the lipoxygenase genes *ALOX12B* and *ALOXE3, LIPN, CERS3* (Radner et al., 2013), *PNPLA1* (Grall et al.,

2012). However, there is poor genotype-phenotype correlation. For example the LI phenotype is frequently, but not exclusively, caused by TGM1 deficiency. The same *TGM1* mutation can cause both LI and NCIE phenotypes, and the LI phenotype can result from mutations other than *TGM1* (Lawlor, 1988, Lefevre et al., 2004, Lesueur et al., 2007, Dahlqvist et al., 2007). Additionally, other variants/subtypes can be distinguished clinically: bathing suit ichthyosis attributed to *TGM1* mutations and the self-resolving collodion baby associated with *TGM1, ALOXE3* and *ALOX12B* mutations.

1.4.2.1 Lamellar Ichthyosis (LI) (MIM 242500)

The incidence of LI is estimated at 1:200000 (Eckl et al., 2005) but is more common in certain regions [(1:90,000 in Norway and 1:122,000 in Galicia in NW Spain due to a founder effect (Rodriguez-Pazos et al., 2011)]. Affected individuals are often (90%) (Burns et al., 2010) born with a parchment-like collodion membrane that is replaced in the first weeks of life by coarse, dark, plate-like scales (Williams and Elias, 1985). Due to the impaired skin barrier they are endangered by dehydration, sepsis and thermodysregulation (Huber et al, 1995). Eclabium and/or ectropion, with incomplete closure of the eye-lids, leading to conjunctivitis and keratitis, scarring alopecia, palmoplantar hyperkeratosis, hypoplasia of auricular and nasal cartilage, severe heat intolerance due to hypohidrosis may be noted (Griffiths et al. 2016).

1.4.2.2 Nonbullous Congenital Ichthyosiform Erythroderma (NCIE) (MIM 242100)

In nonbullous congenital ichthyosiform erythroderma, after desquamation of the collodion membrane in the first weeks of life, erythroderma develops with fine white-gray semiadherent scales which become large and plate-like on the lower limbs. Erythroderma often improves during childhood. Sites of predilection for scales are the face, arms and trunk. In up to about

70 % of patients, palmoplantar hyperkeratosis is present (Burns et al., 2010). Further frequent characteristics are ectropion, eclabium, mild nail dystrophy and heat intolerance (Burns et al., 2010).

1.4.2.3 Transglutaminase-1 (*TGM1*)

Of the many genes implicated in ARCI a variety of loss-of-function mutations in *TGM1* (Huber et al., 1995, Russell et al., 1995, Laiho et al., 1997, Akiyama et al., 2001), are most common accounting for over a third of this group (Fischer, 2009). The most typical phenotype of *TGM1*-linked ARCI is that of (classic) lamellar ichthyosis but *TGM1* mutations are reported to underlie NCIE phenotype (Laiho et al., 1997, Akiyama et al., 2001).

1.4.2.3.1 *TGM1*: Other genotype-phenotype correlations

Other than the phenotypes mentioned above *TGM1* mutations are also responsible for self-healing collodion baby (Vahlquist et al., 2010), limited lamellar ichthyosis and bathing suit ichthyosis (Oji et al., 2006). In self-healing collodion baby, the collodion membrane heals with no or only very mild ichthyosis, and bathing suit ichthyosis, characterized by pronounced scaling in the bathing suit areas but sparing of the extremities and the central face (Vahlquist et al., 2010, Oji et al., 2006). Bathing suit ichthyosis is thought to be a temperature-sensitive phenotype where the enzyme activity decreases at temperatures >33°C (Trindade et al., 2010). In this very rare condition there appear to be areas of normal looking skin and areas of skin with abnormal plate-like scaling. The amount of normal skin may vary at any one time.

1.4.2.3.2 *TGM1*: Gene

The *TGM1* gene localizes to chromosome 14 and contains 15 exons. To date, over 115 different mutations have been identified in this gene in 234 individuals from diverse

racial/and ethnic backgrounds (Herman et al., 2009). Most reported mutations are missense followed by nonsense, deletion and insertion (Herman et al., 2009). The most severe cases of LI are caused by nonsense and missense mutations resulting in loss of functional protein (Russell et al., 1995). The c.877-2A>G is the most commonly reported *TGM1* mutation and it had been shown that this mutation is common among North American and Norwegian patients due to a founder effect (Herman et al., 2009).

1.4.2.3.3 *TGM1*: Protein

TGM1 is mainly expressed on the upper spinous and granular layers of the stratified epidermis (Huber et al., 1995). It is a 92 kDa membrane-bound, calcium-dependent enzyme that is involved in CE assembly (by catalysing the N-y-glutamyl lysine) by cross-linking of precursor proteins such as involucrin, small proline-rich proteins and loricrin (Steinert and Marekov, 1995). Additionally it plays a role in covalently linking ω-hydroxyceramide, a constituent of the CLE, by ester bonds to CE proteins, most abundantly to involucrin (Candi et al., 2005).

1.4.2.3.4 Transglutaminases (TGs): The superfamily

Transglutaminases are encoded by a family of structurally and functionally related genes. Nine TG genes have been identified, eight of which encode active enzymes (Esposito and Caputo, 2005). A four-sequential domain arrangement is highly conserved in TG isoforms (Esposito and Caputo, 2005). The enzymes catalyze transamidation of glutamine resides a reaction associated with a wide variety of physiological processes including blood clotting, keratinization and fertilization (Huber et al., 1995). It consists of an N-terminal, a catalytic and two C-terminal ß-barrel domains. The epidermis harbours four of the nine TG isoforms (TG1, TG2, TG3 and TG5). TG2 is only detected in the basal layers and it is not involved in

cornification. TG1, TG3 and TG5 are expressed in the upper layers (Esposito and Caputo, 2005). These play consecutive and complementary roles in the formation of CE (Esposito and Caputo, 2005) on the intracellular surface of the plasma membrane of keratinocytes undergoing terminal differentiation. Although TGM3 and TGM5 are involved in the assembly of the CE, TGM1 is the major subtype involved (Yamanishi et al., 1992, Kim et al., 1992); TG 3–/– mice display no obvious defect in skin development nor in barrier function suggesting that epidermal loss of TG3 can be compensated for by other family members (John et al., 2012) and mutations in TGM5 lead to another type of ichthyosis, acral peeling skin syndrome MIM 609796. The fact that TGM1–/– mice die soon after birth with impaired skin barrier is the strongest validation of the importance of TG1 for cornified-envelope formation (Kuramoto et al., 2002).

1.4.2.3.5 TGM1: Role in Barrier function

Although TGM1 plays a role in CE formation, the barrier defect is paracellular as seen by lanthanum tracer studies (Elias et al., 2002). Ultrastructural studies reveal that the CEs are focally attenuated at all levels of the SC and abnormalities in extracellular lipid structures are evident and these correspond to regions where the cornified envelope is attenuated (Hohl et al., 1993, Paige et al., 1994, Elias et al., 2002). Furthermore, alterations in the lipid fatty acid synthesis pathway, following microarray analysis, in a rat epithelial organotypic model have been reported (O'Shaughnessy et al., 2010). Thus, mutations in *TGM1* secondarily cause defects in the intercellular lipid layers in the SC, leading to defective barrier function and to the ichthyotic phenotype seen in LI patients (Elias et al., 2002) and in transglutaminase 1 knockout mice (Kuramoto et al., 2002). *Ex vivo* gene replacement of TGM1, followed by transplantation to SCID mice, successfully corrects the ARCI phenotype, including the barrier abnormality (Choate et al., 1996).

1.4.2.3.6 *TGM1* expression

TGM1 is expressed on cell borders in the granular layer of healthy skin. In patients with *ALOX12B*, *ALOXE3* and *NIPAL4* mutations, the expression of *TGM1* is altered and extends into the stratum corneum and in several layers of the viable epidermis (Li et al., 2012). *TGM1* and eLOX-3 are found to colocalize mainly in the granular layer of healthy control skin and this colocalization is markedly increased in patients with *ALOX12B* and *ALOXE3* mutations (Li et al., 2012). Additionally, loss of *TGM1* is reported to cause changes in epithelial differentiation markers (increase in keratins 1, loricrin and downregulation of involucrin) in a rat epidermal keratinocyte organotypic model (O'Shaughnessy et al., 2010).

1.4.2.4 ALOX12B/ALOXE3

In 2002, mutations in two lipoxygenase genes, *ALOXE3* and *ALOX12B*, on chromosome 17p13, coding lipoxygenase-3 and 12(R)-lipoxygenase, respectively, were reported to underlie LI/NCIE (Jobard et al., 2002). They represent the second most common cause of ARCI after TGM1 (~15% of ARCI patients) (Eckl et al., 2009, Fischer, 2009). Most reported mutations are missense but deletions, insertions, splice site mutations leading to frameshift and mutations resulting in premature termination codons in both genes have been reported. Although *ALOX12B* mutations are distributed throughout the gene, two significant hotspots for mutations in *ALOXE3* were found in one study of 250 patients (Eckl et al., 2009). All mutations are loss of function mutations, either impairing enzyme activity or ablating protein synthesis thus confirming the crucial role of the LOX in barrier formation (Eckl et al., 2009) as evidenced by 12R-LOX and eLOX-R deficient mice that display a postnatal lethal phenotype due to severely impaired barrier function (Epp et al., 2007, Moran et al., 2007, Krieg et al., 2013).

1.4.2.4.1 LOX: Lipoxygenases family

Lipoxygenases (LOX) represent a widely distributed family of non-heme, iron-containing dioxygenases that insert molecular oxygen into polyunsaturated fatty acids producing highly active metabolites that play important roles in cell signaling or modification of membrane structures (Brash, 1999). Within the mammalian LOX family, a distinct subclass of epidermal-type LOX has been found to be preferentially synthesized in the skin and few other epithelial tissues (Brash et al., 1997, Boeglin et al., 1998). The genes for the human epidermal LOX, 15-LOX-2, 12R-LOX, and eLOX-3, map closely together on human chromosome 17p13.1 (Krieg et al., 2001). Their differentiation-dependent expression pattern in the epidermis suggests a common physiological role in epidermal differentiation. The epidermal 12R-LOX and eLOX-3 differ from all other mammalian LOX in their unique structural and enzymatic features (Boeglin et al., 1998, Krieg et al., 1999) as both proteins contain an extra domain located at the surface of the catalytic subunit. 12R-LOX represents the only mammalian LOX that forms products with R chirality (i.e. spatial arrangement of molecules with R chirality are mirror images of molecules with S chirality), and, unlike all other LOX, eLOX-3 does not exhibit dioxygenase activity but acts as a hydroperoxide isomerase (Yu et al., 2003).

1.4.2.4.2 LOX:12R-LOX/eLOX-3

Both 12R-LOX and eLOX-3 are localized to the stratum granulosum. Because the same phenotype is caused by mutation of either gene, the encoded proteins 12R -lipoxygenase (12R -LOX) and epidermal lipoxygenase-3 (eLOX3) are proposed to function in the same pathway of skin barrier formation. It is thought that both enzymes act in sequence: 12R-LOX to convert fatty acid substrates to R-hydroperoxides and eLOX3 in turn converts the 12R-LOX product into a specific epoxyalcohol derivative.

1.4.2.4.3 Lipoxygenase-3 and 12(R)-lipoxygenase: Role in terminal differentiation

With arachidonic acid as a substrate, the 12R-LOX/eLOX-3 pathway results in the production of specific R-epoxyalcohol metabolites which are known to function as signaling molecules involved in regulating keratinocyte differentiation (Brash et al., 2007, Eckl et al., 2005).

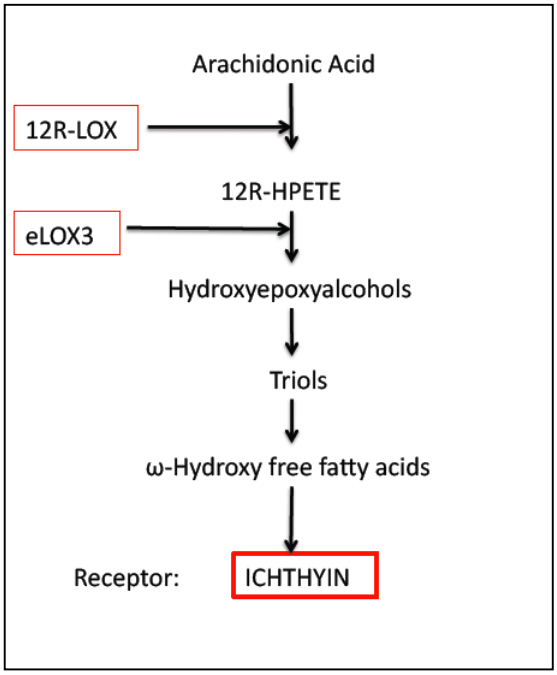

Figure 1.5: Postulated role of 12R-LOX and eLOX-3 in the same metabolic pathway. 12R-LOX converts fatty acid substrates to 12R-hydroperoxyeico- satetraenoic acid (12R-HPETE) and eLOX3 converts the 12R-LOX product into the corresponding hepoxilin- like epoxyalcohol, 8R-hydroxy-11R,12R-epoxyeicosatrienoic acid. Ichthyin is thought to the putative receptor for the end products of this pathway.

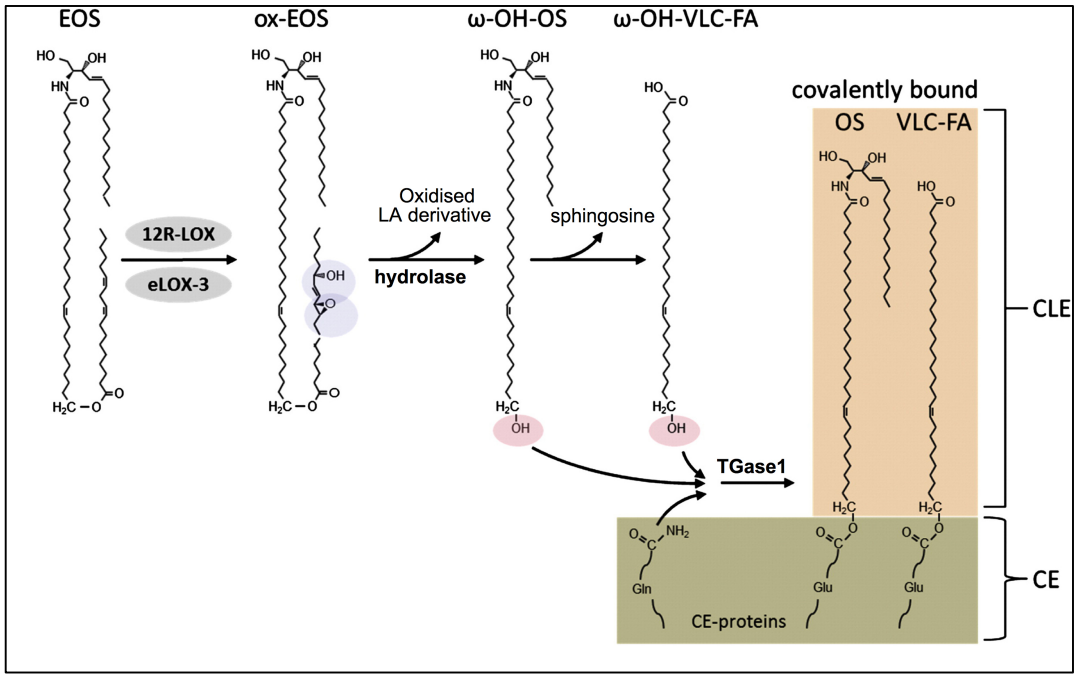

Figure 1.6: Involvement of 12R-LOX and eLOX-3 in ceramide processing.
The linoleate moiety of linoeoyl-ω-hydroxy-ceramide (EOS) is successively oxidised by 12R-LOX and e-LOX-3. This LOX induced oxidation facilitates further hydrolysis to ω-hydroxyacyl-sphingosine (ω-OH-OS) and ω-OH-very long chain fatty acid (ω-OH-VLC-FA). The resulting ω-OH derivatives are esterified by transglutaminase 1 (TGase 1) to glutamines in the cross-linked proteins of the cornified envelope (CE). Protein-bound OS ceramides and VLC-FA form the corneocyte-bound lipid envelope (CLE).
Adapted from (Krieg et al., 2014)

1.4.2.4.4 LOX: Structural role in skin barrier formation (CLE)-defective ceramide processing

Here, linoleate-containing EOS ceramide is the substrate. It is catalysed by 12R-LOX/eLOX-3 to an oxidized linoleate moiety which is hydrolysed further resulting in a free hydroxyl on the ceramides for coupling to the cross-linked proteins of the CE and forming the CLE (Krieg et al., 2013, Zheng et al., 2011). Thus, it has been proposed that the LOX pathway may play a role in ceramide processing and consequently in the formation of the CLE (Zheng et al., 2011).

1.4.2.5 Ichthyin

1.4.2.5.1 LI/NCIE phenotypes due to Ichthyin mutations

In patients with Ichthyin mutations LI/NCIE phenotypes have been noted, with a slightly increased prevalence of the NCIE phenotype, but the spectrum of clinical variability is very

wide, even among members of the same family, (Wajid et al., 2010) ranging from NCIE to LI to a mixture of both. Palmoplantar keratoderma is present in most cases. Some patients are born with a collodion membrane (Lefevre et al., 2004, Dahlqvist et al., 2007). Other features such as hypohidrosis, itching, joint contractures, clubbing and ectropion have also been reported.

1.4.2.5.2 *Ichthyin*: Gene

Ichthyin, also known as *NIPAL4*, defects were reported to be associated with ARCI in 2004. (Lefevre et al., 2004). The gene is localized on chromosome 5q33 and has 6 exons. Homozygous mutations reported include 6 missense mutations (most commonc.527C ->A), 2 splice site mutations and 1 nonsense mutation (Wajid et al., 2010).

1.4.2.5.3 Ichthyin: Protein

The protein belongs to a new family of proteins and is predicted to have several transmembrane domains. Ichthyin-like proteins are localized in the plasma membrane, and share homologies to both magnesium transporters and G-protein coupled receptors (Lefevre et al., 2004). In normal skin, Ichthyin is expressed in the viable part of epidermis with highest expression in the SG with localization to the cell borders in a honeycomb pattern (Li et al., 2013, Wajid et al., 2010). On electron microscopy it localises to keratin throughout the viable epidermis and desmoplakin (Dahlqvist et al., 2012). (Interestingly, patients with mutations in keratin 1 and desmoplakin have palmoplantar keratoderma, a feature observed in this ichthyotic phenotype).

In patients with Ichthyin mutations no loss of Ichthyin protein has been observed (Dahlqvist et al., 2012) but relocation to the cytoplasm as well as weak expression of the protein in the

stratum corneum has been detected (Li et al., 2013). Ultrastructurally, aggregation of mutant ichthyin protein is seen (Dahlqvist et al., 2012). These findings suggest altered or loss of functional protein in mutant Ichthyin.

1.4.2.5.4 Ichthyin: Role in lipid metabolism

The function of Ichthyin is unknown. It has been proposed to function both as a receptor for metabolites produced by the 12R-LOX and eLOX-3 lipoxygenases in the hepoxilin pathway (Lefevre et al., 2004) and as a magnesium transporter (Goytain et al., 2008) with a possible role in lipid metabolism; In support of this, structural changes in the SG (empty or partially filled vacuolar and vesicular structures, which are thought to represent defective LB and perinuclear elongated membranes) due to ichthyin deficiency have been seen on electron microscopy (Dahlqvist et al., 2007) and abnormal lipid accumulation within cells (but not in the intercellular space) is seen in the SG and SC on Nile Red lipid analysis (Dahlqvist et al., 2012, Wajid et al., 2010). Further support for the role of Ichthyin in lipid metabolism comes from another finding; Ichthyin is found to colocalize with FATP4 protein in the SG. The putative function of FATP4 is that of acyl-CoA synthetase with some predilection for long and very-long FFA (Lenz et al., 2011). It is thought to be essential for lipid deposition in the cornified layer and lack of fatty acid transport protein, FATP4, leads to a syndromic ichthyosis in the neonatal period called Ichthyosis Prematurity Syndrome. Down-regulation of Ichthyin results in the up-regulation of FATP4 expression possibly reflecting a compensatory feedback mechanism (Li et al., 2013). FATP4 is known to be a magnesium-dependent enzyme and it may be possible that it requires ichthyin for Mg^{2}+ recruitment (Li et al., 2013).

1.4.2.5.5 Ichthyin: Putative receptor for products of the lipoxygenase pathway

The expression of Ichthyin is upregulated in ALOX12B$^{-/-}$, ALOXE3$^{-/-}$ and TGM1$^{-/-}$ mutations.

In turn, along with altered localization of ichthyin, ALOX12B, ALOXE3 are upregulated with increased colocalisation in ICHTHYIN$^{-/-}$ (Li et al., 2012, Li et al., 2013) suggesting abnormal enzyme turnover due to a chain of events in which these ARCI genes may be involved.

However, the exact mechanisms of how *Ichthyin* mutations can cause an ichthyotic phenotype and interact with other ichthyosis genes, in particular *ALOX12B* and *ALOXE3* along a common pathway, remains to be clarified.

1.5 Hypothesis

The monogenic non-syndromic ichthyoses (ichthyosis vulgaris, X-linked ichthyosis, congenital ichthyosiform erythroderma, lamellar ichthyosis, harlequin ichthyosis) cause a similar clinical phenotype of varying severity that affects terminal differentiation in skin with compromise of the cornified envelope due to genetic defects arising from different underlying gene mutations located on separate chromosomes.

The null hypothesis states that despite the common phenotype the individual ichthyosis do not have interlinking pathomechanisms and biological pathways. In this study I test this as follows:

Aims and objectives

1. Development of in-vitro 2D (and where possible 3-D) models of the ichthyoses.
2. *RNA-Seq* on generated models from the same genetic background with knockdown of relevant ichthyosis genes using primary human keratinocytes from neonatal foreskin.
3. Analysis of the results to identify pathways and/or biological processes involved in disease pathogenesis.

Chapter 2: Materials and Methods

2.1 Ethics

This study was conducted according to the Declaration of Helsinki Principles and was approved by the East London and City Health Authority Research Ethics Committee and cooperating centres (Ethics reference: 08/H1102/73).

2.2 Cell culture

2.2.1 Primary Keratinocyte culture

Primary human keratinocytes were derived from neonatal foreskins and purchased from Invitrogen (Cat. No. C-001-5C).

2.2.1.1 Isolation of primary keratinocytes from neonatal foreskin

Foreskin was obtained following circumcision from neonatal Caucasian males. The skin was delivered post-operatively in transport medium [DMEM Dulbecco's Modified Eagles medium (E4) containing 10% (v/v) foetal bovine serum (FBS), 1% (v/v) L-glutamine (200 mM), 1% (v/v) penicillin-streptomycin (P/S)] and processed the same day or the following day after overnight storage at 4°C. Skin was placed on a sterile Petri dish containing Versene (EDTA). Excess dermis and subcutaneous fat were removed. The skin pieces were washed with Versene and cut into small 1-2mm fragments. The fragments were placed in 1x trypsin in a 15 ml tube and incubated at 37°C, 10% CO_2 for 2 hours. At 30-minute intervals and at the end of the incubation the tube was shaken vigorously. The cell suspension was transferred into a sterile tube and resuspended in an equal volume of DMEM:Ham's F12 (3:1) growth medium supplemented with 10% (v/v) (FBS), 1% (v/v) L-glutamine (200 mM), 1% (v/v) P/S and 1x RMplus (see Table 2.1) (keratinocyte growth media) and shaken vigorously for 5 minutes.

Table 2.1: RM+ supplement

RMplus supplement
0.4 μg/ml hydrocortisone
0.5 μg/ml insulin
10 ng/ml epidermal growth factor
0.1 nM cholera toxin
5 μg/ml transferrin
20 pM Liothyronine

The cell suspension was filtered through a sterile gauze into another Falcon tube and centrifuged (1200 rpm, 5 min, RT). The cell pellet was resuspended in keratinocyte growth media containing 2.5 μg/ml amphotericin, the cells counted in a haemocytometer, and plated at densities of $2x10^6$cells/T75 flask on a feeder-layer of 3T3 ($2x10^6$cells/flask) mouse fibroblasts that that had previously been growth arrested by lethal irradiation-6000Gy (Rheinwald and Green, 1975). Cells were grown at 37°C, 10% CO_2 and media were changed 2-3 times/week. Old feeders were removed by incubating cells in Versene for 5 min at 37°C, and new growth arrested 3T3 cells were added every 2-3 days to maintain optimal 3T3 density. Primary keratinocytes are seen to grow in colonies.

2.2.1.2 Subcultivation of keratinocytes

The 3T3 feeders were removed by incubating cells in Versene for 5 min and the cells were incubated with 0.02% trypsin-EDTA at 37°C until cells were seen to be rounded and detached over a period of 5-7 minutes. Trypsin was neutralised with an equal volume of serum containing media. Cells were then centrifuged (1200 rpm, 5 min, RT) and frozen, subcultured for amplification, or seeded for experiments.

2.2.1.3 Subculture with 3T3-mouse fibroblast feeders

For cultivation of primary keratinocytes on a feeder-layer of irradiated 3T3 fibroblasts (Rheinwald and Green, 1975), 3T3 fibroblasts were seeded into T75 flasks at $2x10^6$ cells/flask and grown in DMEM Dulbecco's Modified Eagles medium (E4) containing 10% FBS overnight at 37°C, 10% CO2. The following day, primary keratinocytes were resuspended in keratinocyte growth media, and seeded at approximately 1.5-2 million cells per T75 flask containing the growth- arrested 3T3 fibroblasts. Cells were grown at 37°C, 10% CO_2 and media were changed every 2-3 days. Old feeders were removed by incubating cells in Versene for 5 min, and new growth arrested 3T3 cells were added every 2-3 days. When the primary keratinocytes were 70-80% confluent, feeders were removed, and keratinocytes were frozen, subcultured for amplification, or seeded for experiments.

2.2.1.4 Subculture in serum-free conditions

Primary human keratinocytes derived from neonatal foreskins, nHEK, either isolated as above or purchased from Invitrogen, were expanded and cultured according to the company's instructions. Briefly, cells were thawed and seeded into a T75 flask pre-coated with rat-tail collagen type I (2mg/ml, Firstlink), containing 14 ml of pre-warmed serum-free growth media (EpiLife Medium with growth supplement, HKGS (S-001-5), Invitrogen). Cells were incubated at 37°C, 5% CO2. Once the cells were 70-80% confluent, they were passaged. Old culture medium was removed, were washed once in Phosphate buffered saline (PBS), and then subcultured by incubation with pre-warmed 0.02% trypsin-EDTA at 37°C in stages (1-2min) over a period of 5-7 minutes. Trypsin was neutralised with an equal volume of growth medium containing serum. Cells were then centrifuged (1200 rpm, 5 min, RT), and resuspended in serum free media. Cell counts were obtained using a haemocytometer, and cells were then resuspended and subsequently seeded at $5x10^3$ cells/cm^2 in collagen I coated

flasks for further amplification, or at variable densities for experiments. Cells were frozen for long-term storage as above.

2.2.1.5 Cryopreservation of cells

To maintain cell stocks for experiments, cells were cryopreserved. For this, following trypsinisation, cells were resuspended at a density of 1-2x10^6 cells/ml in freezing media containing 10% Dimethyl Sulfoxide (DMSO), and 90% complete growth medium, cooled in a Mr. Frosty™ Freezing Container (ThermoFisher Scientific) at -80°C o/n and then stored in liquid nitrogen.

2.2.1.6 Thawing Cells

Ampoules of cryopreserved cells were thawed rapidly by incubation in a water bath at 37°C. The ampoule was swabbed with 70% ethanol before opening. The cells were diluted in media containing 10% FBS, then pelleted by centrifugation (as above) and resuspended and plated as required.

2.2.2 Primary fibroblasts

Primary human fibroblasts were isolated from the separated dermis of neonatal foreskins by overnight incubation in collagenase D (1 mg/ml) (Roche) in DMEM supplemented with 10% FBS, 1% L-glutamine (200 mM) and 1% P/S (Fibroblast growth medium) at 37°C. Cells were collected by centrifugation and expanded until the second passage, at this point stocks of fibroblasts were cryopreserved and stored in liquid nitrogen. For routine culture primary fibroblasts were plated into T175 flasks at a density of 6,000 cells per cm^2 in fibroblast growth media and growth until 70-80% confluent. Subculturing was performed as described above in fibroblast growth media.

2.2.3 Immortalised keratinocyte (nTERT) culture

The immortalised cell line, nTERT, expressing the catalytic subunit of telomerase (nTERT) combined with deletion or mutation of p16INK4a, was obtained from cryopreserved departmental stocks (Rheinwald et al., 2002). The cell line was grown in keratinocyte growth media, and incubated at 37°C, 10% CO_2. Media were changed every 2-3 days until the cells were confluent. Cells were passaged and split 1:5 or counted and seeded depending on experimental requirements. For cryopreservation $1x10^6$ cells were resuspended in FBS containing 10% dimethyl sulfoxide (DMSO) as a cryoprotectant. Freezing was performed at a rate of -1°C/min to a temperature of -80°C. At this stage the tubes were transferred to -180°C liquid vapour phase cryostore.

2.2.4 RNAi for terminal differention genes in nHEKs

For transient transfection, custom made siRNAs (Invitrogen, UK) sequence-specific to the genes of interest were transfected into nHEKs.

Table 2.2: siRNA sequences

Gene	siRNA used	siRNA sequence
STS	2	CCUCAGAACAGCACAUCCAUCUGGA
FLG	1	ACAGAAAGCACAGUCAUCAUGAUAA
ABCA12	1	GACCGAACUUCUUUGUGAAUCUGAA
TGM1	3	CGGGAGGACAUCACCUACCUCUAUA
ICHTHYIN	3	CAAGAACGUCCUUGUGGACAAUAUA
ALOX12B	2	CCAUAAGCAGCUGCUGAACCACUUU

Control non-targeting primer sequences were not made available by Invitrogen.

Transfection was performed according to the HiPerFect transfection protocol (Quigen, UK) and optimised for a 6-well plate format. nHEKs were plated at a density of $1.5x10^5$ per well

and incubated in Epilife media (Cascade Biologics, UK) in a 6-well plate, and incubated at 37°C/5% CO_2. After 24 h, nHEKs of 50–60% confluency using HiPerFect were transfected with a siRNAs for *STS, FLG, ABCA12, TGM1, ICHTHYIN and ALOX12B* (table 2.2) and the non-targeting control. For transfection, siRNA duplexes (5-25nM) and 15 μl of HiPerFect transfection reagent were diluted with 95 μl Epilife media, vortexed and incubated at room temperature (RT) for 10 min. After incubation the volume was made up to 2 ml in Epilife growth media and pipetted onto primary keratinocytes and incubated overnight at 37°C/5% CO_2. The following day transfection media was replaced with Epilife growth media. Cells transfected with non-targeting siRNAs, (Invitrogen, UK) at the same final concentration were used as negative controls.

2.2.5 Calcium shift assay

nHEKs were transfected as described previously. After 12 h, the cells were shifted to high calcium (1.3 mM) Epilife media and incubated for 24 h. Calcium was added to Epilife media as $CaCl_2$ (Sigma-Aldrich, UK), and the media filter-sterilised using a vacuum-driven filtration system (Millipore, UK). Cells incubated in low calcium media for 24 h were kept as a control. Cells were harvested in RLT Plus Buffer or QIAzole lysis reagent (Qiagen) for RNA analysis and 1x Triton-lysis buffer for Western Blotting.

2.2.6 Organotypic cultures on de-epidermalised dermis (DED)

Sterilised glycerol-preserved skin (Euro Skin Bank, Beverwijk, The Netherlands) was washed three times in PBS and incubated in PBS containing antibiotic mix (600 U/ml penicillin-G, 600 μg/ml streptomycin sulphate, and 2.5 μg/ml amphotericin) for 10 days at 37°C. After incubation the epidermis was scraped off the dermis using the blunt side of a scalpel, and cut into 1.5 cm^2-squares. Each square of DED was placed into a well of a 6-well plate with the

reticular side facing up onto which a stainless steel ring was placed. $5x10^5$-primary human fibroblasts in 500 µl fibroblast growth media (DMEM supplemented with 10% FBS, 1% L-glutamine (200 mM) and 1% P/S) were seeded into each ring. Fibroblasts were cultured on the DED for 2 weeks with media changes every 2 days. Then, the DED was flipped over so that the papillary side was facing up, which allowed the seeding of $5x10^5$ keratinocytes in 500 µl Epilife growth media into rings placed on the papillary side of the DED. After 48 hours the cultures were raised to the air-liquid interface on stainless steel grids in a 6-well plate. Keratinocyte growth media containing 50 µg/ml ascorbic acid (vitamin C) was added and refreashed every 2 days. After 10 days the cultures were harvested and bisected, with one half being fixed in 4% PFA and paraffin embedded and the other half was snap frozen in liquid nitrogen, cryo-embedded in Bright Cry-M-Bed (Jencons), and stored at -80°C.

2.3 RNA methods

2.3.1 Extraction of RNA using the RNeasy Plus Mini kit

Total RNA was extracted from primary keratinocytes using RNeasy Plus Mini Kit (Qiagen, West Sussex, UK) according to the manufacturer's instructions. Briefly, cells were harvested by adding 350 µL of lysing Buffer RLT Plus (containing β-Mercaptoethanol; 10 µl for 1 ml of RLT buffer). The lysates were homogenised by centrifugation for 2 minutes at maximum speed in a QIAshredder spin column (Qiagen) and placed in a collection tube. The homogenised lysate was transferred to a genomic (g) DNA eliminator spin column (Qiagen) and centrifuged for 60 s at 10,000 rpm to remove gDNA. One volume of (600 µl) of 70% ethanol was added to the flow-through and mixed well. The sample was then applied to an RNeasy spin column and centrifuged for 30 seconds at 10,000 rpm and the flow-through discarded. The column was washed with RW1 buffer (700 µl) followed by two washes with RPE buffer (500 µl). After a final centrifugation for 1 minute at 14,000 rpm for 1 min, the

RNeasy column was then transferred to a new 1.5 ml collection tube and RNA eluted by adding 25 µl of RNase free water and centrifuging. A second elution step with a further 25 µl was performed before quantifying the RNA. Purified RNA was stored at –80°C in RNase-free water.

2.3.1.2 Spectrophotometric quantification of RNA

RNA concentration was determined by measuring the absorbance at 260 nm with a spectrophotometer after RNA extraction (Nanodrop, ND-1000 Spectrophotometer) and samples were stored at -80°C.

2.3.2 Complementary DNA (cDNA) synthesis using Superscript VILO cDNA Synthesis Kit

cDNA was synthesised from total RNA using the Superscript VILO cDNA synthesis kit (Invitrogen, Paisley, UK) according to manufacturer's instructions. Briefly, 2 µg of total RNA was added to a mixture containing 1X SuperScript enzyme mix (containing, SuperScript III RT, RNaseOUT recombinant ribonuclease inhibitor, and a property helper protein), 1X VILO reaction mix (containing, random primers, $MgCl_2$, and dNTPs), and DEPC-treated water to a final volume of 20 µl. The mixture was placed in the DNA Engine Tetrad 2 Peltier Thermo Cycler (MJ Research, CA) and incubated at 25°C for 10 minutes, and then at 42°C for 60 minutes. To terminate the reaction the sample was heated to 85°C for 5 minutes. cDNA was stored at 20°C. cDNA was quantified using the NanoDrop and then stored at -20°C.

2.3.3 Polymerase chain reaction

PCR is a method used to amplify specific DNA sequences that are selected by specific primers. To do this, oligonucleotide primer sequences (Sigma, Poole, UK) were designed

around the region of interest. Primer sequences were designed using the internet-based Primer3 program and were checked with the mRNA sequence of interest. In the case that multiple isoforms exist for the same gene, all isoforms were aligned together using the ClustalW alignment tool and primers were designed to overlap a region common to all the isoform sequences (Larkin et al., 2007). To check the specificity of the primers, both forward and reverse primer sequences were input into the NCBI Nucleotide BLAST search tool which searches the primer sequence against other genes (Altschul et al., 1990). This prevents the amplification of other genes that may have a similar sequence which would give a false positive result.

qPCR was performed with 200 ng of cDNA using The ReddyMix® PCR Mastermix kit (Fisher Scientific, Leicestershire, UK). cDNA was mixed with ReddyMix® (12.5 µl), 25 mM MgCl2 (1 µl), 1 µM primer template (2 µl). The mix was adjusted to a reaction volume of 20 µl with RNase free water. For genes that have lower expression, the cDNA and/or primer concentration was increased. For a negative control, a reaction mix was made with cDNA substituted with an equal volume of H_2O. PCR reactions were performed using the PTC-240 DNA Engine Tetrad 2 Peltier Thermal Cycler (MJ Research, USA) with the following cycle sequence: initiation at 95°C for 5 minutes, 45 cycles of denaturation at 95°C for 20 seconds, annealing for 20 seconds (optimised primer annealing temperature ranging from 57°c to 64°C), and extension at 72°C for 25 seconds and a final extension at 72°C for 25 seconds.

PCR products were then run on a 1% agarose gel to confirm the presence of the right size amplified PCR fragment; a 0.6% (w/v) agarose gel (Fisher Scientific, Leicestershire, UK) was prepared in 1x TAE solution (48.4 g Tris, 11.4 ml 17.4 M glacial acetic acid, 3.7 g

EDTA made upto 1 L with distilled water. Diluted 1:10 (v/v) with distilled water) and repeatedly boiled until the agarose crystals were fully dissolved. The agarose solution was cooled for 1 minute with cold tap water before GelRed was added at 1 µl/ml (Biotium, CA, USA). The solution was then poured into a gel castor with a comb and left to solidify. The PCR reaction products were loaded onto the gel (placed in gel tank, submerged in 1x TAE) along with DNA Hyperladder II. The gel was run at 90 V until the size of the PCR product was determinable compared to the DNA ladder.

2.3.4 Quantitative polymerase chain reaction (qPCR)

qPCR was performed with 200 ng of cDNA using the Rotor-Gene SYBR green PCR kit (Qiagen, West Sussex, UK). cDNA was mixed with SYBR mix (12.5 µl), 25 mM $MgCl_2$ (1 µl), 1 µM primer template-forward and reverse (2 µl). The mix was adjusted to a reaction volume of 20 µl with RNase free water. For primer sequences refer to Table 2.3. The qPCR reaction was carried out using Rotor-Gene Q (Qiagen, West Sussex, UK) with the following cycle sequence: initiation at 95°C for 5 minutes, 35 cycles of denaturation at 95°C for 5 seconds, annealing at 60°C for 5 seconds, and extension at 60°C for 10 seconds. A house-keeping gene was used as an endogenous control and gene expression was normalised to the house-keeping gene (details in section 3). Technical triplicates were used for each sample. Water (no template, cDNA excluded) was included as a negative control. Data analysis was performed using Microsoft Excel 2008. The relative mRNA expression values were calculated using the $x=2^{-\Delta\Delta Ct}$ formula where x represents the induction value and Ct represents the average threshold cycle of the triplicate samples. ΔCt refers to the difference between the Ct values of the gene of interest and the housekeeping reference gene. ΔΔ Ct represents the difference between the ΔCt of the cDNA sample compared to the control sample.

Table 2.3 Primer sequences used for qPCR

GENE	Primer Sequence
GAPDH	F-GCCTTCCGTGTCCCCACTGC R-GCTCTTGCTGGGGCTGGTGG
B2M	F-GATGAGTATGCCTGCCGTGTG R-CAATCCAAATGCGGCATCT
TBP	F-CACGAACCACGGCACTGATT R-TTTTCTTGCTGCCAGTCTGGAC
RPLOPO	F-ATCAACGGGTACAAACGA GTC R-CAGATGGATCAGCCAAGAAGG
YWHAZ	F-ACTTTTGGTACATTGTGGCTTCAA R-CCGCCAGGACAAACCAGTAT
GUSB	F-GCTCTTGCTGGGGCTGGTGG R-CAGATGGATCAGCCAAGAAGG
STS	F-AACTCACTCAGCACCTGGCA R-GGGAGGAAGACCAGCCTCTT
FLG	F-TACAGTCACGTGGCAGTCCT R-CCAAACGCACTTGCTTTACA
ABCA12	F-CACTGGCCTTGATGGGAAA R-ATGCCAACCTGGTACAGAG
TGM1	F-AATCCTCTGATCGCATCACC R-GTGCGGACTGTGAACTGAAA
ICHTHYIN	F-GACGGAATCTCCGTTGTTGT R-CTGCCTCCAAAGAGGAAGTG
ALOX 12B	F-CCTCCTGGAGCACAGAAAAG R-TGAGGAAGGAGTAGCGGAGA

2.3.5 Next Generation Sequencing (*RNA-Seq*) Experiment

Tranfection was performed as described in section 2.2.4 for the genes of interest (*STS, FLG, ABCA12, TGM1, ICHTHYIN ALOX12B*) and three negative controls (non-targeting siRNA, mock and untreated). For mock conditions, 2 ml of culture media with transfection reagent

were added per well and for untreated cells 2 ml of culture media were added per well and incubated at 37°C/5% CO_2. For untreated cells 2 ml of culture media were added per well and incubated at 37°C/5% CO_2. 12 h post-transfection, a calcium switch assay was performed as described in section 2.2.5. RNA was extracted 3 days post-calcium switching as described in section 2.3.1. RNA concentration was determined as described in section 2.3.1.2. RNA (from triplicated biological replicates) was sent to GSK (RD Molecular Discovery Research, GlaxoSmithKline, Collegeville, PA, USA) for sequencing. The laboratory at GSK confirmed that all samples had an RNA Integrity Number of >8. Dr Harpreet Saini (Dr Anton Enright group) carried out analysis of the sequenced reads at European Bioinformatics Institute (EBI), Cambridge (described in section 5.0) and differentially expressed gene (DEG) lists were provided. The DEGs were analysed further using DAVID, REACTOME and GeneMANIA (chapter 5). Heatmaps were generated using ggplot2 by Dr Harpreet Saini at EBI (chapter 6).

2.3.5.1 Extraction of RNA using the miRNeasy Mini Kit and MaXtract High Density gel tube

RNA was extracted from primary keratinocytes using miRNeasy Mini Kit and MaXtract High Density gel tubes (Qiagen, West Sussex, UK). MaXtract High Density gel tubes enables improved recovery of nucleic acids and ensures ease of handling when working with standard organic extraction mixtures. It acts as a barrier between the organic and aqueous phases, allowing the nucleic acid-containing phase to be easily removed by decanting or pipetting. Compared to traditional organic extraction methods, use of MaXtract High Density gel can result in the recovery of 20–30% more nucleic acid. Cells were harvested by washing in PBS, lysed in 700 µL of QIAzol Lysis Reagent and the lysate was transferred into a prespun (13000 rpm for 30s) MaXtract High Density gel tube (Qiagen). 140 µl chloroform was added to the tube containing the homogenate and the tube was shaken vigorously for 15 s. The tube was left at RT for 15 s and then centrifuged at 4°C at 13000 rpm to separate the phases. After

centrifugation, the sample separated into 3 phases: an upper, colourless, aqueous phase containing RNA; a white interphase (MaXtract High Density gel); and a lower, red, organic phase containing protein. The upper, aqueous phase was decanted into a fresh tube with 525 µl of 100% ethanol and mixed thoroughly by pipetting up and down several times. The sample was washed as described previously (section 2.3.1). Each RNA sample was eluted with 50 µl of nuclease-free water and divided into a 2µg aliquot for *RNA-Seq* and the remainder kept for qPCR.

2.4 Protein analysis

2.4.1 Western Blotting

2.4.1.1 Antibodies

The antibodies used for this project together with their dilutions for Western blotting are listed as follows:

Table 2.4 Antibodies used for Western Blotting

Antibody	Species	Company, Catalogue Number	Dilution
STS	R	Abcam, ab83668	1:250
TGM1	M	B.C1	1:1000
ICHTHYIN	R	Ichthyin (P-12) sc-133280	1:250
GAPDH	R	Abcam, ab9485	1:5000

The secondary antibodies (goat anti-rabbit #P0448, goat anti-mouse #P0447) for Western blotting were purchased from Dako, UK and used at 1:5000 dilution.

2.4.1.2 Total cell lysate preparation

Cell extracts were prepared from keratinocytes that were 80% confluent in a 6 well plate. At the appropriate time points, media were removed from the cells, cells were washed with PBS and lysed for approximately 30 min on ice in a 1XTriton lysis buffer (20mM Tris pH 7.4, 137 mM NaCl, 2 mM EDTA pH 7.4, 1 % Triton X-100 and 10 % glycerol) containing a complete protease inhibitor cocktail 2 mM N-ethylmaleimide (NEM), 1 mM phenylmethylsulfonyl fluoride (PMSF), and 10 mM EDTA (Roche, UK) and collected using a cell scraper. Lysates were sonicated for 10 seconds and cleared by centrifugation at 12000 rpm for 15 minutes at 4°C.

For quantification of protein concentration 20 µl of the lysate was put into a 1.5 ml tube for quantification using the Bio-Rad DC Protein Assay kit (Bio-Rad, MA, USA). 2 µl of Solution S and 98 µl of Solution A were added to the tube and mixed. 800 µl of Solution B was added

to each tube and mixed at which point, the mix changed colour. A high protein concentration creates stronger blue colour intensity. A set of diluted standards was used to generate a standard curve. Using a spectrophotometer, the protein absorbance (AU) measured at a wavelength of 655 nm. A standard curve was generated using the AU measurements obtained from known concentrations of bovine serum albumen (BSA, Sigma, Poole, UK).

2.4.1.3 SDS-PAGE electrophoresis in Laemmli system

Equal protein amounts were separated by SDS-PAGE with 10% polyacrylamide resolving gels using electrophoresis apparatus from Hoefer Inc., USA. Samples were diluted in 5x sample buffer (6% (w/v) SDS, 180 mM Tris-HCl pH 6.8, 15% (w/v) β-mercaptoethanol, 60% (v/v) glycerol, and 6% (w/v) bromophenol blue), boiled for 5 minutes at 95°C and loaded onto the polyacrylamide gel. Samples were boiled with the sample buffer for 2 min at 80°C, spun down and then loaded into wells created in the 5% stacking gel. 7 µl of Precision Plus Protein Kaleidoscope Standards (Biorad, UK) were loaded in a separate lane to visualize progress and to evaluate the molecular weight of separated proteins. Electrophoresis was performed in 1x running buffer (25 mM Tris-HCl pH 8.3, 0.2 M glycine, 0.1% (w/v) SDS) at 90 V until samples reached the resolving gel, then at 120 V for approximately 90 min to separate the proteins. Proteins were electrotransferred from the polyacrylamide gel onto Amersham Hybond-C Extra (GE Healthcare, UK) nitrocellulose membrane in transfer buffer (25mM Tris-HCl pH 8.3, 0.2 M glycine, 0.01% (w/v) SDS, 20% (v/v) methanol) at a 70 V current for approximately 120 min at 4°C. Transfer quality was assessed in Ponceau S (Sigma-Aldrich MO, USA) solution for 5 minutes followed by de-staining in ddH_20.

Membranes were blocked in 5% milk (Marvel) in TBST (20 mM Tris-HCl, pH 7.5, 150 mM NaCl, 0.1% Tween-20) for 1 hour at RT to block non-specific antibody binding to the

membrane. Membranes were incubated with primary antibody (Table 2.4) at the appropriate dilution in 5% milk o/n (4°C) with gentle agitation. After washing three times with TBST, the membranes were incubated with horseradish peroxidase-conjugated secondary antibody (1/5000 in 5% milk in TBST) for 1 hour at RT. After membranes were washed again (as described above) and incubated in ECL plus Mix Solution (GE Healthcare, UK), and exposed to chemiluminescence sensitive film (GE Healthcare, UK) and developed.

2.4.2 Haematoxylin and Eosin (H&E) staining of DEDs

Haematoxylin and Eosin (H&E) staining of paraformaldehyde (PFA) fixed paraffin embedded and cryo-embedded organotypic culture sections was undertaken. Sections (5 μm-thick) of 4% PFA-fixed and paraffin-embedded organotypic cultures were cut. Sections were de-paraffinised in two changes of xylene for 5 and 3 minutes and hydrated in descending grades of ethanol (100% twice, 90% and 30%) for 3 minutes each. Sections were washed in distilled water for 5 minutes. Nuclei were stained with Haematoxylin for 5-8 minutes, washed in running tap water, differentiated by immersing briefly in 1% acid alcohol, and rinsed in water. The cytoplasm was stained with Eosin for 5 minutes. Sections were then dehydrated by ascending grades of ethanol followed by xylene (inverse of described above). Sections were mounted with DePex mounting medium (Fisher Scientific).

2.4.3 Immunohistochemistry

Cryosections (5 μm-thick) of frozen samples mounted in optimal cutting temperature, ,OCT, (Tissue-Tek®, NL) were cut in a cryostat, placed on a Poly-lysine plus coated slide and stored at -80°C. For H&E staining, sections were air-dried at room temperature for 30 minutes and the same procedure as described above was used with the exception of the de-paraffinisation step.

Specimens were mounted in paraffin and sectioned at 5 μm. Haematoxylin and eosin staining was performed first, then sections were deparaffinized, quenched with 3% hydrogen peroxide to block endogenous peroxidases, and antigen retrieval was achieved by boiling in a microwave in antigen unmasking solution (10 mM citrate buffer pH=6.0), for 10 minutes. Sections were blocked with 2.5% normal horse serum, and probed with primary antibodies either overnight at 4°C, or for one hour at RT. Peroxidase conjugated secondary antibodies were then applied, and DAB substrate kits were used for peroxidase detection (Vector Laboratories).

2.4.4 Immunofluorescence (IF) staining of PFA-fixed paraffin embedded and cryo-embedded sections

The PFA-fixed paraffin embedded sections were cut, de-paraffinised and hydrated as described above (Section 2.4.4.1). Antigen retrieval was performed by heating sections in 10 mM citrate buffer (pH 6.0) in a water bath set to 95°C for 10 minutes. Sections were washed in distilled water for 5 minutes and PBS for 5 minutes before proceeding to IF staining protocol. Cryoembedded sections of 5 μm were cut on a cryostat microtome (Thermoscientific cryotome FSE) and placed on electrostatically charged slides (Superfrost plus, BDH). Frozen sections were dried and either fixed in 4% PFA at room temperature for 10 minutes or fixed in 1:1 methanol: acetone for 10 min before proceeding to the IF staining protocol.

Slides were washed three times for 5 minutes in phosphate-buffered saline (PBS). Non-specific binding was blocked with PBS containing 0.3% Bovine Serum Albumin (BSA) for 20 min at RT and washed as previously. The sections were incubated with primary antibody diluted in PBS containing 1% BSA (Table 2.5), overnight at 4°C. The sections were washed

again and the secondary antibody, Alexa Fluor 568-red or 488-green, goat anti-rabbit or goat anti-mouse was applied at a dilution of 1:800 in the same dilutant at room temperature for 40 min. The samples were light protected thereafter. Sections were washed twice in PBS before counterstaining with 4',6-Diamidino-2-phenylindole (DAPI, 1:20,000 in PBS) nuclear stain for 5 min at room temperature. After a further washing step, sections were mounted with ImmuMount mounting medium (Thermo-Fisher Scientific).

Table 2.5 Antibodies used in Immunohistochemistry and Immunofluorescence.
R= rabbit, M= mouse

Antibody	**Species**	**Company, Catalogue Number**	**Dilution**
STS	R	Abcam, ab83668	1:50
TGM1	M	B.C1	1:1000
ICHTHYIN	R	Ichthyin (P-12) sc-133280	1:800
GAPDH	R	Abcam, ab9485	1:5000
Keratin 10	M	CRUK (LHK10)	1:1000
K14 MM	M	CRUK (LL002)	1:100
LOR	R	Abcam ab85679	1:100
ABCA12	R	Abcam ab98976	1:500
FLG	M	Novocastra (NCL-FILAGGRIN)	1:100
ALOX12B	R	Thermo Scientific PA5-23608	1:50

2.5 Functional Protein analysis

2.5.1 Stimulation of siRNA transfected keratinocytes with ligands

Transfection was performed as described in section 2.2.4 for the genes of interest (*STS, FLG, ABCA12, TGM1, ICHTHYIN and ALOX12B*) and negative control, non-targeting siRNA (*C*). 12 h post-transfection, a calcium switch assay was performed as described in section 2.2.5. 24 h following calcium switching, keratinocytes were stimulated with peptidoglycan (PGN) from Staphylococcus aureus (10 ug/ml), Poly I:C (10 ug/ml) and flagellin (Salmonella Typhimurium 1 ug/ml) (in duplicate for each condition). Culture supernatants were recovered at 12 and 24 hours thereafter for cytokine measurement. Total RNA was extracted 24 hours following addition of ligands as described in section 2.3.1.

2.5.2 BD™ CBA Human Inflammatory Cytokines Kit

The (Cat No. D8000C) was used to quantitatively measure interleukin-8 (IL-8), interleukin-1β (IL-1β), interleukin-6 (IL-6), interleukin-10 (IL-10), tumor necrosis factor (TNF), and interleukin-12p70 (IL-12p70) protein levels in a single sample using flow cytometry.

Six bead populations with distinct fluorescence intensities had been coated with capture antibodies specific for IL-8, IL-1β, IL-6, IL-10, TNF, and IL-12p70 proteins i.e. each capture bead in the kit had been conjugated with a specific antibody. The six bead populations were mixed together to form the bead array. A single set of diluted standards was used to generate a standard curve for each analyte. The inflammatory cytokine capture beads were mixed with the recombinant standards or samples, containing recognized analytes, and incubated them with the detection reagent, phycoerythrin (PE)-conjugated detection antibodies which provides a fluorescent signal in proportion to the amount of bound analyte, to form sandwich complexes (capture bead + analyte + detection reagent). Flow cytometry was used to measure

these complexes. The intensity of PE fluorescence of each sandwich complex correlated with the concentration of that cytokine. FCAP Array™ software was used to generate results in graphical and tabular format.

2.6 Replicates and Statistical analysis

Technical triplicates were used for all qPCR experiments. Biological triplicates were used for the RNASeq experiment and western blots. Biological duplicates were used for cytokine analysis using the BD™ CBA Human Inflammatory Cytokines Kit. Ten measurements from each organotypic were taken at random from different positions using the measuring tool with Image J. Statistical analysis was performed using an paired two-tailed *t*-test using Prism v7.od (GraphPad software Inc. Ca, USA). Cell count quantification was done using cell profiler (http://cellprofiler.org). Statistical analysis was performed using an paired two-tailed *t*-test using Excel.

Chapter 3: RNAi for Terminal Differentiation genes in Primary Human Keratinocytes

3.1 Introduction

RNA interference (RNAi) is the process of mRNA degradation that is induced by double-stranded RNA in a sequence specific manner. This process was first discovered to occur endogenously in plants (Napoli et al., 1990) and subsequently in the nematode *Caenorhabditis elegans* (Tabara et al., 1999), humans (Elbashir et al., 2001a) and other mammalian cells (Hammond et al., 2000). The mechanism of RNAi exists to protect the host from molecular invaders such as viruses and transposons. Double stranded RNA (dsRNA) entering a cell will be targeted for immediate destruction via this pathway. Using RNAi as a molecular tool allows the investigator to study the function of one gene at a time, as the process of gene knockdown is usually very specific (Moazed, 2009).

RNAi is a two-step process. The first step involves the cleavage of long dsRNA into 21 to 23 bp siRNA with dinucleotide 3' overhangs by the enzyme Dicer (Zamore et al., 2000). Dicer is a type III endoribonuclease and is a ubiquitous member of the proteome. In the second step, one strand of siRNA (the guide strand) is assembled into an RNA-inducing silencing complex (RISC) that cleaves the target mRNA leading to down regulation of the protein encoded by that gene (Elbashir et al., 2001b). The siRNA is thought to provide target specificity of RISC through base pairing of the guide strand with the target mRNA. Assessing the phenotype of a cell after suppressing expression of a specific gene by siRNA transfection has become a powerful tool in laboratory research.

3.1.1 Aim

The aim of this chapter was to establish an *in vitro* disease model for the non-syndromic ichthyoses by knockdown of *STS, FLG, ABCA12, TGM1, ICHTHYIN* and *ALOX12B* in normal keratinocytes from neonatal skin. Transient knock-down of the Ichthyosis genes was achieved by using siRNAs in normal human keratinocytes. This will enable analysis

of the effect of knockdown in keratinocytes with the same genetic background.

3.2 Results

3.2.1 Transfection of primary keratinocytes with siRNA to knockdown ichthyosis genes: *STS, FLG, ABCA12, TGM1, ICHTHYIN* and *ALOX12B*

3.2.1.1 Optimisation of the siRNA-transfection conditions

Low transfection efficiency will result in a lower level of silencing, and the transfection efficiency may vary between cells and cell lines and should be optimised for each cell line. Therefore, prior to transfecting the siRNA sequence-specific to the ichthyosis genes into the normal human keratinocytes (nHEKs), the transfection efficiency was optimised by determining the volume of lipid-based HiPerFect transfection reagent (Qiagen) having least impact on cell viability and the highest efficiency of siRNA delivery.

Three different volumes (according to the range suggested by the manufacturer) of the transfection reagent (12, 15 and 18 μl) were tested on nHEKs. Cells were plated in a 6-well plate and incubated with the transfection solution containing the respective amount of HiPerFect, according to the manufacturer's instructions. Cell number and morphology were analysed under bright-field microscopy twenty-four hours post-incubation. Further cell count quantification was done using cell profiler (http://cellprofiler.org). A significant reduction ($p=0.004$) was found between 12μl and 18μl but no significant difference in cell count was observed between 12 μl and 15μl or 15 μl and 18 μl of transfection reagent.

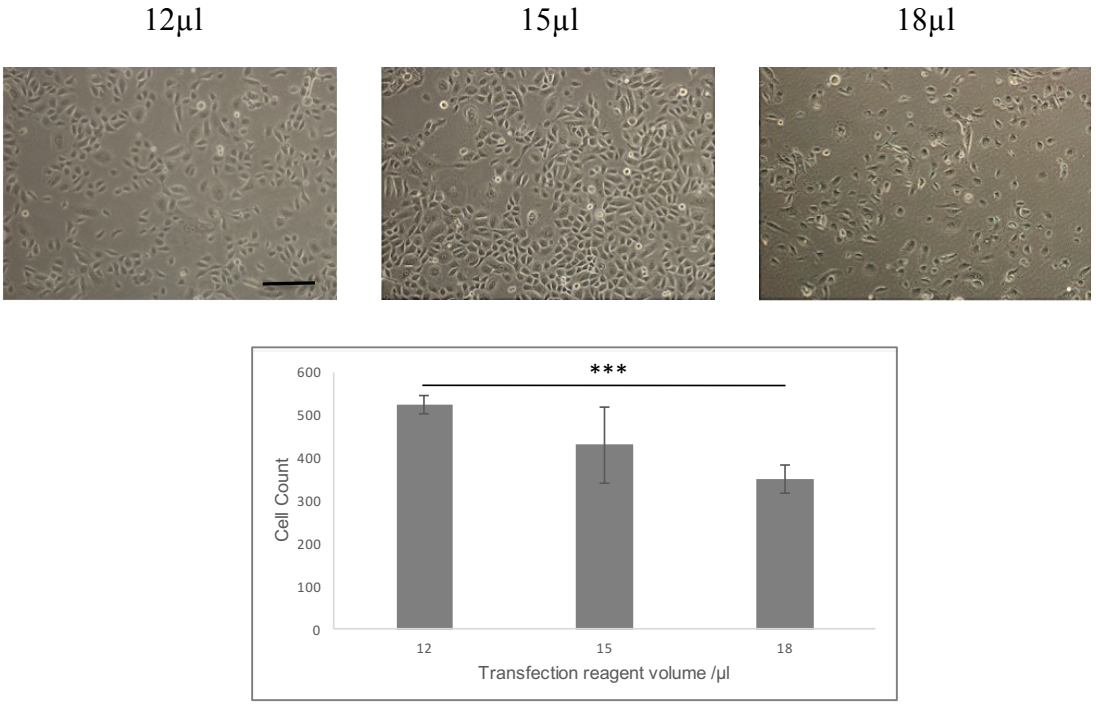

Figure 3.1: The effect of HiPerFect transfection reagent quantity on nHEKs viability.
Representative photomicrographs of nHEKs 24 h after incubation with different volumes of HiPerFect transfection reagent diluted in 2 ml of medium: 12 µl (HiPerFect-12 µl) or 15 µl (HiPerFect-15 µl) or 18 µl (HiPerFect-18 µl). Pictures were taken under brightfield microscopy. Scale bars represent 50 µm. Cell count quantification for different volumes of HiPerFect transfection reagent using Cell Profiler. Significant difference between 12 and 18 µl is noted. Data represent mean ± standard deviation (n=4) with *** P =0.004.

Then, it was determined which of the following volumes 12, 15 or 18 μl of transfection reagent, provided the highest siRNA-delivery efficiency into these cells at 24 or 48 hours. For that, a siRNA control fluorescently labelled with the fluorophore Cy3", si*GLO*" siRNA, was used. The uptake of si*GLO*" siRNAs can be visualised with the appropriate filters on a microscope. Analysis of transfected cells under fluorescence microscopy showed that all volumes of transfection reagent were effective in delivering the siRNA molecules into the cells. Cells transfected with 15 μl of HiPerFect reagent at 24 hours, showed increased fluorescence compared to 12 or 18μl viability, thereby suggesting that transfection of these cells under these conditions gives the best results.

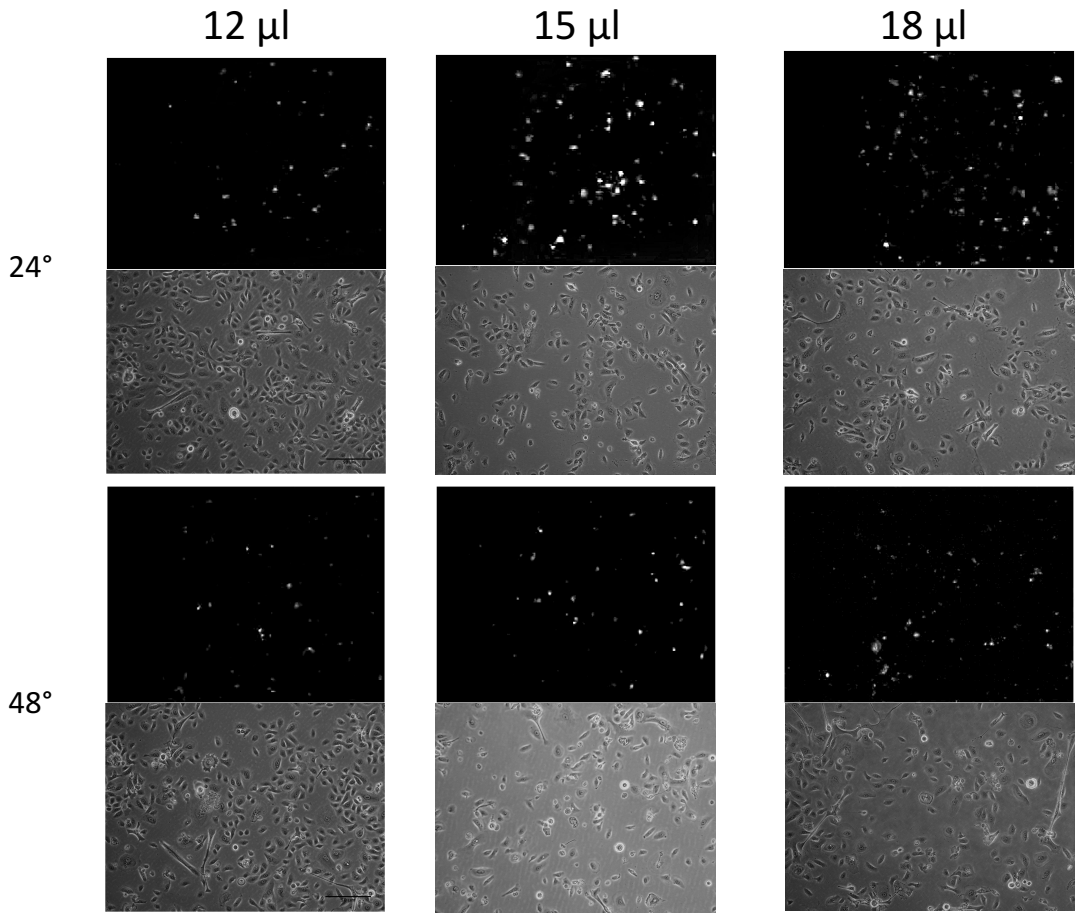

Figure 3.2: The effect of HiPerFect transfection reagent quantity on siRNA delivery into nHEKs.
Representative photomicrographs of nHEKs transfected with the si*GLO*" siRNA (siRNAs fluorescently labelled with the fluorophore Cy3" for easy detection) and different volumes of HiPerFect transfection reagent diluted in 2 ml of medium: 12 µl (HiPerFect-12 µl), 15 µl (HiPerFect-15 µl) and 18 µl (HiPerFect-18 µl) Twenty four and fourty-eight hours after, cells were analysed under brightfield (top panel) and fluorescence (bottom panel) microscopy (n=3). The presence of fluorescently labelled-siRNAs (white) inside the cells can be detected with fluorescence microscopy. Scale bars represent 50 µm.

3.2.1.2 Cell density at transfection

The optimal cell confluency for transfection should be determined for every new cell type to be transfected and kept constant in future experiments. This is achieved by counting cells before seeding and by keeping the interval between seeding and transfection constant. This ensures that the cell density is not too high and that the cells are in optimal physiological condition at transfection. For transfection a 50-60% cell density at the time of transfection is optimal. To determine the optimal seeding density nHEKs were seeded at three different cell

counts, 100,000, 200,000 and 300,000, according to the manufacturer's instructions. Cell density was determined the following day.

Collagen is the most widely used extracellular matrix protein and has been shown to be involved in cell attachment and differentiation. Type I collagen can be used as a thin film to promote cell attachment and/or proliferation *in vitro*. To evaluate if collagen I affected nHEK cell proliferation and differentiation, cells were seeded, as above, on collagen uncoated and coated six well plates. Higher cell proliferation and epithelioid morphology was observed with collagen-coated plates. 50-60% cell density for transfection was observed with a cell count of 150,000 cells.

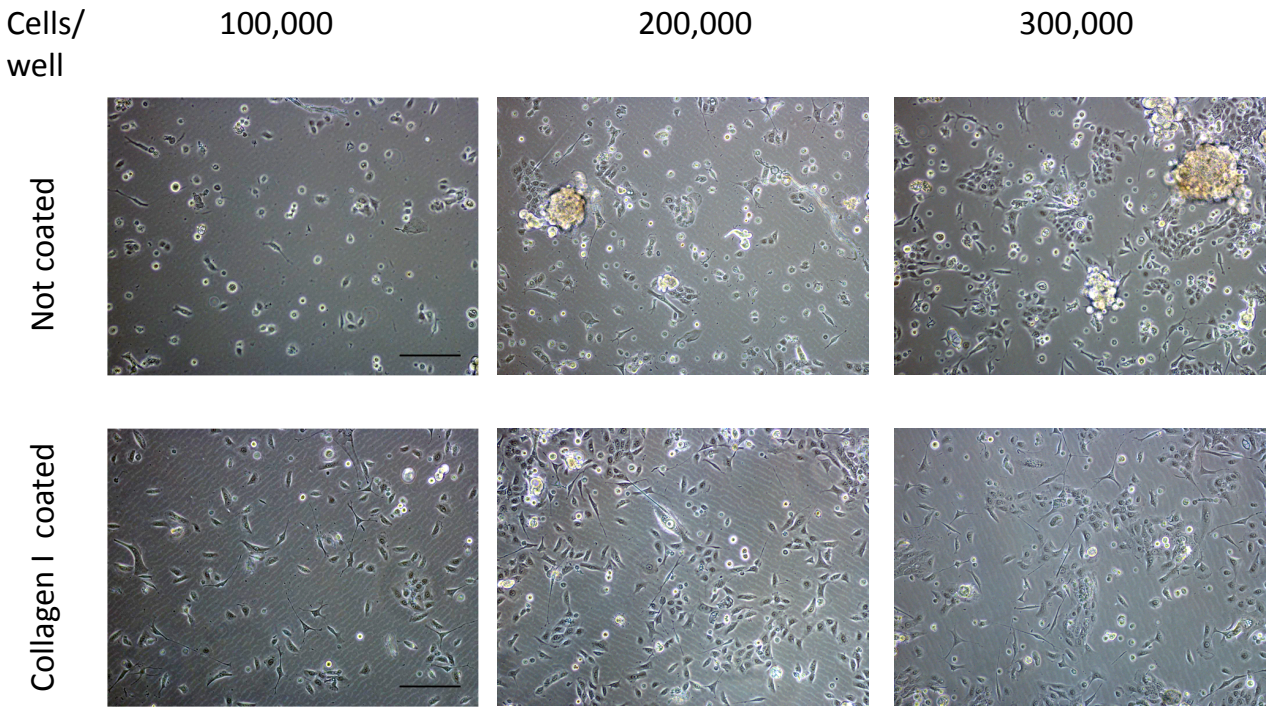

Figure 3.3: Optimistion of cell density at transfection for nHEKs.
Representative photomicrographs of nHEKs 16 hours after seeding 100,000, 200,000 and 300,000 cells/well in a six-well plate uncoated and coated with rat tail Collagen I. Photomicrographs were taken under brightfield microscopy (n=2). Scale bars represent 100 μm.

3.2.1.3 RNAi knock-down expression of ichthyosis genes of interest

Three custom made Stealth siRNAs (25bp each) targeting different regions in the mRNA for the gene of interest and a high and low GC negative control, designated CH and CL respectively, were obtained from Invitrogen. The siRNA was transfected into nHEKs of 50–60% confluency using HiPerFect. siRNAs were used at a concentration of 25nM each. The degree of gene expression down-regulation was determined at mRNA level two days post-transfection using quantitative, real-time PCR (qPCR). For that, RNA was extracted, total cDNA synthesised and used for qPCR with specific primers for each gene of interest. Relative quantitation of gene expression was calculated using the Comparative CT method. Expression of each gene of interest was normalized to expression of the housekeeping gene, *GUSB*. Each siRNA sequence for each gene of interest down-regulated gene expression at the mRNA level. The most effective siRNA sequence for each gene was used in subsequent experiments. Since the GC content of siRNA used for subsequent experiments was between 36-52% a low GC negative control was used as advised by the manufacturer.

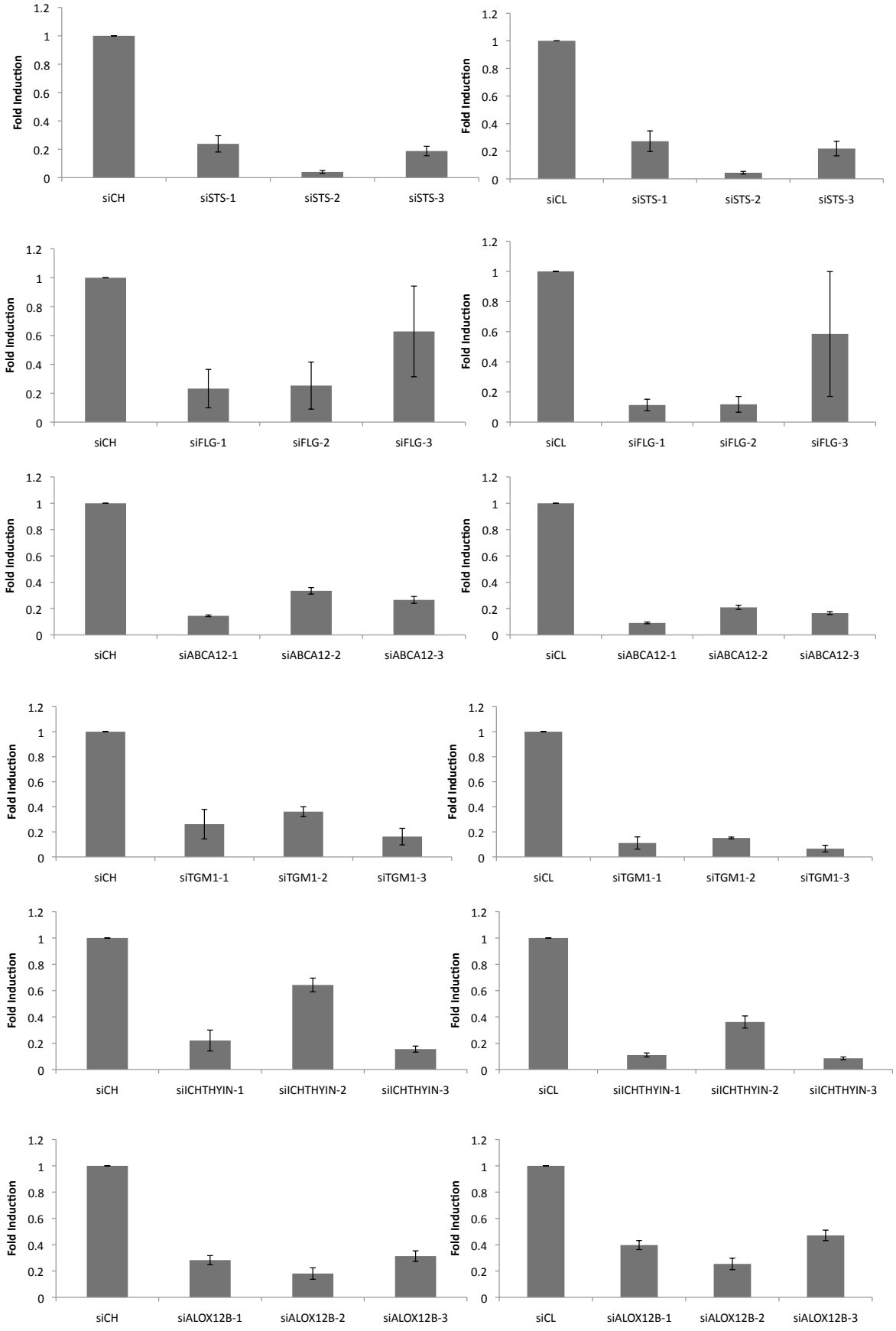

Figure 3.4: qPCR showing downregulation of Ichthyosis genes.
Each siRNA sequence targeting the gene of interest lead to significant down-regulation of gene expression. qPCR analysis of *STS, FLG, ABCA12, TGM1, ICHTHYIN and ALOX12B* expression in nHEKS two days post transfection with three different siRNA sequences targeting each gene of interest. Two different non-targeting controls, CL and CH, were used. Values derived from qPCR for siC were set at 1 (fold induction) and the relative expression levels of cells transfected with the experimental siRNA (n=3). Error bars represent mean ± standard deviation.

3.2.1.4 Optimal siRNA concentration to minimize off-target effects in RNAi experiments

Studies have indicated that transfection of siRNA can result in off-target effects, in which siRNAs affect the expression of non-homologous or partially homologous gene targets. The mechanisms of off-target effects are not fully understood. They may be caused by siRNA targeting mRNA with close homology to the target mRNA, by siRNAs functioning like miRNAs, or by a cellular response to siRNA toxicity. Off-target effects, which may produce misleading results in RNAi experiments, can be largely avoided by using low siRNA concentrations. To evaluate the lowest concentration of siRNA for each gene of interest that will allow gene silencing without compromising knockdown efficiency nHEK cells were transfected with 5 nM, 10 nM and 25 nM of siRNA. Low GC non-targeting siRNA, siC, was used as a negative control. Gene expression was determined at the mRNA level, 2 days after transfection, by qPCR.

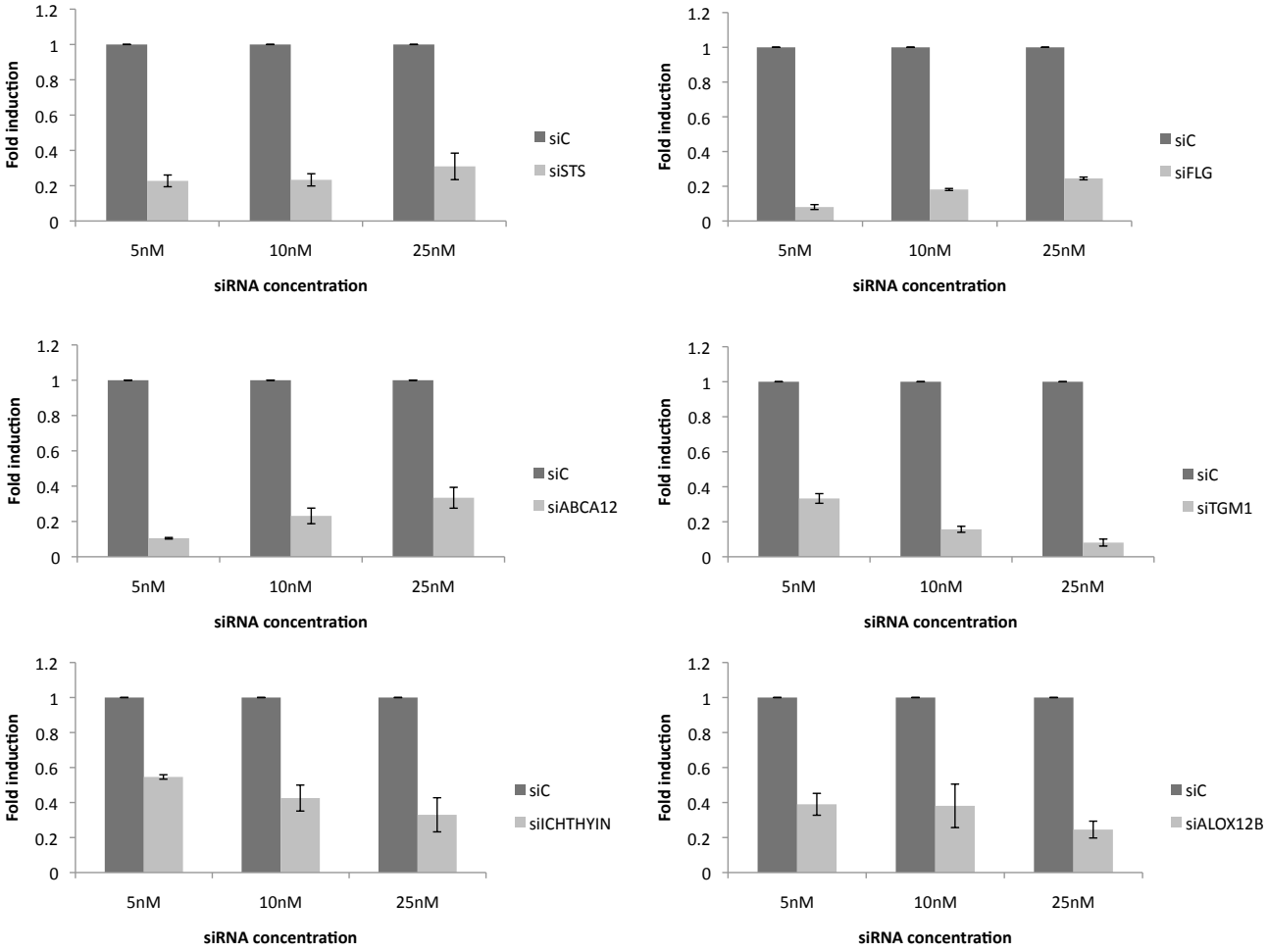

Figure 3.5: qPCR analysis of nHEK cells transfected with different concentrations of siRNA targeting the gene of interest.

nHEK cells were transfected with three different concentrations, 5 nM, 10 nM and 25 nM, of siRNA targeting *STS, FLG, ABCA12, TGM1, ICHTHYIN and ALOX12B* . Nonsilencing siRNA, siC, was also transfected. 2 days later, cells were harvested for qPCR. Values derived from qPCR for siC were set at 1 (fold induction) and the relative expression levels of cells transfected with the experimental siRNA (n=3). Error bars represent mean ± standard deviation.

3.2.2 Reference gene selection for qPCR in siRNA transfected primary keratinocytes

For qPCR to yield meaningful results, it is necessary to normalise expression of the gene of interest to a stably expressed endogenous control. Housekeeping genes are genes coding proteins responsible for maintaining basic functions of cells. They are thought to be relatively constitutively expressed and therefore are candidates for internal control genes in qPCR. However, evidence shows that these and other housekeeping genes are not as resistant to internal and external environmental changes as previously thought and that mRNA expression of housekeeping genes may show alterations depending on applied experimental conditions (Balogh et al., 2008).

The current study involved establishing expression profiles for 6 putative housekeeping genes (*GAPDH, B2M, RPLOPO, TBP, YWHAZ* and *GUSB*) with different functions in cellular maintenance to study gene expression of *STS, FLG, ABCA12, TGM1, ICHTHYIN,* and *ALOX12B* in neonatal human epidermal keratinocytes, nHEKs, following gene silencing using 3 different primer siRNA sequences targeting each gene of interest, as previously described.

The stability of gene expression for candidate HKGs was analyzed using the geNorm analysis program. Genes with different cellular functions were chosen because selecting genes that share identical biochemical pathways could bias analyses (Bär et al., 2009). The geNorm algorithm expresses the internal control gene-stability measurement as M. Genes with the lowest M-values exhibit the most stable expression and are thought to be more reliable for normalization (Allen et al., 2008). Genes with a M-value under 0.5 are considered acceptable for valid HKG (Minner and Poumay, 2009). This analysis revealed that the cutoff M-value of *GUSB* was below 0.5 thus supporting the choice of *GUSB* as HKGs in experiments to study

differentiation of keratinocytes by real-time qPCR.

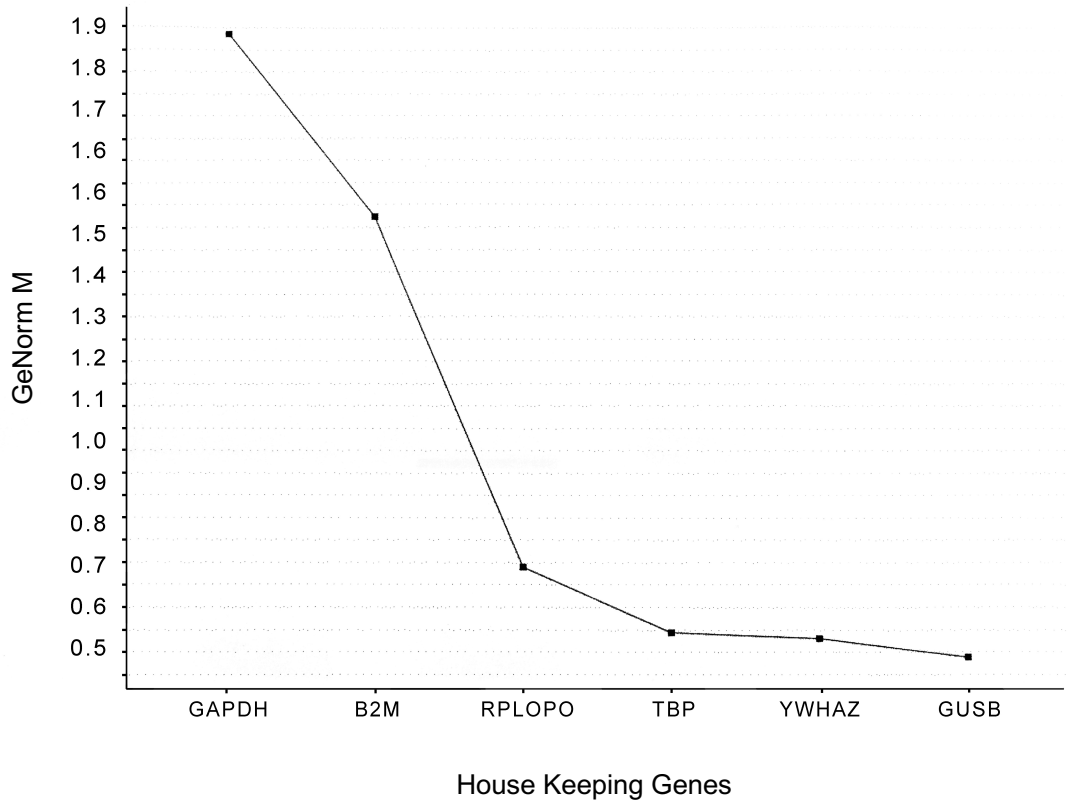

Figure 3.6: Genorm Analysis of HKGs.
Average expression stability values, M. M-values under 0.5 are considered acceptable for valid HKG (Minner and Poumay, 2009). *GUSB* was the only gene with an M value below 0.5. Following transfection with siRNA gene expression of the ichthyosis genes was analysed; Total RNA was extracted, reverse transcription was performed and cDNA was analyzed (n=3), by qPCR.

To further confirm the stability of HKGs qPCR analysis was undertaken using three different HKGs-*GAPDH*, *YWHAZ* and *GUSB*. *GUSB* and *YWHAZ* were chosen because they had the lowest M values. *GAPDH* was chosen because it is a commonly used HKG in nHEK experiments.

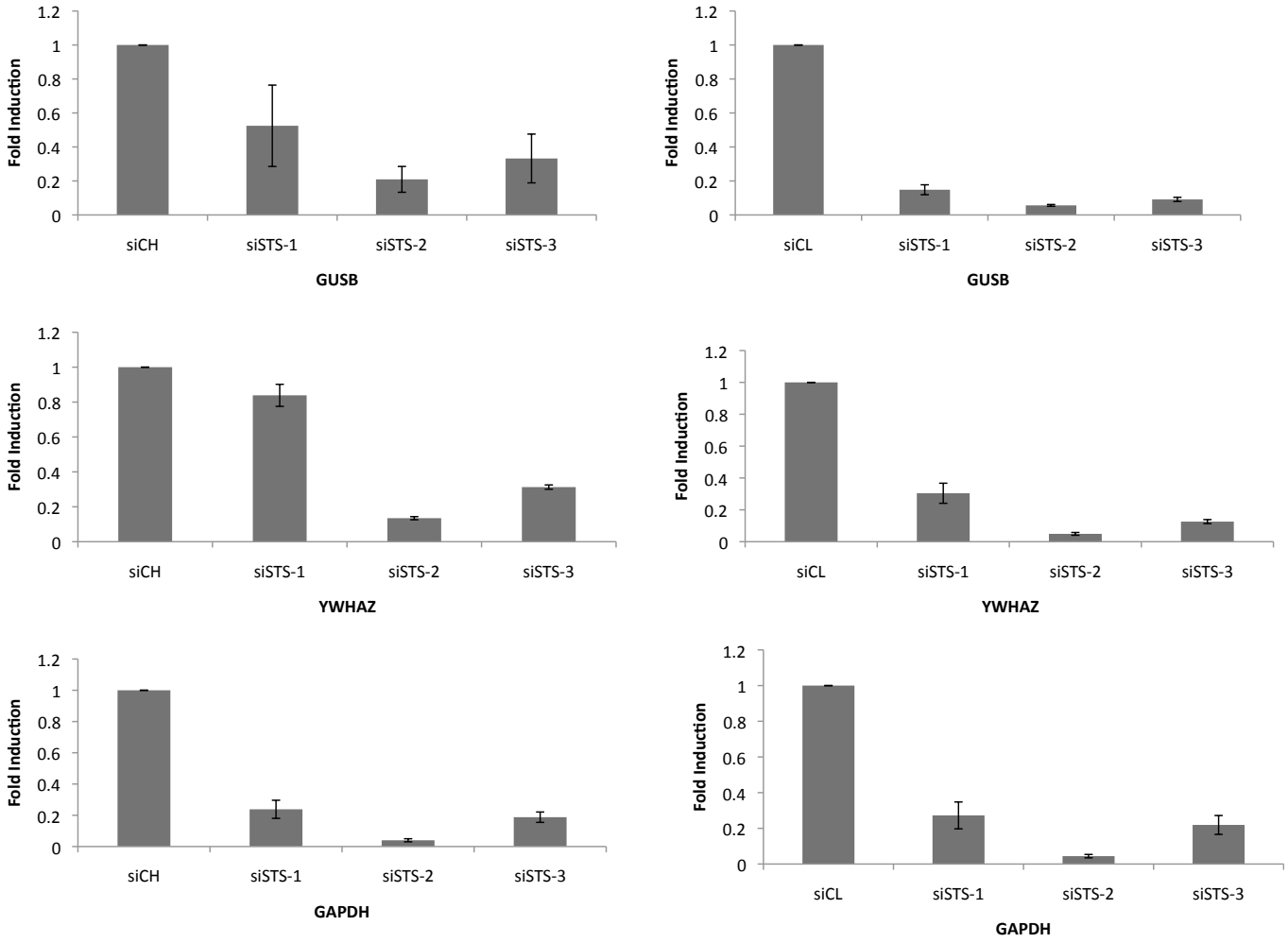

Figure 3.7: *STS* knockdown assessment following normalization with 3 different HKGs.
STS expression is consistent directionally with quantitative changes observed in *siSTS-1* compared to controls, siCH and siCL, following normalization with *GAPDH* (least stable HKG) when compared to *GUSB* and *YWHAZ* (n=3). Error bars represent mean ± standard deviation.

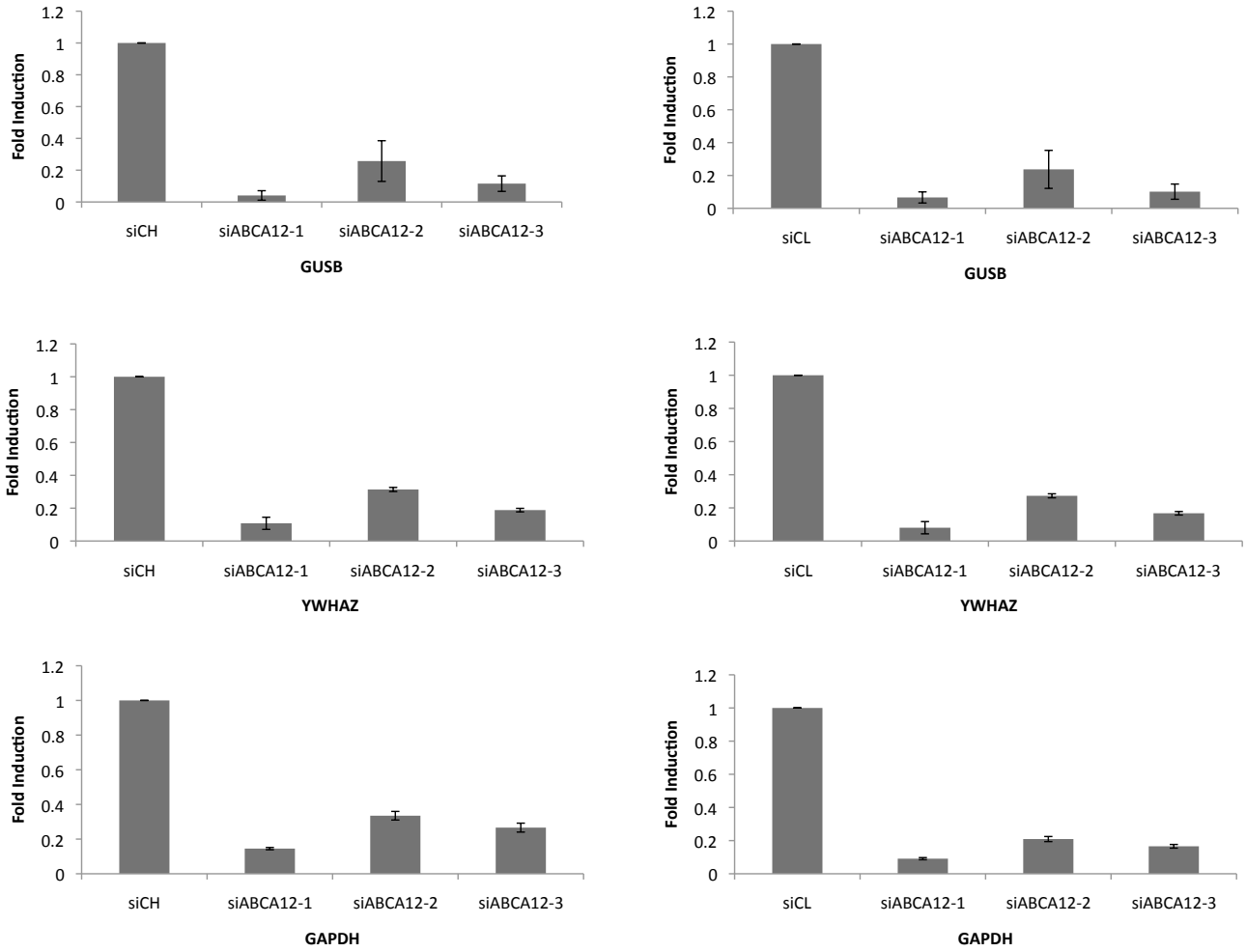

Figure 3.8: *ABCA12* knockdown assessment following normalization with 3 different HKGs.
ABCA12 expression is consistent directionally and quantitatively following normalization with all three HKGs (n=3). Error bars represent mean ± standard deviation.

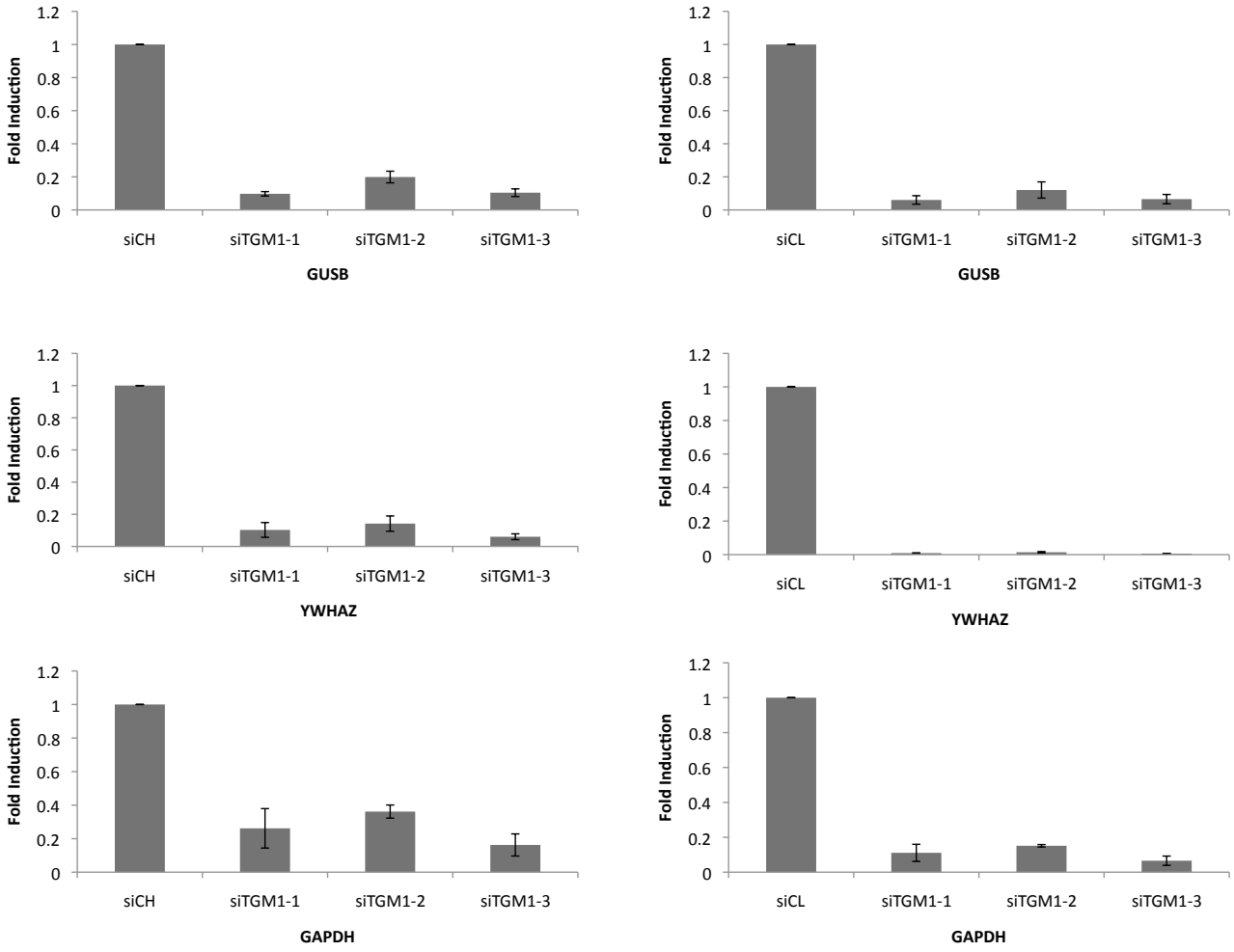

Figure 3.9: *TGM1* knockdown assessment following normalization with 3 different HKGs.
TGM1 expression is consistent directionally and quantitatively following normalization with all three HKGs (n=3). Error bars represent mean ± standard deviation.

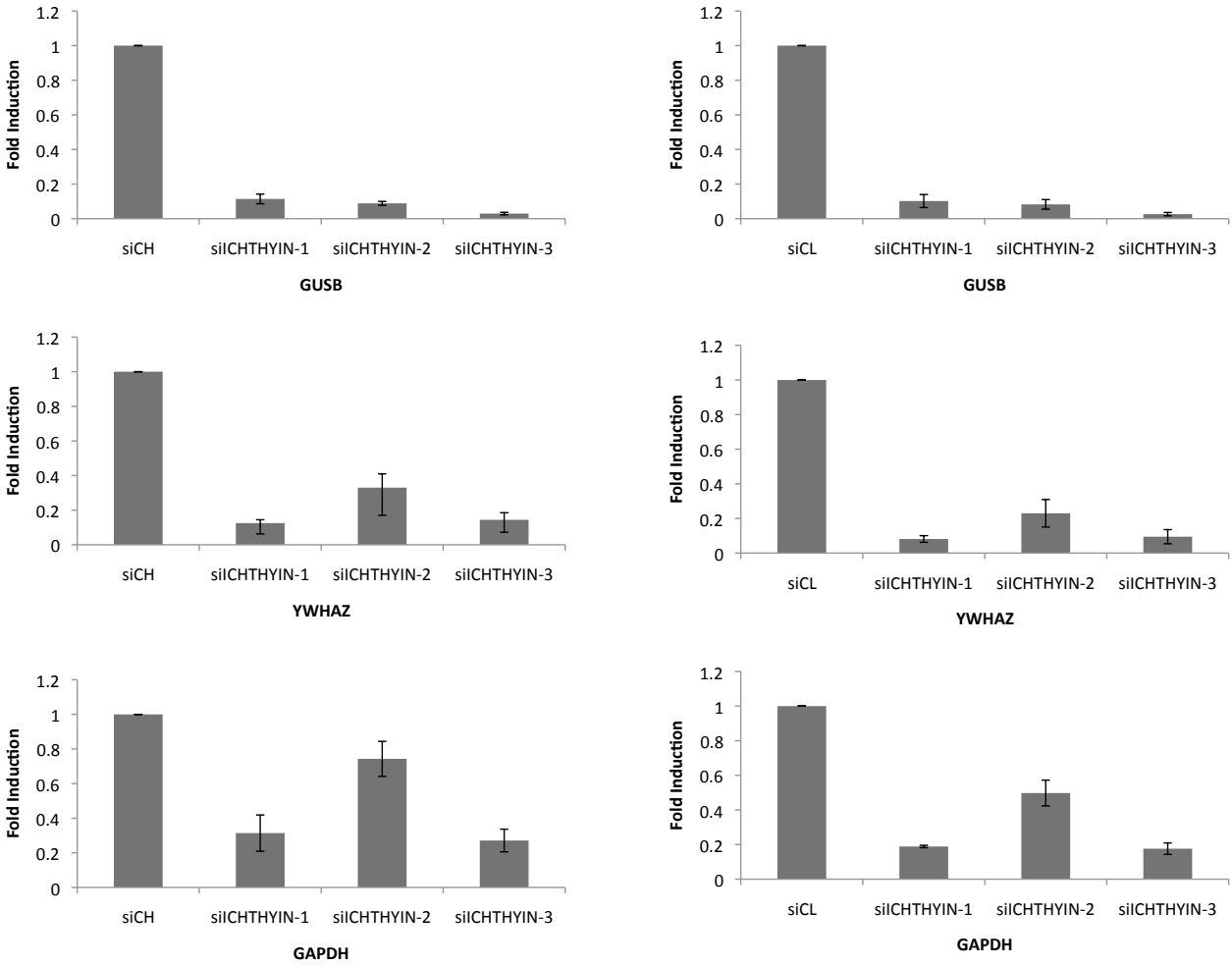

Figure 3.10: *ICH* knockdown assessment following normalization with 3 different HKGs.
ICH expression is consistent directionally with some quantitative changes observed with *GAPDH* (least stable HKG) when compared to *GUSB* and *YWHAZ*, following normalization with all three HKGs (n=3). Error bars represent mean ± standard deviation.

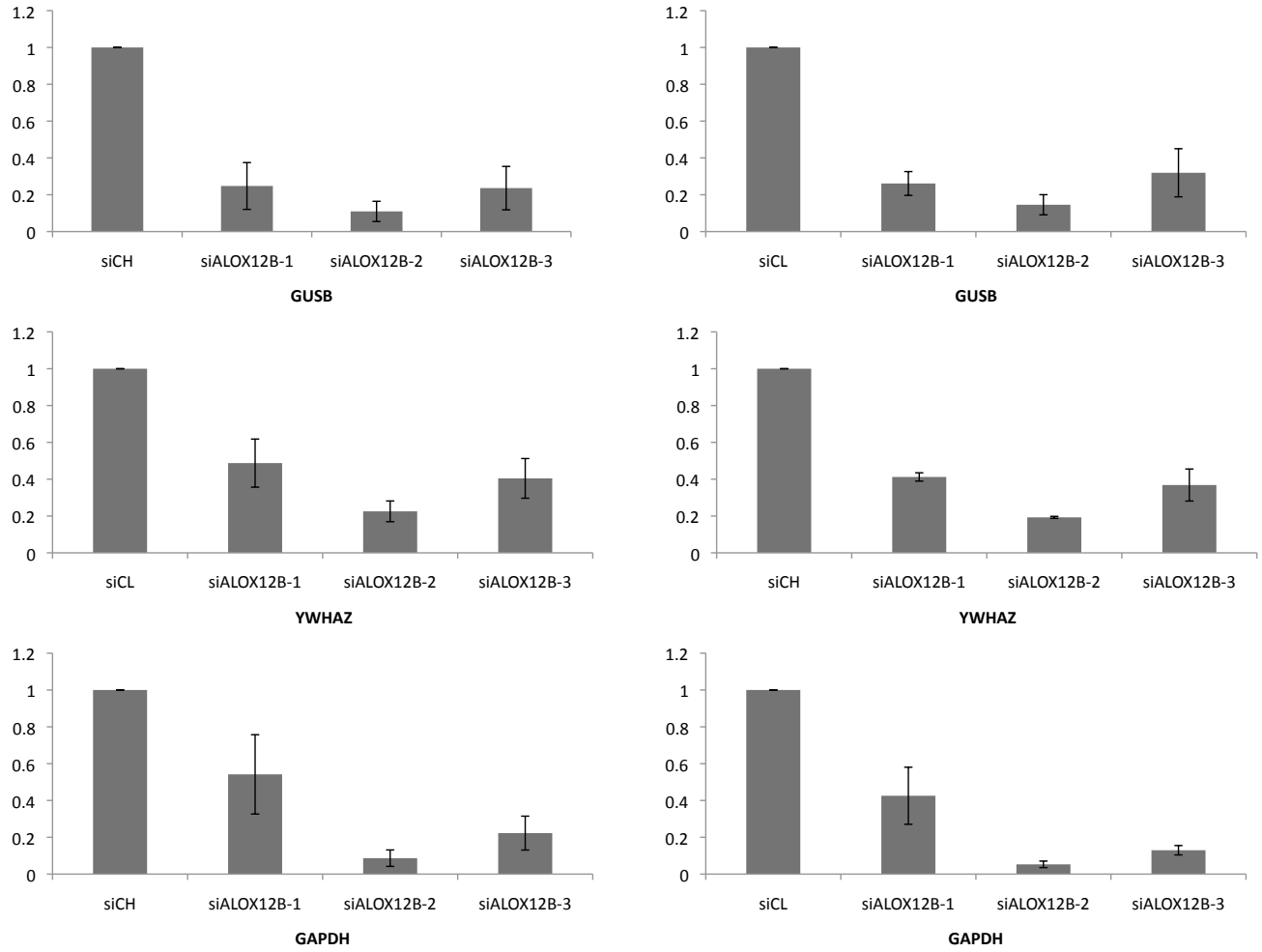

Figure 3.11: *ALOX12B* knockdown assessment following normalization with 3 different HKGs.
ALOX12B expression is consistent directionally with some quantitative changes observed, following normalization with all three HKGs (n=3). Error bars represent mean ± standard deviation.

In order to understand what impact reference gene selection might have on expression data of the genes of interest, the expression of siRNA transfected nHEKs was measured and normalized versus the most stable reference genes (*GUSB* and *YWHAZ*) and least stable reference gene (*GAPDH*) calculated by geNorm analysis. For all genes of interest all three HKGs showed directionally similar results i.e. reduced expression compared to control. Some quantitative differences were noted between the HKGs.

3.2.3 Establishing an experimental system for epithelial differentiation in monolayers

Mammalian epidermis displays a characteristic calcium gradient, in the non-linear gradient in human skin with a low concentration in the basal layer, the lowest concentration being in the supra-basal / early spinosum layers and with a marked increase in the late spinosum, granular and corneum layers (Leinonen et al., 2009). Calcium has been shown to be a major factor in controlling keratinocyte differentiation (Hennings et. al., 1980). *In vitro*, nHEKs can be selectively cultured and grown optimally in monolayers in media having a calcium concentration <0.1mM with protein markers characteristic of basal cells. Calcium addition (1.2mM or above) to cultures leads to inhibition of cell proliferation followed by induction of terminal differentiation characterized by a series of coordinated morphological changes such as formation of adherens junctions and desmosomes coupled with the increased expression of terminal differentiation markers such as involucrin (Micallef et al., 2009). Although *in vitro* results cannot be directly extrapolated to the *in vivo* situation (e.g. due to the impact of the dermis on the epidermis) much has been learned about calcium-regulated differentiation from *in vitro* studies, that is applicable to the *in vivo* epidermis (Bikle et. al., 2012).

3.2.3.1 Morphological changes shown in normal human keratinocytes cultured in high calcium media

nHEKs were plated at a density of $1.5x10^5$ and calcium switched as described in section 2.2.4. After 12 h, the cells were shifted to high calcium (1.3 mM) Epilife media and incubated for 24 h (section 2.2.5). Cells incubated in low calcium media for 24 h were kept as a control. Cell morphology was observed with brightfield microscopy. 24 hr post calcium switch, morphological changes such as cell-cell adhesion and stratification were noted in HC media due to calcium addition.

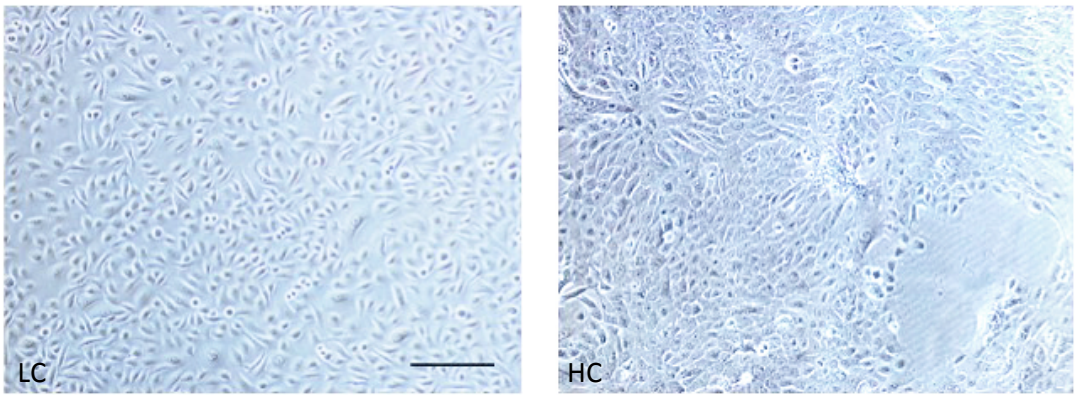

Figure 3.12: Morphological changes in normal human keratinocytes due to different calcium ion concentrations.
Morphological changes in nHEKs cultured in low calcium (LC) and high calcium (HC) medium for 24 hours shown by phase contrast microscopy (n=2). Scale bars represent 50 μm.

STS, FLG, ABCA12, TGM1, ICHTHYIN and ALOX12B expression are induced by calcium switch from LC to HC media in nHEKs. For all qPCR experiments, results are shown comparing mRNA expression on days 1, 3, 5 and 7 following calcium switch to gene expression in cells grown in LC media indicated as baseline. The expression of all genes except *FLG* was elevated 24 h post calcium switching and was maintained for 7 days for *STS*, *ICHTHYIN, FLG AND ALOX12B* but not for *TGM1* and *ABCA12*. However gene expression was upregulated during days 3 and 5 for all genes of interest. All genes had sufficient baseline expression in LC on day 1 to serve as controls. Further gene expression knock-down experiments using siRNA with this model were performed on day 3.

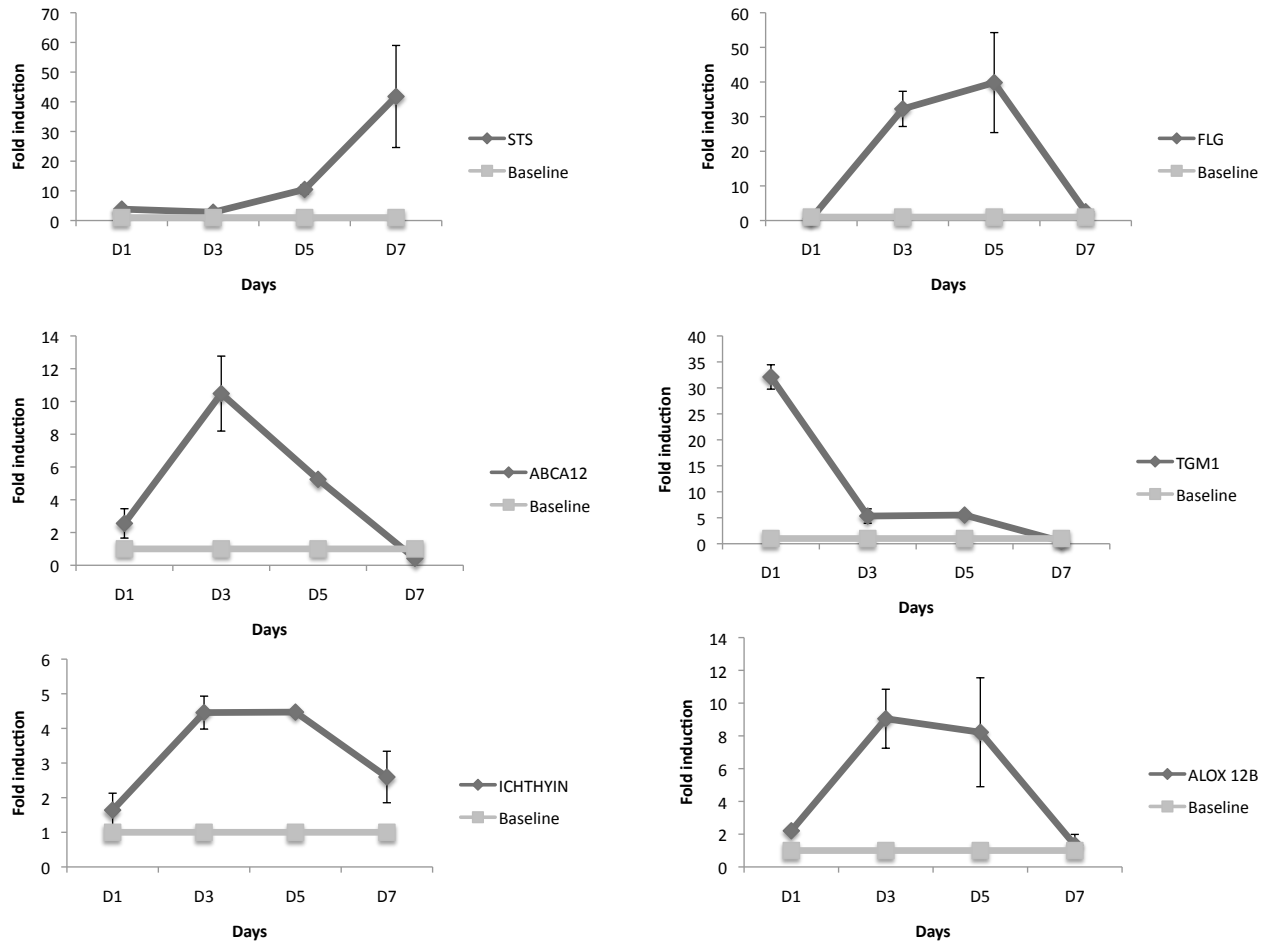

Figure 3.13: qPCR of *STS, FLG, ABCA12, TGM1, ICHTHYIN and ALOX12B* gene expression over 7 days in nHEKs cultured in high Ca media compared to low Ca media. Analysis by qPCR of the *STS, FLG, ABCA12, TGM1, ICHTHYIN and ALOX12B* mRNA expression in nHEKs in low (0.06 mM) set at fold induction 1 to serve as baseline or high (1.3 mM) extracellular calcium concentrations during 7 days. For each gene, mRNA levels were normalized with a house keeping gene, as described previously (n=3). Error bars represent mean ± standard deviation.

3.2.3.2 Comparison of expression of *STS, FLG, ABCA12, TGM1, ICHTHYIN* and *ALOX12B* in low and high Ca media following transfection with siRNA 2 days post-transfection

nHEKs were plated at a density of $1.5x10^5$ per well in incubated in low calcium (0.06 mM) Epilife (Cascade Biologics, UK) medium a 6-well plate, and incubated at 37°C/5% CO2. After 24 h, nHEKs were transfected with siRNAs for *STS, FLG, ABCA12, TGM1, ICHTHYIN and ALOX12B* and the non-targeting control, as described previously. After 12 h, the cells were shifted to high calcium (1.3 mM) Epilife media and incubated for 24 h. Additionally, transfected cells for each gene were incubated in low calcium media for 24 h and kept as a control. Optimal suppression with siRNA targeting all genes of interest was achieved 2 days post-transfection (Figure 3.15).

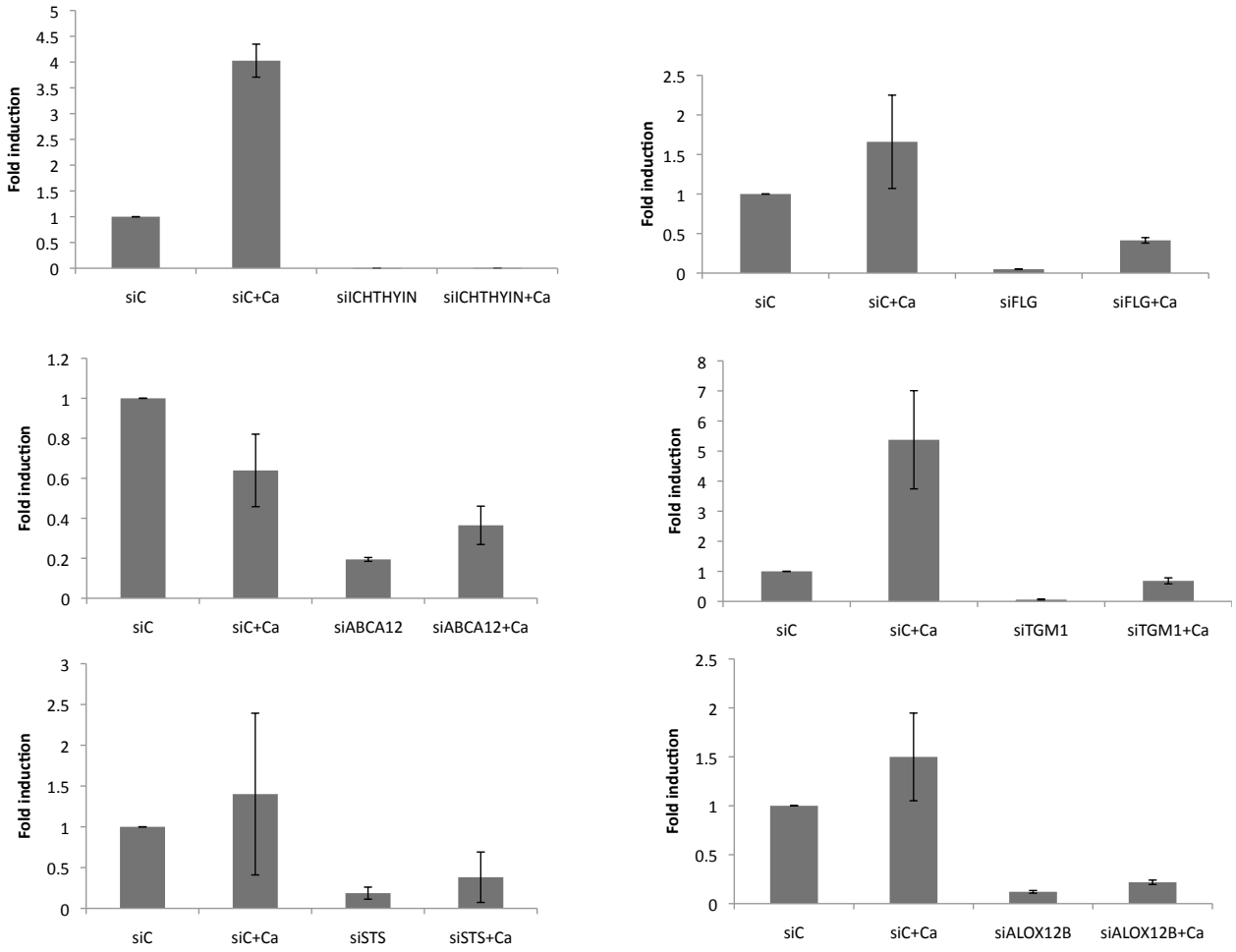

Figure 3.14: qPCR showing optimal suppression with siRNA targeting all genes of interest in low and high Ca media 2 days post-transfection.
Transfection with siRNA targeting *STS, FLG, ABCA12, TGM1, ICHTHYIN and ALOX12B* respectively in low and high Ca media 2 days post-transfection. Optimal suppression with siRNA targeting all genes of interest was achieved (n=3). Error bars represent mean ± standard deviation.

3.2.3.3 Time-course analysis of *STS, FLG, ABCA12, TGM1, ICHTHYIN and ALOX12B* down-regulation

The degree of *STS, FLG, ABCA12, TGM1, ICHTHYIN and ALOX12B* down-regulation in nHEKs after transfection with the siRNA targeting the gene of interest and after induction of differentiation by calcium switching as described was assessed for 8 days. Cells were harvested at day 2 and 8 post-transfection and *STS, FLG, ABCA12, TGM1, ICHTHYIN and ALOX12B* expression analysed by qPCR. There was significant down-regulation of expression of all genes on day 2 but this was maintained significantly for *STS, FLG, ABCA12* only by day 8 (Figure 3.16) suggesting that this is a good monolayer model for all 6 knockdowns on day 2 but not day 8.

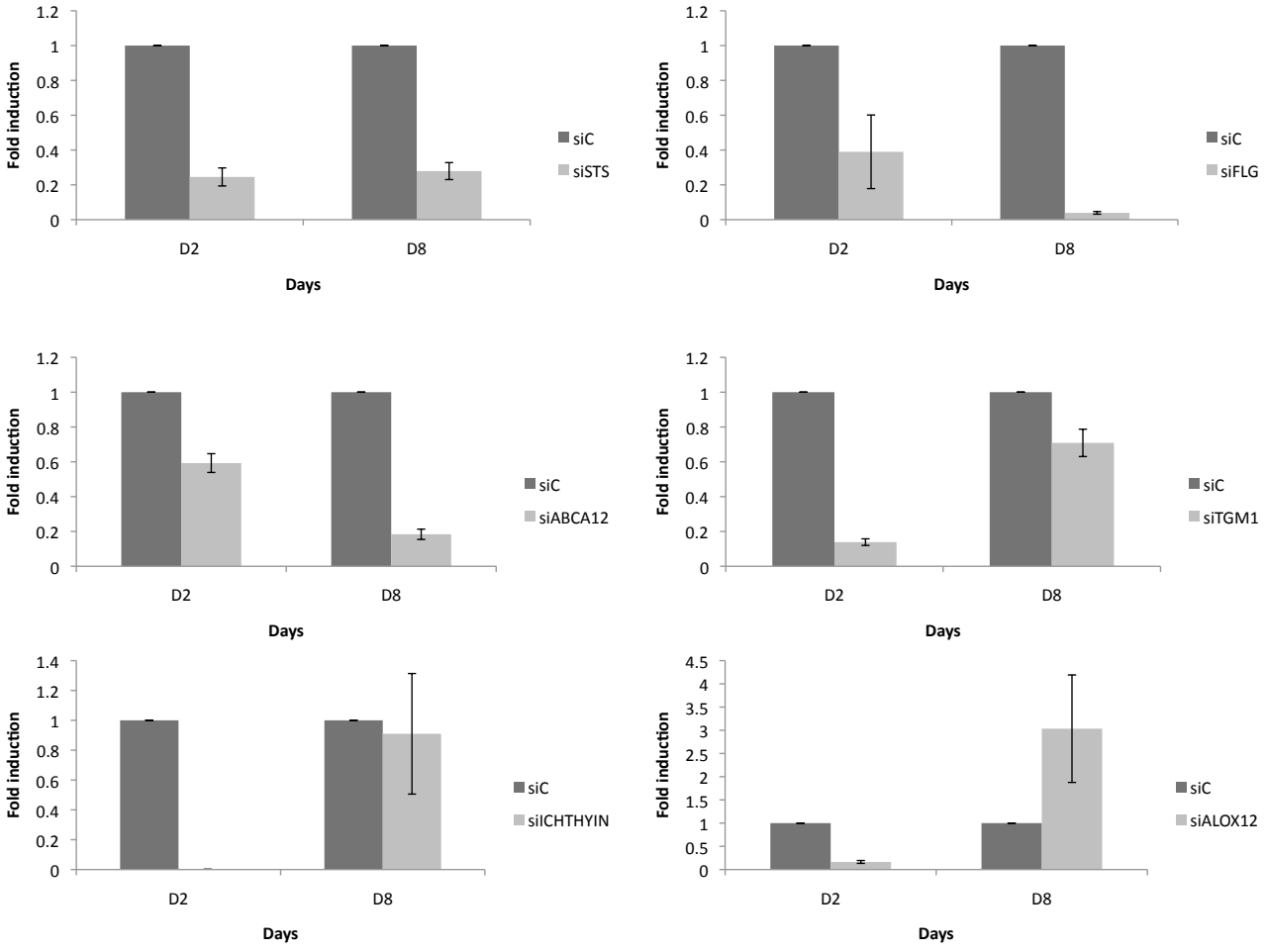

Figure 3.15: qPCR showing expression of *STS, FLG, ABCA12, TGM1, ICHTHYIN and ALOX12B* in nHEKs posttransfectiona over a period of 8 days following calcium switch.
Time course of mRNA expression of *STS, FLG, ABCA12, TGM1, ICHTHYIN and ALOX12B* at day 2 (D2), and 8 (D8) after siRNAs transfection into nHEKs following calcium switch 1 day post-transfection (n=3). Error bars represent mean ± standard deviation.

3.2.3.4 Optimal knock-down of *STS, FLG, ABCA12, TGM1, ICHTHYIN and ALOX12B* 4 days post transfection in differentiated nHEKs

The degree of *STS, FLG, ABCA12, TGM1, ICHTHYIN and ALOX12B* down-regulation in nHEKs 4 days post transfection (mRNA expression of all genes was upregulated Figure 3.13) was assessed in differentiated cells using three negative controls (non-targeting, mock and untreated) as described in section 2.3.5. For non-targeting control cells were transfected with non-targeting siRNA, for mock cells were cultured in media with transfection reagent and for untreated cells were cultured in culture media only. Cells were harvested in QIAzole lysis reagent and RNA extracted using miRNeasy Mini kit (Qiagen) from triplicated biological replicates. cDNA was made as previously and gene expression assessed by qPCR. Knock-down of *STS, FLG, ABCA12, TGM1, ICHTHYIN and ALOX12B* compared to each control used was noted (figure 3.17). RNA was sent to GSK for sequencing (section 2.3.5).

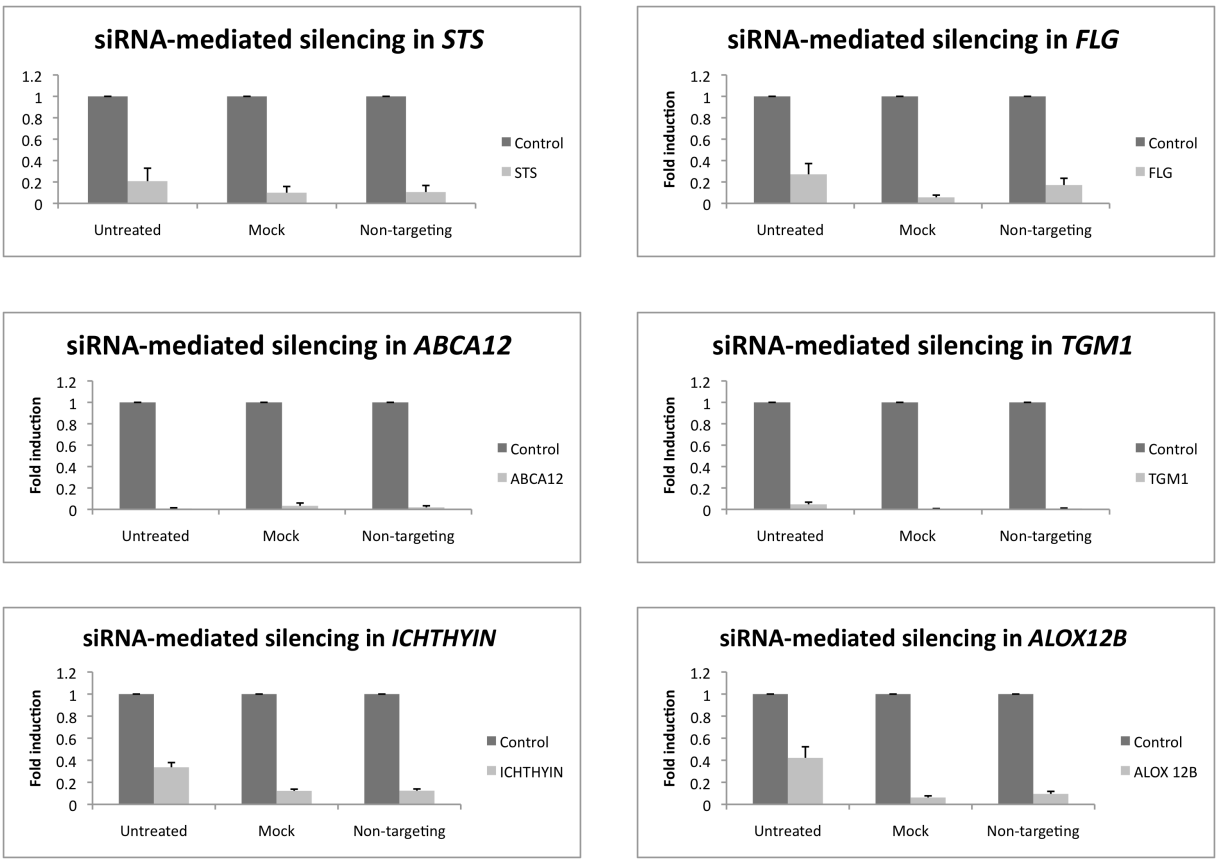

Figure 3.16: qPCR showing expression of *STS, FLG, ABCA12, TGM1, ICHTHYIN and ALOX12B* in nHEKs cultured in high calcium medium 4 days post transfection.
Analysis of siRNA mediated silencing in of *STS, FLG, ABCA12, TGM1, ICHTHYIN and ALOX12B* in nHEKs cultured in high calcium medium 4 days post transfection using three different controls, non-targeting, mock and untreated, (n=3). Error bars represent mean ± standard deviation.

3.2.4 Optimal knock-down of *STS, TGM1* and *ICHTHYIN* in HEKs 4 days post transfection in differentiated nHEKs leads to loss of protein confirmed by western blotting

Significant knock-down of *STS, TGM1 and ICHTHYIN* in HEKs 4 days post transfection in differentiated cells (differentiation induced the day following transfection as previously described) was confirmed at protein level by Western blotting.

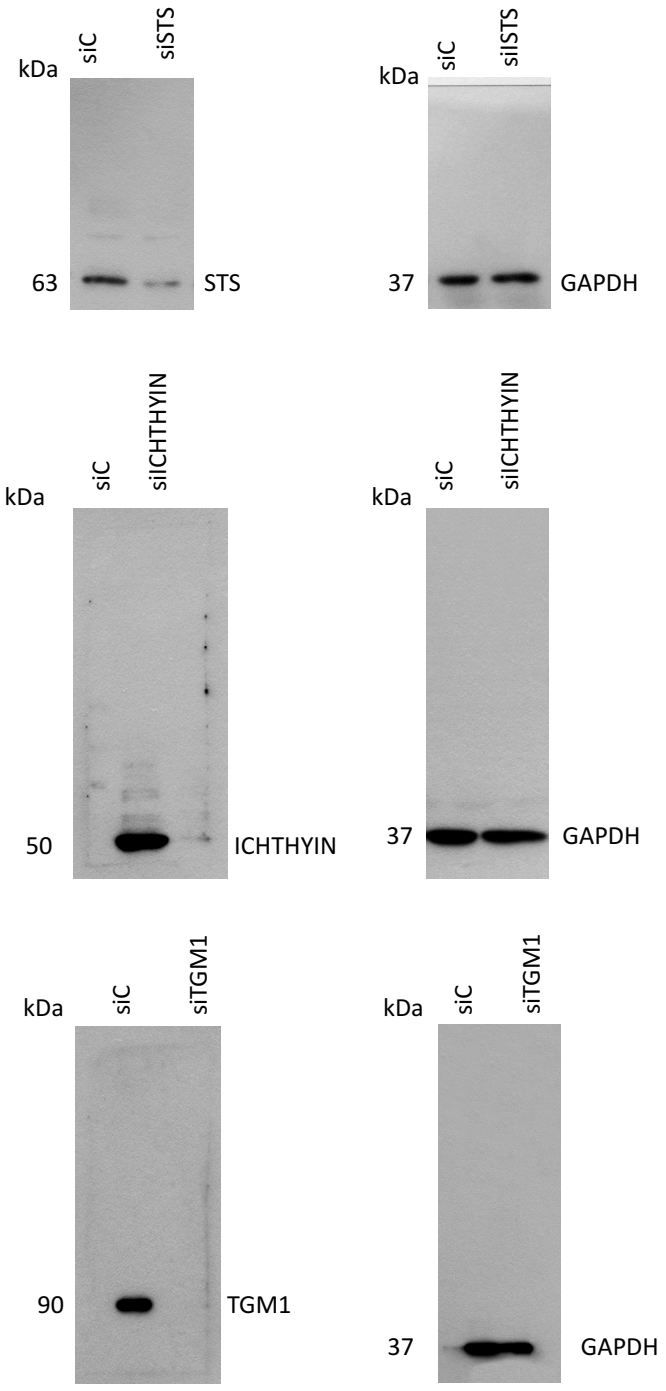

Figure 3.17: Western blot analysis showing siRNA-mediated silencing of STS, Ichthyin and TGM1.
Representative Western blots of 3 biological repeats. Separate blots for knockdown and HKG shown because following transfer the membrane was cut in two for immunoblotting.

3.3 Discussion

In this chapter *in vitro* disease models for the non-syndromic ichthyoses by knockdown of *STS, FLG, ABCA12, TGM1, ICHTHYIN* and *ALOX12B* in normal keratinocytes derived from neonatal foreskin were developed. Primary keratinocytes were selected as a model because they are more physiologically relevant to keratinocytes *in vivo* than a cell line (Pan et al., 2009). However, as they have a limited passage capability siRNA was used to induce a transient knockdown (rather than stable knockdown where intracellular expression of siRNAs is induced). This enabled analysis of the effect of knockdown in keratinocytes with the same genetic background.

The efficiency of transfection was optimised for the primary keratinocytes as low transfection efficiency usually results in lower levels of gene knock-down. This happens because mRNA expression from untransfected cells will contribute to the total observed mRNA level. Optimal transfection reagent volume (HiPerFect-15 µl) with highest efficiency of siRNA delivery with least impact on cell viability and optimal cell plating density (150,000 cells/well on collagen I coated plate) were determined. Three custom made siRNAs targeting different regions in the mRNA for the gene of interest. Demonstration of the siRNAs′ specificity by providing the appropriate controls is crucial (Hüttenhofer et al., 2003). Two different non-targeting controls, a high and low GC negative control, designated CH and CL respectively, were used. Each siRNA sequence for each gene of interest down-regulated gene expression at the mRNA level detected 2 days after transfection. The most effective siRNA sequence for each gene was used in subsequent experiments. Since the GC content of siRNA used for subsequent experiments was between 36-52% a low GC negative control was used as advised by the manufacturer.

For RNAi to be a useful tool in gene knock-down experiments, it is critical that siRNA-mediated silencing is specific i.e. limited to the specific knock-down of the target gene.

Down-regulation of unintended gene targets, i.e. off-target effects, is a result of non-specific silencing and can be a consequence of siRNA methods. Sequence independent off-target effects can result from high siRNA concentration introduction as this can displace endogenous miRNAs from RISC (Khan et al., 2009). The lowest concentration of siRNA (5-25nM) for each gene of interest that would allow gene silencing without compromising knockdown efficiency nHEK cells was evaluated.

For qPCR to yield meaningful results, it is necessary to normalise expression of the gene of interest to a stably expressed endogenous control (Bustin et. al.; 2005, Huggett et.al.; 2005). The stability of gene expression for 6 candidate HKGs (*GAPDH, B2M, RPLOPO, TBP, YWHAZ* and *GUSB*) was analyzed using Genorm analysis and further by qPCR for the 2 most stable genes *GUSB* and *YWHAZ* and the commonly used *GAPDH*. The overall findings supported the choice of *GUSB* as HKG to study gene suppression in siRNA transfected nHEKs by qPCR and hence it was used as HKG for this project.

The ichthyosis genes play a role in terminal differentiation and the genes of interest in this study are expressed late in differentiation. Induction of genes in monolayer cultures was achieved by switching low calcium media to high calcium media. Gene expression was upregulated during days 3 and 5. All genes had sufficient baseline expression in LC on day 1 to serve as controls. In one study, a 3 day calcium switch lead to induction of *TGM1* but, in contrast to our study, not in *FLG* and induction of *FLG in vitro* was attributed to increased cell confluency (Borowiec et al., 2013). These differences may be explained by different cell culture conditions (serum and cell confluency). Use of a negative control (cells cultured in low calcium media) in this study confirms that gene induction was due to calcium switching in this project. It has been suggested that calcium switch is a potent model for inducing

calcium- dependent genes but not for studying differentiation of *in vitro* keratinocytes (Borowiec et al., 2013). In this study, induction of all genes of interest was noted at transcriptome level following calcium switch. Confirmation of gene induction at protein level to allow for post-translational modifications would allow further validation of this model. To assess whether the experimental conditions in this project serves as an appropriate model for keratinocyte differentiation other genes involved in differentiation e.g. genes involved in induction of the ER stress response (Sugiura et al., 2009) can be assessed at transcriptome and/or protein level.

Following calcium switch optimal suppression with siRNA targeting all genes of interest was achieved on day 3 (confirmed using three different controls). The silencing potential of the siRNAs targeting the ichthyosis genes was maintained for 8 days for *STS, FLG, ABCA12* but not for the other genes. Knockdown was confirmed at protein level for *STS, TGM1 and ICHTHYIN* by Western blotting on day 3. Further gene expression knock-down experiments using this model were performed at this time point.

In summary, a model to study transient knockdown of genes expressed in late differentiation in monolayer cultures was developed. By optimizing transfection conditions (including calcium switching) and by using the appropriate controls a highly reproducible protocol for consistent, efficient and specific knock-down in *STS, FLG, ABCA12, TGM1, ICHTHYIN and ALOX12B* nHEKs was established at transcriptome level and confirmed at protein level for *STS, TGM1 and ICHTHYIN* by Western blotting. This paves the way for further experiments where the specific effect of *STS, FLG, ABCA12, TGM1, ICHTHYIN and ALOX12B* loss on nHEKs can be determined.

3.4 Further work

The limitation of siRNA as a method for protein knockdown is that the knockdown is transient; therefore it is desirable to generate a stable knockdown so that long-term experiments can be carried out. For example, although the effects of siRNAs are sustained for longer in organotypic skin model than in monolayers (Mildner et.al.; 2006) longer lasting experiments could be performed. For this a keratinocyte cell line such as N/TERT-1 would be appropriate because it was shown that normal keratinocyte differentiation was maintained after immortalisation (Dickson et al., 2000). To produce a stable induction of RNAi, endogenous expression of short-hairpin RNAs (shRNAs) by expression plasmids or viral vectors is commonly used (Paddison et al., 2002, Stegmeier et al., 2005). shRNAs are processed by Dicer to produce siRNAs. Upon binding to the cell the viral genome is transported into the cytoplasm where it undergoes reverse transcription into DNA. The DNA is then integrated into the host genome, allowing the shRNA to be constitutively expressed. Additionally keratinocytes from ichthyosis patients with known mutations could be used.

Chapter 4: Characterisation of 3D Organotypic Cultures of Keratinocytes Following Knockdown of Ichthyosis Genes

4.1 Introduction

Organotypic culture is a form of three-dimensional tissue culture where cultured cells are used to reconstruct a tissue or organ *in vitro* the objective being to allow the cells to exhibit as many properties of the original organ as possible. Three-dimensional organotypics (3D organotypics) are superior to monolayers of keratinocytes because they preserve the physiological 3D architecture of the skin, with cell proliferation occurring in the basal layers and cell differentiation towards the surface. Gene silencing by means of RNA interference (RNAi) is a powerful tool for gene function analyses *in vitro*. The combination of RNA interference technology and human organotypic skin cultures is an efficient method to study gene functions in epidermal development (Mildner et al., 2006, Kuchler et al., 2011, Vavrova et al., 2014, (O'Shaughnessy et al., 2010).

The skin consists of a stratified cellular epidermis composed mainly of keratinocytes and an underlying dermis composed predominantly of fibroblasts in a collagen-rich stroma. Full thickness skin models contain both epidermal and dermal compartments. The best *in vitro* model that best mimics normal skin are organotypic cultures of keratinocytes on a fibroblast populated scaffold where a SC is formed indicating terminal differentiation and complete barrier formation. Terminal differentiation of keratinocytes can be induced by culturing keratinocytes at an air/liquid interface resulting in a multilayer stratified tissue modelling normal skin. The keratinocytes used for epidermis formation can vary in that either keratinocyte cell lines or primary keratinocytes can be used. In addition, there are a number of possible dermal materials/scaffolds that can be used for organotypic cultures of skin such as de-epidermalised dermis, type I collagen gels (Boelsma et al., 1999), and collagen and Matrigel mixtures (Sobral et al., 2007).

In vitro skin models (using siRNA in primary keratinocytes using dermal scaffolds) provide a way of mimicking monogenic skin disorders. This is advantageous in that it allows the gene specific effects to be evaluated without other possibly contributing factors. However it does not mimic *in vivo* skin and lacks other epidermal cells-melanocytes, Langerhans cells, Merkel cells. Additionally the amount and composition of SC lipids in *in vitro* models varies from that of skin (Vavrova et al., 2014). Furthermore, the dermal scaffolds do not represent the vascularized dermis, including circulating immune cells, and appendageal structures such as hair follicles and sweat glands. Additionally, the underlying subcutaneous layer is not represented.

For this study, fibroblasts were cultured in de-epidermalised dermis for two weeks prior to seeding primary keratinocytes. Primary keratinocytes were grown at the air/liquid interface for 10 days.

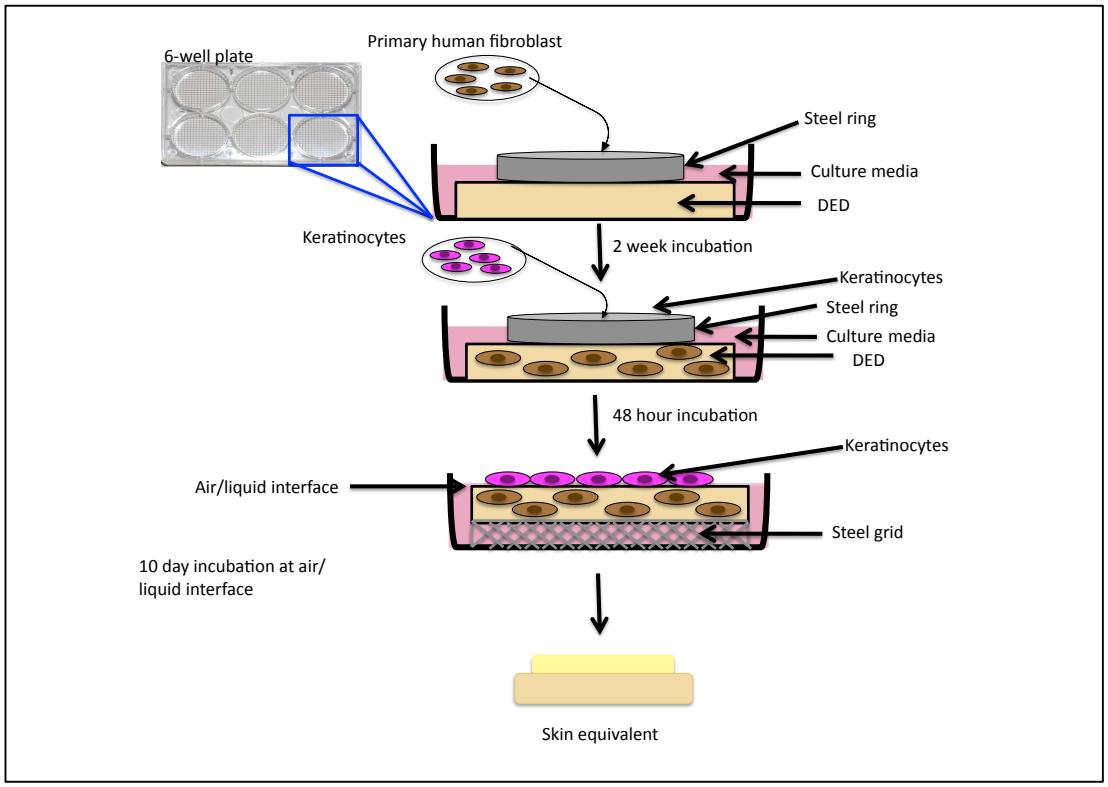

Figure 4.1: Organotypic culture of primary keratinocytes on fibroblast populated de-epidermalised dermis grown at the air/liquid interface (10 days) on a steel grid.

4.1.1 Development of skin models to study the ichthyoses *in vitro*

In recent decades a number of murine models have been developed for the ichthyoses. The flaky-tail mouse, which lacks processed murine filaggrin because of a frameshift mutation in the gene encoding profilaggrin, has impaired barrier function (Presland et al., 2000, Fallon et al., 2009). However this mouse model has another recessive hair mutation, *matted* and it was found that the latter gene, rather than filaggrin, causes development of spontaneous development of AD with increased IgE levels (Sasaki et al., 2014, Sasaki et al., 2013). Subsequently, the $FLG^{-/-}$ mouse model was generated. These mice have dry skin, enhanced percutaneous allergen priming but do not develop spontaneous dermatitis under specific pathogen-free conditions (Kawasaki et al., 2012). Thus, it has been suggested that the flaky tail mouse is not a true model of filaggrin deficiency and all of the previous work on these models needs to be re-evaluated (Moniaga et al., 2010, Moniaga and Kabashima, 2011, Oyoshi et al., 2009, Scharschmidt et al., 2009, Moniaga et al., 2013).

Skin from the 12R-LOX mice transplanted onto wild-type nude mice develops an ichthyosiform phenotype (de Juanes et al., 2009). Mice knockouts for *ABCA12* have been described as having a post-natal lethal phenotype with skin resembling that of newborn HI skin (Smyth et al., 2008, Yanagi et al., 2008). The expression of *ABCA12* in normal foetal skin development and the grafting of HI keratinocytes on immunodeficient mice have also been described (Yamanaka et al., 2007). Mice knockouts for *TGM1* do not recapitulate the human skin phenotype and die within the first hours of life (Matsuki *et al*., 1998). A TGM1 deficient skin-humanized mouse model for LI has been reported (Aufenvenne et al., 2012).

In vivo models of the skin such as murine animals provide a 3D model however interspecies transferability of the results and ethical issues remain a problem. Reconstructed human

epidermis serve as effective models for the study of skin disorders. *In vitro* human *FLG* (Mildner et al., 2010), *ALOX12B*, *ALOXE3*, *TGM1*, *ICH/NIPAL4*, *ABCA12* (Thomas et al., 2009, Eckl et al., 2011) models using siRNA in primary human keratinocytes and a rat *in vitro* model (O'Shaughnessy et al., 2010) have been described. These have not been fully characterized. No 3D *in vitro* models for *STS* or ichthyin are known.

Skin models to study the ichthyoses were developed using siRNA transfected primary keratinocytes and harvested 10 days post transfection.

4.1.2 Aim

The aim of this chapter was to study the role of the ichthyosis genes (*FLG, STS, TGM1, ALOX12B, NIPAL4,* and *ABCA12*) in epidermal differentiation and maturation of the epidermal barrier by establishing (and characterizing) full-thickness human skin models for the common ichthyosis and the autosomal recessive congenital ichthyosis. Organotypic cultures were generated using primary keratinocytes with knockdown of *FLG, STS, TGM1, ALOX12B, ICH,* and *ABCA12* using siRNA. The effect on epidermal differentiation was investigated in these cultures compared to control.

4.2 Results

4.2.1 Haematoxylin and Eosin staining of ichthyoses organotypic culture following ichthyosis protein knock-down using de-epidermalised dermis

Organotypic cultures on a fibroblast populated de-epidermalised dermis were generated with primary keratinocytes with knockdown of the ichthyosis genes: *STS, FLG, TGM1, ALOX12B, ICH,* and *ABCA12* (siSTS, siFLG, siABCA12, siTGM1, siALOX12B, siICH). A non-targeting siRNA was used as a control (siC). Figure 4.2 shows H&E staining of siSTS, siFLG,

siABCA12, siTGM1, siALOX12B, siICH and siC organotypic cultures. A multi-layered fully differentiated epidermis was observed in all cultures. The *stratum corneum* was present confirming that the keratinocytes have successfully undergone terminal differentiation. The nucleated epidermis of the ichthyosis gene knock-downs were thicker (i.e. more acanthotic) as well as the SC (i.e. compact hyperkeratosis) compared to the control suggesting that the ichthyosis knock-downs have an influence on keratinocyte differentiation and SC development.

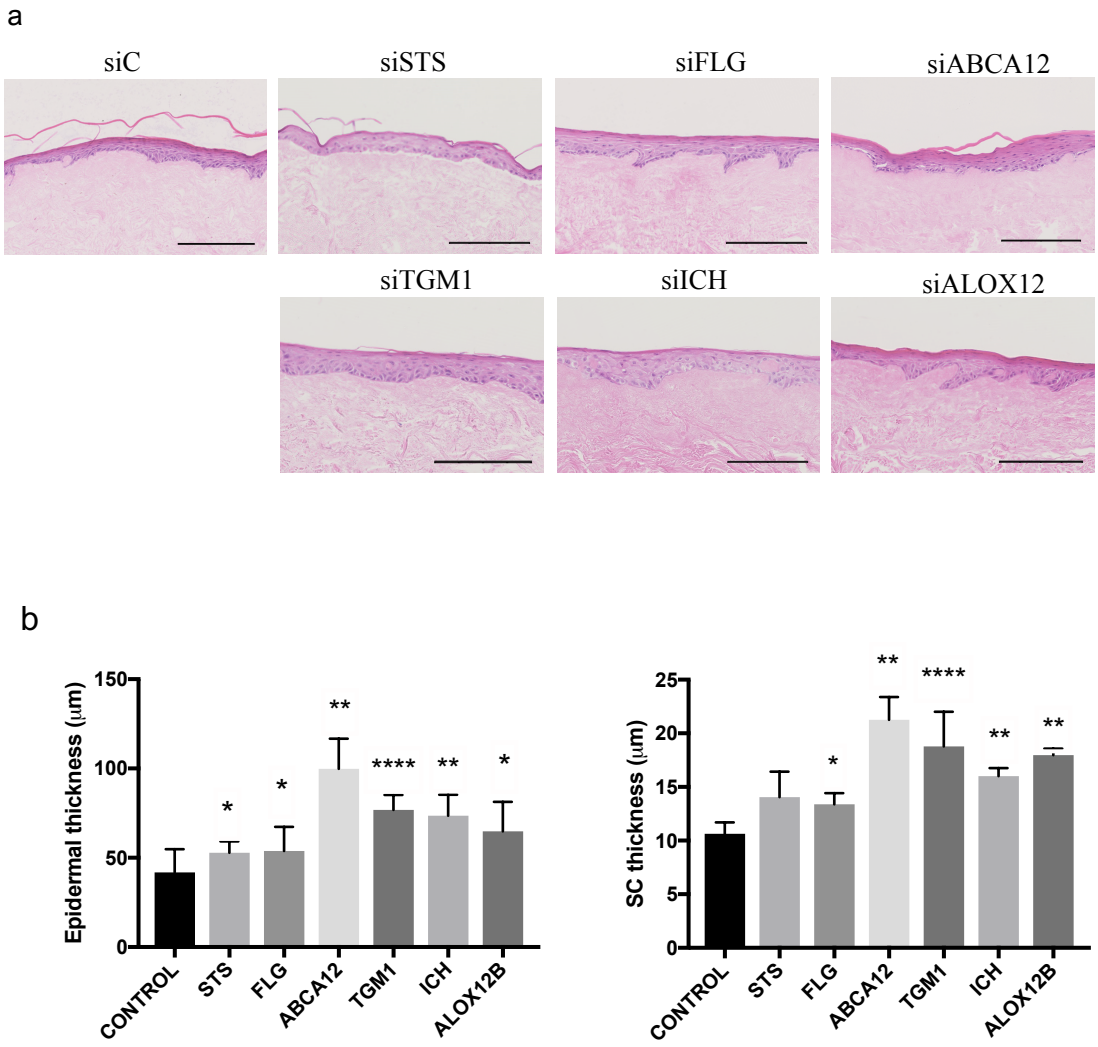

Figure 4.2: Organotypic cultures of primary keratinocytes following ichthyosis gene knockdown.
(a) Haematoxylin and eosin staining of 3D organotypic cultures on a fibroblast populated de-epidermalised dermis were generated with primary keratinocytes with knockdown of the ichthyosis genes: *STS* (siSTS), *FLG* (siFLG), *TGM1 (*siTGM1), *ALOX12B (*siALOX12B), *ICH* (siICH), and *ABCA12* (siABCA12). Non-targeting siRNA was used as a control (siC). Sections were stained with haematoxylin, which stains the cell nucleus purple, and eosin, which stains the cytoplasm pink. Scale bars represent 200μm (b) Graphs showing epidermal and stratum corneum (SC) thickness (* $P < 0.05$, ** $P < 0.01$, **** $P < 0.0001$).

4.2.2 Ichthyosis protein expression in primary keratinocyte organotypic cultures

Due to the transient nature of siRNA knockdown it was important to confirm knockdown was still present in organotypic cultures of primary keratinocytes. There was efficient knockdown of FLG as measured by IF staining (Figure 4.3) and of TGM1, ICH and ABCA12 as measured by IHC (Figure 4.4-4.6 respectively).

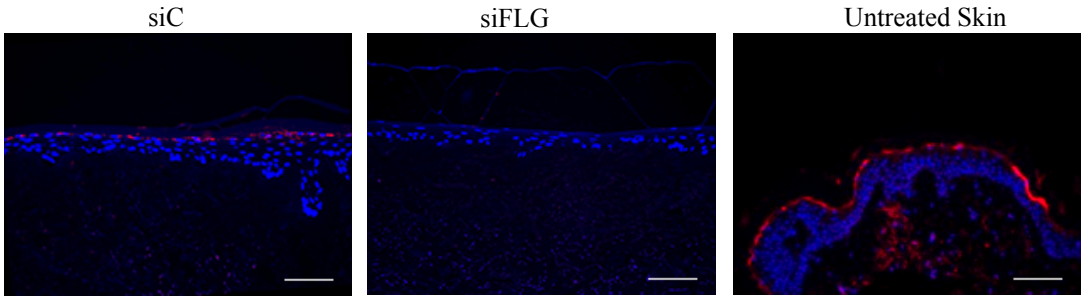

Figure 4.3: IF staining of Filaggrin (red) in siC, siFLG organotypic cultures and skin sections.
IF staining of Filaggrin (red) in siC, siFLG organotypic culture and skin sections. DAPI (blue) was used as a nuclear stain. Scale bars represent 100μm in siC and siFLG and 200 μm in Untreated Skin panels.

In normal skin filaggrin staining was observed in the SG and SC, as expected. In siC organotypics, filaggrin expression was observed in the upper layer of the epidermis. However, this was absent in the siFLG cultures in keeping with complete knockdown of filaggrin protein.

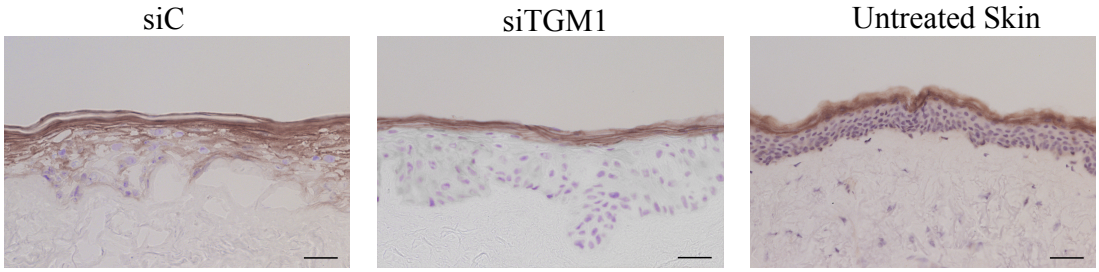

Figure 4.4: IHC staining of TGM1 in siC, siTGM organotypic cultures and skin sections using DAB.
IHC staining of TGM1 in siC, siTGM organotypic cultures and skin sections. DAPI was used as a nuclear stain. Scale bars represent 100μm in siC and siTGM1 and 200 μm in Untreated Skin panels.
.

The TGM1 protein is expressed primarily in the SC in normal skin. In siC it is expressed throughout the entire epidermis but primarily in the SC, SG and upper SS. In the *TGM1* knockdown TGM1 expression is limited to the SC only.

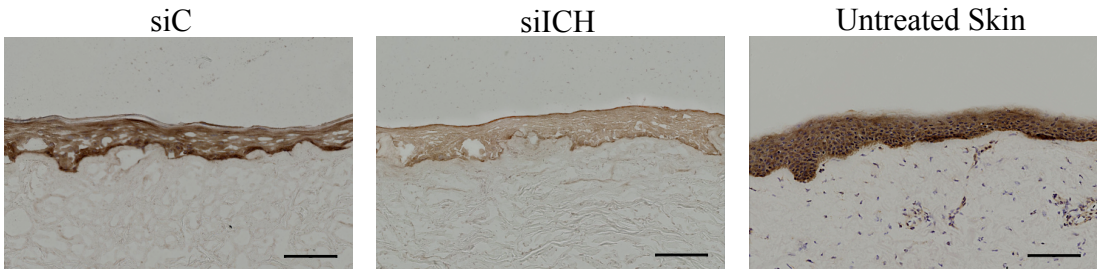

Figure 4.5: IHC staining of Ichthyin in siC, siICH organotypic cultures and skin sections using DAB. IHC staining of Ichthyin in IHC staining of Ichthyin in siC, siICH organotypic cultures and skin sections. DAPI was used as a nuclear stain. Scale bars represent 200 μm.

Expression of Ichthyin was examined by IHC. Ichthyin is expressed throughout the viable and non-viable epidermis in normal skin and siC. In the *ICH* knockdown reduced expression is noted throughout the epidermis.

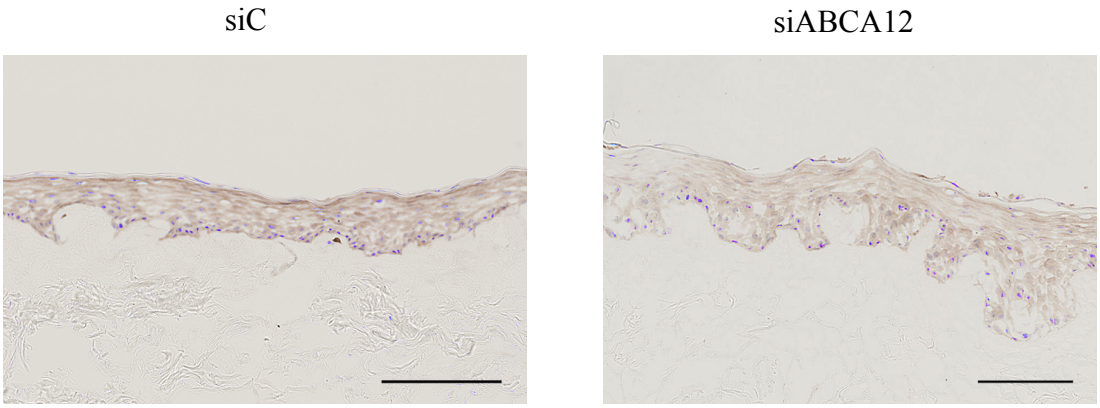

Figure 4.6: IHC staining of ABCA12 in siC, siABCA12 organotypic cultures and skin sections using DAB. IHC staining of ABCA12 in siC, siABCA12 organotypic cultures and skin sections. DAPI was used as a nuclear stain. Scale bars represent 200 μm.

IHC demonstrated *ABCA12* was expressed throughout the epidermis with apparent increased expression in the upper epidermis. This could be an edge artefact, but is in keeping with staining pattern in normal skin (Thomas et al., 2009). In the *ABCA12* knockdown reduced staining is noted throughout the epidermis.

4.2.3 Further characterisation of organotypic cultures 4.2.3.1 Characterization of *FLG* organotypic culture

To further characterize *FLG* 3D model loricrin (LOR) and keratin10 (K10)-late and early differentiation markers respectively-were used. Furthermore, IF staining was done using

keratin14 (K14) to evaluate changes in the SB. LOR was expressed in the SC in normal skin and siC. There was loss of expression of LOR following *FLG* silencing. K10 is expressed in the suprabasal layers of the epidermis and a typical staining pattern is shown in siC and normal skin sections. There is reduced expression of K10 in siFLG. K14 expression is most evident in the basal layer as seen in normal skin. There is increased expression of K14 in siC and siFLG and it is seen in the suprabasal layers compared to normal skin. Suprabasal K14 has been noted previously in 3D epidermal models (Lamb and Ambler, 2013).

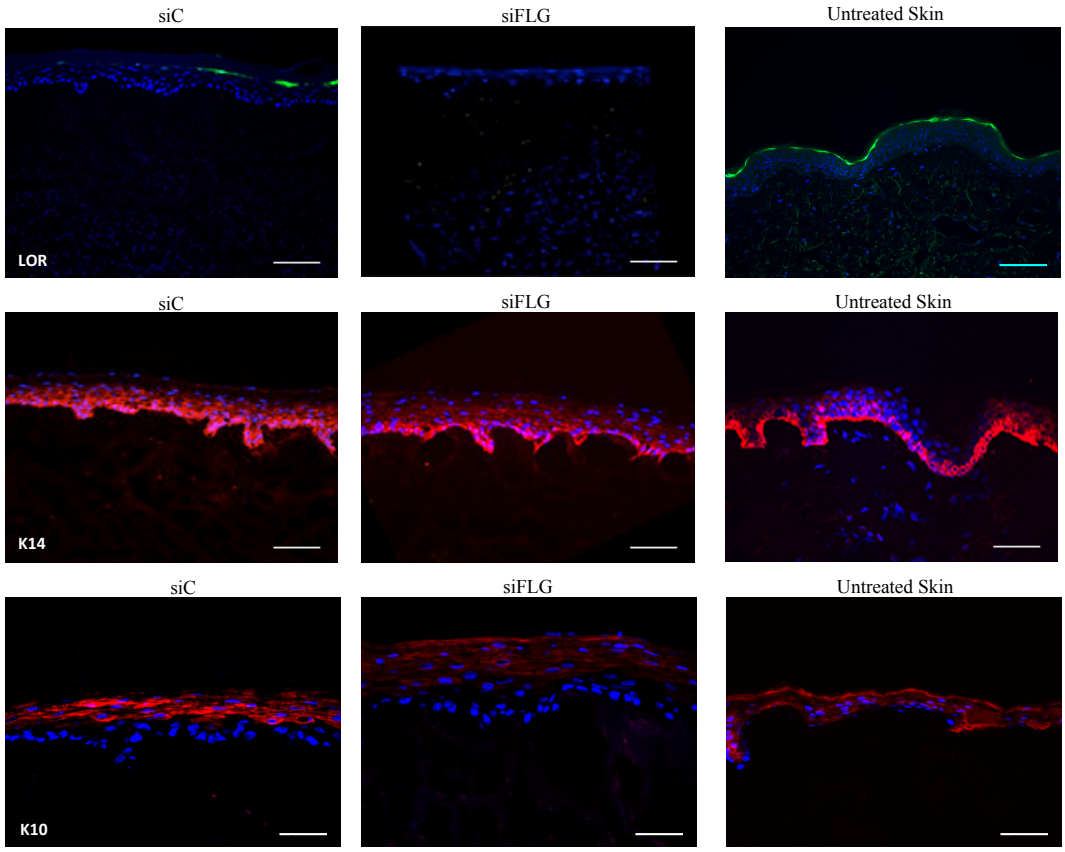

Figure 4.7: IF staining of the epidermal differentiation marker LOR, K10 and K14 in siC, siFLG and normal skin.
IF staining of LOR (green) and K14 (red) and K10 (red) in siC, siFLG and skin. DAPI (blue) was used as a nuclear stain. Scale bars represent 100μm.

4.2.3.2 Characterization of *ABCA12* knockdown organotypic culture

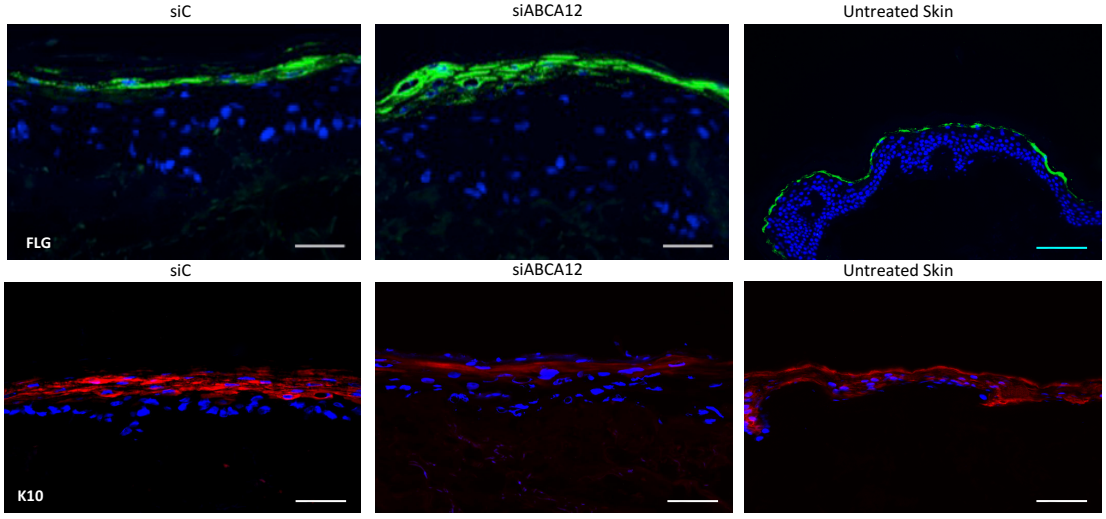

Figure 4.8: IF staining of filaggrin and K10 in siC, siABCA12 and skin sections.
IF staining of the terminal differentiation marker FLG (green) and early differentiation marker K10 (red) in siC, siABCA12 and normal skin. DAPI (blue) was used as a nuclear stain. Scale bars represent 100μm.

To further characterize the siABCA12 organotypic culture filaggrin a late differentiation marker and K10 expression were evaluated. There was expression of filaggrin in the SG in siC and siFLG but also in the SS in the latter lending support to premature termination differentiation in an *ABCA12* knockdown (immortalized cell) model (Thomas et al., 2009). Early differentiation marker K10 is expressed in the suprabasal layers of the epidermis as seen in siC and normal skin sections. K10 expression is limited to the upper spinous layer in siABCA12.

4.2.4 Epidermal differentiation of ichthyoses organotypic cultures

The localization TGM1 in normal skin was assessed by IHC (fig.4.4) and was primarily in the SC. On comparison to siC TGM1 expression was altered in the remaining ichthyoses knockdowns suggesting dysregulation of terminal differentiation (Figure 4.9); there was reduced expression of TGM1 in *TGM1* knockdown as expected but also in the *STS* and *ICH* knockdowns. In siFLG, siALOX12B and siABCA12 there was increased expression in the SS; increased expression was noted in the upper SS the lower SS in siFLG and siABCA12

suggesting premature terminal differentiation in these disease models. This was most striking in siABCA12 which is representative of the most severe ichthyosis phenotype.

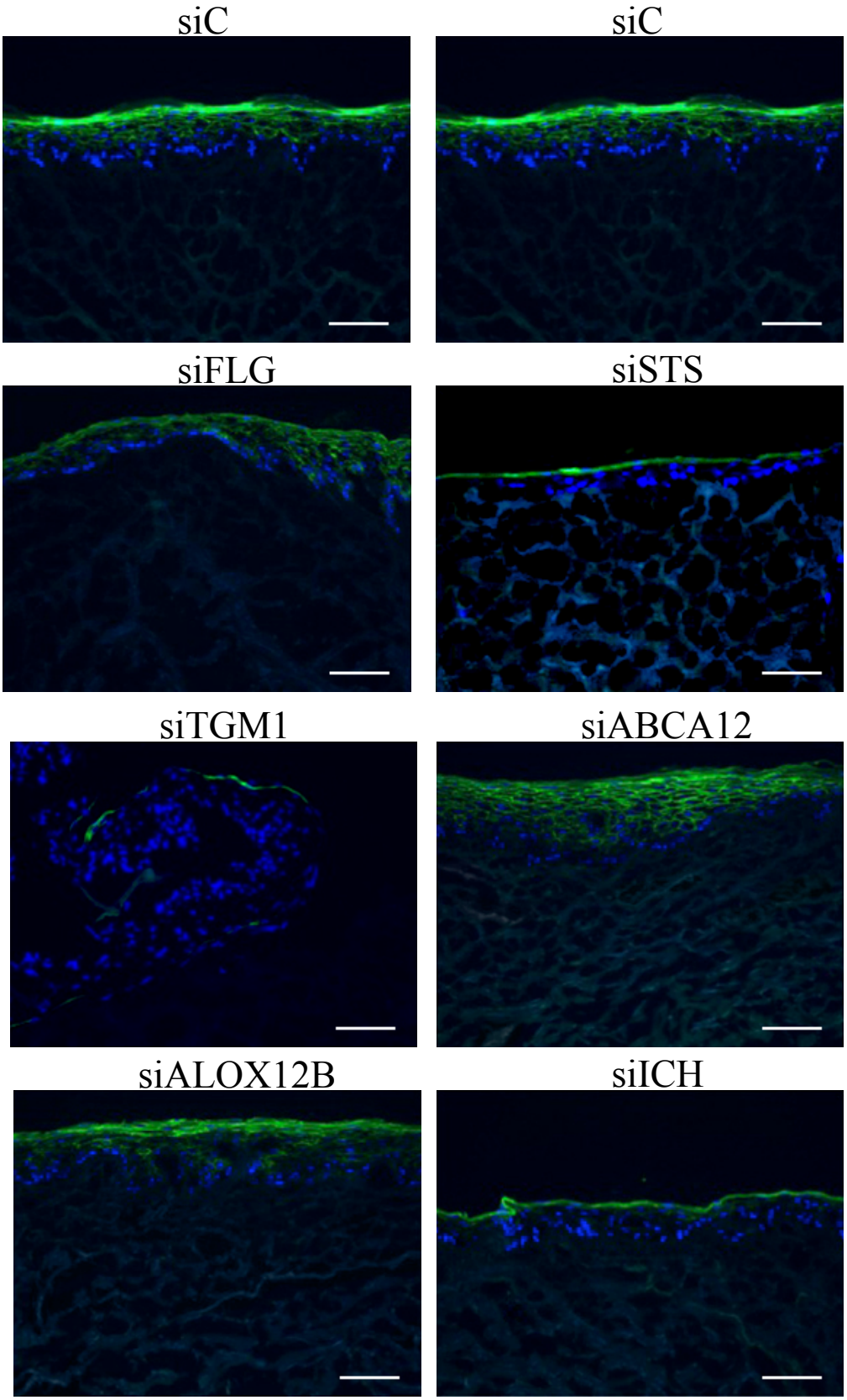

Figure 4.9: IF staining of the epidermal differentiation marker TGM1 in siC, siSTS, siFLG, siABCA12, siTGM1, siALOX12B and siICH organotypic cultures.
IF staining of TGM1 (green) in siC, siSTS, siFLG, siABCA12, siTGM1, siICH and siALOX12B organotypic cultures. DAPI (blue) was used as a nuclear stain. Scale bars represent 100μm.

4.3 Discussion

In this study, *in vitro* human skin models were generated for the common ichthyoses and the autosomal recessive congenital ichthyoses. Organotypic cultures were generated using primary keratinocytes with knockdown of *FLG, STS, TGM1, ALOX12B, ICH/NIPAL4,* and *ABCA12* using siRNA on a de-epidermalised dermis. Full thickness epidermis was generated for each organotypic culture and loss of protein assessed (where possible) by IHC or IF. Further characterization by staining with differentiation markers was undertaken to assess the effect of knockdown on epidermal differentiation.

Novel ichthyosis *in vitro* disease models for *STS* and *ICH* knockdowns were developed. H&E staining in the *STS* knockdown demonstrated a fully differentiated epidermal compartment with all viable layers and SC. The SC appeared more compact and thicker (compact hyperkeratosis) and the viable layers slightly thicker (slight acanthosis) than that of control as noted *in vivo* (Calonje et al.; 2012). Immunofluorescent staining did not reveal any changes compared to control or normal skin. For the *ICH* knockdown compact hyperkeratosis, nuclei in the SC (parakeratosis) and acanthosis were noted on H&E staining. *ICH* mutations lead to LI/NCIE phenotypes and several of the observed histological features in the generated model have been noted in affected patients; hyperkeratosis, moderate acanthosis and parakeratosis in NCIE phenotype and orthohyperkeratosis, moderate acanthosis, normal or reduced granular layer and mild irregular undulation of the epidermal surface (papillomatosis) are seen in lamellar phenotype (Fischer et al., 2007). The loss of the target protein following knockdown was further demonstrated by IHC analysis of diseased skin compared to normal skin equivalent. However, the staining pattern noted throughout the epidermis may not be representative of Ichthyin expression but may be non-specific due to the polyclonal antibody used; polyclonal antibodies target multiple epitopes of the same antigen and are less specific

than monoclonal antibodies that recognize one epitope of an antigen only. IHC with another antibody would verify these findings.

In addition to the novel models generated, *in vitro* cultures were established for the remaining ichthyoses using primary keratinocytes (neonatal) from the same genetic background i.e. same donor. In the *FLG* knockdown H&E staining demonstrated, a fully differentiated epidermal compartment with all viable layers and SC. Morphology of the SC did not appear to be compromised. The impact of *FLG* knock down on filaggrin protein expression in the skin construct was verified by IF. Immunofluorescence labeling of filaggrin in the granular layers of control organotypic and normal skin was seen. Notable reduction of fluorescence staining intensity in *FLG* knock down in comparison to normal control was noted most likely due to loss of keratohyalin granules in the granular layer. Further characterization revealed loss of *LOR* and reduced expression of *TGM1* confirming that it affects terminal differentiation and leads to disturbed maturation of the epidermis in contrast to previous studies (Mildner et al., 2010). These differences are most likely due to the shorter cultivation period of seven days; it is thought that the influence of filaggrin deficiency on epidermal maturation does not become visible until cultivation periods exceed one week in duration (Kuchler et al., 2011). No changes were noted on IF staining with K14 (expressed in the basal layer) confirming that it does not impact on the SB as shown in previous studies (Mildner et al., 2010). IHC of three-dimensional organotypic cultures expressing siRNA to *ALOX12B* showed reduced expression of *ALOX12B* throughout the epidermis compared to complete loss of *ALOX12B* protein noted by IF in another reported model reflecting the differences in technique used-IHC being more sensitive than IF (Eckl et al., 2011). *TGM1* knockdown displayed compact hyperkeratosis and acanthosis. IF and IHC staining showed a reduction in *TGM1* staining in the viable epidermis compared to C and skin. This is in keeping with another *TGM1 in vitro* model

using primary keratinocytes (Eckl et al., 2011). A HI model using primary keratinocytes was generated in this study; This bears out several features related to epidermal differentiation noted in HI skin; hyperkeratosis and acanthosis were noted. Furthermore nuclei were seen in the SC (parakeratosis) and there was irregular undulation of the epidermal surface (papillomatosis). Protein knockdown was confirmed by IHC. Terminal differentiation was altered in the HI model with increased expression of both TGM1 and filaggrin in the viable epidermis compared to control suggesting premature terminal differentiation as noted previously in HI skin (Thomas et al., 2009); filaggrin expression was in keeping with HI skin and involved the upper spinous layers adding further support to the previously reported error in filaggrin processing in HI skin (Thomas et al., 2009). TGM1 expression was limited to the suprabasal layers rather than the entire epidermis as seen in HI skin and NEB1 organotypic model in another study (Thomas et al., 2009). This may be because of the different antibodies used in the two studies. In addition, there was a reduction of K10 expression implying altered early differentiation in HI.

Assessment of terminal differentiation of all disease models (from the same genetic background) generated in this study was undertaken to evaluate comparative changes in terminal differentiation by IF staining of TGM1. All the ichthyosis knockdowns impact on TGM1 expression suggesting dysregulation of terminal differentiation. Transglutaminase 1 (TGM1) is an enzyme involved in the cross-linking of the components of the CE proteins (Candi et al., 2005). The CE functions as a platform for cross-linking organized lipid layers-which is essential for the barrier function of the skin (Lorand and Graham, 2003). Additionally, TGM1 contributes to the formation of the CLE by attachment of long-chain omega-hydroxyceramides to involucrin (Nemes et al., 1999). Thus, interactions between TGM1 and ALOX12B (involved in lipoxygenase pathway) and ICH (putative receptor for the

end products of this pathway) may be explained by perturbations in omega ceramide synthesis that compromises CLE formation and TGM1 expression. How these changes come about mechanistically in the remaining ichthyoses is unclear. This could result from impairment of barrier function leading to compensatory changes as observed in other barrier diseases, AD and psoriasis, where upregulation of TGM1 has been observed (de Koning et al., 2012).

In summary, all the ichthyosis knockdowns in this study impact on TGM1 and changes in *ABCA12* alter early differentiation in addition to terminal differentiation. In addition, in this study 3D *in vitro* cultures using primary keratinocytes for the ichthyosis of interest, from the same genetic background, were developed including a novel models (*STS* and *ICH* knockdown) in order to study the individual ichthyosis and make comparative assessments and evaluate impact on epidermal biology.

4.4 Future work

Further characterization of the ichthyosis models (other than for *FLG* knockdown) to assess changes in SB and SS can be undertaken by IF staining with K14 and K10 respectively (for *ABCA12* knockdown further K14 IF staining).

The ichthyoses are disorders of cornification and impair the skin barrier. To investigate functional barrier assessment a penetration assay using Lucifer yellow can be applied on fully differentiated organotypic skin cultures for the disease models and control. Lucifer yellow can be added on top of the organotypic cultures and its penetration measured, which is indicative of a functional SC (Mansbridge and Knapp, 1993). The cultures can be harvested 2 hours post application for permeation studies.

As lipid composition is crucial for epidermal barrier function alterations in the composition of total lipids by Nile Red analysis of lipids can be performed to compare the lipid profile between the knockdowns and control. Nile Red fluoresces green in the presence of nonpolar lipids (such as ceramides) and red in the presence of polar lipids (such as phospholipids and sphingomyelin) (Thomas et al., 2008). Furthermore lipids extracted from 3D organotypics (control and knockdowns) can be investigated using mass spectroscopy.

Organotypic cultures of skin are a model for the *in vivo* environment; therefore it is important to confirm that the phenotype observed due to ichthyosis knockdown is biologically relevant. Ichthyosis patient samples could be used to see if the above *in vitro* findings are also seen *in vivo*.

RNAi, leads to gene-specific silencing but can also lead to off-target effects. Rescue experiments remain the gold standard control to confirm the specificity, and hence the validity of RNAi data (Hüttenhofer et al., 2003). There are two main methods used (Cullen, 2006); if the siRNA used was designed to bind to a sequence in the mRNA open reading frame, then this resistance can be achieved by mutation of the mRNA, without changing the encoded protein, by taking advantage of the redundancy of the genetic code. Alternatively, the siRNA can be designed to target the 3′ untranslated region (UTR) of the mRNA, and rescue of expression can then be achieved by expressing a form of the mRNA lacking its normal 3′ UTR. Another acceptable approach is to show that two or three distinct siRNAs targeted to different regions of the mRNA exert the same phenotypic effect (Hüttenhofer et al., 2003).

Stable knock-down models can be used to investigate the role of the icthyosis genes in epidermal differentiation and barrier function by using primary keratinocytes with stable

knockdown. This can be achieved by lentiviral shRNA infection. Clustered regularly interspaced short palindromic repeats (CRISPR)/Cas9 system (CRISPR-CAS9) can be also be used for performing targeted editing to alter or knockout gene expression of the ichthyosis genes. This system requires a Cas nuclease and a single guide RNA (sgRNA) against the target sequence to function as a site-specific nuclease.

In this project, transcriptome analysis was undertaken on a 2D models. A more robust approach would be evaluation of the transcriptome using the epidermal component of the generated skin equivalents.

Chapter 5: *RNA-Seq* analysis of keratinocytes following ichthyosis genes knockdown

5.0 Introduction

RNA sequencing (*RNA-Seq*) is a powerful method for transcriptome analyses. The transcriptome is the complete set of transcripts in a cell, and their quantity, for a specific developmental stage or physiological condition. Understanding the transcriptome is essential for interpreting the functional elements of the genome and revealing the molecular constituents of cells and tissues, and also for understanding development and disease (Wang et al., 2009). Various technologies have been developed to deduce and quantify the transcriptome. The automated Sanger method is considered as a 'first-generation' technology and the newer methods, which include *RNA-Seq* (this supersedes the automated Sanger method), are referred to as next-generation sequencing (NGS) (Metzker, M.L., 2010). *RNA-Seq* generates huge amounts of data, which poses a challenge both for data storage and analysis, and consequently often necessitates the use of powerful computing facilities and efficient algorithms (Trapnell., 2012).

In this project, RNA (from triplicated biological replicates) was sent to GSK for sequencing. Analysis of the sequenced reads was performed in collaboration with the Enright group at European Bioinformatics Institute, Hinxton (http://www.ebi.ac.uk/research/enright) and differentially expressed gene (DEG) lists were provided. The DEGs were analysed further using DAVID, KEGG, REACTOME and GeneMANIA.

RNA was converted to a library of cDNA fragments and adaptors attached to one or both ends. Following amplification each molecule was sequenced in a high-throughput manner using the Illumina platform to obtain sequences from both ends i.e. pair-end sequencing (the alternative is single-end sequencing where sequences are from one end) with read length of 50bp (the reads are typically 30–400 bp). The reads were not strand specific.

RNA sequencing data was analysed using the pipeline as shown in Figure 5.1:

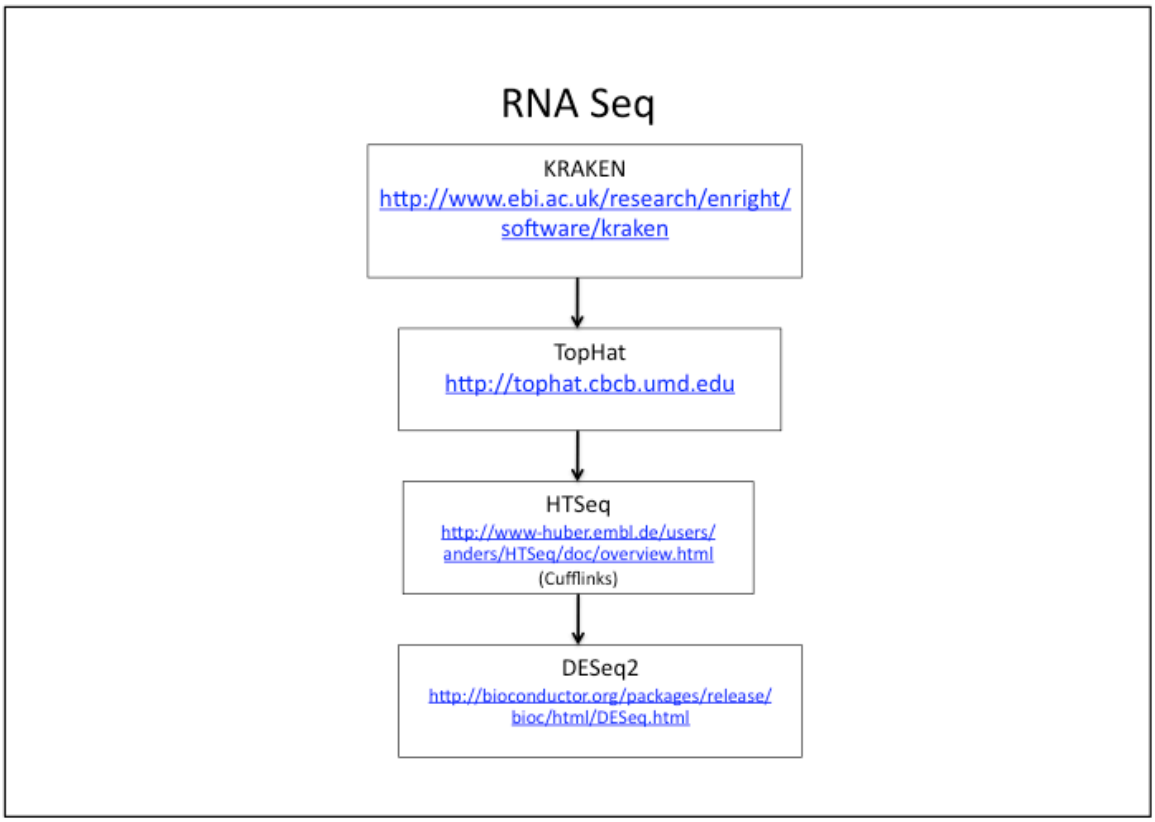

Figure 5.1: Summary of workflow.
Software used in the workflow and the main functions of each tool. All tools used are fully documented on the web and actively maintained by a team of developers.

KRAKEN (http://www.ebi.ac.uk/research/enright/software/kraken) pipeline, used for quality control, developed in the Enright lab was used to process the *RNA-Seq* data. It consists of 3 tools: Reaper, Tally and Minion. Reaper is a program for demultiplexing, trimming adapter sequences and filtering sequencing data. First, the Reaper command was used to trim the 3' adaptor sequences. The 3' adaptors were stripped using the criteria: 14-nt alignment stretch with no more than 2 mismatches and no gaps. Low complexity sequences were then removed with a dust score cut-off of 20. Complexity scores range from 0 to 100. Higher scores imply lower complexity. Then, Tally was used to reduce identical reads to a single entry while

keeping the depth values. A file with unique reads and their corresponding counts was generated for each sample.

The final processed unique paired-end reads were aligned to the reference human genome (GRCh37/hg19) with Tophat v2.0.4. TopHat2 aligns *RNA-Seq* reads to the genomes using the short read aligner BOWTIE, and then analyzes the mapping results to identify splice junctions between exons.

For transcript quantification, the number of reads mapped to transcripts (Homo_sapiens.GRCh37.74.gtf from Ensembl) were obtained from Tophat2 aligned sam files using the HTSeq-count command from the HTSeq library (http://wwwhuber.embl.de/users/anders/HTSeq/doc/). HTSeq was used to assemble individual transcripts from the reads. Longer transcripts produce more sequencing fragments than shorter transcripts. Therefore the read count to each transcript's length must be normalized and differential expression calculated using the Bioconductor DESeq2 package (http://www.bioconductor.org/packages/release/bioc/html/DESeq2.html). DeSeq2 calculates expression levels of transcripts from different conditions and tests the statistical significance of observed changes. Differential gene expression analysis was based on a negative binomial distribution.

Bioconductor provides tools for the analysis and comprehension of high-throughput genomic data. Bioconductor uses the R statistical programming language, and is open source and open development (http://bioconductor.org/packages/release/bioc/html/DESeq.html). For functional grouping of differentially expressed genes lists of the differentially expressed genes, DEGs, (upregulated and downregulated) were then analysed via two internet based bioinformatics resources Database for Annotation, Visualization and Integrated Discovery

DAVID (https://david.ncifcrf.gov) (Huang da et al., 2009) and REACTOME (http://www.reactome.org) (Fabregat et al., 2016). DAVID is a gene annotation tool that highlights biological processes and functions from list of DEGs. There are a number of annotation categories including protein-protein interactions, protein functional domains, disease associations, gene functional summaries, molecular events and functional annotation clustering. REACTOME is a open-source, curated and peer reviewed of human biological processes. The central unit of this data model is a *Reaction*, and subclasses of *Reaction* model these core biological events (Croft et al., 2014). Reactions are grouped into pathways, which in turn are assembled into a hierarchy of biological processes. This allows indication of whether there were interesting clusters of genes to investigate further as opposed to single genes that may be affected by the suppression of the ichthyosis gene of interest. Kyoto Encyclopedia of Genes and Genomes KEGG database (accessed through DAVID) was used to overlay the list of DEGs onto known signaling pathways. The number of components that are highlighted helps determine the extent by which certain pathways were affected. GeneMANIA (http://genemania.org) (Warde-Farley et al., 2010) performs biological network integration between a gene list and networks generated from available genomic and proteomic data. The list of DEGs was input into GeneMANIA to evaluate physical interactions, shared protein domains or identify DEGs that participate in the same pathway and also to predict functional relationships.

5.1.1 Aim

The overall aim of this chapter was to analyse the transcriptome of siRNA transfected keratinocytes in monolayer in order to identify differentially expressed genes in keratinocytes with knockdown of ichthyosis genes compared to control to evaluate the following:

1. To directly test the null hypothesis at the level of the transcriptome. If the null hypothesis is correct no commonality in gene expression profiles for the *in vitro* disease models will be

observed.

2. To identify key pathways or biological functions for each ichthyosis.

For this lists of DEGs following ichthyosis gene knockdown (*STS, FLG, TGM1, ICH, ALOX12B, ABCA12*) were subjected to analysis using DAVID, KEGG and REACTOME.

5.2 Results

5.2.1 Confirmation of knockdown of siRNA transfected primary keratinocytes by DESeq

For differential expression analysis knockdowns were compared to non-targeting controls for all 6 knockdowns *(STS, FLG, TGM1, ICH, ALOX12B, ABCA12)* using DESeq2 in the R/Bioconductor environment.

There was significant downregulation of all 6 knock-downs:

Table 5.1: Significant downregulation of the ichthyosis genes *STS, FLG, TGM1, ICH, ALOX12B, ABCA12*

Gene Name	log2 FoldChange	FDR <0.01
STS	-1.807514883	1.50E-23
FLG	-1.242284384	3.07E-08
ABCA12	-2.067862732	2.23E-146
TGM1	-2.287142185	2.41E-49
NIPAL4	-1.723383376	5.64E-48
ALOX12B	-1.090237652	2.07E-08

DESeq2 generated a list of differentially expressed genes for each knockdown (*STS*, *FLG*, *ABCA12, TGM1, ICH* and *ALOX12B*) compared to non-targeting, *C*. These lists were modified by selecting genes with a p-value below 0.05 and 0.01. The genes that had the greatest expression changes due to each ichthyosis gene knockdown with p-value below 0.01 are shown in Appendix 1.1.

5.2.2 Common Genes differentially expressed following knockdown of the Ichthyosis genes:

It is important to investigate whether there were any common signaling pathways or biological functions affected following the knockdown of of the ichthyosis genes. 62 genes were significantly down-regulated and 26 genes were significantly up-regulated (FDR < 0.05). Gene clusters were found for cell cycle, humoral immune response, keratin filament/cytoskeleton and apoptosis (Figures 5.2-5.6). In addition genes related to cytokine signaling (*FOS, TREM2, CFH, RIPK1, PIP4K2C*) and metabolism of lipids and lipoproteins (*PPARGC1B, LPCAT4, PIP4K2C*) were noted.

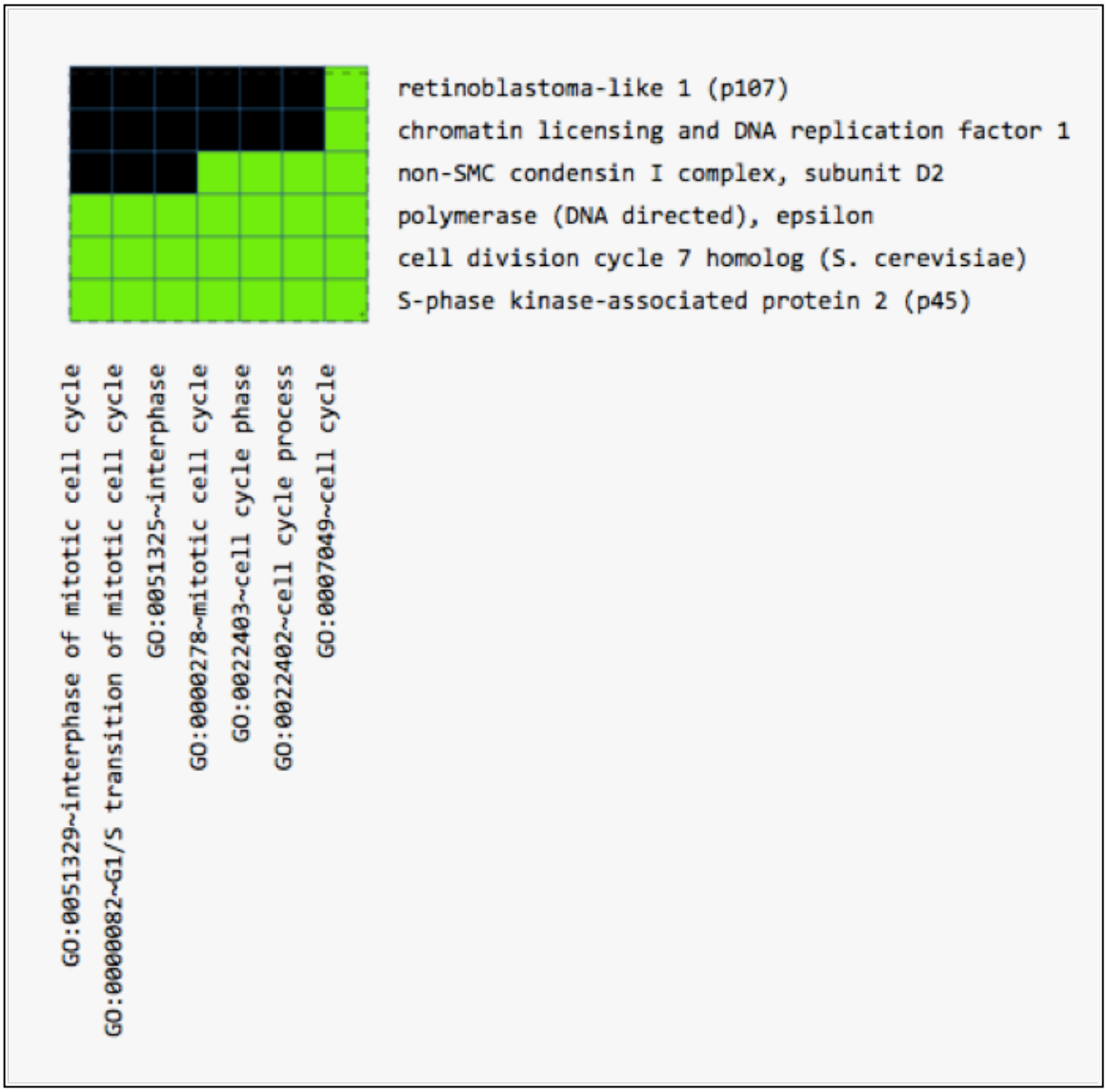

Figure 5.2 2D heatmap showing differentially expressed genes in the cell cycle following knock-down of the ichthyosis genes.
DAVID was used to generate a heat map from differentially expressed genes common to all the ichthyosis gene knockdowns (*STS, FLG, TGM1, ICH, ALOX12B, ABCA12)*. The heatmap shows corresponding gene terms positively associated (green) and corresponding gene terms not associated (black).

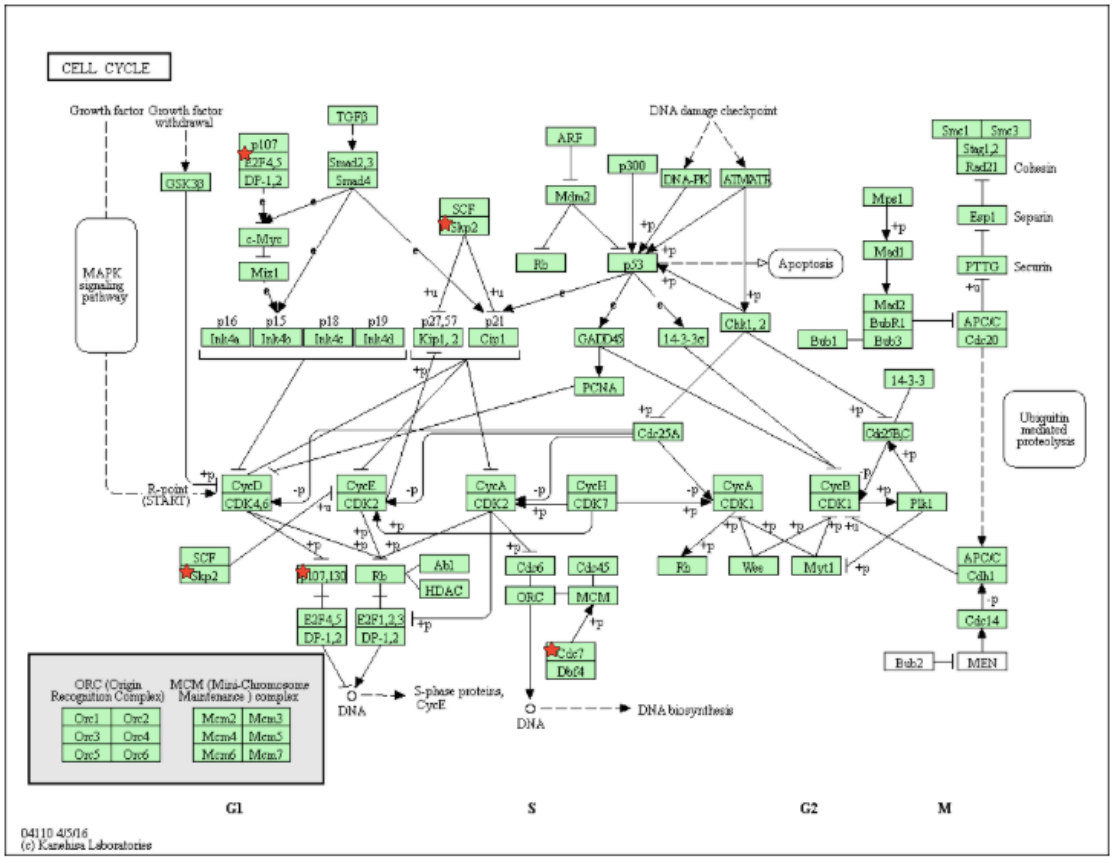

Figure 5.3 Network generated from differentially expressed genes in cell cycle.
DAVID® used defined gene lists onto well known KEGG® pathways to help interpret the data in a network context.*shows differentially expressed genes.

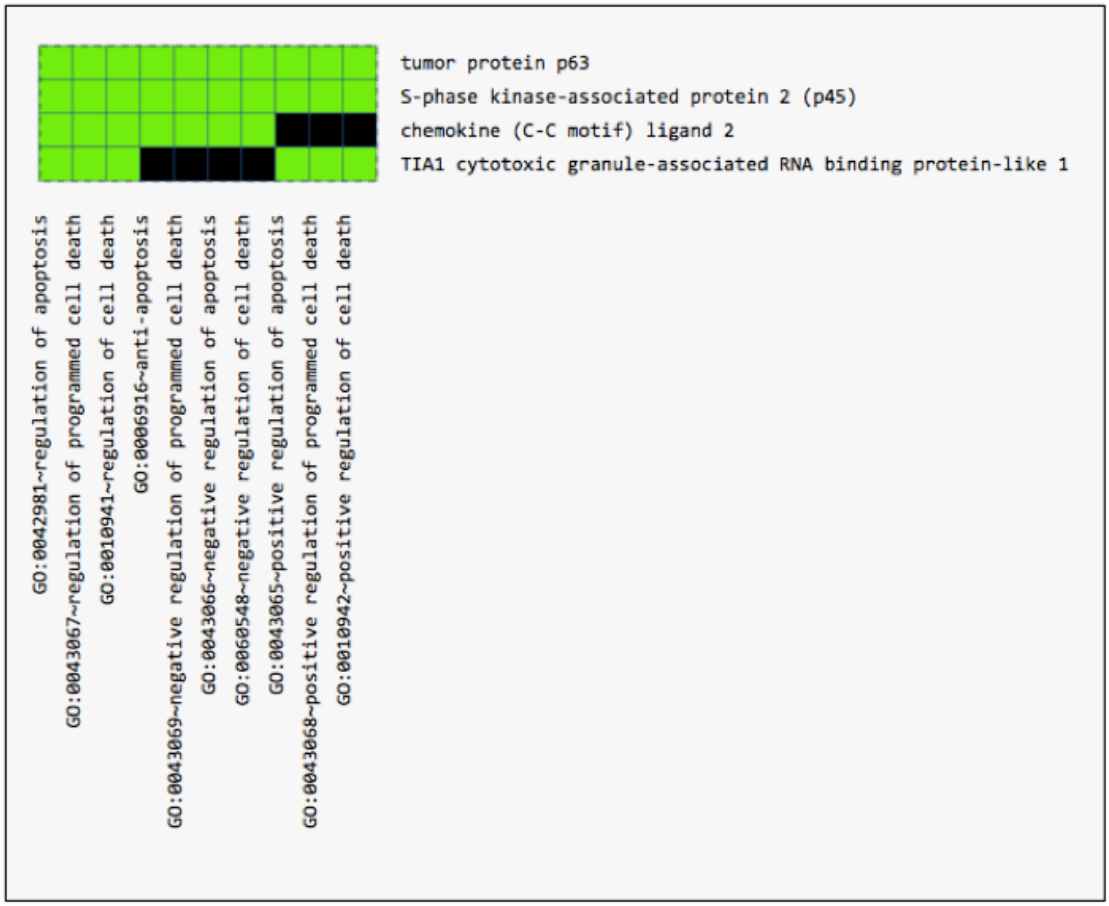

Figure 5.4 2D heatmap showing differentially expressed genes in apoptosis following knock-down of the ichthyosis genes.
DAVID was used to generate a heat map from differentially expressed genes common to all the ichthyosis knockdowns (*STS, FLG, TGM1, ICH, ALOX12B, ABCA12)*. The heatmap shows corresponding gene terms positively associated (green) and corresponding gene terms not associated (black).

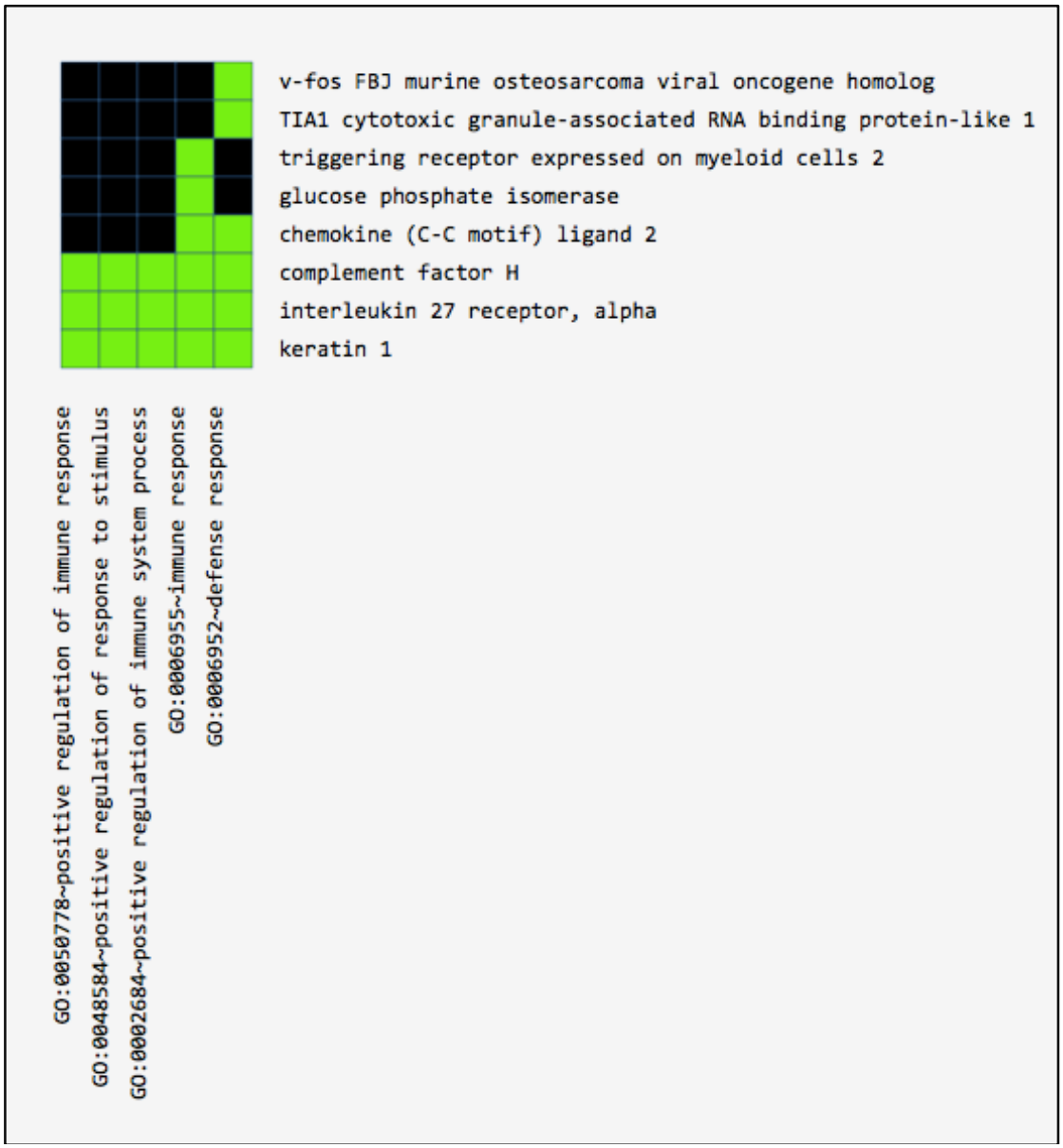

Figure 5.5 2D heatmap showing differentially expressed genes in immune function following knock-down of the ichthyosis genes.

DAVID was used to generate a heat map from differentially expressed genes common to all the ichthyosis knockdowns. The heatmap shows corresponding gene terms positively associated (green) and corresponding gene terms not associated (black).

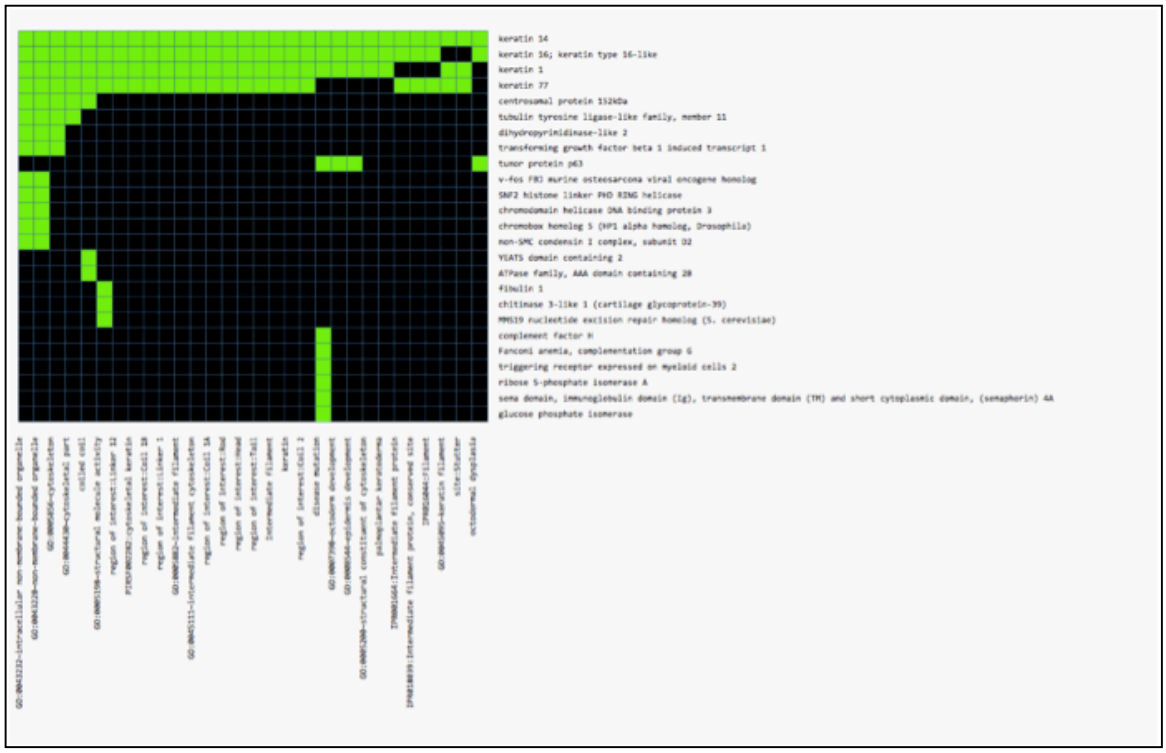

Figure 5.6 2D heatmap showing differentially expressed genes in keratin filament/cytoskeleton function following knock-down of the ichthyosis genes.
DAVID was used to generate a heat map from differentially expressed genes common to all the ichthyosis knockdowns. The heatmap shows corresponding gene terms positively associated (green) and corresponding gene terms not associated (black).

5.2.2.1 Common Ichthyosis (*STS* and *FLG* knockdown) and the Autosomal Recessive Congenital Ichthyosis (*ABCA12, TGM1, ICH*, and *ALOX12B)*:

Venn Diagram for dysregulated genes in the CI and ARCI were made using Venny. (http://bioinfogp.cnb.csic.es/tools/venny/index.html). 68 overlapping genes were common to the CI and 34 for the ARCI. Overlapping genes between two or three knockdowns for the ARCI were also noted (Figure 5.7). Analysis of dysregulated genes in CI and ARCI using GeneMANIA was undertaken. For CI shared protein domains were noted in the epidermal differentiation genes. Pathway connections were noted between FOS and NFIB, SPRR3, LPAR3, CA2, SAP30, CA2, CCL2, MAPK14 and GSTP. Several physical interactions, pathway connections and shared protein domains were noted for CDK2. For ARCI predicted interactions were noted between FOS and OPTN. Pathway connections were noted between

FOS and CA2. Several physical interactions, pathway connections and predicted interactions were noted for CDK2.

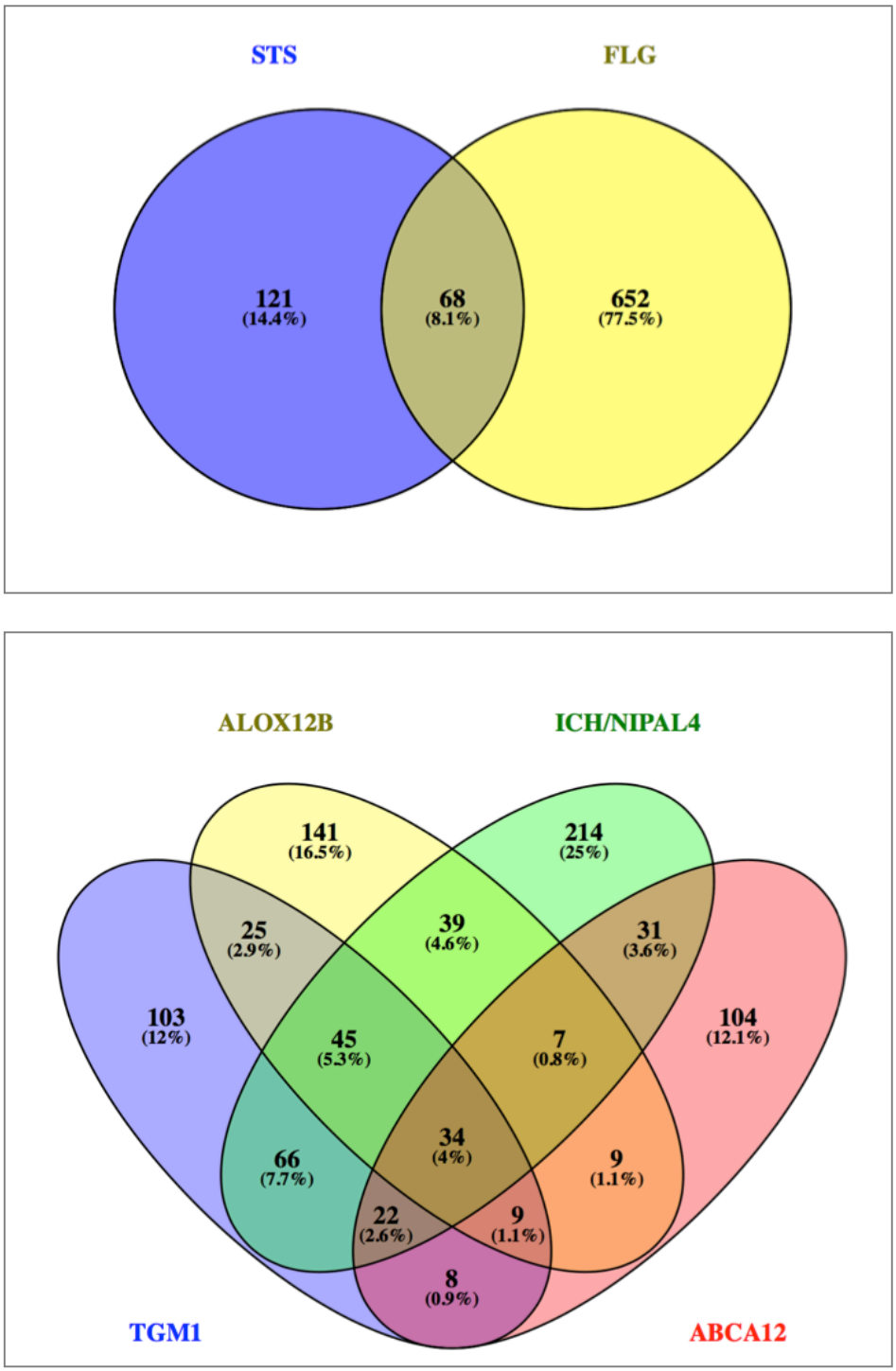

Figure 5.7: Venn Diagram of the number of genes that are dysregulated in the CI and ARCI using Venny. The number of dysregulated genes are displayed for each ichthyosis knockdown in primary keratinocytes. 68 overlapping genes were common to the CI and 34 for the ARCI. For the ARCI, 9 genes were common to *TGM1/ALOX12B/ABCA12* knockdowns, 22 to *TGM1/ICH/ABCA12* knockdowns and 45 to *TGM1/ALOX12B/ICH*. 31 overlapping genes were found for *ICH/ABCA12* knockdowns, 8 for *TGM1/ABCA12* knockdowns, 9 for*ABCA12/ALOX12B* knockdowns, 39 for *ICH/ALOX12B* knockdowns and 66 *ICH/TGM1* knockdowns.

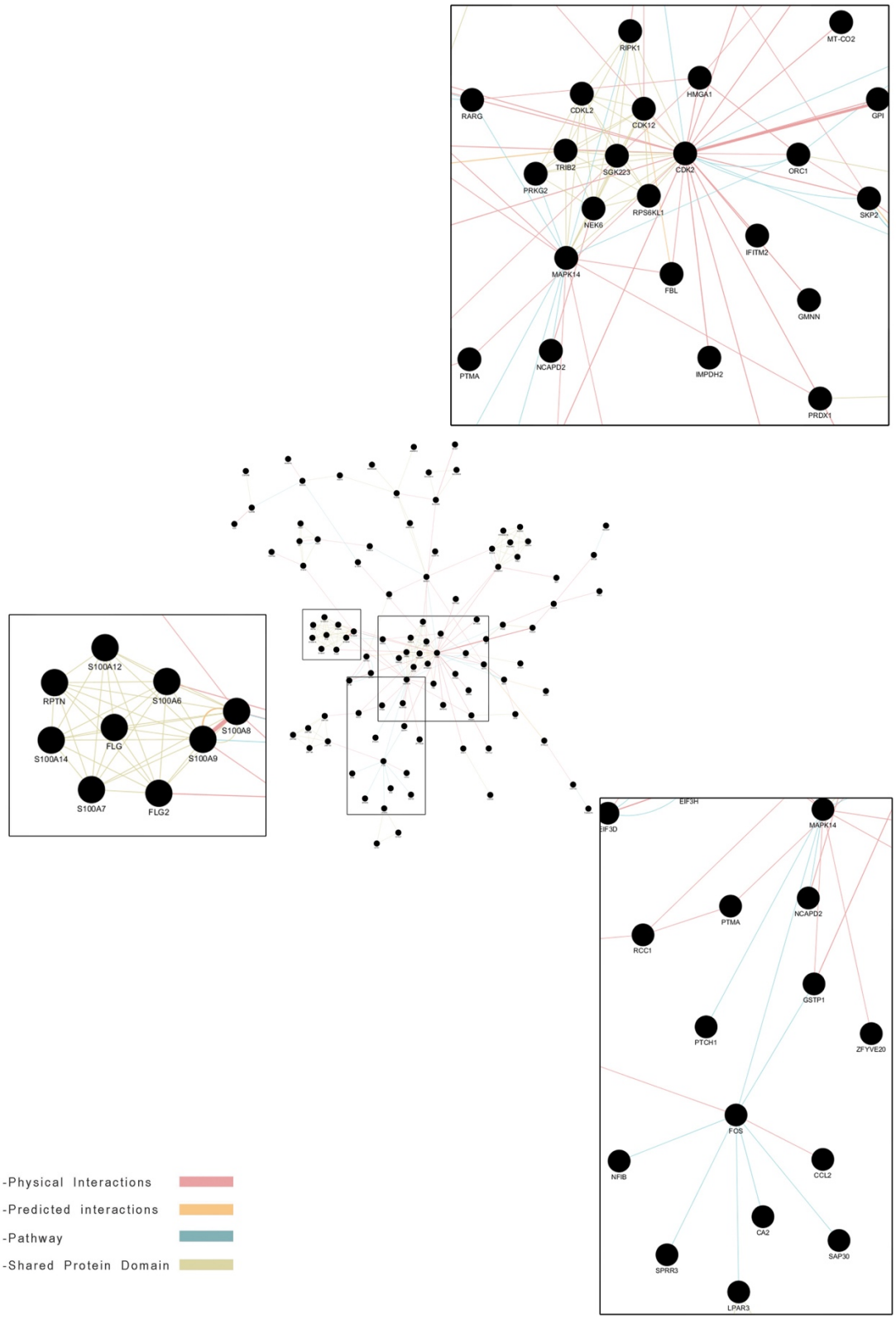

Figure 5.8 Analysis of dysregulated genes in CI using GeneMANIA.
Several gene clusters were noted. Insert: (Left) Shared protein domains were noted in the epidermal differentiation genes. (Bottom) Pathway connections (genes involved in the same pathway) were noted between FOS and NFIB, SPRR3, LPAR3, CA2, SAP30, CA2, CCL2, MAPK14 and GSTP. (Top) Several physical interactions, pathway connections and shared protein domains were noted for CDK2.

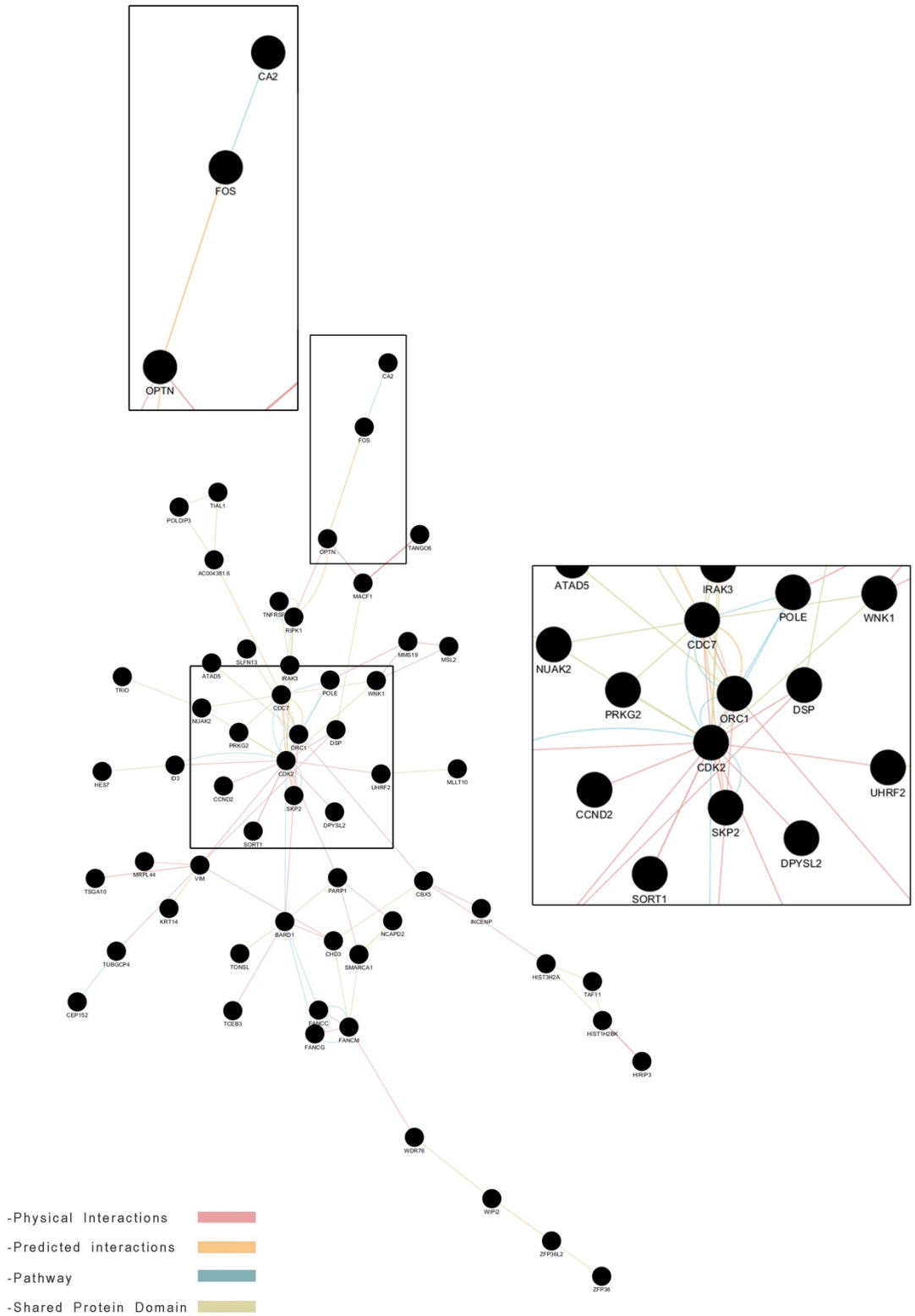

Figure 5.9 Analysis of dysregulated genes in ARCI using GeneMANIA.
Predicted interactions were noted between FOS and OPTN. Pathway connections (genes involved in the same pathway) were noted between FOS and CA2. (Insert) Several physical interactions, pathway connections and predicted interactions were noted for CDK2.

5.2.3 Genes differentially expressed following STS knockdown:

258 genes were significantly down-regulated and 200 genes were significantly up-regulated (FDR < 0.01). Several genes involved in female pregnancy, steroid metabolic process, neurological processes including behaviour, learning and memory and calcium ion homeostasis/binding were noted. *STS* is known to play a role in these processes but genes pertaining to these functions in XLI may be a novel finding.

Altered expression in 27 genes (n = 14) in patients with XLRI has been reported in a study where mRNA expression profiles were determined by oligonucleotide arrays (Hoppe et al., 2012). None of these genes were altered in our study. This discrepancy may be because expression profiling was undertaken on skin containing both epidermis and dermis (obtained by taking punch biopsies) rather than micro-dissected epidermis. In addition, tissue was obtained from volar forearms of the subjects. This location is only mildly affected by ichthyosis in patients with XLRI, and may not be completely representative of their skin barrier function in other places (Hoppe et al., 2012).

Table 5.2: Dysregulation following knockdown of *STS*

Downregulated genes:

DAVID		
	Development/ differentiation	ASPRV1, C1orf68, DHRS9, KRT1, KRT2, SPRR2F, SPRR3, TXNIP
	Lipid metabolism	UGCG, ACER1, HPGD, LIPM, LIPN, PSAPL1, STS
	Female pregnancy	CLIC5, HPGD, JUNB, OXTR, STS, FOS
	Steroid metabolic process	CYP2R1, DHRS2, DHRS9, DIO2, HSD17B2, KLK6, LEP, STS
	Neurological processes including behaviour, learning and memory	HTR1B, S100P, CCL2, CXCL17, CXCL2, CLIC5, CHRNA5, DEFB4A, EGR1, KLK6, LEP, OXTR, KCNQ3, SCG2, FOS
	Calcium ion homeostasis /binding	CCL2, STC1, CCL2/S100P, CLSTN2, CATSPER3, PADI2, PLA2G4D, RPTN, FLG2, SCG2, STS
REACTOME		
	Arachidonic acid metabolism	CYP4F22,HPGD
	Cytokine Signaling in Immune system	IL36B,CNKSR2,SOCS3,CSF3,FGF19,IFNB1,IL37,MX2,EGR1,IL20
KEGG		
	Cytokine-cytokine receptor interaction	CCL2, CXCL2,CSF3,IFNB1,IL20,LEP

Upregulated genes:

DAVID		
	Defense/immune response	EPHA3, ITGB6, SERPINA3, VNN1
REACTOME		
	Cytokine signaling	EDA,PIK3R3
	Metabolism of lipids and lipoprotein	ELOVL3, PIK3R3
KEGG		
	Regulation of actin cytoskeleton	ARHGEF6, ITGA11, ITGB6, PIK3R3

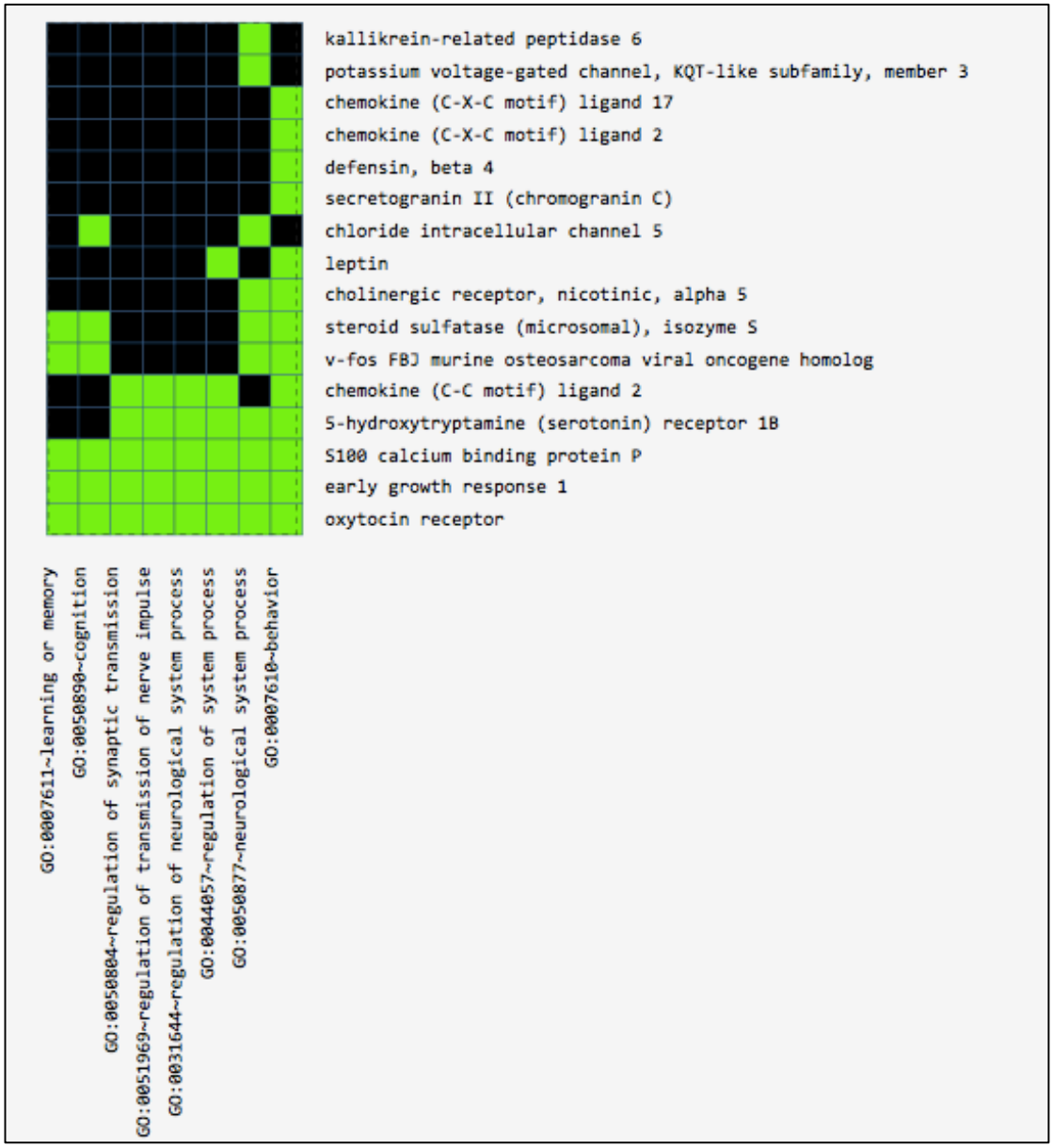

Figure 5.10 2D heatmap showing differentially expressed genes in neurological function following knock-down of the *STS*.

DAVID was used to generate a heat map from differentially expressed genes involved in neurological function following *STS* knockdown. The heatmap shows corresponding gene terms positively associated (green) and corresponding gene terms not associated (black).

5.2.4 Genes differentially expressed following *FLG* knockdown:

There is no published study looking at the transcriptome of IV patients without AD or an IV model. Winge et al looked at the transcriptome of 5 AD/IV FLG -/- patients by microarray analysis and found that several pathways were significantly altered compared to the healthy control group (Winge et al., 2011). Focal adhesion, extracellular matrix receptor interactions, regulation of actin cytoskeleton, ABC transport system and calcium signaling pathways

showed significantly altered expression (Winge et al., 2011).

In this project, knockdown of *FLG* lead to the largest number of dysregulated genes compared to other knockdowns. 395 genes were significantly down-regulated and 327 genes were significantly up-regulated (FDR < 0.01). Interestingly there are 2 interactions noted with the ichthyosis genes of interest in this study-with *TGM1* and *ALOX12B* (Figure 5.9); TGM1 is involved in CE formation and filaggrin-dependent keratin aggregation (by a yet incompletely understood mechanism) yields keratins that remain as the prevailing proteins inside the CEs (Norlen and Al-Amoudi, 2004). In addition to this, genes involved in arachidonic acid metabolism (involving *ALOX12B*) were downregulated. The mechanisms of how *FLG* interacts with *TGM1* and *ALOX12B* needs to be elucidated.

In addition genes involved in acyl-chain remodelling were downregulated. Shorter fatty acid chain lengths have been reported in AD (also caused by *FLG* mutations) which in turn produce abnormalities in lipid organization that most likely compromise permeability barrier function (Ishikawa et al., 2010, Janssens et al., 2012, Janssens et al., 2011).

Several genes involved in the phenotype of IV involving Ca^{2+} dependent membrane targeting were noted. It is known that FLG may be involved in calcium metabolism in the skin (Bieber, 2008), and the calcium gradient is important for epidermal differentiation- a loss of this gradient increases keratinocyte proliferation and decreases differentiation (Jensen et al.; 2005).

Table 5.3: Dysregulation following knockdown of *FLG*
Downregulated genes:

DAVID		
	Keratinocyte differentiation	KRT1,KRT10,KRT14,KRT2,KRT76,KRT77,KRT84,ZNF492
	Epidermis development	BARX2CALML5,CASP14,CRABP2,C1orf68,EMP1,FABP5,,S100A7,UGCG,ALOX12B,ASPRV1,FLG,KRT1,KRT10,KRT14,KRT16,KRT16P2,KRT2,LOR,SPRR3,TXNIP,TGM1,TGM5,
	Defense/ immune response	CD74,S100A12,S100A7,S100A8,S100A9,CCL2,CFD,CFH,CORO1A,HSF1,ITGB6,IFNK,IL12A,IL27RA,KRT1,PGLYRP3,PGLYRP4,PDPN,P2RX7,SAA1,TLR1,TLR2,FOS,
	Cornified envelope	FLG, LOR, RPTM, TGM1
	Leukocyte chemotaxis	S100A9, CCL2, CORO1A, SAA1
	Serine hydrolase	CFD,DPP4,FAP,KLK1,KLK6,PLAT,PRSS21,TMPRSS11D
	Lipid metabolic	ST3GAL5, ST3GAL6, UGCG, ACER1, ITGB8, PSAPL1, P2RX7
	S100/CaBP-9k-type, calcium binding, subdomain	S100A12,S100A2, FLG,S100A9,,S100A7,S100A4,S100A8, FLG2,RPTN
	Cell cycle	CHEK1,E2F2,E2F8,FBXO43,KAT2B,LFNG,SPC25,CENPJ, CDT1,IL12A,KIF20B,KIF22,KNTC1,LZTS1,LIN9,MND1,PDPN, TXNIP,
	MAP kinase	CD74, EGF, P2RX7, IRAK3
REACTOME		
	Acyl-chain remodelling	PLA2G2F, PLA2G4D
	Vesicle mediated transport	CD36,ARRB1,KIF20B,KIF22, RAC2,GJA1, KIF26A,GJB6, SAA1, TUBA4A, TUBA4B, GJB2
	Interleukin-6 family signaling	IL12A, IL27RA
KEGG		
	NOTCH signaling pathway	KAT2B, LFNG, DLL1, HES5, MAML2
	Arachidonic acid metabolism	ALOX12B, PLA2G2F, PLAY2G4E, PTGS1
	Cytokine-cytokine receptor interaction	CCL2,CXCL14,CSF3,EGF,IFNK,IL12A,IL20,IL7R,PDGFRA,TNFRSF18

Upregulated genes:

DAVID		
	Vesicle mediated transport	ANG, FGF2, GRM8, HMOX1, INHBB, SYT1, TAC4, TAC1, TRPV6
	Calcium-dependent membrane targeting	SYT1, SYT2, CADPS2
	Activation of protein kinase activity	ADCY1, ADRB1, ANGANKHD1-EIF4EBP3, AMH, CCK, COL4A3, FGF2
KEGG		
	NOTCH signaling	HEY1, MIR34A, NEURL

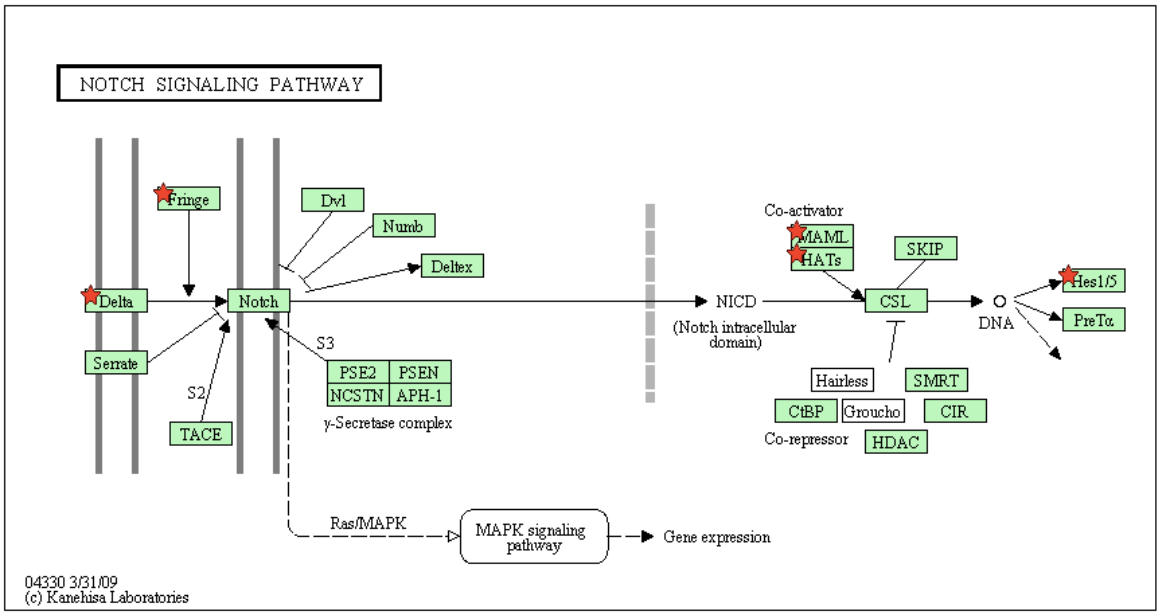

Figure 5.11 Network generated from differentially expressed genes in the NOTCH signaling pathway following *FLG* knockdown.
KEGG® pathway showing network generated from differentially expressed genes in NOTCH signaling pathway following *FLG* knockdown.*shows differentially expressed genes.

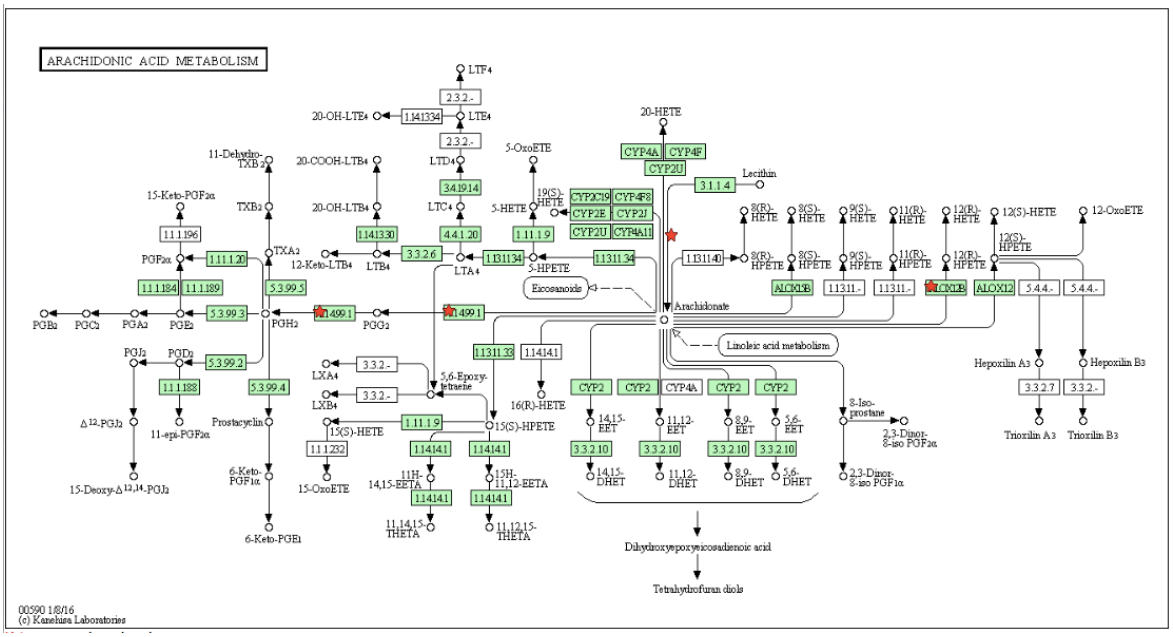

Figure 5.12 Network generated from differentially expressed genes in arachidonic acid metabolism signaling pathway following *FLG* knockdown.
KEGG® pathway showing network generated from differentially expressed genes in arachidonic acid metabolism signaling pathway following *FLG* knockdown.*shows differentially expressed genes.

5.2.5 Genes differentially expressed following *TGM1* knockdown:

163 genes were significantly down-regulated genes and 231 genes were significantly up-regulated (FDR < 0.05). As expected several genes involved in CE formation/peptide cross-linking (a key step in CE formation) were dysregulated. Several of these changes CE proteins (LOR, FLG) have been noted in a proteomic study of a *TGM1* deficient skin-humanized mouse model (Aufenvenne et al., 2012). As noted previously (O'Shaughnessy et al., 2010) changes in fatty acid synthesis pathway and in the inflammatory response were also dysregulated although the genes involved in this project were different. This is most likely due to different disease models-human in this study compared to rat and possibly different gene expression platforms used (microarray in the reported study). Additionally *RNA-Seq* data analysis implies that lipid metabolism is regulated by PPAR-alpha following *TGM1* knockdown. Several genes involved in keratinocyte differentiation, epidermal development and keratin filament organisation were found to be perturbed. *KRT1* expression was downregulated in this study and was found to be alterated in LI in another study

(O'Shaughnessy et al., 2010). No changes in its pairing partner *KRT10* were noted bearing out the findings of a proteomics study (Aufenvenne et al., 2012).

Table 5.4: Dysregulation following knockdown of *TGM1*

Downregulation:

DAVID		
	Cell cycle	CHEK1, DBF4B, E2F2, E2F8, HAUS8, SPC25, CENPJ, CDT1, CCNF, KIF20B, KIF22, KNTC1, LIN9, MND1, CHEK2, SMC4
	Keratinocyte differentiation	S100A7, LCE3A
	Epidermal development	S100A7, CASP14, C1orf68, KRT1, KRT10, LCE3A
	Cornified envelope	TGM1, RPTN, LOR, FLG
	Peptide cross-linking	LOR, TGM1, TGM2, TGM4, TGM5, MAMDC2
	Defense response	S100A7, ANKRD1, DEFB4A, HIST1H2BF, IL27RA, KRT1, FOS
REACTOME		
	Cytokine signaling	IRAK3, FGF1, SOCS3, MT2A, EGR1, TNFRSF18, IL27RA, HLA-DRB1
	Cell cycle	POLE2, HIST1H2BF, CDT1, SPC25, CENPH, CENPJ, SMC4, CHEK2, CHEK1, ORC1, MND1, LIN9, HAUS8, PRIM1, POLA2, KNTC1, LMNB1, E2F2
	Arachidonic acid metabolism	CYP4B1, PTGS1
	Metabolism including lipids and lipoproteins	ANKRD1, GBA3, CYP4B1, PTGS1
	Regulation of lipid metabolism by PPAR alpha	ANKRD1, CYP4B1
KEGG		
	DNA replication	POLA2, POLE2, PRIM1

Upregulation:

DAVID		
	Membrane bound vesicle	CSPG5, C12orf39, NPY1R, SHH, SYT2
	Plasma membrane	ADAM23, DIXDC1, GPR1, RAB33A, ADCY1, CHRM3, CSPG5, DTNA, HDAC6, HAS3, IL1RL1, IL18R1, NPY1R, OLR1, KCNMB3, PRKD1, PTPRB, SGCG, SCN9A, SHH, SYNE1, SYT2, SDC2
	Cytoskeleton	LDB3, HDAC6, IL1RL1, KIF5A, SGCG, SYNE1
REACTOME		
	Fatty acid CoA synthesis	ELOVL2
	Cytokine signaling	IL1RL1, IL18R1, IFI30

5.2.6 Genes differentially expressed following *ALOX12B* knockdown:

150 genes were significantly down-regulated and 159 genes were significantly up-regulated (FDR < 0.01). *ALOX12B* encodes the 12R-LOX enzyme which is a iron-containing dioxygenase that oxygenates lipids (polyunsaturated fatty acids and their esters). In keeping with this several genes annotated to oxidoreductase activity, iron ion binding and lipid biosynthetic process/lipid metabolism were noted. *RNA-Seq* analysis showed several genes involved in keratinocyte differentiation/cytoskeleton organization lending support to its possible role in keratinocyte differentiation (section 1.5.2.4.3). Genes involved in inflammation were also noted thereby implying possible novel functions for *ALOX12B*, whose specific role in skin barrier function is not well understood. Genes involved in regulation of lipid metabolism by PPAR-alpha were also noted.

Table 5.5 Dysregulation following knockdown of *ALOX12B*

Downregulation:

DAVID		
	Cell cycle	BARD1, CHEK1, DBF4B, E2F8, CENPJ, CCNF, KPNA2, KIF20B, KIF22, KNTC1, LZTS1, LIN9, MND1, PTTG1, PLK2, SMC4
	Extracellular matrix	MAMDC2, COL4A2, COL12A1, HMCN1, LUM, MMP19
	Cytoskeleton	CHEK1, ACTG2, CENPJ, CNKSR2, GDPD2, KRT31, KRT77, KIF20B, KIF22, KIF24, KIF26A, KNTC1, LMNB1, LZTS1, TNNT3, VIM
	Intermediate filament	KRT31, KRT77, LMNB1, VIM
	Immune/ defense response	GEM, CCL2, CXCL2, CFH, IL27RA, TLR1, TREM2, FOS
	Lipid localization and transport	ABCG4, SLC1A2, SLCO2A1, SORL1, TC
	Lipid biosynthetic process	ST3GAL5, ALOX12B, CYP1A1, PTGS1
	Oxidoreductase activity, iron ion binding and lipid biosynthetic processes	ALOX12B, BBOX1, CYP1A1, DHRS2, DIO2, DPYD, LOXL2, MOXD1, PTGS1, ST3GAL5
REACTOME		
	Arachidonic acid pathways	CYP1A1, ALOX12B, PTGS1
	TLR cascades	FOS, JUN, TLR1
	Interleukin-6 family signaling	SOCS3, IL27RA
KEGG		
	MAPK signalling	CHP2, FGF1, JUN, FOS
	TLR signaling pathway	JUN, FOS, TLR1

Upregulation:

DAVID		
	Defense response	CCK, INHBB, IL1RL1, KYNU, OLR1, TAC1, VNN1
	Immune response	IFI6, OLR1, TNFSF18, IL1RL1, KYNU, VNN1; latter three genes involved in innate immune response
	Regulation of secretion	GDNF, INHBB, TAC1, TRPV6
	Lysosome	IFI30, LAMP3, SLC29A3
REACTOME		
	Regulation of lipid metabolism by Peroxisome proliferator-activated receptor alpha (PPARalpha)/ PPARA activates gene expression	PLIN2, ANGPTL4, PPARGC1A
	Cytokine signaling	IL1RL1, TNFSF18, RET,GDNF, IFI6, IFI30, IFI27
	Signaling by Interleukins	IL1RL1, RET, GDNF
	Metabolism of lipids and lipoproteins	PLIN2, ANGPTL4, PPARGC1A, CPNE7, PLA2G4D

5.2.7 Genes differentially expressed following *ICH* knockdown:

258 genes were significantly down-regulated and 200 genes were significantly up-regulated (FDR < 0.01). Several genes were down-regulated involved in metabolism of lipids and lipoproteins and vesicle mediated transport most likely through LB. *ICH* is known to encode a magnesium transporter membrane associated protein hypothetically involved in epidermal lipid processing and in lamellar body formation and transport (Goytain et al., 2008). Additionally several genes annotated to keratinocyte differentiation, keratin filament regulation of cell differentiation/epithelial development were noted suggesting that *ICH* is involved in keratinocyte differentiation.

Table 5.6 Dysregulation following knockdown of *ICH*

Downregulated Genes:

DAVID		
	Keratin filament	KRT1, KRT10, KRT2, KRT77
	Regulation of cell differentiation	CNTN1, DLL1, HES7, JAG1, MAML2
	Regulation of immune response	THY1, CFH, HSPD1P5, IL12A, IL27RA, IRAK3, KRT1
	Epithelial development	TBX18, CA2, DHRS9, JAG1, KRT2, TXNIP
	Vesicle mediated transport	ABCA3, CSPG5, C12orf39, GAD1, SHH
REACTOME		
	Metabolism of lipids and lipoproteins	PPARGC1B, FABP5, CYP4B1, UGCG
	Cytokine signaling	IL12A, IFIT1, ACTG1, CNKSR2, IL7R, OAS1, BIRC3, OAS2, OAS3, DDX58, IFIT2, IFIT3, MX1, IL33, MX2, IFITM1, CSF3, PDGFRA, IL27RA, EGR1, FGF1, BST2, EBI3, IL20, IRAK3, UBA7, IFI35, IL1RL2, XAF1, USP18
	Innate immune system	IRAK3, CNKSR2, FGF1, ACTG1, TXNIP, FOS, PDGFRA, TREM2, BIRC3, UBA7, CFH, DDX58
	IL-6-type cytokine receptor ligand interactions	IL12A, IL27RA
KEGG		
	Cytokine/cytokine receptor interaction	CCL2, CXCL2, CXCL6, CSF3, IL12A, IL20, IL7R, PDGFRA
	Cell cycle pathways	CHEK1, E2F2, CDK6, PTTG1, CHEK2

Upregulated Genes:

DAVID		
	Vesicle	ABCA3, CSPG5, C12orf39, GAD1, SHH
	Cytoskeleton	LDB3, DNAH1, SGCG, KIF5A
	Plasma membrane and ion transport	
REACTOME		
	Signal transduction and metabolism	CCK, VIP, SHC2, INHBB, ADRB1, ADCY1, KIF5A, CHRM3, TAS1R3, NEURL, SHH, CDON, HEY1, ATP6V0D2, TNXB

5.2.8 Genes differentially expressed following *ABCA12* knockdown:

Knockdown of ABCA12 produced fewer gene expression changes compared to loss of the other ichthyosis genes with 136 significantly down-regulated and 87 significantly up-regulated genes (FDR < 0.01). In this project, *RNA-Seq* analysis shows several genes annotated to lipids, transportation, secretion and endomembrane systems. This is in keeping

with the known function of ABCA12 as a keratinocyte transmembrane lipid transporter protein associated with the transport of lipids via lamellar granules. Additionally, several genes involved in metabolism of lipids and lipoproteins were dysregulated. Malformation of the intercellular lipid layers in HI skin has been noted previously (Aufenvenne et al., 2012, Dale et al., 1990, Milner et al., 1992, Akiyama et al., 1998). Defective lipid transport due to loss of ABCA12 function leads to the accumulation of intracellular lipids, including glucosylceramides and gangliosides, in the epidermal keratinocytes. The accumulation of gangliosides seems to result in the apoptosis of Abca12−/− keratinocytes (Akiyama, 2014). In this study, several genes involved in cell cycle apoptosis were found to be dysregulated following *ABCA12* knock down in primary keratinocytes.

Table 5.7 Dysregulation following knockdown of *ABCA12*

Downregulated Genes:

DAVID		
	Inflammatory response	CCL2, CFH, FN1, IL6, KRT1, FOS
	Endomembrane system	VGF, CLSTN2, CHST6, CORO1A, DHRS2, HSD17B2, LMNB1, PTGS1
	Cytoplasmic bound vesicle/secretory granules	RAB3B, VGF, ARC, ANXA2P1, CORO1A, FN1
	Epithelial development	GATA6, CA2, LAMA1, TIMELESS
	Cytoskeleton	CHEK1, ARC, CENPJ, CORO1A, HOMER1, KRT1, KIF24, KNTC1, LMNB1, LZTS1
	Cell cycle	CHEK1, DBF4B, E2F2, CDT1, KNTC1, LZTS1, TIMELESS
	Apoptosis	E2F2, GATA6, XAF1, IER3, IFI6, IFNB1, IL6, STAT1, TNFRSF11B, TNFRSF18
REACTOME		
	Cytokine signaling interaction	IFIT1, IFNB1, IL7R, OAS1, OAS2, STAT1, OAS3, DDX58, IL6, IFIT2, TNFRSF18, IFIT3, FN1, PRLR, MX1, MX2, SAMHD1, RSAD2, CD70, EGR1, OASL, BST2, TNFRSF11B, IFI6, ISG15, IFI35, XAF1, USP18
	Fatty acids	CYP4F22
	Arachidonic acid metabolism	CYP4F22, PTGS1
	Metabolism of lipids and lipoproteins and cell cycle	CYP4F22, PTGS1
	Interleukin-6 signaling	STAT1, IL6
KEGG		
	Cytokine-cytokine receptor interaction	CD70, CCL2, IFNB1, IL6, IL7R, PRLR, STST1, FOS, TNFRSF11B, TNFRSF18
	TLR signaling pathway	STST1, IL6, INFB1, FOS

Upregulated Genes:

DAVID		
	Plasma membrane and secretion	C1QTNF4, EGFL6, COL21A1, CRB1, IL34, OLR1, PAMR1, TNXB, VIP, WNT1
	Extracellular region	ENDOU, C1QTNF4, EGFL6, COL21A1, CRB1, IFI30, IL34, OLR1, PAMR1, TNXB, VIP, WNT1
	Transcription and apoptosis	NKX3-2, ARHGEF6, ADCY1, NME5, OLR1, PREX1, PTGER3, RP1L1, TNFRSF10D
REACTOME		
	Metabolism of lipids and lipoproteins	PLA2G4D, PIK3R3, AKR1C2
	Arachidonic acid metabolism	AKR1C2
	Transmembrane transport of small molecules	HEPH, ADCY1, SLC24A3
KEGG		
	Chemokine signaling pathway	ADCY1, PREX1, PIK3R3

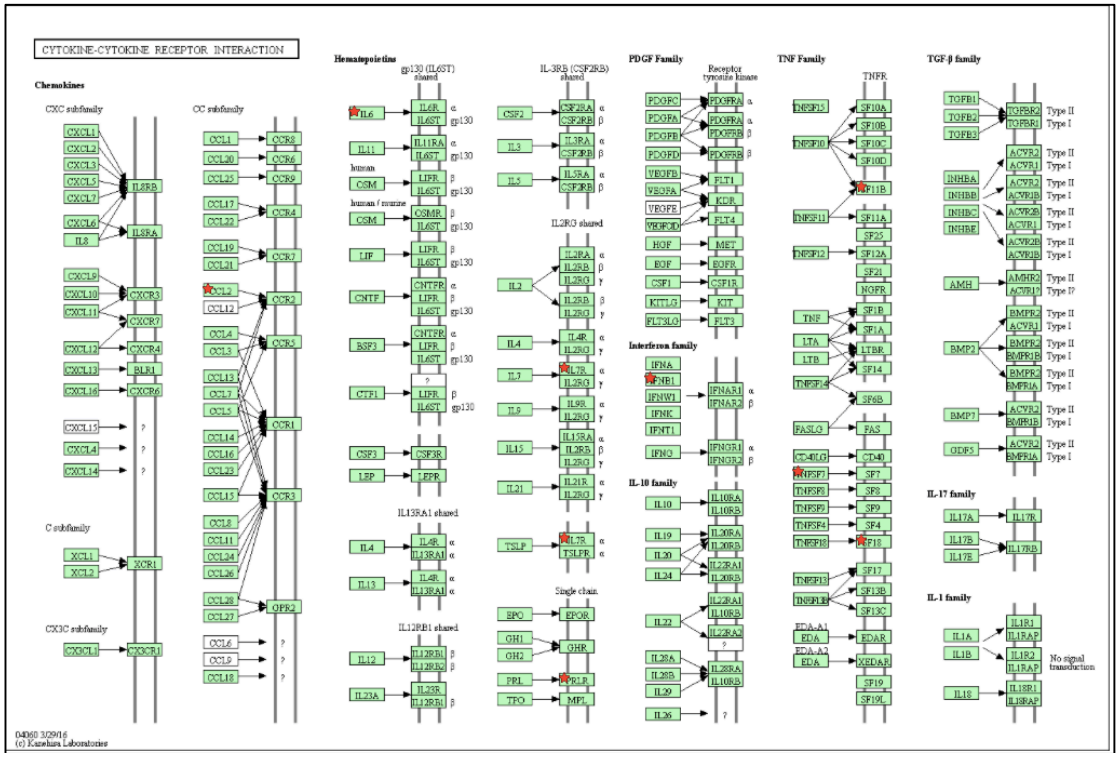

Figure 5.13 Network generated from differentially expressed genes involved in cytokine-cytokine receptor interaction following *ABCA12* knockdown.
KEGG® pathway showing network generated from differentially expressed genes involved in cytokine-cytokine receptor interaction following *ABCA12* knockdown.*shows differentially expressed genes.

5.3 Discussion

RNA-Seq is a powerful method to analyse the transcriptome of cells of interest. In this project *RNA-Seq* analysis was employed to investigate differentially expressed genes following ichthyosis gene knockdown (*STS, FLG, TGM1, ICH, ALOX12B, ABCA12*). The lists of differentially expressed genes generated following ichthyosis gene knockdown underwent gene enrichment and pathway analysis using DAVID and REACTOME.

In this project, analysis of common genes differentially expressed following knockdown of the ichthyosis genes was undertaken to identify any common genes or pathways to provide more insight into the biology of this group of diseases with similar phenotypes. Furthermore, individual ichthyosis knockdowns were analysed separately.

5.3.1 Common Ichthyoses (STS and FLG)

5.3.1.1 Loss of *STS* expression causes neurological abnormalities in X-linked Ichthyosis

Several genes associated with neuronal processes and steroid metabolic processes were altered following *STS* knock-down in primary keratinocytes. It is known that XLI patients demonstrate cognitive behavioral abnormalities, such as attention-deficit disorder and social communication deficits (Trent et al., 2012, Kent et al., 2008). In addition, inactivation of SSase increases aggressive behavior in rodents (Nicolas et al., 2001). These abnormalities have been attributed to altered sterol metabolism in the central nervous system (Kent et al., 2008, Bicikova et al., 2013).

5.3.1.2 *STS* expression is important in lipid metabolism and cholesterol synthesis

Several dysregulated genes annotated to lipid metabolism were noted. SSase is secreted into the intercellular spaces of the SC, along with other lamellar granule-derived lipid hydrolases (Elias et al., 2004) where steroid sulfatase catalyzes the desulfation of cholesterol sulfate generating cholesterol for the barrier. Several genes altered here are related to ceramides and are possibly secondary defects following cholesterol synthesis disruption.

5.3.1.3 Role of AP1 transcription factors in epidermal/keratinocyte differentiation following *STS* suppression

It is known that AP1 (JUN/FOS) transcription factors (*C-JUN, JUNB, JUND, C-FOS, FOSB, FRA-1, AND FRA-2*) are key regulators in epidermal differentiation (Eckert et al., 2013). *RNA-Seq* analysis following *STS* knock-down showed significant dysregulation of genes involved in differentiation. As noted in section 1.4.2.6 cholesterol sulfate is thought to be operate through an AP-1 binding site in the promoter region of several proteins involved in cornified envelope formation thereby regulating their transcription. In this study, both *FOS*

and *JUNB* were downregulated. Several epithelial abnormalities have been noted following perturbations of members of the AP1 transcription family; mice lacking JUNB in keratinocytes display pronounced epidermal hyperproliferation, disturbed differentiation and delayed wound healing (Florin et al., 2006). In addition, simultaneous deletion of C-JUN and JunB in the epidermis produces a psoriasis-like phenotype (Schonthaler et al., 2009).

5.3.1.4 Extracutaneous features/syndromic features following loss of *STS* expression:

XLI recessive may be non-syndromic (phenotype limited to the skin) or syndromic when accompanied by extracutaneous features (Oji et al., 2010).

5.3.1.4.1 Prolonged labor in XLI

Failure of labor either to initiate or to progress due to placental sulfatase deficiency has been noted to occur in pregnancies of XLI fetuses. Following RNA Seq analysis suppression of several genes associated with female pregnancy was noted (Bradshaw and Carr, 1986).

5.3.1.5 Role of NOTCH signaling in Epidermal Differentiation following loss of *FLG* expression:

In this dataset, several genes involved in keratinocyte differentiation, epidermis development, intermediate filament were enriched following loss of *FLG* expression. As discussed in chapter 1, filaggrin is thought to aggregate the keratin cytoskeleton, facilitating the collapse and flattening of cells in the outermost SC to produce flattened anuclear squames (Manabe et al., 1991). Furthermore, the top signaling pathway implicated in this study for the *FLG* knockdown was the NOTCH signaling pathway. NOTCH signaling is essential for keratinocyte differentiation. NOTCH1 is expressed in all epidermal layers, NOTCH2 in the basal cell layer and Notch3 in basal cell and spinous cell layers in normal epidermis. NOTCH

signaling functions as a molecular switch that controls the transition of cells between skin layers during the epidermal differentiation process (Lin et al., 2012). In addition, previous studies have shown involvement of NOTCH signaling in keratinocyte differentiation in embryos of mice and rats (Baker et al., 2006, Takahashi et al., 1996) and NOTCH molecules are thought to cause aberrant expression of K10 and K14 leading to anomalous differentiation of the epidermis in psoriatic lesions (Ota 2014). In this study IF of 3D *FLG* knockdown organotypic model showed reduced expression of K10 in the knockdown and no change in expression of K14 in siFLG and siC (section 4.2.4.1).

5.3.1.6 *FLG* loss causes abnormalities in ABC transport system

Several genes related to vesicle-mediated transport were enriched. Abnormalities in lamellar body loading and secretion in FLG-deficient IV suggest that FLG deficiency produces a cytoskeletal defect sufficient to impair organelle secretion (Man et al., 2008). Thus the immune dysfunction noted may be due to abnormalities in the ABC transport system that delivers antimicrobial peptides through secretion of LB contents (Braff et al., 2005, Oren et al., 2003, Aberg et al., 2008).

5.3.2 Autosomal Recessive Congenital Ichthyosis (*TGM1, ALOX12B, ICH, ABCA12*)

5.3.2.1 Role of Peroxisome proliferator-activated receptor (PPAR)-alpha in ARCI

Peroxisome proliferator-activated receptor (PPAR)-alpha is a fatty acid activated transcription factors that belongs to the nuclear hormone receptor family. There are three PPAR isotypes (alpha, beta/delta, gamma) with variable ligand specificity and metabolic functions. All three PPAR isotypes are expressed in human skin (Westergaard et al., 2001). PPAR-alpha is preferentially expressed in the suprabasal epidermis (Icre et al., 2006, Rivier et al., 1998). It

is known that epidermal differentiation and SC formation are stimulated by activation of PPAR-alpha (Hanley et al., 1997, Man et al., 2006, Rivier et al., 2000, Batheja et al., 2009). There is a strong link between epidermal lipid metabolism and skin barrier function as permeability barrier function is largely determined by extracellular lipids in the SC. PPAR-alpha ligands induce lipid synthesis (Batheja et al., 2009, Rivier et al., 2000) as well as lamellar body formation, secretion and lipid processing, correlating with accelerated skin barrier repair (Man et al., 2006). Chakravarthy et al. identified the oxidised phospholipid, 1-palmitoyl-2-oleoly- sn-glycerol-3-phosphocholine (16:0/18:1-GPC) as a specific PPAR-alpha ligand in the liver (Chakravarthy et al., 2009). It is speculated that epidermal lipoxygenases, including *ALOX12B*, generate oxidized phospholipids in cutaneous tissue (Munoz-Garcia et al., 2014) and may be endogenous PPAR-alpha agonists in the skin. Both PPAR-alpha and *ALOXE3*, have been found to be downregulated *in vitro* following barrier disruption.

In addition to their role in barrier formation PPARs play a role in inflammation and PPAR-alpha expression has been found to be reduced in AD (Plager et al., 2007). It was suggested that downregulation of PPAR-alpha could be involved in AD development or maintenance by affecting the lipid pathway (Plager et al., 2007). The underlying mechanism is thought to involve nuclear factor kappaB signaling (NF-κB) (Daynes and Jones, 2002, Staumont-Salle et al., 2008). Lipoxygenases are thought to play a role in inflammation (Krieg and Furstenberger, 2014); however the specific role of *ALOX12B* in immune responses/inflammation is not known.

In this study, *RNA-Seq* data supports the hypothesis that *ALOX12B* may be a ligand for PPAR-alpha and the changes caused by *ALOX12B* in epidermal differentiation, barrier formation and inflammation may be mediated by PPAR-alpha.

RNA-Seq data analysis also showed dysregulation of genes involved in lipid metabolism regulated by PPAR-alpha following *TGM1* knockdown. PPAR-alpha is an established transcriptional regulator of transglutaminase (Hanley et al., 1998). Alterations in lipid synthesis and desaturation of fatty acids and acute response inflammatory pathways involving the up-regulation of IL1A and NFkappaB/retinoic acid signaling have been reported in an *in vitro TGM1* knockdown rat model (O'Shaughnessy et al., 2010). Additionally IL1A up-regulation from patient skin scrapings with LI were reported at the protein level. Normally, in response to barrier disruption, trauma and in normal keratinocyte homeostasis, the expression of IL1A and IL1RA are tightly controlled and linked (Wood et al., 1994) and NFkappaB activation is the downstream effect of IL1A up-regulation. It is known that the PPAR transcription factors (Michalik and Wahli, 2007), stimulate synthesis of IL1RA, a direct transcriptional target in response to IL-1 increase (Chong et al., 2009).

It has been reported that *ABCA12* expression is upregulated by ceramides via PPAR delta-mediated signaling pathway (Jiang et al., 2009, Feingold and Jiang, 2011) although PPARbeta/delta, PPAR-gamma and LXR activators all stimulate ABCA12 expression in human keratinocytes in a dose- and time-dependent manner (Jiang et al., 2008). In this dataset, no significant changes in *ABCA12* and nuclear hormone receptors were noted. This could be because the effects of ligand activation on keratinocyte proliferation and differentiation may differ between monolayer cultures, 3D equivalents and the *in vivo* setting.

5.3.2.2 Dysregulation in cornified envelope formation following *TGM1* knockdown

In this study, several genes related to CE and peptide cross-linking as well as calcium ion binding site / calcium ion homeostasis were suppressed. TGM1 participates in the formation

of the cornified envelope by catalyzing calcium-dependent cross-linking of several proteins such as involucrin, loricrin, and proline-rich proteins (Kalinin et al., 2002) (Robinson et al., 1997). The CE is missing when TGM1 activity is reduced or nonexistent (Akiyama et al., 2003, Rice et al., 2005). In keeping with this and also with a proteomic study of a *TGM1* deficient skin-humanized mouse model downregulation of *FLG* and dysregulation in *LOR* was noted. Surprisingly no change in involucrin was observed, confirming the findings of the proteomics study (Aufenvenne et al., 2012).

5.3.2.3 *TGM1* suppression may alter lipid metabolism

Several genes involved in lipid synthesis and metabolism including lipids and lipoproteins, linoleic acid metabolism, fatty acid CoA synthesis and arachidonic acid metabolism, were dysregulated following *TGM1* knockdown in primary keratinocytes. TGM1 is responsible for ceramide (thought to be generated by lipoxygenases) coupling to corneocyte proteins. Although the mechanisms are not well understood, all mutations that cause ARCI (except for transglutaminase) are thought to affect some of the above lipid pathways resulting in metabolite deficiency and substrate accumulation. The changes noted in this dataset may be alluding to secondary (compensatory) defects secondary to barrier disruption caused by loss of *TGM1*. The fact that inactivating mutations in all the ARCI genes produce related skin phenotypes supports the idea that they may have common pathomechanisms. Thus, an alternative explanation may be that LOX (by metabolising linoleate) via a novel-signaling pathway may be upregulating/downregulating transglutaminase thus forming an efficient self-regulating system (Munoz-Garcia et al., 2014).

5.3.2.4 *ALOX12B* affects secretion of LG contents:

Several genes annotated to glycosyltransferase (*ST3GAL5, ST3GAL6, GLT8D2, QPRT*) and vesicle-mediated transport (*ARC, MEGF10, SORL1*) were suppressed. From the study of

ALOX12B mutant mouse skin transplants, it was suggested that 12R-LOX deficiency might affect the processing of LGs (de Juanes et al., 2009). Other studies have reported lipid droplets in the cornified cell layers (Harting et al., 2008, Akiyama et al., 2010), and partially disturbed LG content secretion into the intercellular space in the epidermis of a patient with CIE with *ALOX12B* mutations suggesting that partially disturbed secretion of LG contents is involved in the pathogenesis (Akiyama et al., 2010). This study supports the possibility of *ALOX12B* causing these changes either through an independent signaling pathway or in the same signaling pathway as *ABCA12 (*which is located in LG associated with glycosylceramides) (Sakai et al., 2007).

5.3.2.4 Role of TLR signaling pathway in epidermal development by altering *ABCA12* expression

RNA-Seq analysis found several genes related to epidermal development and cytoskeleton were altered. It has been suggested that ABCA12 deficiency leads to differentiation defects in keratinocytes (Akiyama, 2014). The mechanism by which these abnormalities occur is unknown; Non-coding double-strand RNA (dsRNA) has been reported to induce TLR3-dependent increased expression of ABCA12 in human keratinocytes, resulting in increased epidermal lipid and lamellar bodies (Borkowski et al., 2013). Additionally, noncoding dsRNA can stimulate some events in keratinocyte differentiation that are important for skin barrier repair and maintenance via ABCA12 upregulation (Borkowski et al., 2013). In this dataset TLR signaling pathway was downregulated and several genes involved in defense response were identified possibly explaining the aberrant keratinocyte differentiation.

In summary, *RNA-Seq* analysis of keratinocytes with loss of ichthyosis genes has been successfully employed as a technique to analyze gene expression changes in these cells. Knockdown of *FLG* caused the highest number of dysregulated genes. Gene clusters were found for cell cycle, keratin filament/cytoskeleton, apoptosis, humoral immune response, and

metabolism of lipids and lipoproteins common to all knockdowns. In addition, several genes involved in TLR signaling pathway and cytokine signaling were impaired (tables 5.2-5.7). TLRs, in addition to their role in innate immunity, have been reported to play a role in the epithelial barrier (Kuo et al., 2013a, Borkowski et al., 2015, Lin et al., 2011). On further analysis (sections 6.2.8 and 6.2.9) TLR2 and TLR3 were downregulated in all the ichthyoses and TLR5 was downregulated in both *FLG* and *ICH*. Also, changes were predicted in the pro-inflammatory cytokines IL6 and IL8. Thus, the *RNA-Seq* data was validated at protein level (chapter 7) by assessing cytokine profile secretion in unstimulated or stimulated primary keratinocytes (following stimulation of TLR2, 3, 5).

5.4 Future work

RNA-Seq can only provide information at the level of the transcript, therefore it is important to confirm gene expression changes at the protein level. This can be achieved by proteomic analysis for each ichthyosis gene knockdown. Innate immune systems were further investigated in this study (common to all the knockdowns). In the future it will be important to investigate other biological functions identified in this study in order to ensure that new insights are not neglected. It might be possible to integrate the RNA-Seq data with proteomic data, as altered RNA transcript expression does not always translate into changes at the protein level.

Chapter 6: Transcriptome Analysis-Heat Maps

6.1 Introduction

A heatmap can graphically visualize the matrix data by representing individual values with different colours. For visualization, a heat map compacts large amounts of information into a small space to bring out coherent patterns in the data (Weinstein, 2008). This can is useful as it allows selection of regions of interest for further study.

Coherent patterns (patches) of colour can be generated by hierarchical clustering on both horizontal (and vertical axes) to bring like together with like (Weinstein, 2008). Cluster relationships are indicated by tree-like structures adjacent to the heat map, and the patches of colour may indicate functional relationships among genes and samples (Weinstein, 2008). The heat map is one of the most widely used graphs in the biological sciences (Weinstein, 2008).

Recent progress in high-throughput techniques, such as next generation sequencing (NGS) has increased the demand for the visualization of data (Deng et al., 2014) to aid in the recognition of meaningful association patterns involving complex relations between genetics and biological features (Haarman et al., 2015).

In this project, heat maps were generated using the ggplot package in Bioconductor (Gentleman et al., 2004, Huber et al., 2015, Wickham, 2009) in collaboration with the Enright group at European Bioinformatics Institute, Hinxton (http://www.ebi.ac.uk/research/enright). The level of expression of known genes, obtained from NGS, associated with different biological processes (identified by literature review by myself) were represented. Triplicate samples for each knockdown and non-targeting control, C, were analysed. Heatmaps are plotted using the normalized gene expression data i.e. mean centralized using all 27 samples. Each heat map was drawn using this data. Mean centralization was done to visualize deviation

of gene expression in a specific sample from the genes' average across all samples. Thus, genes, which are unchanged, were displayed as white. Up-regulated genes were displayed as red. Down-regulated genes were displayed as blue. The variability colour pertaining to each *in vitro* model (sample) was indicative of how much a gene was expressed in that particular sample. A histogram for each heat map shows fold change on the x-axis (value) and gene counts on the y-axis (count).

6.2 Results

6.2.1 Impact of knock-down on other Ichthyosis genes in this study

Heat maps were made to evaluate the impact of knock-down on other ichthyosis genes.

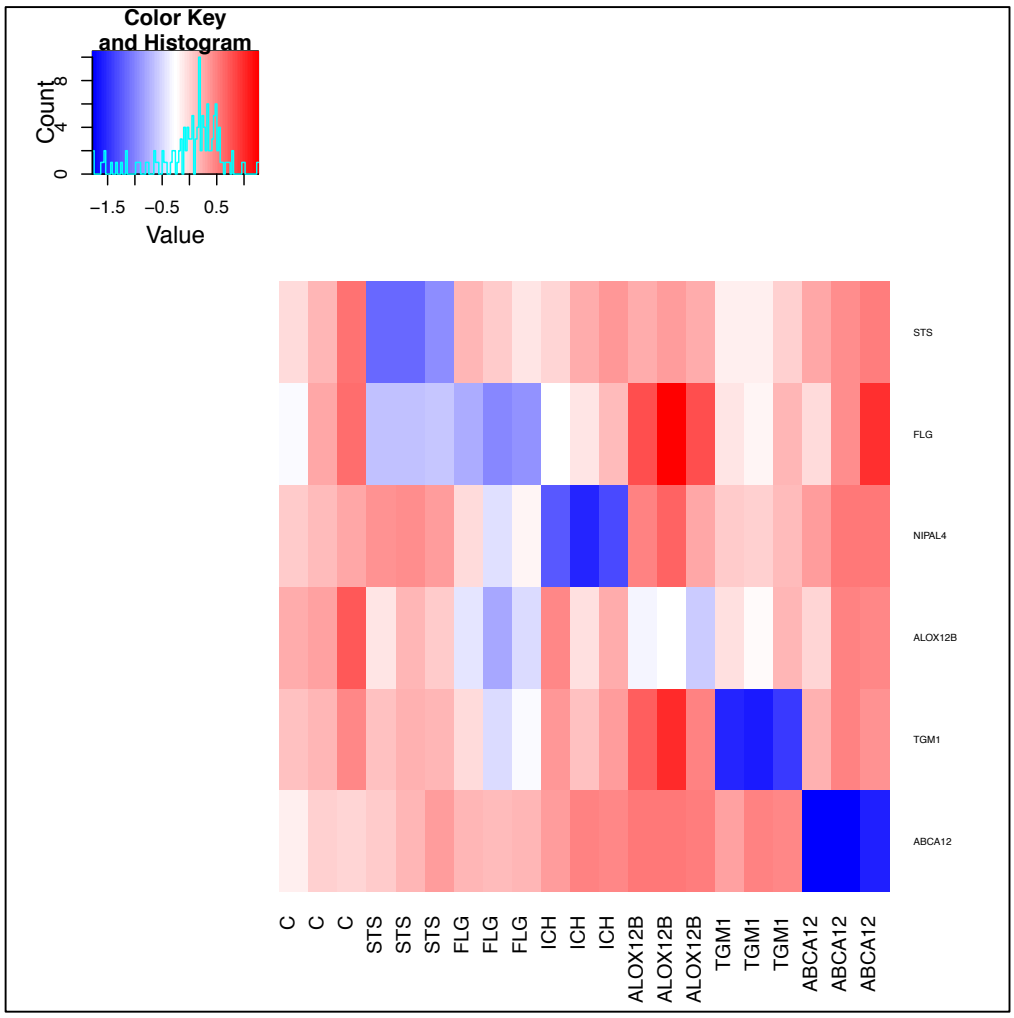

Figure 6.1: Heatmap showing gene expression of *STS, FLG, TGM1, ALOX12B, ICHTHYIN,* and *ABCA12* following *STS, FLG, TGM1, ALOX12B, ICHTHYIN,* and *ABCA12* knockdown.
Reduced expression of the individual genes (blue) following knockdown, compared to C, is seen in *STS, FLG, TGM1, ALOX12B, ICHTHYIN,* and *ABCA12* respectively. Upregulation (red) and downregulation (blue) of other genes is noted following knockdown.

In each ichthyosis studied there is downregulation compared to control. In the *STS* knockdown there was downregulation of *FLG* but this was not significant. *FLG* knock-down showed no changes in *STS* expression but there was downregulation of *ALOX12B* (log2FC -1.26, pval<0.01), *TGM1* (log2FC -1.01, pval<0.01) and *ICH*. In *ALOX12B* knockdown there was upregulation of *FLG, ICH* and *TGM1* but these were not significant. A slight non-

significant downregulation of *STS, FLG* and *ALOX12B* was noted in *TGM1* knockdown. No interactions were noted in the *ICH* and *ABCA12* knockdown models. These findings suggest that there are some interactions between the ichthyosis genes.

6.2.2 Interactions between known genes causing ARCI (LI/CIE) phenotype

Several genes (other than those studied in this project) have been implicated in the pathogenesis of ARCI (section 1.5.2). Interactions between the ichthyosis knockdowns and these genes were evaluated.

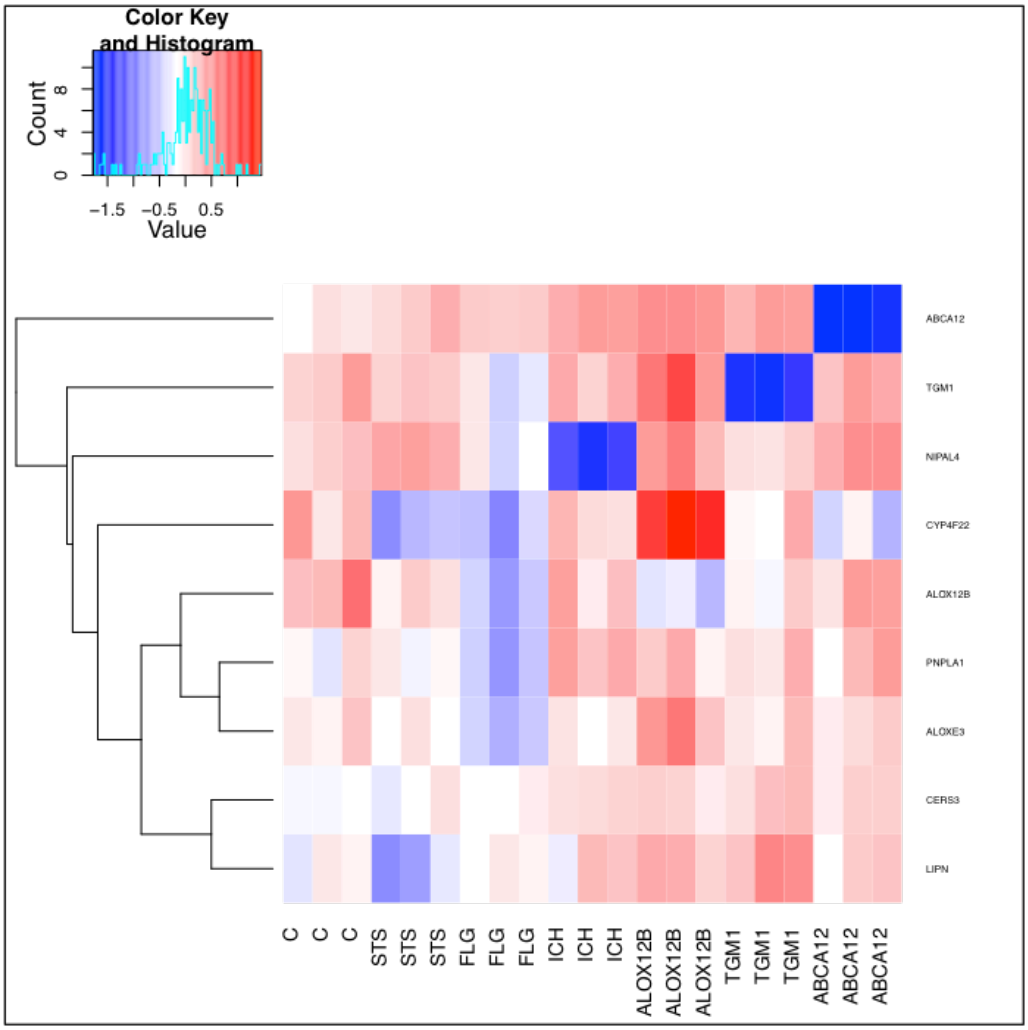

Figure 6.2: Heatmap showing impact of ichthyosis gene knockdown on expression of other known genes causing ARCI.

STS silencing lead to downregulation of *LIPN* (log2FC -1.22, pval<0.01) and *CYP4F22*

(log2FC -2.06, pval<0.01). Several genes were significantly downregulated in *FLG* knockdown including *ALOXE3* (log2FC -1.04, pval<0.01), *PNPLA1* (log2FC -1.22, pval<0.01) and *CYP4F22* (log2FC -1.26, pval<0.01). *CYP4F22* expression was reduced in *ABCA12* knockdown (log2FC -1.51, pval<0.01). Thus, interactions were seen between CI and ARCI genes and between two ARCI genes-*ABCA12* and *CYP4F22*.

6.2.3 Dysregulation of Epidermal Differentiation Complex (EDC)

Many proteins essential for epidermal differentiation are encoded by genes clustered on human chromosomal region 1q21 (Mischke et al., 1996). The genes constitute the EDC. It is known that mutations in the EDC genes are the strongest risk factors for atopic dermatitis (FLG genes) and faulty formation of the CE (*TGM1* deficiency) causes lamellar ichthyosis (Kypriotou et al., 2012). Heat maps were generated to evaluate changes in the EDC genes in the ichthyosis knock-downs.

The clustered organization of the EDC genes suggests duplication of ancestors adapting to changes in terrestrial conditions during evolution (Backendorf and Hohl, 1992). The EDC is divided on the basis of common gene and protein structures, into three clustered gene families (Kypriotou et al., 2012):

(i) S100A calcium-binding proteins;

(ii) Cornified Envelope (CE) precursors-a group of precursor proteins of the CE including involucrin, loricrin, the SPRRs and the 'late cornified envelope' (LCE) proteins (previously LEP, XP5 and SPRRL), and

(iii) S100 fused genes. The 'fused gene' proteins (SFTPs 'S100 Fused Type Proteins') *FLG*, filaggrin-2 (*FLG2*), trichohyalin (*TCHH*), trichohyalin-like protein (*TCHHL1*), hornerin (*HRNR*), repetin (*RPTN*) and cornulin (*CRNN*) evolved from families (i) and (ii).

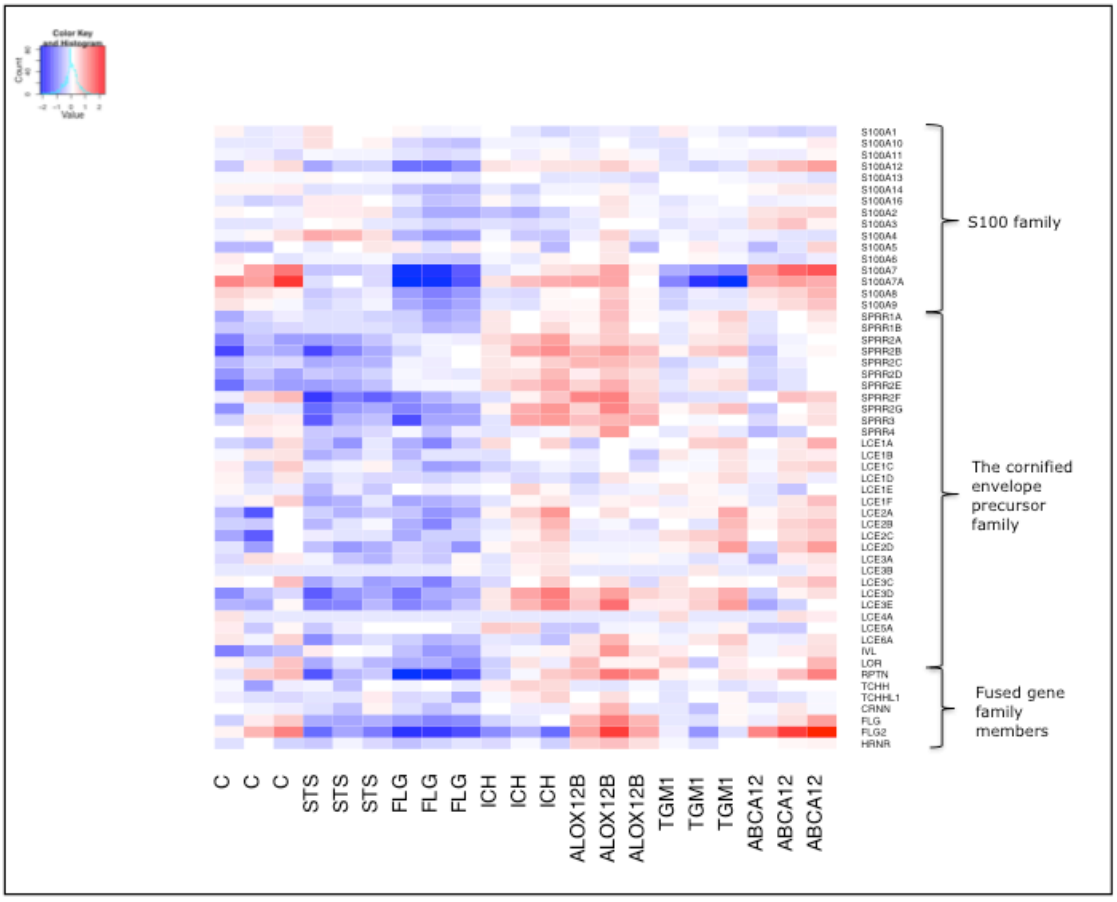

Figure 6.3: Heatmap showing expression of the Epidermal Differentiation Complex genes following *STS, FLG, TGM1, ALOX12B, ICHTHYIN,* and *ABCA12* knockdown.

UCSC Genome Bioinformatics (http://genome.ucsc.edu) was used to generate a list of genes listed on human chromosomal region 1q21. Several genes are significantly downregulated in the common ichthyoses: In *FLG* knockdown a subset of S100 genes [(*S100A2* (log2FC -1.03, pval<0.01), *S100A4* (log2FC -1.32, pval<0.01), *S100A7* (log2FC -2.28, pval<0.01), *S100A8* (log2FC -1.20, pval<0.01), *RPTN* (log2FC -2.81, pval<0.01), *FLG2* (log2FC -3.17, pval<0.01) and *LOR* (log2FC -2.50, pval<0.01)). There is significant downregulation in several other EDC genes in *STS* knockdown *[S100P* (log2FC -1.16, pval<0.01), *RPTN* (log2FC -1.69, pval<0.01) and *FLG2* (log2FC -2.32, pval<0.01)]. A number of EDC genes were also significantly dysregulated in the ARCI; downregulation in *TGM1* [(*S100A7* (log2FC -1.29, pval<0.01), *FLG2* (log2FC -1.55, pval<0.01)) and *ICH* [(*FLG2* (log2FC -2.18,

pval<0.01)) and upregulation in *ALOX12B [(HRNR* (log2FC -1.09, pval<0.01)) knockdowns. Thus, there appears to be significant dysregulation in EDC mRNA expression in the CI and ARCI. Interestingly, there was down regulation of all the EDC genes following *FLG* knockdown.

6.2.3.1 Regulation of EDC

The expression of genes of the EDC is regulated by a pool of transcription factors: Krüppel-like factor 4 (*KLF4*), grainyhead-like 3 (*GRHL3*), and aryl hydrocarbon receptor nuclear translocator (*ARNT*) (Kypriotou et al., 2012). The relationship between the EDC regulatory genes and the knockdowns was evaluated.

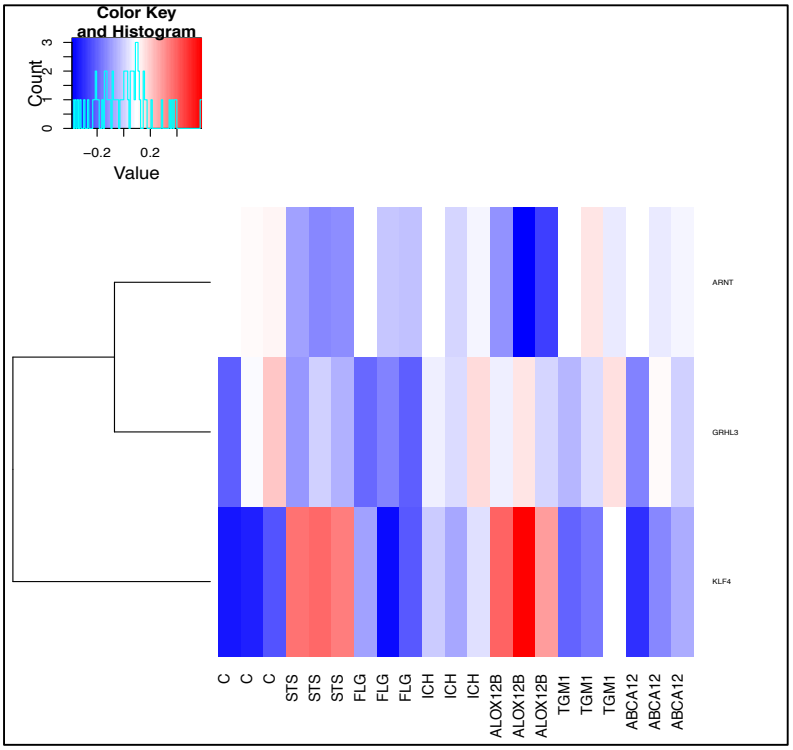

Figure 6.4: Heatmap showing impact of *STS, FLG, TGM1, ALOX12B, ICHTHYIN,* and *ABCA12* knockdown on genes involved in regulating the EDC.

ICH silencing causes significant upregulation of *ARNT* (log2FC 1.11, pval<0.01). Changes were noted in the common ichthyosis genes and *ALOX12B* knockdowns (non significant); in the *STS* knockdown *KLF4* expression was up-regulated whereas *GRHL3* and *Arnt* were down-

regulated. In the *FLG* knockdown there was downregulation of *GRHL3* and *ARNT*. In *ALOX12B* knockdown *KLF4* expression was up-regulated but *ARNT* was down-regulated.

6.2.4 1q21 GENES (not EDC)

Heat maps were also generated for the remaining genes on chromosomal human region 1q21.

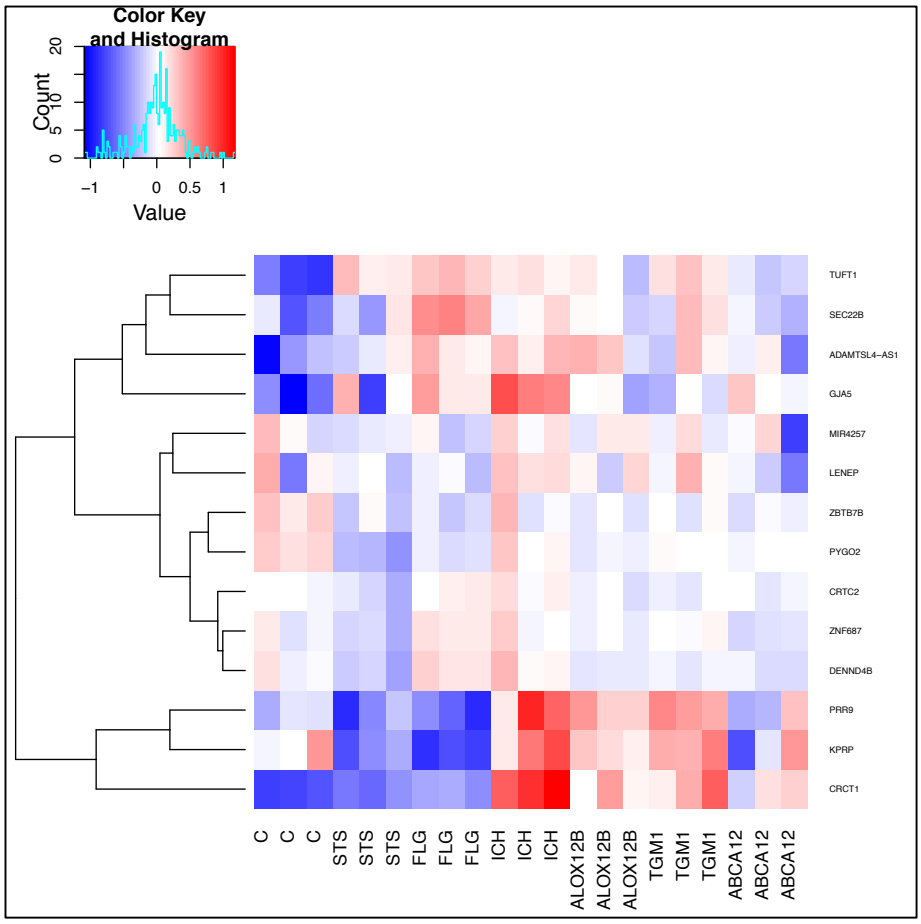

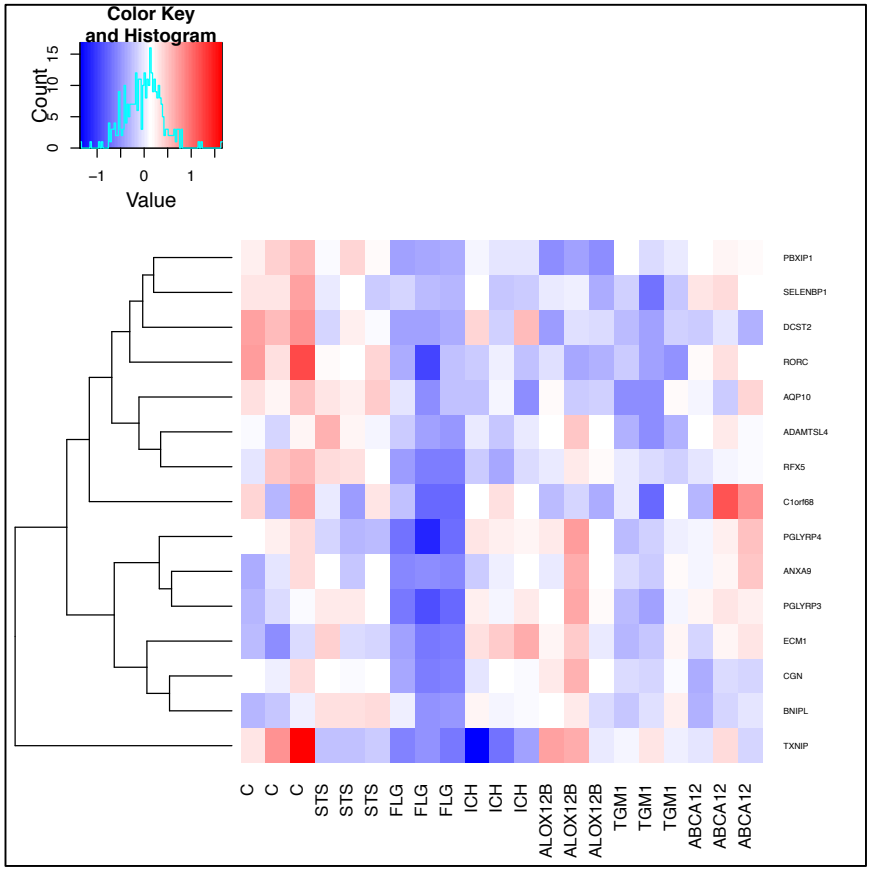

Figure 6.5: Heatmap showing gene expression of genes on 1q21 (not included in EDC) following *STS, FLG, TGM1, ALOX12B, ICHTHYIN,* and *ABCA12* knockdown.

In *STS* and *FLG* knockdowns there was downregulation of *TXNIP* (log2FC -1.69, pval<0.01 and log2FC -1.94, pval<0.01 respectively). Other downregulated genes noted in *FLG* knockdowns were *PGLYRP3* (log2FC -1.34, pval<0.01), *PGLYRP4* (log2FC -1.29, pval<0.01), *C1orf68* (log2FC -3.69, pval<0.01). *ALOX12B* silencing lead to *C1orf68* (log2FC -2.84, pval<0.01) downregulation. This suggests that several genes on chromosome 1q21 outside the EDC are dysregulated in the CI and *ALOX12B* knockdown; Almost all the non-EDC genes on 1q21 were downregulated following *FLG* knockdown.

6.2.5 Cytokeratin downregulation common to all the ichthyoses

Changes in keratins have been reported in the ichthyosis [(Toivola et al., 2015, Chamcheu et al., 2011), Table 1]; Upregulation of K1 has been reported in LI and IV (O'Shaughnessy et al.,

2010) and *KRT1* downregulation is known in HI (Grone, 2002) and in several other non-syndromic ichthyosis (Table 1).

Keratins are structural proteins found in all epithelial cells to which they confer stability when under mechanical stress. Keratins are grouped into two classes, the acidic type I (K9-K20) and the neutral-basic type II (K1-K8) which are expressed in pairs in a tissue and differentiation-specific manner (Smith et al., 2003). Keratin 5 (*KRT5)* and *KRT14* are both expressed in the basal layers of the epidermis, but are down-regulated and replaced by the expression of *KRT1* (*KRT2* in upper spinous and granular layer; *KRT9* in palmoplantar) and *KRT10* in suprabasal keratinocytes (Schnare et al., 2001). Keratin 15 (*KRT15*), is a type I keratin without a defined type II partner. *KRT15* has been shown to be a basal epidermal stem cell (Takeda et al., 2003) and its expression is normally down regulated with epidermal differentiation.

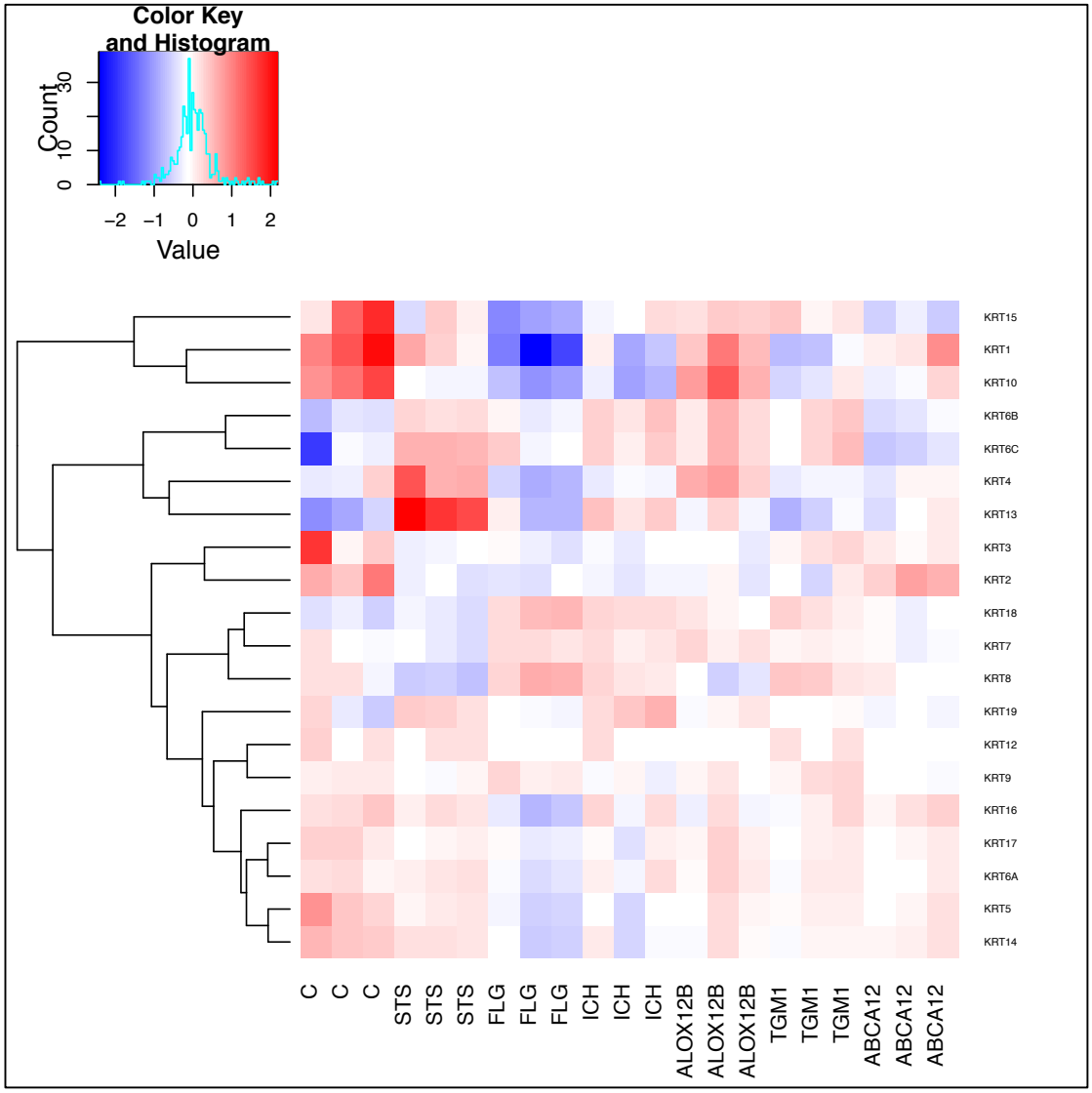

Figure 6.6: Heatmap showing gene expression of cytokeratin genes following *STS, FLG, TGM1, ALOX12B, ICHTHYIN,* and *ABCA12* knockdown.

KRT1 was significantly downregulated in **all** the ichthyoses. Its pairing partner *KRT10* was also downregulated in all the ichthyoses but this was significant in *ICH*, *TGM1, FLG* [(log2FC -1.39, pval<0.01), (log2FC -1.007, pval<0.01) and (log2FC -1.67, pval<0.01) respectively]. The other pairing partner, *KRT2* is downregulated in all knockdowns but this was significant in *STS, FLG* and *ICH* [*STS* (log2FC -1.23, pval<0.05), *FLG* (log2FC -1.37, pval<0.05) and *ICH* (log2FC -1.31, pval<0.01)] other than in *ABCA12*. Basal keratins *KRT5* and *14* were downregulated in all the ichthyoses but *KRT14* expression suppression was significant in *FLG* knockdown (log2FC -1.009, pval <0.01). *KRT15* expression was also

downregulated in all the ichthyoses but was most pronounced in *FLG* and *ABCA12* knockdowns. Upregulation of K1 has been reported in LI (O'Shaughnessy et al., 2010) and *KRT1* downregulation is known in HI (Grone, 2002). Thus, K1 downregulation underlies all the ichthyosis in this study at transcriptome level and this is significant.

6.2.6 Desmosomal Dysregulation

Ichthyin has been found to localise to desmoplakin throughout the viable epidermis (Dahlqvist et al., 2012). Netherton syndrome (OMIM #256500) characterized by congenital ichthyosiform erythroderma, an atopic diathesis, and a characteristic hair-shaft abnormality known as trichorrhexis invaginata is caused by serine protease inhibitor lympho-epithelial Kazal-type-related inhibitor LEKTI (encoded by *SPINK5)* (Sarri et al., 2016) and it is thought that there is premature cleavage of desmosomal proteins (including desmocollin1 (DSC1), desmoglein 1 (DSG1) and corneodesmosin) (Yang et al., 2004, Descargues et al., 2005, Descargues et al., 2006). Changes in desmosomal genes were evaluated in the ichthyosis knockdowns.

Desmosomes are “mechanical” junctions, involved primarily in cell cohesion (Yamamoto et al., 2003a) required for the integrity of epidermis. Desmosomal proteins interact with keratins, 1(2)/10 in the suprabasal layers of the epidermis and provide cytoskeletal structure (Fox et al., 2008). Additionally, they contribute to the correct formation and maintenance of the *stratum corneum* barrier.

The structural components of the desmosomes involve three protein families: Desmosomal cadherins (desmogleins DSGs and desmocollins DSCs), armadillo proteins (desmoplakin DSP and plakoglobin JUP), and the plakophilin family (PKP 1 to PKP 3) (Takeuchi et al., 2000).

Desmosomal cadherins located on adjacent cells mediate intercellular connection via interactions of their extracellular domains. The intracellular ends of desmosomal cadherins are inserted in the molecular network of adaptor proteins, DSP, JUP, PKP 1-3, to which keratin filaments bind.

DSG1-4 and DSC1-3 are expressed in the epidermis. According to the level of keratinocyte differentiation, DSG2 and 3 from the lower epidermal compartment are progressively substituted by DSG1 and 4 in the upper viable epidermal layers. In the same way DSC3 is replaced by DSC1. PKP1, 3 are expressed throughout the viable epidermis but expression is most prominent in the SG (Takeuchi et al., 2000). PKP2 expression is found in the SB only (Yamamoto et al., 2003a).

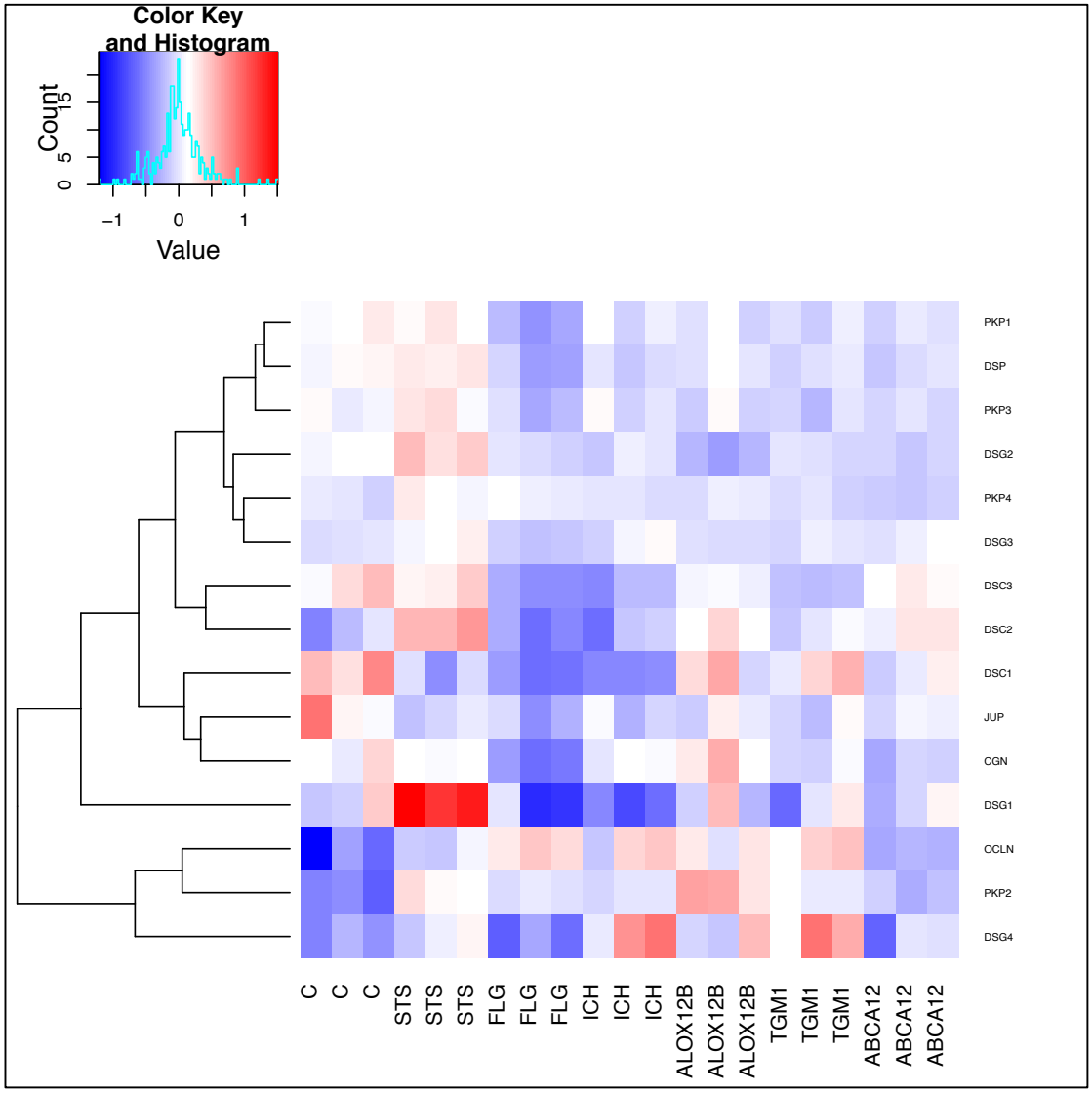

Figure 6.7: Heatmap showing changes in desmosomal genes following *STS, FLG, TGM1, ALOX12B, ICHTHYIN,* and *ABCA12* knockdown.

Dysregulation (downregulation predominantly) of several desmosomal genes in the common ichthyosis knockdowns was noted throughout the viable epidermis: in *STS* knock-down there was upregulation of desmosomal cadherins *DSG1, DSG2, DSC2, DSC3* and downregulation of *DSG4* expression. Additionally, *PKP2, PKP3* and *DSP* were upregulated. In the FLG knock-down downregulation of *DSC1* (log2FC -1), *DSC2* (log2FC -1.04), *DSC3* and *DSG1, DSP, PKP1, PKP3* was seen. In *ICH* knock-down the SG desmosomal cadherins were altered; *DSG1, DSC1* were downregulated but *DSG4* was upregulated. *PKP2* was upregulated in *ALOX12B*. Thus, significant alterations in desmosomal genes were noted.

6.2.7 Antimicrobial peptides (AMP)

Ichthyosis can be complicated by secondary infection (Grahovac et al., 2009, Fleckman et al., 2003). AMP are one of the primary mechanisms used by the skin in the early stages of immune defense to prevent infection from bacteria, viruses and fungi. The production of AMP such as the S100 proteins, psoriasin (S100A7) (Akiyama, 2010) and calprotectin (S100A8/A9 complex) (Umemoto et al., 2011) as well as RNase 7 (Harder and Schroder, 2002) occurs constitutively in the epidermis. Upon recognising the microbe e.g. by TLRs, keratinocytes initiate a defense response by further inducing already present AMP and increasing expression of inducible AMPs such as human beta-defensins DEFB4A, DEFB103A, DEFB103B and the cathelicidin CAMP (LL-37) (de Koning et al., 2012). The impact of the knockdown on AMPs was evaluated.

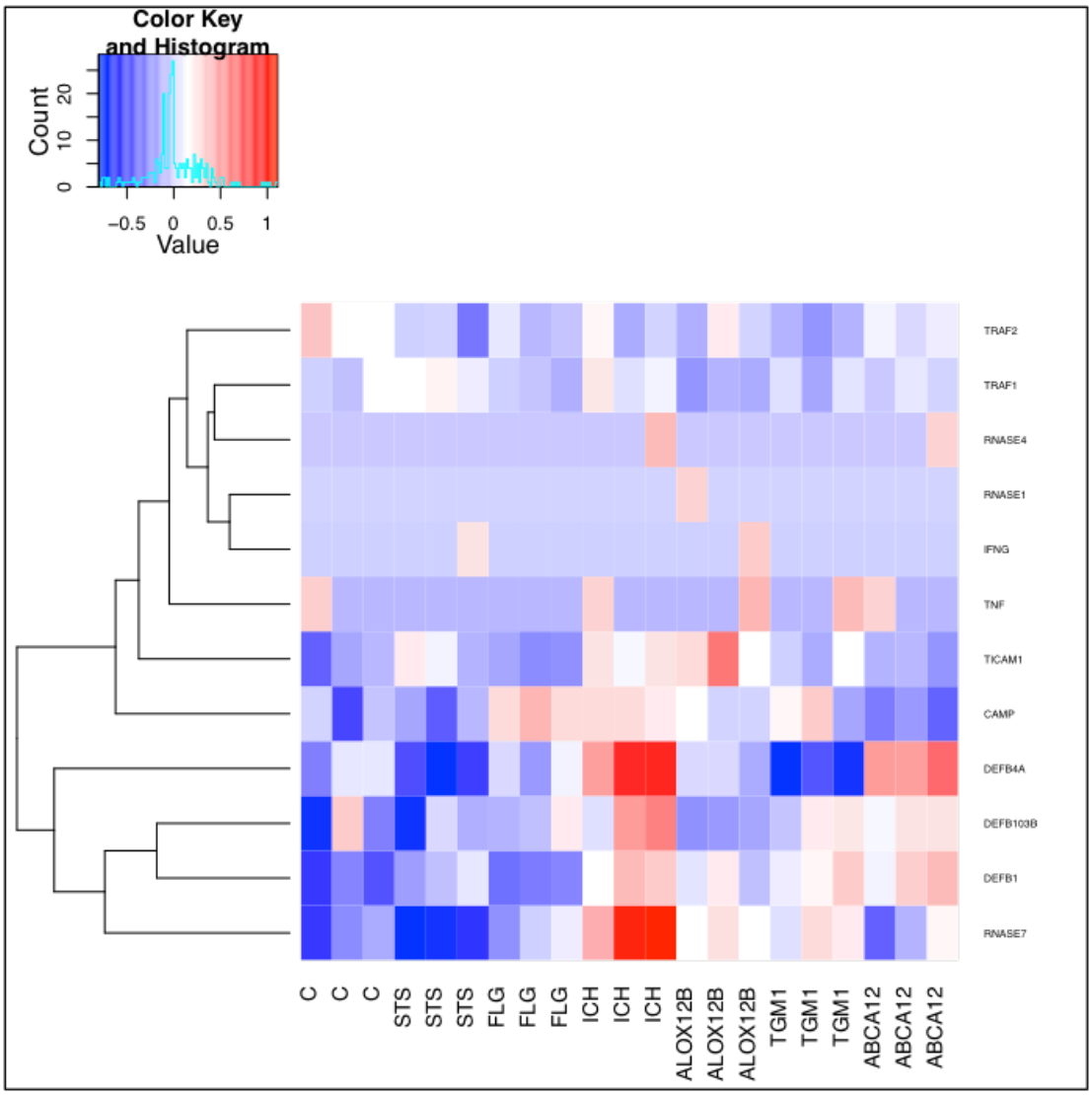

Figure 6.8: Heatmap of changes in gene expression of antimicrobial peptide genes following *STS, FLG, TGM1, ALOX12B, ICHTHYIN,* and *ABCA12* knockdown.

In our dataset, several beta-defensin genes were down regulated. *DEFB4A* (log2FC -1.06, pval<0.01) and *DEFB4B* (log2FC -1.17, pval<0.05) in *TGM1* knockdown. *DEFB4A* in *STS* knockdown (log2FC -1.01, pval<0.01) and *DEFB103B* (log2FC -1.907, pval<0.05) in *ALOX12B* knockdown. Upregulation of *DEFB1, DEFB4A* and *DEFB103B* was seen in *ICH* and *ABCA12* knockdowns but this was not significant. The constitutive AMP, *S100A7* (log2FC -2.28, pval<0.01) and the *S100A8/A9* complex (log2FC -1.2, pval<0.01 / log2FC -1.07, pval<0.01) were downregulated in *FLG*. *S100A7* (log2FC -1.29, pval<0.01) is downregulated in *TGM1* (EDC heatmap, Fig. 6.5).

6.2.8 Toll-like Receptors (TLR)

Human Toll-like receptors (TLRs, numbered 1–10) are found on a variety of different cell types and can recognise various components of microorganisms, subsequently initiating signaling pathways important in the generation of cytokines, chemokines, antimicrobial peptides, and upregulation of adhesion and costimulatory molecules involved in innate and acquired immune responses (Jones et al., 2004). In addition to their antimicrobial effects the function of TLRs has recently extended to include epithelial barrier regulation (Kuo et al., 2013a). Keratinocytes are reported to express TLRs 1,2,3,5,9 and 10 (Hari et al., 2010); the evidence supporting TLR4 expression is conflicting (Hari et al., 2010). In addition, TLRs on keratinocytes are functional and respond to their respective ligands to produce cytokines implying that keratinocytes can initiate immune responses via activation of TLRs (Chong et al., 2004, Yamamoto et al., 2003b); thus TLR2 heterodimererises with TLR1 and recognises bacteria-derived lipoproteins, TLR3 recognizes viral double-stranded RNA, TLR4 recognizes lipopolysaccharide of Gram-negative bacteria and TLR5 recognizes bacterial flagellin (Miller, 2008).

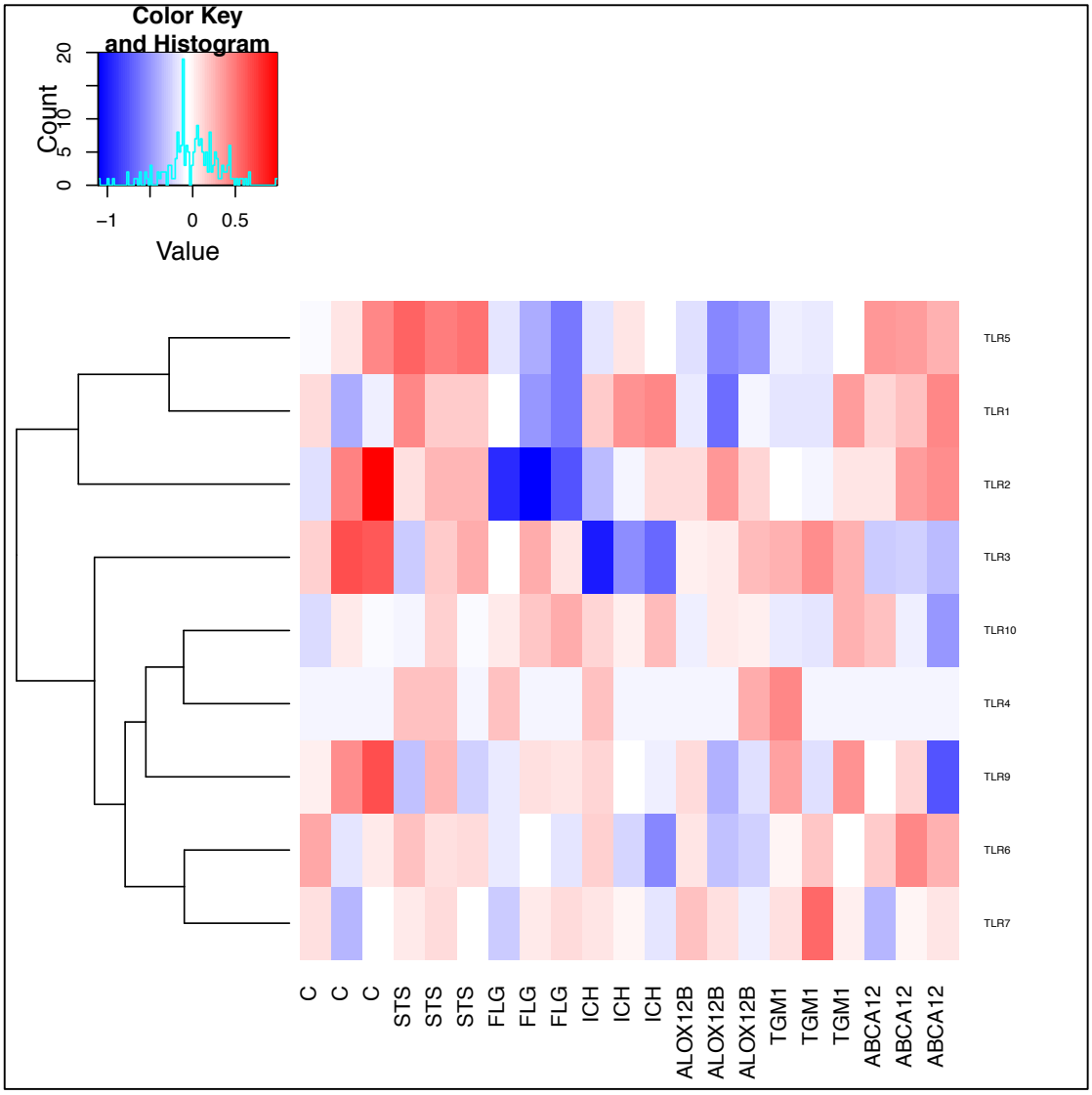

Figure 6.9: Heatmap of gene expression of toll-like receptors following *STS, FLG, TGM1, ALOX12B, ICHTHYIN,* and *ABCA12* knockdown.

In our dataset there is downregulation of *TLR2* and *TLR3* in all the ichthyoses but this is most marked in *FLG* for *TLR2* (log2FC -1.412, pval<0.01) and *ICH* for *TLR3* (not significant). *TLR1* and *TLR5* are downregulated in both *FLG* and *ICH*.

6.2.9 Cytokines

Cytokine production influences keratinocyte proliferation and differentiation processes and may have pleiotropic effects on the immune system (Nedoszytko et al., 2014). Cytokines are produced by keratinocytes, either constitutively or upon exposure to viral or bacterial stimuli (Uchi et al., 2000, Grone, 2002). Altered epidermal cytokine production has been noted after

barrier disruption and may play a role in restoring the cutaneous permeability barrier (Wood et al., 1992) by influencing keratinocyte proliferation and differentiation, atleast in part by modulating the gene expression in these cells (Hanel et al., 2013). The impact of the ichthyosis knockdowns on cytokines was analysed.

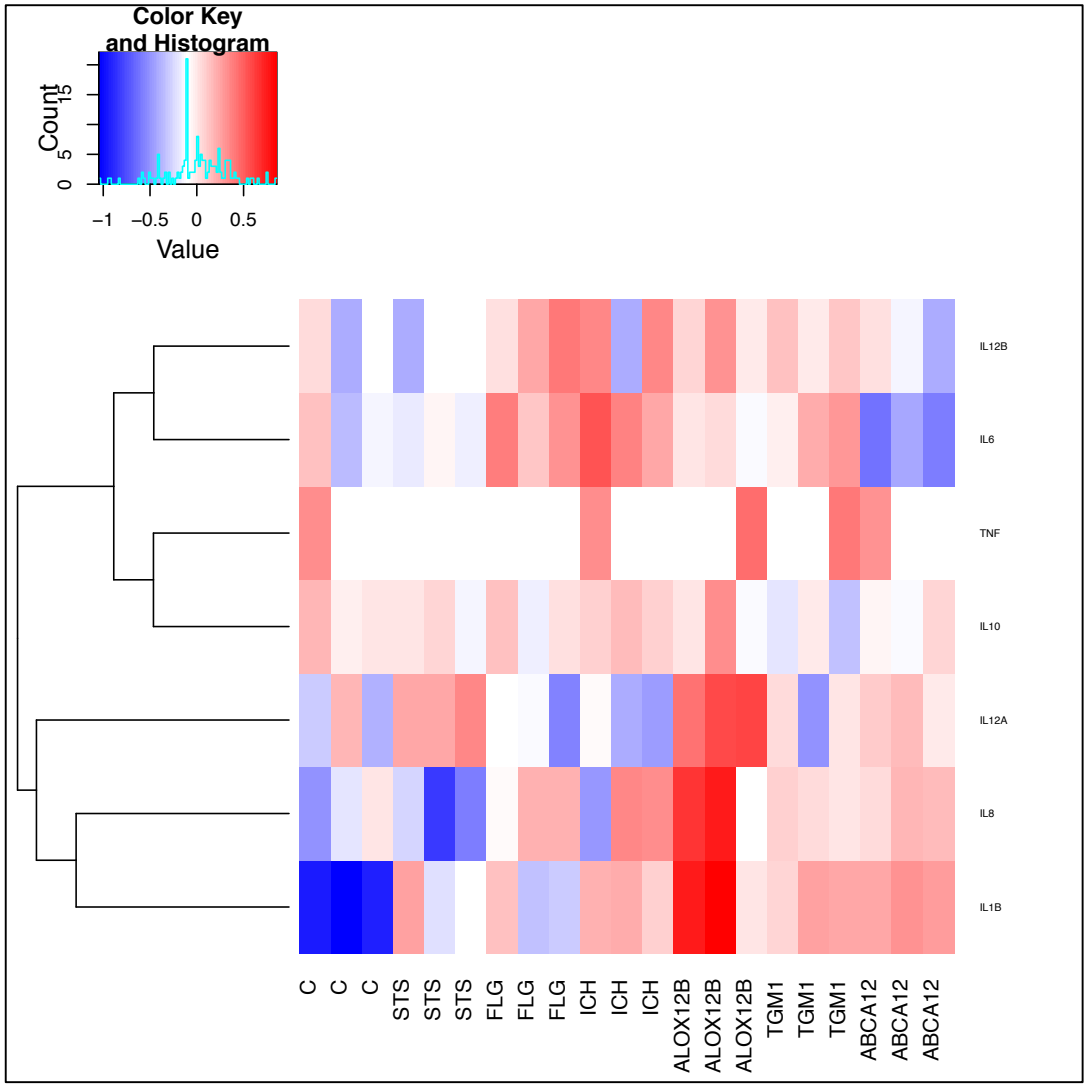

Figure 6.10: Heatmap of impact of *STS, FLG, TGM1, ALOX12B, ICHTHYIN,* and *ABCA12* knockdown on expression of cytokine genes.

In this study, *IL12A* was downregulated in *FLG* (log2FC -1.39, pval<0.01) and in *ICH* (log2FC -1.46, pval<0.01). Other trends noted were that the pro-inflammatory cytokine *IL6* was upregulated in all knock-downs compared to control except in *ABCA12* where it was

down-regulated (log2FC -1.25, pval<0.01). The pro-inflammatory cytokine *IL8* was upregulated in all knock-downs compared to control except in *STS* where it was down-regulated.

6.2.10 Kallikreins (KLKs)

Desquamation (detachment of the superficial corneocytes) requires proteolytic degradation of corneodesmosomes which form connections between corneodesmosomes and is mediated by a cocktail of proteases including serine proteases. Tissue KLKs are the largest family of human secreted serine proteases encoded by 15 genes (Paliouras and Diamandis, 2006). Several kallikreins are expressed in the upper stratum granulosum (SG) and stratum corneum (SC) of the epidermis, including KLKs 1,3,5-11, 14,15 (Shaw and Diamandis, 2007). Kallikrein proteolytic activity in the skin is mostly attributed to the trypsin-like proteases KLK5 and KLK14 and the chymotrypsin-like protease KLK7. In XLI desquamation is thought to be retarded by KLK5 and KLK7 (section 1.4.2.5) and reduction in KLK5 in HI skin has been noted (section 1.5.1.6). The impact of the ichthyosis knockdowns on the KLKs was evaluated.

.

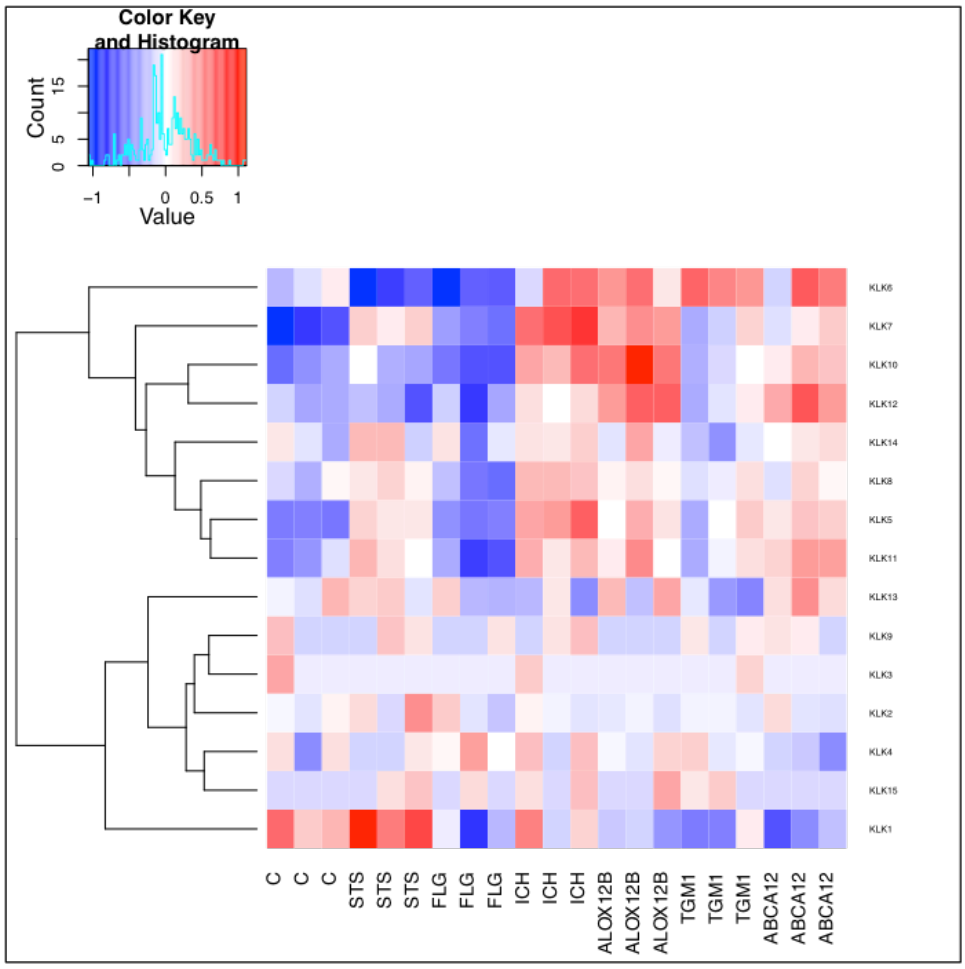

Figure 6.11: Heatmap of gene expression changes in kallikreins after *STS, FLG, TGM1, ALOX12B, ICHTHYIN,* and *ABCA12* knockdown.

KLK6 was significantly down regulated in the common ichthyoses *STS* (log2FC -1.61, pval<0.01), *FLG* (log2FC -1.65, pval<0.01) and upregulated in the ARCI. *KLK1* was significantly downregulated in *FLG* (log2FC -1.63, pval<0.01) and several ARCI knockdowns *ALOX12B* (log2FC -1.46, pval<0.01); *TGM1* (log2FC -1.48, pval<0.01); *ABCA12* (log2FC -1.86, pval<0.01). *KLK* 5 and 7 showed upregulation in all the ARCI and *STS* knockdowns and a slight upregulation in *KLK14* was seen in *ICH* and *ABCA12* knockdowns but these changes were not significant.

6.2.11 Lipids

The permeability barrier resides in the SC which is composed of corneocytes embedded in a

matrix of lipid-enriched lamellar sheets. Impairment of the skin permeability barrier leads to several cutaneous disorders, including ichthyosis. SC lipids consist free fatty acids (FA), ceramides and cholesterol in nearly equimolar ratios (Lampe et al., 1983). The adequate balance of these major components is imperative for a proper structure and maintenance of SC barrier competence (Janssens et al., 2011). The impact of the ichthyosis knockdowns on the known SC lipid genes involved in synthesis, activation (where applicable) and transportation were evaluated.

6.2.11.1 FA Transportation/Activation

Fatty acids (FA) used in the epidermis can be synthesized *de novo* by keratinocytes or taken up from the diet or extracutaneous sites of the body (e.g. linoleic acid and other essential fatty acids are unable to be synthesized by keratinocytes) in a process that likely involves protein transporters. Several proteins have been proposed to facilitate FA uptake including fatty acid translocase (FAT/CD36) (Weinstein, 2008), fatty acid binding protein (FABP) (O'Shaughnessy et al., 2010), and members of the fatty acid transport protein/very long-chain acyl-CoA synthetase (FATP/ACSVL) family (Cuzick et al., 2013).

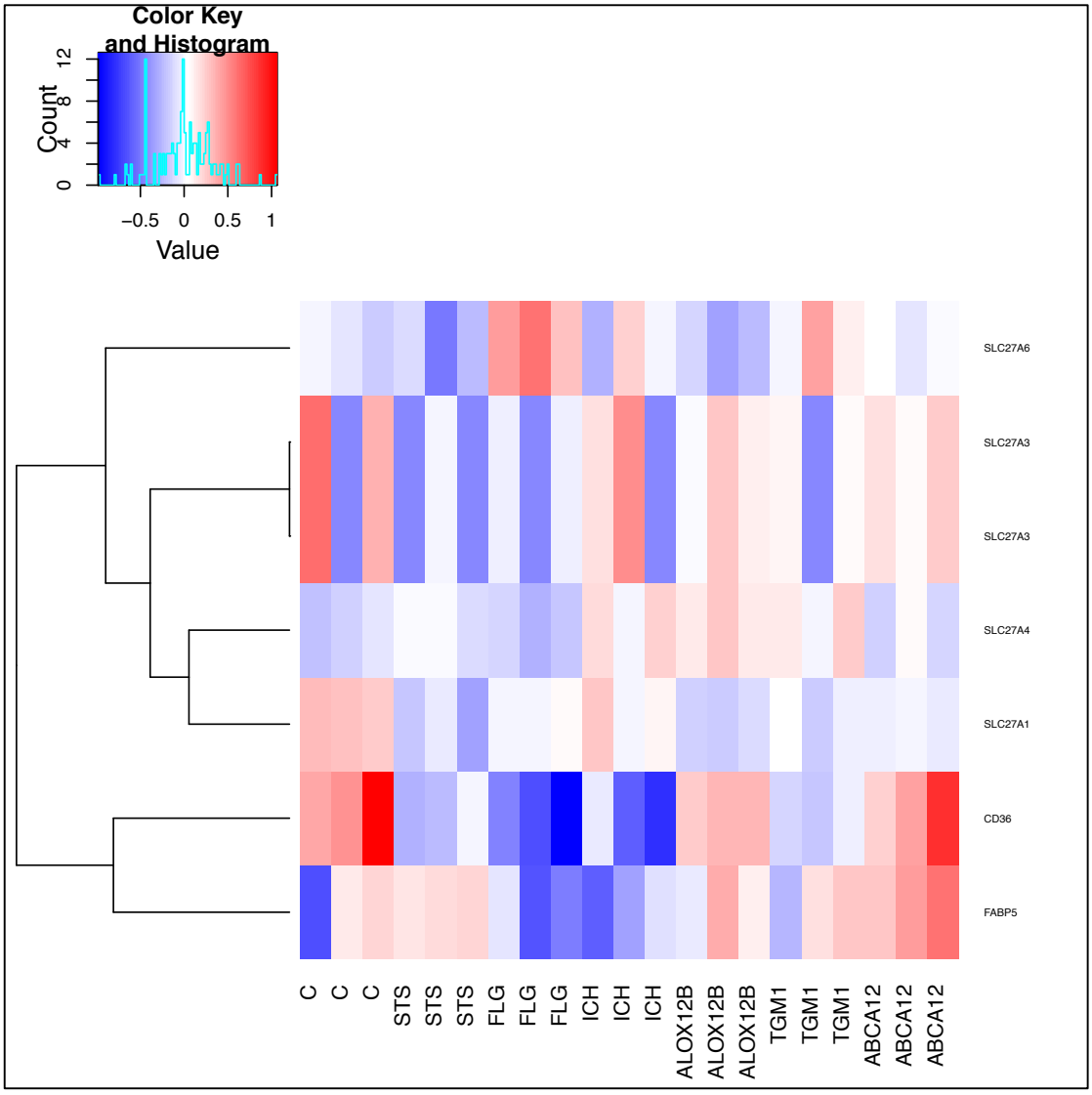

Figure 6.12: Heatmap showing alteration in expression of genes involved in FA transportation/activation after *STS, FLG, TGM1, ALOX12B, ICHTHYIN,* and *ABCA12* knockdown.

6.2.11.1.1 FAT/CD36

FAT/CD36 functions as a transmembrane protein that facilitates the translocation of FA across the plasma membrane (Maloney et al., 1984). It is not normally expressed in human epidermis, but it is detected in skin lesions of patients with ichthyosis vulgaris (IV), psoriasis and several other dermatological diseases (Grone, 2002) (Rearick et al., 1987). In this dataset there is downregulation of *CD36* in the common ichthyoses i.e. *STS* and *FLG* (log2FC -1.27, pval 0.01) and *ICH* and *TGM1* knockdowns.

6.2.11.1.2 FABP5

In contrast to *CD36 FABP5* is expressed in the normal epidermis (Epstein et al., 1984). *FABP5* expression was downregulated in *FLG* (log2FC -1.07, pval 0.01) and *ICH* (log2FC -1.02, pval 0.01). In contrast its expression is upregulated in psoriasis and eczema (Yanagi et al., 2011) (Zuo et al., 2008) possibly highlighting the differences in pathomechanisms of the barrier diseases.

6.2.11.1.3 SLC27A /FATP

The FATP family consists of six integral membrane proteins that are encoded by solute carrier family 27 member 1 to 6 genes (*SLC27A1* to *SLC27A6*). *SLC27A1, -3, -4,* and *-6* are normally expressed in human epidermis (Akiyama et al., 2005). In addition to FA transportation SLC27A/FATP proteins play a central role in activation of fatty acids. Activation of FA is a pre-requisite before they can be directed to different metabolic pathways (Watkins and Ellis, 2012).

6.2.11.1.3.1 SLC27A4/FATP4

A recent report of a functional linkage between *SLC27A4* and *ICH* highlighted the possible involvement of *SLC27A4* in common pathways essential for lipid processing in the epidermis (Li et al., 2013). SLC27A4 has also been implicated in a syndromic ARCI, ichthyosis prematurity syndrome. It is up-regulated in several ARCI (*ICH/ALOX12B/TGM1*).

6.2.11.1.3.2 SLC27A Others

SLC27A1 (or *FATP1*) is the most closely related protein to *SLC27A4*. Thus it may exhibit similar substrate specificities. It is downregulated in all knockdowns (albeit slight reduction in ICH) and *SLC27A6* expression is upregulated in FLG knockdown only.

6.2.11.2 Biosynthesis of very long-chain fatty acids (VLC-FA) or ultra long-chain fatty acids (ULC-FA)

6.2.11.2.1 Synthesis of FA

In addition to FA taken up from the diet or extracutaneous sites of the body FA up to 16 carbons in length can be synthesized *de novo* by the enzyme complex fatty acid synthase (FASN) in keratinocytes (Uchiyama et al., 2000).

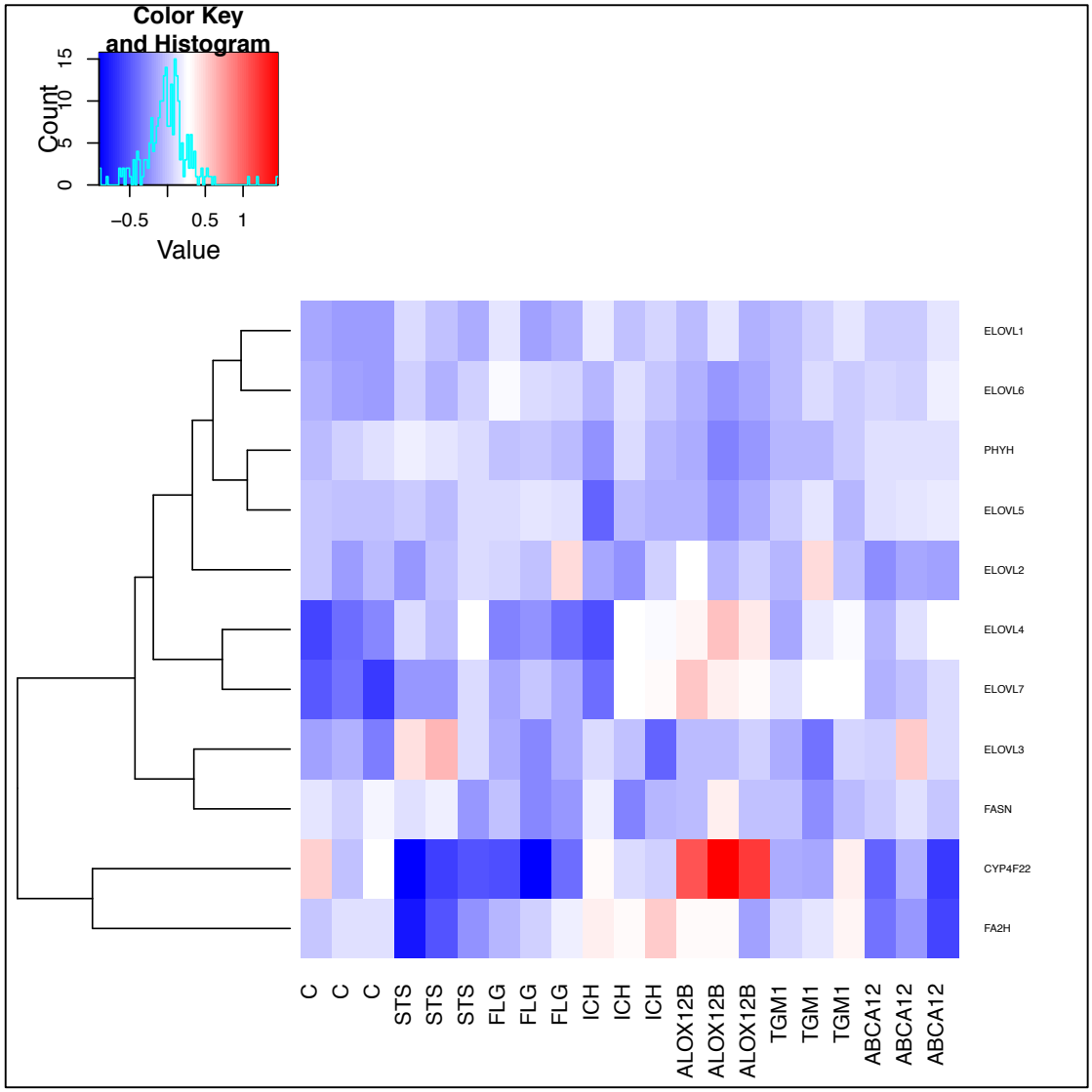

Figure 6.13: Heatmap of changes in expression of genes involved in synthesis VLC-FA or ULC-FA following *STS, FLG, TGM1, ALOX12B, ICHTHYIN,* and *ABCA12* knockdown.

6.2.11.2.2 Elongation of FA

Fatty acids synthesized by FASN or taken up from an extracellular source can be further elongated into VLCFA or ULCFA containing 18 or more carbon atoms (Jakobsson et al., 2006). Each elongation cycle requires four reactions: acyl chain elongation, reduction, dehydration and another reduction step. The rate-limiting step is the initiation of elongation by a family of seven enzymes, elongation of very long chain fatty acids 1–7, ELOVL1–7 (Guillou et al., 2010). ELOVLs 1, 3 and 4 have been detected in skin (Jakobsson et al., 2006). The ELOVLs exhibit a preference for selected substrates depending on their hydrocarbon chain length and degree of unsaturation; ELOVL 1 and ELOVL 4 are crucial to generate ULC-FAs with ≥26 carbon atoms; ELOVL 1 accepts activated FA with a chain length of C18 to C26 (Ohno et al., 2010) and the biosynthesis of FAs longer than 24 carbon atoms depends exclusively on ELOVL4 (Guillou et al., 2010) (Jakobsson et al., 2006, Ohno et al., 2010).

There was dysregulation of several *ELOVL* genes in our dataset. Broadly, there was upregulation of several *ELOVLs* in the knockdowns; *ELOVL1* and 7 in all, *ELOVL2* in *ALOX12B* and *TGM1* knockdowns (log2FC 1.5, pval<0.01; log2FC 1.13, pval<0.05), *ELOVL3* in *STS, ALOX12B* and *ABCA12* knockdowns (log2FC 1.2, pval<0.05) and *ELOVL4* in all except *FLG* knockdowns. *ELOVL 5, 6* expression was downregulated in *ALOX12B* knockdown but the latter was upregulated in all the other models.

6.2.11.2.3 Cutaneous FA hydroxylation

Epidermal fatty acid may be hydroxylated in the α- or ω-position. Hydroxylation in the ω-position is unique to the epidermis.

6.2.11.2.4 α-Hydroxylation

The epidermal enzyme with capacity for α-hydroxylation remains unidentified. Two potential candidates are fatty acid 2-hydroxylase (FA2H) and phytanoyl-CoA 2-hydroxylase (PHYH) (Rabionet et al., 2014). In this dataset *FA2H* expression in *STS* and *ABCA12* knockdowns was

downregulated.

6.2.11.2.5 ω-Hydroxylation of FA

Fatty Acids (and possibly also ceramides containing ULC-FAs) can undergo ω-hydroxylation most likely catalyzed by a cytochrome P450 isoform, *CYP4F22* (Behne et al., 2000). It is known that human mutations in *CYP4F22* cause ARCI (Lefevre et al., 2006). *CYP4F22* was downregulated in the common ichthyoses *STS* (log2FC -2.067, pval<0.01) and *FLG* (log2FC -2.067, pval<0.01) and in *ABCA12* (log2FC -1.1516, pval<0.05) knockdown. It was upregulated in *ALOX12B* knockdown. Thus, perturbations in the CI genes and *ABCA12* (which is not thought to be involved in the 12R-LOX pathway) lend support to the additional role of CYP4F22 in ω-hydroxylation in addition to its proposed involvement in the 12R-LOX pathway.

6.2.11.3 Ceramide Synthesis

Ceramides are composed of a FA acid amide linked to a sphingoid base. The heterogeneity of the sphingoid bases and the huge variety of FA moieties (variation in carbon chain length, degree of saturation, hydroxylation) confer epidermal ceramides with an immense structural complexity.

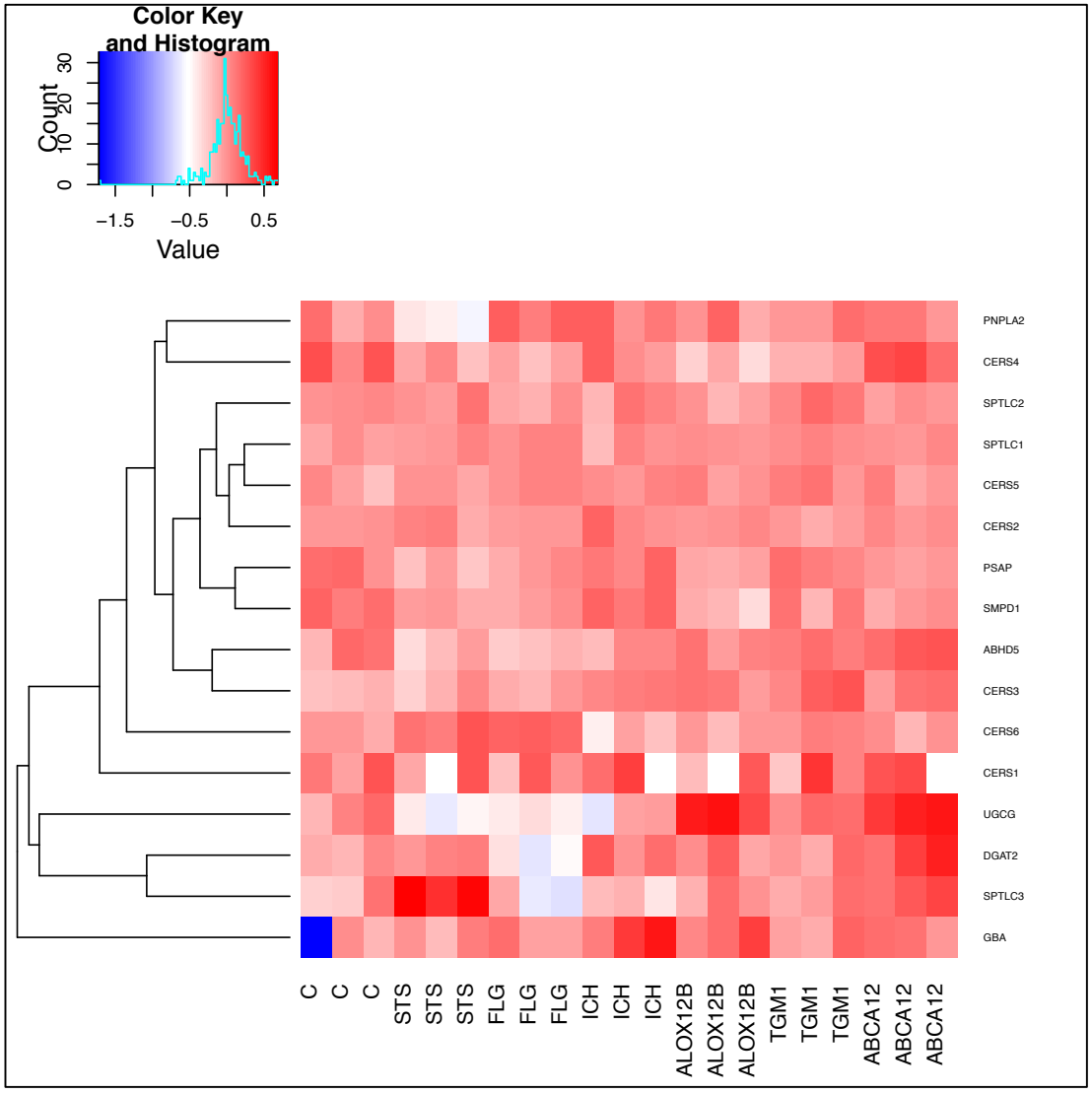

Figure 6.14: Heatmap of genes involved in ceramide synthesis following *STS, FLG, TGM1, ALOX12B, ICHTHYIN,* and *ABCA12* knockdown.

6.2.11.3.1 Generation of Sphingoid bases

Serine palmitoyltransferase (SPT) is a key enzyme in generating sphingoid bases (by the condensation of palmitoyl-CoA and L-serine) at the ER. It is a heterodimer of subunits, Serine Palmitoyltransferase Long-Chain SPTLC 1 either with SPTLC 2 or with SPTLC 3 (Hornemann et al., 2007). Significant reductions of *SPT* expression and of ceramide levels have been reported in psoriatic lesions compared with non-lesional skin (Hong et al., 2007). *SPTLC3* was downregulated in *FLG* and to a lesser extent in *ICH* knockdowns but upregulated in *STS*.

6.2.11.3.2 Generation of ω-acyl-ceramide (and ω-acyl-(glycosyl) ceramide)

Unique epidermal ceramides are acylceramides. Along with α- or ω-hydroxylated ceramides they have an essential function in the formation of lipid lamellae. In addition, acylceramides are also important as a precursor of protein-bound ceramide, which functions to connect lipid lamellae and corneocytes. After the removal of linoleic acid, the exposed ω-hydroxyl group of acylceramide is covalently bound to corneocyte proteins, forming a corneocyte lipid envelope.

Acylceramides have C28–C36 ULCFAs, which are ω-hydroxylated and ω-esterified to FA (>95% of the esterified FA consists of linoleic acid) forming hydrophobic ULC-acylceramides (acylCer).

The linoleate is derived from triacylglycerides (TAG) by an unidentified triacylglyceride lipase activated by CGI-58 (gene *ABHD5*) (Grone, 2002). *ABDH5* mutations cause Chanarin-Dorfman syndrome. This is a rare autosomal recessive lipid storage disorder characterized by ichthyosis, liver disease and lipid vacuolations in neutrophils (also called neutral lipid storage disease).

The final step of TAG biosynthesis is catalysed by diacylglycerol acyltransferase 2 (DGAT 2). This enzyme is decreased in human psoriatic skin (Ilves et al., 2015). Downregulation of *DGAT2* was seen in *FLG* knockdown. *PNPLA2* (known cofactor of adipose TAG lipase) was downregulated with *STS* knockdown.

6.2.11.3.3 Glucosylation of acylceramides

Ceramide biosynthesis increases along with keratinocyte differentiation. They are further processed to glycosylated ceramides (GlcCers) and sphingomyelins (SM) in the Golgi

apparatus. Glucosylation of ceramides is by UDP-Glucose Ceramide Glucosyltransferase (UGCG) (Edwards et al., 2003). UGCG expression was downregulated in the common ichthyoses *STS* (log2FC -1.25, pval<0.05) & *FLG* (log2FC -1.18, pval<0.01). SMs and GlcCers are then recruited into lamellar bodies (LBs) for transport and exocytosis into the extracellular space. After secretion, they are degraded back to ceramides predominantly at the interface between SG and SC as described in Section 6.1.11.4.

Currently it is unclear if ω-OH-ceramides are glucosylated first to ω- OH-GlcCer and then acylated to acylGlcCer.

6.2.11.3.4 Extracellular processing of probarrier lipids

Probarrier lipids synthesized (acylGlcCers, acyl-Cers, ULC-FAs etc.) are recruited into lamellar bodies for transport and exocytosis into the extracellular space at the interface of the SG and SC. In the extracellular space the linoleic moiety is stepwise oxidized by 12R lipoxygenase (12R-LOX) and epidermal lipogenase 3 (eLOX3) (Zheng et al., 2011) followed by generation of ceramides by deglucosylation of acylGlcCers (catalyzed by LB-secreted β-glucocerebrosidase, *GBA*, and its co-factor Saposin-C, *SAP-C*) and SM (by Sphingomyelin Phosphodiesterase 1, Acid Lysosomal, *SMPD1*. Ceramides derived from acylGlcCers ultimately generate protein-bound ceramides thereby forming CLE (ceremides derived from SM do not form the CLE). A slight upregulation of *GBA* and *SMPD1* in the *ICH* knockdown was seen (not significant).

6.2.11.4 Topology and Transport

Despite the crucial role of LBs in lipid transport and ultimately in epidermal barrier homeostasis, our understanding of LB formation and transport is rather superficial. *ABCG1*, a member of the *ABCA12* family, is thought to play a role in normal LB formation and secretion

(Cheung et al., 2010). Lack of the Golgi pH regulator (Gpr89), an anion channel protein essential for normal acidification of the Golgi apparatus, has also been suggested to be prerequisite for proper LB formation. In the SG, newly made ceramides are quickly transported to the Golgi apparatus for GlcCer and SM formation. The current literature suggests that this transport is carried out by both a vesicular-dependent and a vesicular-independent route (Sawada et al., 2012). Vesicular flow is believed to be the major mode for transport of ceramides to the cis-Golgi cisternae for GlcCer synthesis at the cytosolic site (Wang et al., 2004). The non-vesicular transfer of ceramides to the trans-Golgi is mediated by the ceramide transport protein, Collagen, Type IV, Alpha 3 (Goodpasture Antigen) Binding Protein (*COL4A3BP*) for luminal synthesis of SM (Arican et al., 2005).

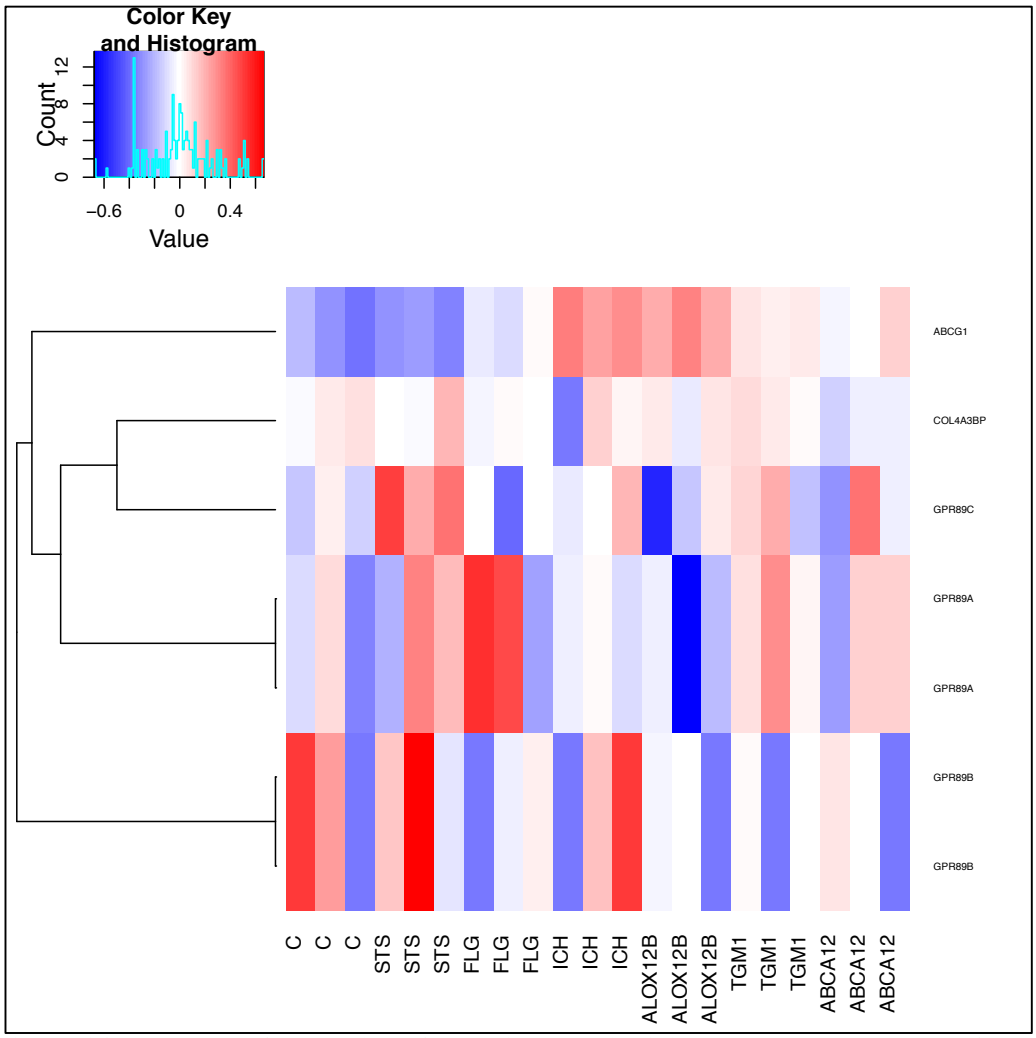

Figure 6.15 Heatmap of expression of genes involved in lipid topology and transport following *STS, FLG, TGM1, ALOX12B, ICHTHYIN,* and *ABCA12* knockdown.

In this dataset *GPR89A* was downregulated in *ALOX12B* knockdown (log2FC -1.47, pval<0.01). *ABCG1* expression is increased in all the knockdowns except *STS*. Conversely, *GPR89C* is upregulated in *STS* knockdown only (non significant). Expression of *COL4A3BP* was downregulated in *ABCA12* knockdown.

6.2.12 Others

6.2.12.1 AP-1 family of transcription factors:

In XLI, abnormal desquamation as well as the permeability barrier abnormality is attributed to disruption of this cholesterol sulfate cycle. In the epidermis, cholesterol sulfate increases from 1% to 5% of the total lipid content as keratinocytes move from the basal to the granular layer,

and then declines again to 1% as corneocytes move, from inner to outer *stratum corneum* (Long et al., 1985, Rearick et al., 1987). An 'epidermal cholesterol sulfate cycle' in which cholesterol is first sulfated in the lower epidermis, and then desulfated back to cholesterol in the outer epidermal nucleated layers has been proposed as an explanation (Epstein et al., 1984). It has been proposed that the increase in cholesterol sulfate that occurs in conjunction with keratinocyte differentiation may not just be a marker of differentiation but may in fact be a signaling molecule that plays a role in inducing keratinocyte differentiation mediated by the AP-1 family of transcription factors or by activating the η isoform of protein kinase C (PRKCH) (section 1.4.2.6). This was evaluated for *STS* and the other ichthyosis gene knockdowns.

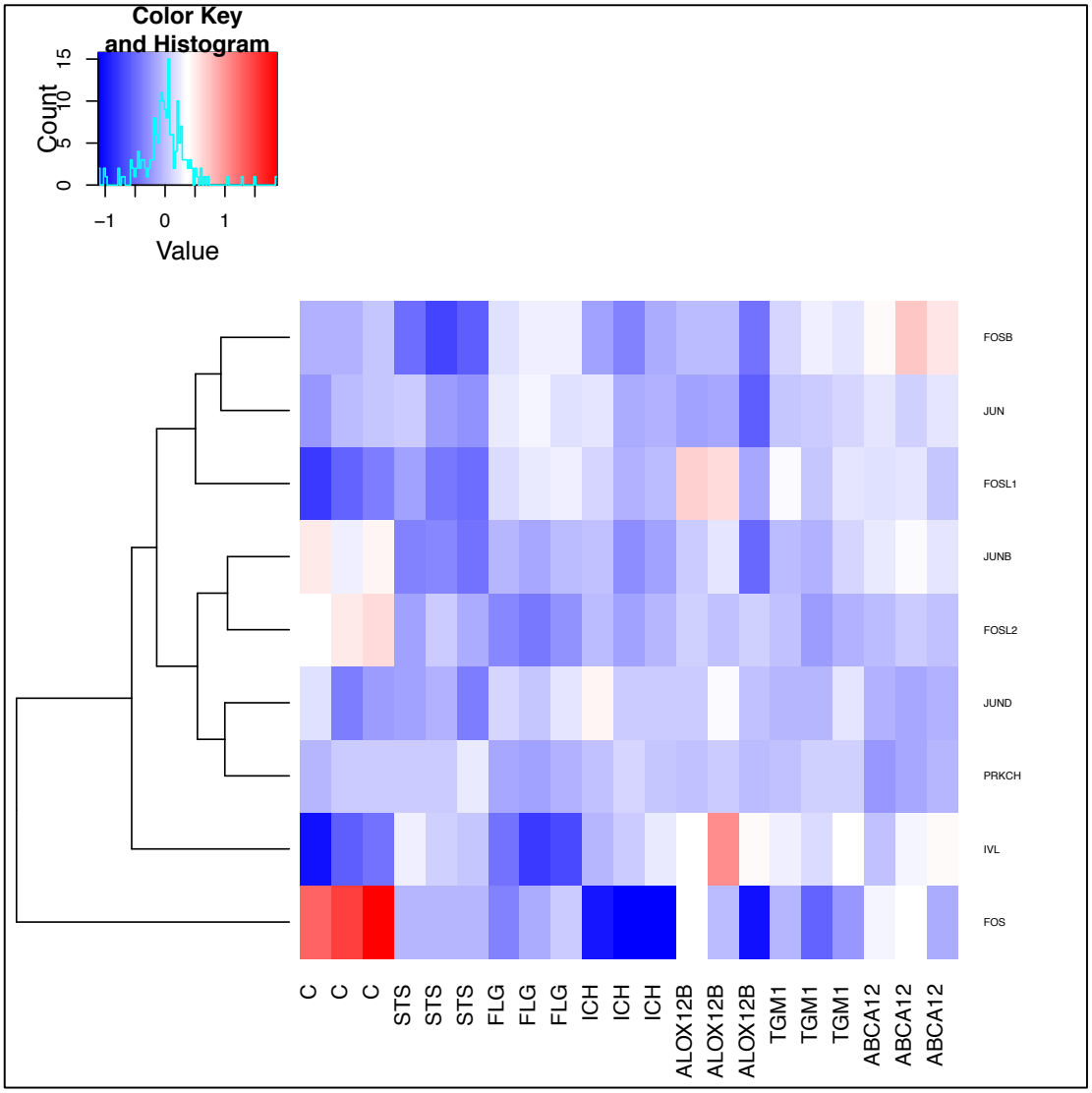

Figure 6.16: Heatmap of gene expression of AP-1 family of transcription factors following *STS, FLG, TGM1, ALOX12B, ICHTHYIN,* and *ABCA12* knockdown.

Our data show that expression of members of the AP-1 family of transcription factors, *FOS,* was significantly downregulated in all the ichthyoses in this study. Additionally *JUNB* (significant in STS silencing, log2FC-1.27, pval<0.01) and FOSL2 (*FRA-2*) was in all the knockdowns (not significant). There was reduced expression of *JUN* (log2FC-1.01, pval<0.01) in *ALOX12B*. This suggests that all the ichthyosis genes studied play a role in keratinocyte differentiation and this may be mediated by the AP-1 family of transcription factors in particular *FOS*.

6.2.12.2 Apoptosis

It has been suggested that keratinocyte apoptosis is involved in the pathomechanisms of HI (Yanagi et al., 2011). Defective lipid transport due to loss of *ABCA12* function leads to the accumulation of intracellular lipids and it is thought that may result in the apoptosis of *Abca12*−/− keratinocytes. In addition, AKT signaling pathway has been demonstrated to help survival of *ABCA12*−/− keratinocytes during keratinization (Yanagi et al., 2011). Furthermore, PPARδ and RXRα are candidate anti-apoptotic molecules in *ABCA12*−/− keratinocytes (Yanagi et al., 2011).

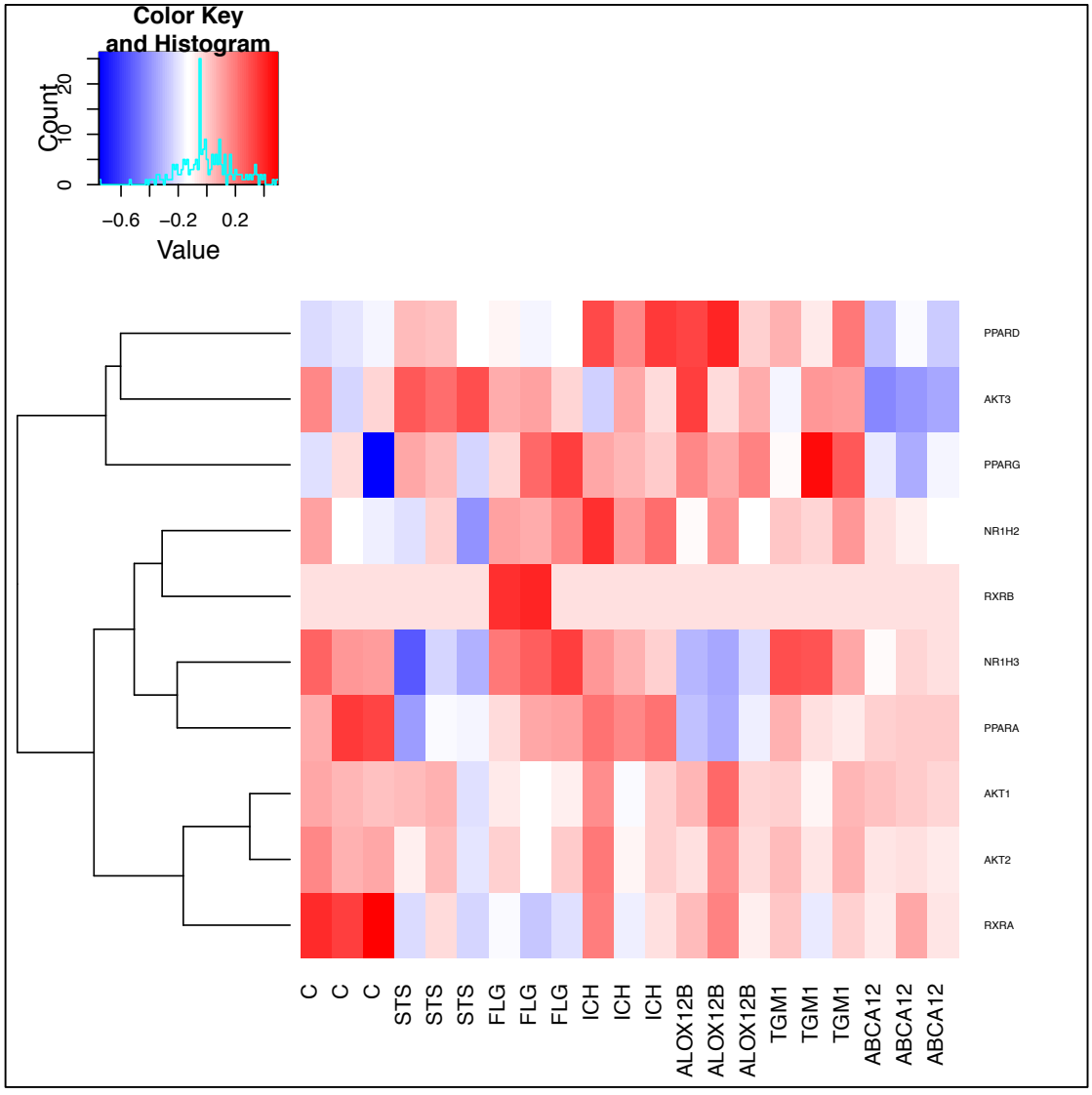

Figure 6.17: Heatmap showing expression of genes involved in keratinocyte apoptosis following *STS, FLG, TGM1, ALOX12B, ICHTHYIN,* and *ABCA12* knockdown.

In this dataset no significant changes were observed. Several trends were noted: *RXRA* is downregulated in all the ichthyosis knockdowns. *PPARA* and *NR1H3* are downregulated in *FLG* and *ALOX12B* knockdowns. *PPARD* was upregulated following *ALOX12B* silencing and *AKT3* is downregulated in *ABCA12* knockdown.

6.3 Discussion

6.3.1 Common Ichthyoses

6.3.1.1 STS

STS silencing lead to *FLG* down regulation; however this was not significant. A subset of patients with XLRI have STS as well as FLG mutations. It is known that *FLG* mutations appear to have a modifying effect on XLRI subjects; those with a mutation in *FLG* as well as mutations in the *STS* gene appear to have a more severe phenotype and greater barrier defects than patients with XLRI with wild-type *FLG* (Janeway and Medzhitov, 2002). Additionally, there was statistically significant down-regulation of *LIPN* and *CYP4F22* genes that are implicated in the ARCI; *LIPN* (log2FC –1.22, pval<0.01) encodes one of six acid lipases known to be involved in triglyceride metabolism and mutations in this gene lead to late onset ARCI (Hari et al., 2010). *CYP4F22* (log2FC –2.06, pval<0.01) has been suggested to be involved in the 12(R)-LOX pathway.

Significant downregulation of the suprabasal keratins *KRT1* and *KRT2* was seen. Several genes in the EDC were significantly downregulated (*S100P*, *FLG2*, *RPTN)*.

STS silencing is thought to lead to accumulation of cholesterol sulfate. Cholesterol sulfate is a potent transcriptional regulator (van Smeden et al., 2014a). *Hanley et al* demonstrated that cholesterol sulfate increased the expression of *Fra-1*, *Fra-2*, and *JunD*, members of the AP-1

family of transcription factors (Danso et al., 2014). Our data show that expression of members of the AP-1 family of transcription factors *FOS*, *JUNB*, *FOSB*, *Fra-2* (*FOSL2*) were downregulated suggesting that it could play a role in keratinocyte differentiation/proliferation. Changes in cell cycle in XLI have been reported previously (Jensen et al., 1989).

Several genes involved in lipid synthesis *UGCG*, *ELOVL3* and *CYP4F22* were dysregulated.

The hyperkeratosis in XLI largely reflects delayed desquamation, the early stages of which are thought to be due to reduced activity of *KLK 5* and *7* (see Section 1.4.2.5). *KLK 5* and *7* were upregulated at the transcriptome level but this was not statistically significant. Post translational modifications may explain these findings. In our dataset, significant downregulation of *KLK6* was noted. There is some suggestion that *KLK6* may be a desquamatory protease (Borgono et al., 2007).

6.3.1.2 FLG

Contrary to the observation in STS knockdown, where *FLG* expression was downregulated, there was no alteration in *STS* expression in the FLG knockdown. Several ARCI genes-*ALOX12B* (significant) and *ALOXE3* (downstream of *ALOX12B* in the LOX pathway), *TGM1* (significant) and *ICH* were downregulated. *FLG* expression was upregulated in the *ALOX12B* knockdown but remained unchanged in the remaining knockdowns. Additionally, there was significant down regulation in *CYP4F22*, mutation in which is known to cause ARCI (Lefevre et al., 2006).

Structural changes were noted in the viable and non-viable epidermis. Several keratins were significantly downregulated throughout the viable epidermis-*KRT1*(2)/10 in the suprabasal layer and *K14* in the basal layer. Additionally, expression of LOR (component of the CE) in the SC was significantly downregulated. Downregulation in the other SB keratins *KRT5/15*

was also noted. Additionally, desmosomal genes *DSC1*, *DSC2* were significantly downregulated thereby reducing cell-cell adhesion. (*DSC3* and *DSG1*, *DSP*, *PKP1*, *PKP3* were also downregulated but this was not significant).

The expression of *TLR2* was significantly downregulated. Keratinocytes mainly signal through *TLR2* once activated with *Staphlococcus aureus* and *Candida albicans* (Hari et al., 2010). Expression of the constitutive AMP genes was also significantly downregulated but not of beta-defensins and cathelicidin perhaps indicating that an adequate response upon stimulation to pathogens is mounted thereby explaining the relatively low rate of infection in IV patients compared to the other ichthyoses.

FLG is located in the EDC. The impact of FLG knockdown on the other EDC genes was evaluated. Several genes in the S100, CE precursors family and fused gene family were downregulated. Several other genes on the chromosome 1q21 but not thought to be part of the EDC were also downregulated; suggesting that they may play a role in epidermal differentiation. Interestingly, there was down regulation of all the EDC genes following *FLG* knockdown (*S100A2, S100A4, S100A7*, *S100A8*, RPTN, *FLG2* and *LOR* significant*)*. In addition, almost all the non-EDC genes on 1q21 were downregulated following *FLG* knockdown (*TXNIP*, *PGLYRP3*, *PGLYRP4*, *C1orf68* significant*)*. Furthermore, there was downregulation of two EDC regulatory genes *GRHL3* and *ARNT*. This suggests that FLG may play a key role in the EDC.

The permeability barrier defect, in IV, lies in the lipid-enriched extracellular space. The effect of *FLG* mutations on SC lipids is contradictory. In populations of northern European descent eczema or atopic dermatitis (AD) occurs primarily due to inherited abnormalities in FLG

(Irvine et al., 2011). In IV, caused by FLG mutations but, unlike in AD, there is no inflammation. Changes in lipid composition have also been reported in AD patients (van Smeden et al., 2014b, Ishikawa et al., 2010, Janssens et al., 2012). These have been attributed to reduction in FFA chain length and associated reduction in ceramide chain length suggesting a common synthetic pathway (van Smeden et al., 2014b). Therefore knowledge of the role that *FLG (*also known to cause AD) plays in epidermal lipids is of interest not only in IV but also in AD.

In this dataset, significant downregulation of FA transporters *CD36* and *FABP5* (*SLC27A1* downregulated but not significant) was observed. No changes in *SLC27A4/FATP4* were noted (loss-of-function mutations in *FATP4* has been associated with AD) (Khnykin et al., 2012). *SLC27A6* expression was upregulated. Expression of fatty acid elongases, *ELOVL1* and *ELOVL4* remained unaltered in contrast to reduced levels of ELOVL isoforms that have been seen in a murine AD model (Park et al., 2012). In addition, UGCG involved in glucosylation of acylceramides and *CYP4F22* involved in ω-hydroxylation (Ohno et al., 2015) are downregulated. Our data suggests that some enzymes involved in FA transportation and ceramide synthesis may contribute to lipid abnormalities due to *FLG* knockdown in addition to altered FFA chain length. Kallikrens, *KLK1* and *-6* were both downregulated.

6.3.2 Autosomal Recessive Congenital Ichthyoses

6.3.2.1 ALOX12B

There was significant downregulation of *ALOX12B* following *FLG* silencing. There was upregulation of *FLG* (not significant) in the *ALOX12B* knockdown suggesting that these two genes may interact with each other: with *FLG* being downstream of *ALOX12B*. Additionally, another CE gene *TGM1* was slightly upregulated in *ALOX12B* knockdown (not significant). Upregulation of these CE genes is consistent with previous studies where LOX deficiency

was reported to affect proteins of the CE (including disturbed processing of pro-FLG to FLG) in addition to severely affecting the lipid components causing barrier dysfunction (Krieg and Furstenberger, 2014).

There was a slight upregulation of *ICH* in keeping with the observation that patients with mutations in *ALOX12B* have up-regulation of ichthyin, the putative receptor for the end products of the LOX-pathway (Li et al., 2013). There is upregulation (not significant) of *ALOXE3* (thought to be downstream of *ALOX12B*) and *CYP4F22* (also involved in the LOX pathway) genes suggesting an attempt to compensate for the absence of *ALOX12B*.

In this study, other significantly dysregulated genes in the *ALOX12B in vitro* model were noted: *KRT1* was significantly downregulated. *HRNR,* a component of the EDC, is upregulated in *ALOX12B* knockdown. *KLK1* is significantly downregulated. *KLK1* is known to be expressed in the skin (Fischer and Meyer-Hoffert, 2013) but it's role as desquamatory protease is unknown. The beta-defensin gene *DEFB103B* was down regulated in *ALOX12B* suggesting that it may play a role in cutaneous infections in the LI/CIE patient group. *GPR89A* (prerequisite for proper LB formation) was downregulated in *ALOX12B* knockdown (log2FC -1.47, pval<0.01) suggesting a role in lipid transportation. The FA elongase gene *ELOVL2* was upregulated.

6.3.2.2 ICHTHYIN/NIPAL4

Changes in the other ichthyosis genes were not seen. Suprabasal keratins *KRT1/2* and *10* were significantly downregulated in *ICH* knockdown indicating structural changes in the suprabasal viable epidermis.

ICH silencing causes significant downregulation of *FLG2* (in the EDC) and upregulation of the EDC regulatory gene, *ARNT.* Expression of FA transporter genes was altered; *FABP5* was reduced. Upregulation of *SLC27A4* was noted and although this was not significant it confirmed previous reports that downregulation of *ICH* results in upregulation of *SLC27A4* (Li et al., 2013). Cytokine *IL12A* was downregulated in the *ICH* model.

6.3.2.3 TGM1

FLG knockdown lead to a significant reduction in expression of *TGM1* suggesting an interaction. Both the suprabasal keratins *KRT1* and *10* were significantly down regulated in *TGM1* knockdown. Overexpression of keratin 1 has been noted in LI patients (O'Shaughnessy et al., 2010).

There was downregulation of EDC genes (*S100A7* and *FLG2).*

The gene *ELOVL2* was significantly upregulated. Genes involved in fatty acid biosynthesis were also perturbed in a rat epithelial organotypic model although the genes involved in the latter were not significantly altered in this study (O'Shaughnessy et al., 2010).

6.3.2.4 ABCA12

No interactions with the other ichthyosis genes were noted. The suprabasal keratinocyte marker *KRT1* was significantly downregulated in keeping with previous studies (Grone, 2002). Its pairing keratin *KRT10* was also downregulated (not significant). Downregulation of *KRT15* was seen (not significant) but no change was seen in the other basal keratins. This lends further evidence to *ABCA12* deficiency leading to differentiation defects in keratinocytes.

In this study *FLG* expression was not significantly altered at the mRNA level suggesting that the defective profilaggrin/filaggrin conversion noted in previous studies (Grone, 2002) is due to post-transcriptional changes.

The expression of *KLK1* was significantly downregulated and mRNA expression of several *KLKs* including *KLK5* was upregulated (not significant). This is in keeping with Yanagi et al. findings in that upregulated *KLK5* mRNA expression was reported although the protein expression was reduced (Coutinho et al., 2005).

CYP4F22 thought to be involved in ω-hydroxylation was found to be significantly downregulated in *ABCA12* knockdown cells. ω-Hydroxyceramides are essential for intact barrier function of the SC. A significant reduction in linoleic esters of long-chain ω-hydroxyceramides and a corresponding increase in their glucosylceramide precursors have been noted in the skin of *ABCA12*-disrupted HI model mice (Zuo et al., 2008). In addition *ELOVL3* was significantly upregulated suggesting involvement in FA elongation. *IL6* expression was significantly reduced following *ABCA12* silencing and this may possibly explain the prevalence of skin infections in this patient group.

6.4 Summary

In summary, in this chapter heatmaps were generated in collaboration with EBI to look at known biological processes and genes related to the ichthyosis knockdowns. Significant changes noted in this study were as follows:

Some interactions were found in the ichthyosis genes in this study; *FLG* silencing downregulated *ALOX12B* and *TGM1* expression. Interactions were seen between other CI and

ARCI genes-other than those studied in this project (*STS* with *LIPN* and *CYP4F22*, *FLG* with *ALOXE3*, *PNPLA1* and *CYP4F22)* and between the ARCI genes *ABCA12* and *CYP4F22.*

Two genes were significantly altered in all the *in vitro* ichthyosis models; *KRT1* and *FOS*; *KRT1* expression was significantly reduced in all the generated models. Its pairing partners were significantly disrupted in some but not all the ichthyoses. *FO*S was significantly downregulated in all the ichthyoses in this study. Other trends were noted in other AP-1 family of transcription factors; down regulation of *JUNB* (significant following *STS* silencing), *FRA-2* (*FOSL2*) in all the ichthyosis. Cell cycle related changes in the ichthyosis have been reported previously (Jensen et. al., 1989, Penneys et al., 1970).

Several EDC genes (clustering of genes on 1q21 that fulfil important functions in epidermal differentiation) were significantly downregulated in the CI; all were downregulated in *FLG* knockdown (significant *S100A2, S100A4, S100A7*, *S100A8*, RPTN, *FLG2* and *LOR)* and all were dysregulated (most downregulated) in *STS* knockdown *(*significantly downregulated *S100P, RPTN* and *FLG2).* A number of EDC genes were also significantly dysregulated in some ARCI-*TGM1* (downregulation of *S100A7, FLG2* and *ICH)* and *ALOX12B* knockdowns (*HRNR* upregulation). Although no significant EDC gene dysregulation was observed in *ICH,* significant upregulation *Arnt* (EDC regulatory gene) (Kypriotou et al., 2012) was observed following *ICH* silencing. Downregulation of all the genes in the EDC in the *FLG* knockdown suggests that it may be the master regulatory gene for the EDC.

Several genes not in the EDC, on chromosomal human region 1q21, were also dysregulated with changes noted in almost all genes following *FLG* knockdowns (significant downregulation of *TXNIP* in *STS* and *FLG* knockdowns, other downregulated genes noted in

FLG knockdowns were *PGLYRP3*, *PGLYRP4*, *C1orf68)*. *ALOX12B* silencing lead to *C1orf68* downregulation. This suggests that several genes on chromosome 1q21 outside the EDC are deregulated in the CI and *ALOX12B* knockdown and these non-EDC genes may also be regulated by *FLG*.

In our dataset TLRs and cytokines (components of the innate immune system but also play a role in epithelial barrier function) were found to be altered in all the ichthyoses. Significant findings were: downregulation of *TLR2* in *FLG* knockdown. The cytokine *IL12A* was downregulated in *FLG* and in *ICH* knockdown models. *IL6* expression was reduced following *ABCA12* silencing. Several beta-defensin genes were down regulated in several knockdowns; *TGM1 (DEFB4A* and *DEFB4B)*, *STS (DEFB4A)* and *ALOX12B (DEFB103B)*. The constitutive *AMP* (*AMP S100A7* and *S100A8/A9* complex) were downregulated in *FLG* and in *TGM1 (S100A7)*. These may be responsible for the impaired antimicrobial barrier in these ichthyoses.

Desmosomal genes were predominantly down regulated. *KLK6* was down regulated in the CI and *KLK1* in *FLG* and several *ARCI* knockdowns (*ALOX12B TGM1* and *ABCA12*). KLK 5, 7 implicated in XLI and *KLK5* in HI were not significantly altered at transcriptome level implying that this may be a post-translational modification.

Several genes involved of biosynthesis of FA and ceramide synthesis were dysregulated. Novel findings were downregulation of genes involved in FA transportation was noted-*CD36* in the *FLG*, *FABP5* in *FLG* and *ICH* knockdowns and FA elongation *ELOVL3* in *ABCA12* knockdowns. Genes involved in ceramide synthesis: *CYP4F22* (involved in ω-Hydroxylation

of FA) and *UGCG* (involved in glucosylation of acylceramides) were downregulated in the CI.

Chapter 7: Validation of *RNA-Seq* analysis- Innate Immunity following Ichthyosis gene knockdown

7.1 Introduction

7.1.1. Innate Immunity and Toll-like receptors (TLRs)

The epidermis, the multilayered stratified epithelium of the skin, provides a first line defense barrier for the host. The epidermis consists of three main resident cell populations: the keratinocytes, Langerhans' cells and melanocytes. Keratinocytes represent the major cell population of the epidermis. Keratinocytes produce various cytokines, either constitutively or upon exposure to viral or bacterial stimuli (Uchi et al., 2000, Grone, 2002) suggesting that they play a role in innate immunity of the skin and are a key component of the epithelial antimicrobial barrier (Kupper and Fuhlbrigge, 2004).

The cytokines produced by keratinocytes include interleukin (IL)-1, -6, -7, -8, -10, -12, -15, -18, -20, -IL23, -IL33, IL34, -TGF-beta, -VEGF, GM-CSF, tumor necrosis factor-alpha (TNF) and interferons (IFN) -alpha, -beta, and -gamma (Grone, 2002). Such cytokine production by keratinocytes has multiple consequences for the migration of inflammatory cells, influences keratinocyte proliferation and differentiation processes, affects the production of other cytokines by keratinocytes and may have pleiotropic effects on the immune system.

The innate immune system has evolved to recognize a broad spectrum of pathogens as a first line of defense. Innate immune cells also instruct adaptive immune responses with information required for this most effective and specific second line response, which helps eradicate the pathogen (Medzhitov, 2001). Recognition of pathogens by innate immune cells is mediated by pattern recognition receptors that recognize conserved pathogen associated molecular patterns (PAMPs). One major group of pattern-recognition receptors is formed by the Toll-like receptors (TLRs) (Medzhitov, 2001, Akira et al., 2001).

In humans, at least ten TLRs have been identified. In the epidermis these receptors are expressed on several cells including keratinocytes, melanocytes, and Langerhans cells. Keratinocytes are reported to express TLRs -1, -2, -3, -5, -9, and -10 (Hari et al., 2010); the evidence supporting TLR 4 expression in keratinocytes is conflicting (Hari et al., 2010). TLRs detect a variety of ligands, which include viral double-stranded RNA (TLR 3), and bacterial flagellin RNA (TLR 5) (Hemmi et al., 2003, Takeda et al., 2003). TLR2 either forms a heterodimer with TLR1 or TLR6 resulting in the distinction between bacterial- and mycoplasma-derived lipoproteins (Brightbill et al., 1999). Keratinocytes, once activated with Staphylococcus aureus (S. aureus) or Candida albicans, mainly signal through TLR 2 (Hari et al., 2010). Once stimulated TLRs activate the transcription factor NF-kB, leading to the production of pro-inflammatory cytokines, chemokines and antimicrobial peptides (Akira and Hemmi, 2003).

In addition to their antimicrobial effects the function of TLRs has recently extended to include epithelial barrier regulation (Kuo et al., 2013a). It has been demonstrated that TLR2 activation by bacterial ligands promotes aspects of the skin barrier; enhances the barrier function of tight junctions (Yuki et al., 2011, Kuo et al., 2013) and treatment of human epidermis wounded by repeated tape stripping (e.g., model of mechanical injury) with TLR2 agonists enhances skin barrier recovery (as measured by transepidermal water loss). Additionally, *TLR2*$^{-/-}$ mice display a skin barrier repair defect (Kuo et al., 2013, Yuki et al., 2011). Desmosomes and tight junctions play an important role in forming a functional skin barrier (Furuse et al., 2002). Activation of TLR3 has been shown to induce expression and function of tight junctions and expression of skin barrier repair genes *ABCA12, GBA, SMPD1 and TGM1* (Borkowski et al., 2015). Mice lacking TLR3 demonstrate a decreased capacity to restore permeability barrier function (Borkowski et al., 2015, Lin et al., 2011).

This skin barrier can be divided into three lines of defense: the physical barrier against pathogens and mechanical injuries, the chemical/biochemical barrier with antimicrobial activity, and a barrier against the unregulated loss of water and solutes (Hanel et al., 2013). In the ichthyoses there is abnormal barrier function. The permeability barrier and antimicrobial barrier, which keeps out pathogens, are closely related (Fischer et al., 2014). In keeping with this, clinically, colonization with pathogens e.g. Staphylococcus aureus (manifesting as maceration, irritation and odour) and recurrent skin infections have been noted clinically in ichthyosis patients.

7.1.2 Aim:

RNA-Seq analysis identified that keratinocytes with knockdown of ichthyosis genes had altered expression of genes associated with innate immunity and defense responses (**Section 6.7**). The aim of this chapter was to assess the following:

1. Cytokine profile of STS, FLG, ABCA12, TGM1, ICH and ALOX12B knock-downs compared to non-targeting control in unstimulated primary keratinocytes.
2. Cytokine profile of *STS, FLG, ABCA12, TGM1, ICH* and *ALOX12B* knock-downs compared to non-targeting control following stimulation of TLR -2, -3, -5 in primary keratinocytes using PGN, Poly I:C and Salmonella typhimurium respectively.

7.2 Results

The cytokine profile of IL-8, IL-1β, IL-6, IL-10, TNF, and IL-12p70 was examined in *STS, FLG, ABCA12, TGM1, ICH* and *ALOX12B* knock-downs compared to non-targeting control, C for stimulated and unstimulated in duplicate samples as described in section 2.4. There was no detection of IL-10 and IL-12p70 in all samples and no detection of IL-1B for

unstimulated samples. TNF, IL6 and IL8 were analyzed further.

7.2.1 Cytokine profile in unstimulated keratinocytes

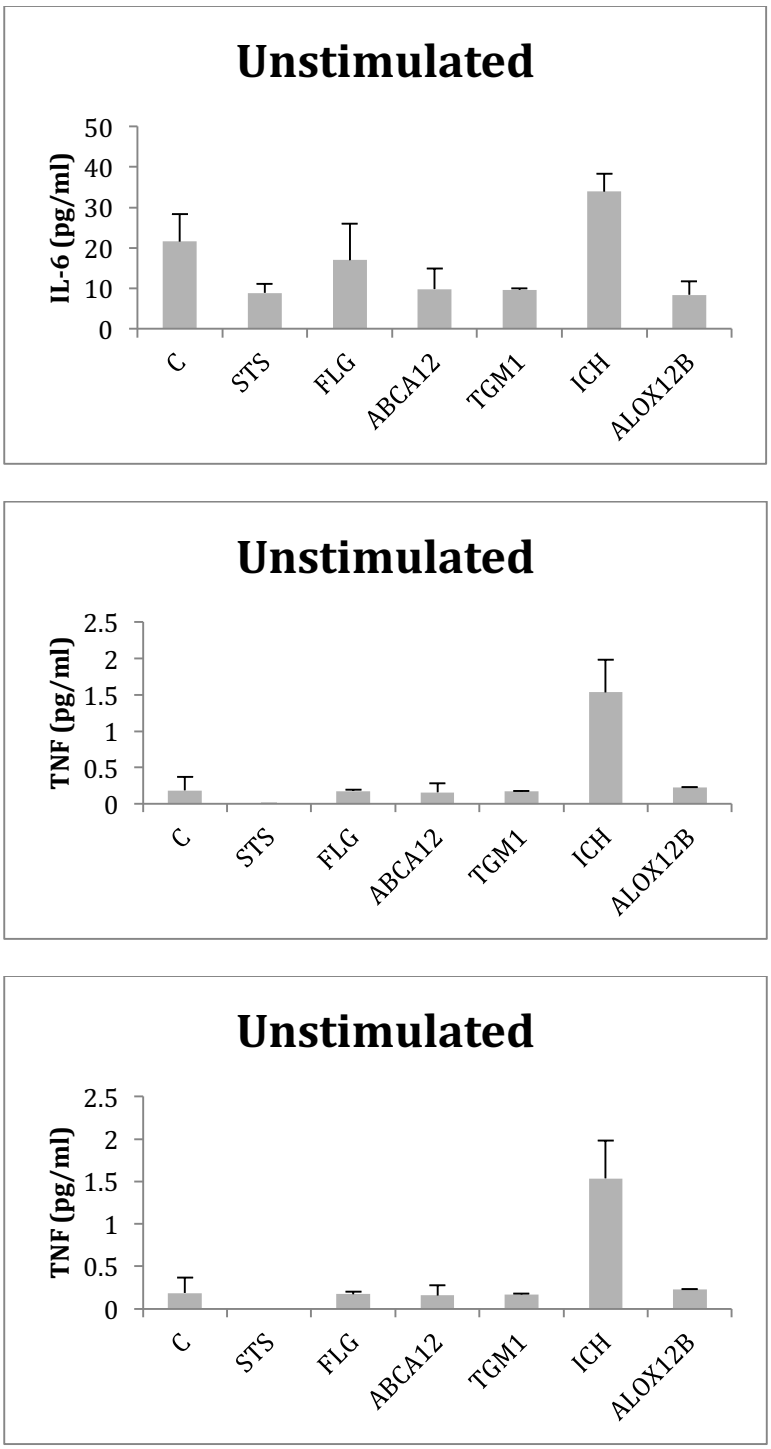

Figure 7.1: Cytokine profile of IL-8, IL-6 and TNF.
Cytokine profile of IL-8, IL-6 and TNF in *STS, FLG, ABCA12, TGM1, ICH* and *ALOX12B* knock-downs compared to non-targeting control, C, in unstimulated primary keratinocytes. Constitutive IL8 induction was noted in both C and knock-downs. Weak induction of IL6 and minimal induction of TNF was also noted in both C and knock-downs as evaluated by BD™ CBA Human Inflammatory Cytokines Kit in duplicates.

Altered IL6, IL8 and TNF profiles were noted in *STS, FLG, ABCA12, TGM1, ICH* and *ALOX12B* knock-downs compared to non-targeting control, *C.* in unstimulated primary keratinocytes (Figure 7.1). TNF was detectable at very low levels only. IL6 was downregulated in *STS, FLG, ABCA12, TGM1* and *ALOX12B* compared to C but was upregulated in *ICH.* IL8 was the most abundant cytokine expressed constitutively in the C and the knockdowns. It was downregulated in *STS*, *FLG*, *ABCA12* and *TGM1* compared to C but was upregulated in *ICH* and *ALOX12B* knockdowns.

7.2.2 Cytokine profile in stimulated keratinocytes

Primary keratinocytes were stimulated with three different TLR ligands: TLR2 ligand PGN, TLR3 ligand poly (I:C) and TLR5 ligand S. typhimurium.

7.2.2.1 Induction of cytokine IL-6

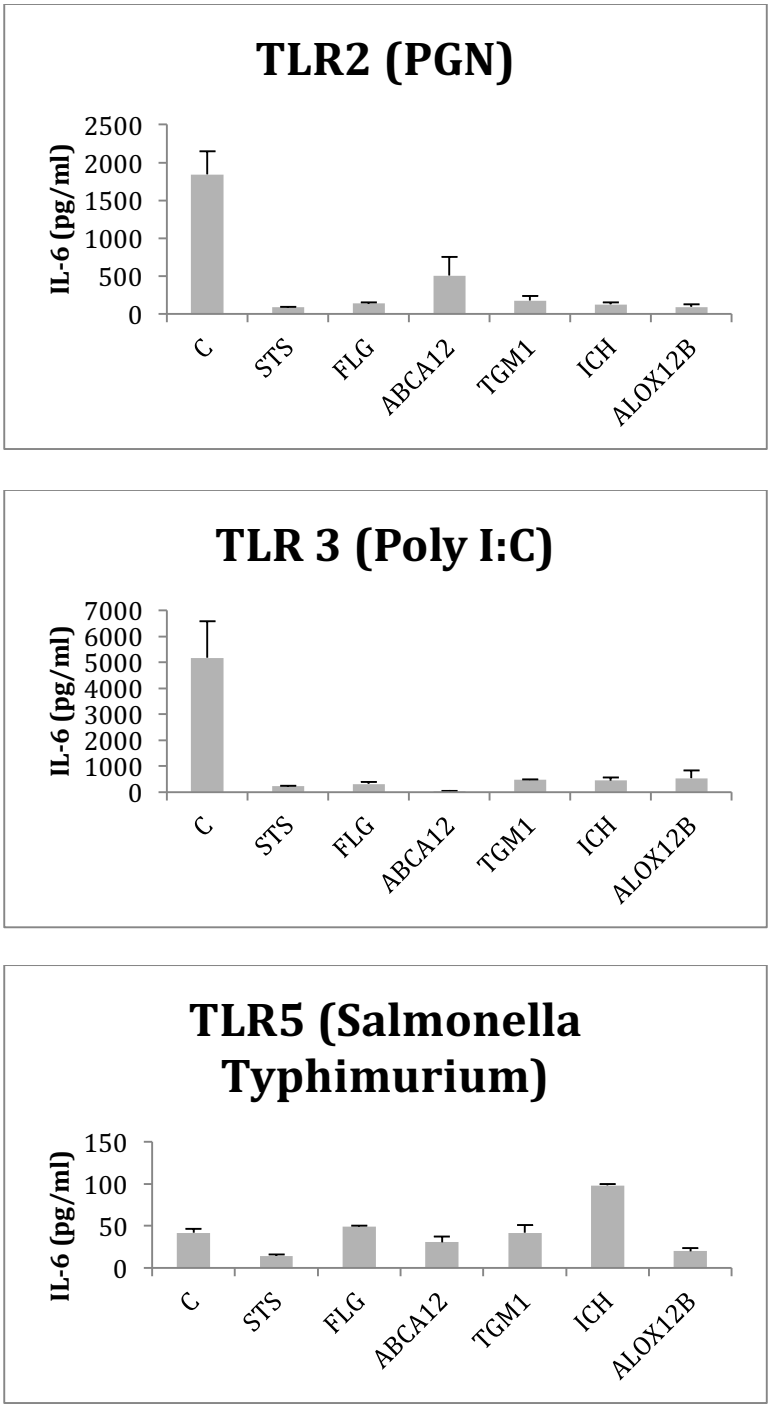

Figure 7.2: Cytokine profile of IL-6.
Cytokine profile of IL-6 in *STS, FLG, ABCA12, TGM1, ICH* and *ALOX12B* knock-downs compared to non-targeting control, C, in primary keratinocytes after stimulation with various TLR ligands. Samples were stimulated at indicated final concentrations: peptidoglycan (PGN) from S aureus (10 ug/ml), Poly I:C (10 ug/ml) and flagellin (Salmonella Typhimurium 1 ug/ml). All three receptors were found to be functional. Results for stimulated were normalized to unstimulated for each ichthyosis gene and then compared to control, also normalized, for meaningful results.

Activation of all three TLRs by the appropriate ligands was seen (Figure 7.2). The TLR3 ligand poly (I:C), a synthetic analogue of double-stranded viral RNA, lead to the strongest activation of primary keratinocytes followed by TLR2 ligand (PGN) and TLR5 (S. typhimurium). Induction of IL6 was reduced in all knockdowns compared to control following TLR2 and TLR3 induction. Following TLR5 activation there was downregulation of IL6 secretion in *STS, ABCA12* and *ALOX12B* knock-downs but upregulation was seen in *FLG* and *ICH* knock-downs.

7.2.2.2 Induction of cytokine TNF

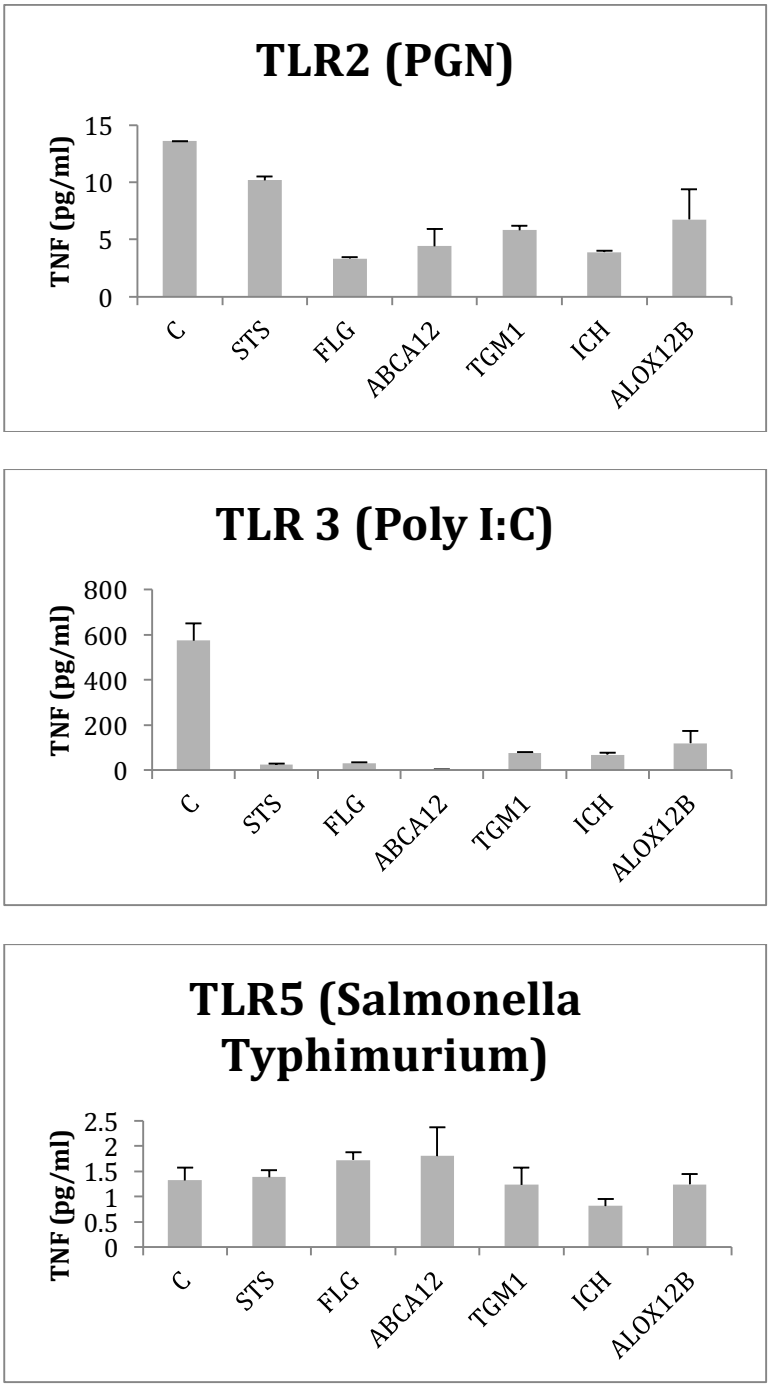

Figure 7.3: Cytokine profile of TNF
Cytokine profile of TNF in *STS, FLG, ABCA12, TGM1, ICH* and *ALOX12B* knock-downs compared to non-targeting control, C, in primary keratinocytes after stimulation with various TLR ligands. Samples were stimulated at indicated final concentrations: using peptidoglycan (PGN) from S aureus (10 ug/ml), Poly I:C (10 ug/ml) and flagellin (Salmonella Typhimurium 1 ug/ml). All three receptors were found to be functional. TLR3 was stimulated more than TLR2. There was minimal stimulation of TLR5.

All three TLRs were functional (Figure 7.3). Induction of TNF was reduced in all knockdowns compared to control following TLR2 and TLR3 stimulation. TLR5 activation lead to downregulated secretion in *TGM1* and *ICH* knock-downs. Increased secretion was seen in *STS, FLG, ABCA12* and *ALOX12B* knock-downs.

7.2.2.3 Induction of cytokine IL8

All three TLRs were stimulated but several values were not within range i.e. were above the maximum range.

7.3 Discussion

RNA-Seq analysis is a powerful method to investigate the effect of protein knockdown by identifying differentially regulated genes. In this study *RNA-Seq* analysis revealed that genes important in innate immunity response were altered as a result of ichthyosis gene knockdown in primary keratinocytes. The aim of this chapter was to validate these results and show that these changes in gene expression are functionally relevant.

The RNA Seq data showed alterations in cytokine genes as a result of knockdown of ichthyosis genes. The *RNA-Seq* data predicted changes in pro-inflammatory cytokine IL6 and IL8 (section 6.2.9). These predictions were evaluated by examining the cytokine profile of *STS, FLG, ABCA12, TGM1, ICH* and *ALOX12B* knock-downs compared to non-targeting control in unstimulated primary keratinocytes. IL6 was downregulated in *STS*, *FLG*, *ABCA12*, *TGM1* and *ALOX12B* knock-downs compared to C but was upregulated in *ICH*. IL8 was downregulated in *STS*, *FLG*, *ABCA12* and *TGM1* compared to C but was upregulated in *ICH* and *ALOX12B* knockdowns. Thus, these changes confirmed the *RNA-Seq* findings for IL6 secretion in *ICH* and *ABCA12* knock-downs but were not consistent for the remaining

ichthyoses. For IL8 *STS, ICH* and *ALOX12B* knock-downs were in keeping with the *RNA Seq* data but for the remaining ichthyoses did not show the same expression changes as the *RNA-Seq* data. This discrepancy may be explained by the ligand chosen for TLRs.

Cytokine profile of *STS, FLG, ABCA12, TGM1, ICH* and *ALOX12B* knock-downs compared to non-targeting control following stimulation of TLR-2, -3, -5 in primary keratinocytes using PGN, Poly I:C and Salmonella typhimurium respectively. After stimulation of primary keratinocytes with three different TLR ligands-TLR2 by ligand PGN, TLR3 by ligand poly (I:C) and TLR5 by ligand S. typhimurium respectively induction of pro-inflammatory cytokines IL6 , IL8 and TNF-α was seen in *STS, FLG, ABCA12, TGM1, ICH* and *ALOX12B* knock-downs. Stimulation of all three receptors was noted suggesting that TLR2, -3, -5 were functional in *STS, FLG, ABCA12, TGM1, ICH* and *ALOX12B* knock-downs in cultured human primary keratinocyes and responded by induction of pro-inflammatory cytokines IL6, IL8 and TNF to appropriate stimuli. For IL8 several values were out of range (very highly stimulated) and further deductions could not be made. There was reduced induction of cytokine secretion in all knock-downs compared to C for IL6 and TNF following TLR2 and -3. This may be due to down-regulation of TLR2 and -3 genes as shown by the *RNA-Seq* data. IL6 secretion was observed predominantly following TLR2 and TLR3 stimulation. TNF induction was predominantly through TLR3 stimulation. These findings suggest that, although reduced compared to C, a more effective cytokine response is produced in the ichthyosis knock-downs following viral compared to bacterial stimulation.

IL-6 and IL-6 receptor expression is increased and localized to all nucleated epidermal layers after barrier disruption. In a human epidermal keratinization model IL-6 reduces the amount of ceramide in the SC but increases the total epidermal ceramide level. The expression of

genes encoding key enzymes accountable for the synthesis of ceramides was also inhibited by IL-6 treatment (Sawada et al., 2012). IL6−/− mice exhibit a delay in skin permeability barrier repair after tape stripping whereas the application of IL-6 enhances this repair process in a concentration dependent manner (Wang et al., 2004). The role of IL6 in bacterial infection has been highlighted following reports that IL6R blockade with Tocilizumab (approved for the treatment of rheumatoid arthritis) shows an inverse relationship to bacterial infection (Lang et al., 2012).

Filaggrin expression is decreased in AD and is reversely associated with IL-6 (Ilves et al., 2015) and interruption of IL-6 receptor signaling improves the severity of AD (Wong et al., 2012). Reduced epidermal TLR2 expression has been observed in AD patients (Kuo et al., 2013b). This suggests that IL6 secretion may be due factors other than stimulation of TLR2 (keratinocytes) in AD. It has been reported that a functional amino acid change in the IL-6 receptor (IL-6R Asp358Ala; rs2228145) was significantly associated with AD (Esparza-Gordillo et al., 2013). IL6 has been implicated in another skin barrier condition, psoriasis; Increased skin and serum IL-6 levels are a feature of psoriasis (Arican et al., 2005). IL-6 is a key mediator of IL-23/Th17-driven cutaneous inflammation (Fujishima et al., 2010). Serum levels of IL-6 are regarded as a marker of the inflammatory activity in psoriasis as well as an indicator of treatment response (Neuner et al., 1991, Grossman et al., 1989, Arican et al., 2005); a positive correlation between IL-6 serum levels and clinical severity of psoriasis before treatment has been described (Balato et al., 2014). Additionally, serum IL-6 levels have been reported to decrease after effective treatment with methotrexate or UVB phototherapy (Mizutani et al., 1997, Lo et al., 2010). The role of IL6 in the ichthyoses has not been studied before. In this dataset, there is marked reduction in secretion of IL6 following stimulation of TLR2 and TLR3 in the knock-downs compared to controls.

The transcription factor STAT3 is activated by cytokines of the IL-6 family. After ligand-induced dimerization of the IL-6 receptor, the associated kinases JAK1 and JAK2 cross-phosphorylate tyrosine residues of adjacent glycoprotein 130 (gp130) subunits of the complex. The SH2 domain of STAT3 binds to newly phosphorylated tyrosines, followed by the phosphorylation of Y705 of STAT3 (Heinrich et al., 2003). Two phosphorylated STAT3 monomers then dimerize and translocate to the nucleus, where they activate the transcription of many downstream genes whose products mediate the diverse effects of STAT3 in development and disease (Levy and Darnell, 2002). STAT3-dependent gene expression also causes upregulation of inhibitory proteins of the SOCS family that interfere with JAK activity (Naka et al., 1997, Starr et al., 1997, Ernst et al., 2001).

STAT3-deficient mice die during early embryogenesis (Takeda et al., 1997). However, analyses of tissue-specific STAT3-deficient mice indicate that STAT3 plays a crucial role in a variety of biological functions including cell differentiation, cell growth, suppression and induction of apoptosis, and cell motility (Hirano et al., 2000, Akira, 2000). Phenotypically the mutant mice had marked acanthosis with hyperkeratosis and scaling. In addition there was aberrant hair follicle expression with pronounced inflammatory infiltration and fibrosis throughout the dermis (Akira, 2000). Also, STAT3 regulates the migration of keratinocytes (Hirano et al., 2000) and is therefore important for wound healing.

Activation/phosphorylation of transcription factor STAT3 has been reported during permeability barrier repair and topical application of IL-6 or Hyper-IL-6, a complex of IL-6 linked to the soluble IL-6 receptor, enhanced epidermal barrier repair in wild-type mice

(Wang et al., 2004). However phosphorylation was markedly reduced, but not completely absent, in IL-6-deficient mice compared with wild-type mice suggesting that IL-6 is an important (Ernst et al., 2001), though not sole, regulator of STAT3 phosphorylation in the skin (Wang et al., 2004) and is involved in permeability barrier repair. Thus it may be hypothesised that in the ichthyosis the effects of IL6 in barrier disruption may be mediated by STAT3.

Interleukin (IL)-8 is a pro-inflammatory cytokine that has a direct effect on immune cells, including polymorphonuclear cells (Jiang et al., 2012). Keratinocytes are a rich source of IL-8. In this dataset constitutive expression of IL8 was observed to be higher than all other cytokines both in the C and the knockdowns. There was reduced secretion in *STS, FLG, ABCA12* and *TGM1* compared to C but there was increased secretion in *ICH* and *ALOX12B* knockdowns. The profiles of pro-inflammatory cytokines IL6 and IL8 were identical for all knock-downs except in *ALOX12B*.

TNF-α is overexpressed in the epidermis of psoriasis skin (Kim et al., 2011) and has a pivotal role in the pathogenesis of psoriasis and TNF-α antagonists are highly effective therapeutic agents in most patients (Kim et al., 2011). TNF-α was recently shown to modulate filaggrin expression via a c-JUN N-terminal kinase dependent pathway (Kim et al., 2011). Psoriasis patients treated with a TNF-α antagonist had significant enhancement of epidermal barrier protein expression, suggesting that TNF-α acts to inhibit key skin barrier proteins and use of specific antagonists may improve barrier protein expression. Thus, specific immunomodulatory therapy could be of benefit in other diseases with epidermal barrier abnormalities including the ichthyoses. In this dataset secretion of TNFα is noted and is higher following TLR3 stimulation than following TLR2 stimulation. There was minimal

stimulation of TLR5. There is reduced secretion in all knockdowns compared to control following both TLR2 and TLR3 stimulation. The gene STS encodes SSase. TNFα upregulates SSase enzyme activity (Elias et al., 2014). TNF stimulates keratinocyte differentiation and increases cholesterol sulfotransferase activity (Elias et al., 2014). TNFα-mediated induction of human STS occurs by transcriptional activation via a mechanism involving PI 3-kinase/Akt pathway in human prostate cancer cells as well as in human mammary cancer cells (Suh et al., 2011). In addition, TNFα has been shown to inhibit the proliferation of keratinocytes and it is involved in sphingomyelin cycle with a subsequent increase in intracellular ceramide which in turn induces cell differentiation (Geilen et al., 1997).

Transcriptome analysis showed downregulation of TLR2 and TLR3 in all the ichthyoses but this was most marked in FLG for TLR2 (log2 FC -1.412, $p < 0.01$) and ICH for TLR3 (not significant). TLR5 was downregulated in both FLG and ICH. The TLR3 ligand poly (I:C), a synthetic analogue of double-stranded viral RNA, led to the strongest activation of primary keratinocytes compared to TLR2 and TLR5 ligands. TLR3 stimulation in all knock-downs was found to be less than in controls. It has been suggested that TLR3, in addition to its role in viral defense, may have other functions in the skin including a role in barrier repair after recognition of dsRNA, which keratinocytes detect following epidermal injury (Borkowski et al., 2013). In addition it has been demonstrated that TLR3 activation of keratinocytes leads to alterations in some of the ichthyosis genes; an increase in transcript abundance of ABCA12, and TGM1 in a TLR3-dependent manner (Borkowski et al., 2013). Additionally non-coding double-strand RNA was reported to induce TLR3- dependent increased expression of ABCA12 in human keratinocytes, resulting in increased epidermal lipid and lamellar bodies

(Borkowski et al., 2013). Thus, reduction in TLR3 gene expression in the ichthyosis knock-downs may play a role in reduced epithelial repair mechanisms.

A reduction of TLR2 expression in AD skin epithelium has been noted (Kuo et al., 2013a). In addition, TLR2 has been shown to play a role in the maintenance of tight junction integrity in response to barrier insults (Kuo et al., 2013a). There is a downregulation of TLR2 expression in all the knock-downs (significant in FLG) in the transcriptome dataset and reduced secretion of IL6 and TNF for all the knock-downs compared to control following TLR2 stimulation with staph aureus. Thus, there may be an association between the ichthyosis genes, reduced TLR2 expression that may contribute to barrier defects.

7.4 Summary

In summary, the cytokine profiles of stimulated and unstimulated primary keratinocytes in the ichthyoses of interest: *STS*, *FLG*, *ABCA12*, *TGM1*, *ICH* and *ALOX12B* knock-downs compared to control were examined.

The cytokine profile is altered in unstimulated primary keratinocytes in the ichthyoses of interest compared to control. On comparison of the cytokine secretion to cytokine gene expression IL6 secretion in *ICH* and *ABCA12* knock-downs confirmed the *RNA-Seq* findings but were not consistent for the remaining ichthyoses. For IL8 *STS, ICH* and *ALOX12B* knock-downs were in keeping with the *RNA Seq* data but did not show the same expression changes for the remaining ichthyoses.

Cytokine profile following stimulation of TLR -2, -3, -5 in primary keratinocytes is altered in the ichthyoses of interest in this study, compared to control. Induction of pro-inflammatory

cytokines IL6, IL8 and TNF was observed in response to appropriate stimuli. There was reduced induction of cytokine secretion in all knock-downs, compared to control, for IL6 and TNF following TLR2 and -3. Secretion of IL6 was observed predominantly following TLR2 and TLR3 stimulation. Induction of TNF was predominantly through TLR3 stimulation.

In conclusion, altered expression levels of several TLR receptors as well as dysregulated production of pro-inflammatory cytokines (IL-6, IL8) is observed in the ichthyoses of interest.

7.5 Future Work

It is important to validate TLR 2, 3 and 5 expression pattern of IL6 and TNF cytokine expression in organotypic cultures and patient samples by IF staining to ensure the *in vitro* findings are observed *in vivo.* As changes in IL8 cytokine expression were noted these could be evaluated by BD™ CBA Human Inflammatory Cytokines Kit with higher reference ranges or by ELISA. Furthermore, plasma IL6, IL8, TNF levels in uninfected, colonized and infected ichthyosis patients would allow validation of cytokine profiles observed in this study.

Chapter 8: Discussion

8.1 Introduction

In this study the non-syndromic monogenic ichthyoses were studied to evaluate any genes or biological processes common to them and to identify key genes and pathways pertaining to each individual ichthyosis. This group of monogenic diseases comprises of ichthyosis vulgaris (loss of *FLG*), X-linked ichthyosis (loss of *STS*), lamellar ichthyosis/congenital ichthyosiform erythroderma (due to mutations in *ALOX12B, ICH, ABCA12*) and harlequin ichthyosis (due to mutations in *ABCA12*). They all affect the cornified layer and manifest as scaly conditions along a spectrum ranging from mild (as in ichthyosis vulgaris) to having a major impact on quality of life (as in lamellar ichthyosis/congenital ichthyosiform erythroderma) to severe (as in harlequin ichthyosis).

In this study the effect of ichthyosis gene knockdown (*STS, FLG, ABCA12, TGM1, ICH* and *ALOX12B*) was examined using RNAi technology (siRNA in primary keratinocytes) targeting each gene in monolayers and organotypic 3D cultures. *RNA-Seq* analysis was undertaken and compared to control to identify differentially regulated genes following gene knockdown. Functional analysis was undertaken to evaluate changes in TLRs and cytokines (altered at transcriptome level).

8.2 A novel *in vitro* 3D model generated for XLI

No previous 3D i*n vitro* models for XLI have been reported before. In this study a novel 3D organotypic culture models for this condition were generated using primary keratinocytes using de-epidermalised dermis as scaffold. Loss of expression for the causative gene *STS* was confimed at transcriptome and protein level by qPCR and Western blot respectively. Changes in terminal differentiation (*TGM1)* were noted (figure 4.7). *RNA-Seq* analysis revealed 458 dysregulated genes that are involved in cutaneous and extracutaneous processes suggesting

that *STS* may directly contribute to contiguous gene defects in *XLI*. Validation of these results by IF or western blotting is important to confirm these findings.

8.3 Filaggrin may play a key role in EDC regulation

Down regulation of all the EDC genes and almost all the non-EDC genes on 1q21 following *FLG* knockdown was noted. This novel finding suggests that FLG may be a key regulator of the EDC. This was further supported by complete loss of *LOR* (an EDC gene) in the 3D *FLG* knockdown model. FLG is one of several genes that comprises the EDC, a 2Mb region on chromosome 1q21, that encodes proteins that fulfil an important role in terminal differentiation in the epidermis (Hoffjan et al., 2007). EDC protein expression is regulated in a gene and tissue-specific manner. Several transcription factors including Klf4, Grhl3 and Arnt (Kypriotou et al., 2012) and interaction of Fra-2/AP-1 with Ezh2 and ERK1/2 (Wurm et al., 2015) have been reported as regulators of EDC. To validate the hypothesis that FLG is a key regulator of the EDC (and non-EDC genes on 1q21) IF on *FLG* knockdown 3D organotypic models and/or Western blotting of the other EDC (and non-EDC genes on 1q21) proteins could be undertaken.

8.4 Epidermal differentiation is altered in all the ichthyoses knockdowns

This study shows that both early and late differentiation is altered in the ichthyoses. *KRT1* downregulation, early differentiation marker, was found to underlie all the ichthyosis in this study (at transcriptome level) and altered TGM1, a terminal differentiation marker, was noted in all the ichthyosis 3D organotypic models. Interestingly *RNA-Seq* analysis did not show significant changes in *TGM1* gene expression in all the ichthyosis knockdowns highlighting the difference between the transcriptome and the functionally relevant proteome. In addition

to downregulation of *KRT1,* its pairing partner *KRT10* was significantly downregulated in *ICH*, *TGM1, FLG* and the other pairing partner, *KRT2* was significantly suppressed in *STS, FLG* and *ICH*. These findings are limited to mRNA level and further validation at protein level is required by IF staining of organotypic cultures and patient samples to confirm these gene expression changes.

This study also provided novel insights for the individual ichthyosis; Loss of *FLG* confirmed changes in terminal differentiation (LOR, TGM1) and implies that a disrupted CE is formed. These changes may be explained by gene alterations noted in the NOTCH signaling pathway (Lin et al., 2012). Premature terminal differentiation was noted following *ABCA12* knockdown (with increased expression of filaggrin and TGM1 in the viable epidermis) confirming findings seen in HI skin (Thomas et al., 2009); In addition, reduction of K10 expression was noted implying altered early differentiation in HI possibly due to premature terminal differentiation. Noncoding dsRNA (via TLR stimulation) have been reported to stimulate some events in keratinocyte differentiation that are important for skin barrier repair and maintenance via ABCA12 upregulation (Borkowski et al., 2013). Our data showed downregulated TLR signaling which may explain the aberrant keratinocyte differentiation. Validation of genes involved in the NOTCH and TLR pathways by qPCR, Western blotting and IF would be required to confirm these findings.

8.5 Innate immune system is dysregulated in all the ichthyoses

In this project altered TLRs and cytokines in unstimulated and stimulated cytokines in all the ichthyoses were noted. Clinically colonization with pathogens and recurrent skin infections have been noted in the ichthyoses (Grahovac et al., 2009, Fleckman et al., 2003); most in HI

followed by the ARCI and may be explained by severity of the impaired permeability barrier (most in HI followed by the other ARCI) impacting on the antimicrobial barrier. In addition, differences in infection prevalence and inflammation are noted between atopic dermatitis and ichthyosis vulgaris (higher in the former), both caused by loss of *FLG* expression. In addition to their role in the innate immune system TLRs and cytokines also play a role in epithelial barrier function (Wood et. al., 1992, Hanel et al., 2013). Mechanistic insights following further study of these components of the innate immune system may explain these observations. It may be hypothesised that the effects of IL6 in barrier disruption may be mediated by STAT3 in the ichthyoses (section 7.3).

8.6 Dysregulation in stratum corneum lipids in all the Ichthyoses

The ichthyoses cause a defect in the epidermal barrier. Epidermal lipids are critical to epidermal barrier formation/function in the SC. The SC is composed of corneocytes that are filled with water and keratin that is surrounded by a cornified envelope, CE, which consists of a densely crosslinked layer of proteins such as filaggrin, loricrin and involucrin. A monolayer of non-polar lipids (ω-hydroxylated ceramides and free fatty acids, FFA) referred to as the cornified lipid envelope, CLE, is esterified to the cornified envelope, mainly to glutamate residues of involucrin (Lazo et al., 1995, Marekov and Steinert, 1998, Swartzendruber et al., 1987). The CLE is suggested to form a template for the formation of the intercellular lipid layers (Sandhoff, 2010, Schuette et al., 1999, Wertz et al., 1989). The cornified envelope, together with the CLE allows proper formation of the lipid matrix.

In this project genes annotated to lipid metabolism were dysregulated in all the ichthyosis knockdowns and arachadonic acid pathway (in all but *ICH* knockdown). Metabolism of

arachidonic acid by *ALOX12B* is known (section 1.5.2.4.3). In the *FL*G knockdown DEGs which included *ALOX12B* in arachidonic acid metabolism were noted implying that there are interactions between *FLG* and *ALOX12B* (section 5.2.4). ICH it is thought to the putative receptor in the same metabolic process as *ALOX12B* (i.e. metabolism of arachidonic acid) (Dahlqvist et al., 2007, Lefevre et al., 2006). It is therefore surprising that genes altered in this pathway were not dysregulated in this knockdown.

Dysregulated lipid metabolism in the other ichthyoses may be explained secondary to the following; irregular lipid matrix formation resulting from a deficient CE following *TGM1* loss have been noted (Meguro et al., 2000, Behne et al., 2000, Li et al., 2007, Downing, 1992). In support of this several genes involved in peptide cross-linking and CE including *FLG* were dysregulated in the *TGM1* knockdown. In addition to its role in the arachidonic acid pathway ALOX12B is known to oxidise the ω-esterified linoleic acid moiety which serves as the substrate for generation of ω-hydroxylated-(glucosyl) ceramides (section 1.5.2.4.4), a prerequisite for CLE formation (Zheng et al., 2011). CLE and bound ceramides are almost entirely absent in ARCI caused by mutations in *ALOX12B (Krieg et al., 2013, Epp et al., 2007)*. In keeping with this genes involved in several lipid processes-lipid localization and transport, lipid biosynthetic process, oxidoreductase activity, iron ion binding and lipid biosynthetic process were altered. The role of ichthyin in epidermal biology is poorly understood; as noted it is the putative receptor in the same metabolic process as *ALOX12B* (Dahlqvist et al., 2007, Lefevre et al., 2006) and it may play a role in the formation, transport or fusion of LBs with the plasma membrane (Dahlqvist et al., 2007). Several genes annotated to vesicle mediated transport were downregulated. Furthermore, a novel finding was involvement of genes in FA/FA biosynthesis. ABCA12 is involved in lipid transportation via LB to the intracellular layers in the SC. Transmembrane transport in this study. Lipid

abnormalities due to loss of *FLG* have been attributed to reduction in FFA chain length and, as some FFAs are components of ceramides, in ceramides (van Smeden et al., 2014). *RNA-Seq* data confirmed these findings. In addition genes involved in lipid transportation and ceramide synthesis were altered. The basis for the permeability barrier abnormality due to loss of *STS* in XLI has been attributed to excess cholesterol sulfate and also in part to the decreased cholesterol content of the SC (section 1.4.2.2) and lipid and arachidonic acid metabolism have not been reported.

8.7 Conclusions and Final Remarks

In this study of the non-syndromic monogenic ichthyosis, my original null hypothesis was that despite a common phenotype the individual ichthyoses have different underlying pathomechanisms and biological pathways. For this *in vitro* models for the CI (IV/XLI) and ARCI (LI/CIE) were developed by transient knockdown of *STS, FLG, ABCA12, TGM1, ICH* and *ALOX12B* in monolayers and 3D organotypic cultures (including a novel XLI model) by using siRNA in primary keratinocytes (neonatal). Knockdown of ichthyosis genes in monolayers was confirmed by qPCR and where possible by western blotting. In the generated 3D models architectural changes and altered terminal differentiation were noted. *RNA-Seq* on generated 2D models from the same genetic background was successfully undertaken.; Altered gene clusters were found for cell cycle, keratin filament/cytoskeleton, innate immune response, and metabolism of lipids and lipoproteins. Functional studies showed altered TLR and cytokine profile in all the ichthyoses. Altered differentiation was noted in all the ichthyosis (early and late differentiation). Furthermore, expression of *FOS*, a member of the AP-1 family of transcription factors, was significantly downregulated. Changes in cell cycle have been noted in the ichthyosis previously (Jensen et al., 1989, Penneys et al., 1970). As it is clear that in this knockdown model of the ichthyoses, there are common pathways altered in

all 6 gene knockdowns, I can partially disprove the null hypothesis. A future hypothesis to interrogate might be that the common phenotype of each individual ichthyosis is caused by changes in the cell cycle and this may be mediated by the AP-1 family of transcription factors, in particular *FOS*. However, it is clear that individual ichthyosis genes also have major effects which may be relevant to the individual gene, such as the major effect of loss of FLG on the EDC or the effect of loss of STS on steroid hormone and ceramide pathway genes which is congruent with the null hypothesis. A large data set, such as the data set generated by this thesis could generate many more hypotheses. Further protein analysis (proteomics/lipidomics) would be required to firm up possible biomarkers or therapeutic targets and this work is in progress.

References

ABERG, K. M., MAN, M. Q., GALLO, R. L., GANZ, T., CRUMRINE, D., BROWN, B. E., CHOI, E. H., KIM, D. K., SCHRODER, J. M., FEINGOLD, K. R. & ELIAS, P. M. 2008. Co-regulation and interdependence of the mammalian epidermal permeability and antimicrobial barriers. *J Invest Dermatol,* 128**,** 917-25.

AKIRA, S. & HEMMI, H. 2003. Recognition of pathogen-associated molecular patterns by TLR family. *Immunol Lett,* 85**,** 85-95.

AKIRA, S., TAKEDA, K. & KAISHO, T. 2001. Toll-like receptors: critical proteins linking innate and acquired immunity. *Nat Immunol,* 2**,** 675-80.

AKIRA, S. 2000. Roles of STAT3 defined by tissue-specific gene targeting. *Oncogene,* 19**,** 2607-11.

AKIYAMA, M. 1999. The pathogenesis of severe congenital ichthyosis of the neonate. *J Dermatol Sci,* 21**,** 96-104.

AKIYAMA, M. 2006. Pathomechanisms of harlequin ichthyosis and ABCA transporters in human diseases. *Arch Dermatol,* 142**,** 914-8.

AKIYAMA, M. 2011. The roles of ABCA12 in keratinocyte differentiation and lipid barrier formation in the epidermis. *Dermatoendocrinol,* 3**,** 107-12.

AKIYAMA, M., DALE, B. A., SMITH, L. T., SHIMIZU, H. & HOLBROOK, K. A. 1998. Regional difference in expression of characteristic abnormality of harlequin ichthyosis in affected fetuses. *Prenat Diagn,* 18**,** 425-36.

AKIYAMA, M., KIM, D. K., MAIN, D. M., OTTO, C. E. & HOLBROOK, K. A. 1994. Characteristic morphologic abnormality of harlequin ichthyosis detected in amniotic fluid cells. *J Invest Dermatol,* 102**,** 210-3.

AKIYAMA, M., SAKAI, K., YANAGI, T., TABATA, N., YAMADA, M. & SHIMIZU, H. 2010. Partially disturbed lamellar granule secretion in mild congenital ichthyosiform erythroderma with ALOX12B mutations. *Br J Dermatol,* 163**,** 201-4.

AKIYAMA, M., SAKAI, K., SATO, T., MCMILLAN, J. R., GOTO, M., SAWAMURA, D. & SHIMIZU, H. 2007a. Compound heterozygous ABCA12 mutations including a novel nonsense mutation underlie harlequin ichthyosis. *Dermatology,* 215**,** 155-9.

AKIYAMA, M., SAKAI, K., SUGIYAMA-NAKAGIRI, Y., YAMANAKA, Y., MCMILLAN, J. R., SAWAMURA, D., NIIZEKI, H., MIYAGAWA, S. & SHIMIZU, H. 2006a. Compound heterozygous mutations including a de novo missense mutation in ABCA12 led to a case of harlequin ichthyosis with moderate clinical severity. *J Invest Dermatol,* 126**,** 1518-23.

AKIYAMA, M., SAKAI, K., WOLFF, G., HAUSSER, I., MCMILLAN, J. R., SAWAMURA, D. & SHIMIZU, H. 2006b. A novel ABCA12 mutation 3270delT causes harlequin ichthyosis. *Br J Dermatol,* 155**,** 1064-6.

AKIYAMA, M. 2010. ABCA12 mutations and autosomal recessive congenital ichthyosis: a review of genotype/phenotype correlations and of pathogenetic concepts. *Hum Mutat,* 31**,** 1090-6.

AKIYAMA, M., SUGIYAMA-NAKAGIRI, Y., SAKAI, K., MCMILLAN, J. R., GOTO, M., ARITA, K., TSUJI-ABE, Y., TABATA, N., MATSUOKA, K., SASAKI, R., SAWAMURA, D. & SHIMIZU, H. 2005. Mutations in lipid transporter ABCA12 in harlequin ichthyosis and functional recovery by corrective gene transfer. *J Clin Invest,* 115**,** 1777-84.

AKIYAMA, M., TAKIZAWA, Y., SUZUKI, Y. & SHIMIZU, H. 2003. A novel homozygous mutation 371delA in TGM1 leads to a classic lamellar ichthyosis phenotype. *Br J Dermatol,* 148**,** 149-53.

AKIYAMA, M., TAKIZAWA, Y., KOKAJI, T. & SHIMIZU, H. 2001. Novel mutations of TGM1 in a child with congenital ichthyosiform erythroderma. *Br J Dermatol,* 144**,** 401-7.

AKIYAMA, M., TITEUX, M., SAKAI, K., MCMILLAN, J. R., TONASSO, L., CALVAS, P., JOSSIC, F., HOVNANIAN, A. & SHIMIZU, H. 2007b. DNA-based prenatal diagnosis of harlequin ichthyosis and characterization of ABCA12 mutation consequences. *J Invest Dermatol,* 127**,** 568-73.

AKIYAMA, M. 2014. The roles of ABCA12 in epidermal lipid barrier formation and keratinocyte differentiation. *Biochim Biophys Acta,* 1841**,** 435-40.

AKIYAMA, M., SAKAI, K., YANAGI, T., TABATA, N., YAMADA, M. & SHIMIZU, H. 2010. Partially disturbed lamellar granule secretion in mild congenital ichthyosiform erythroderma with ALOX12B mutations. *Br J Dermatol,* 163**,** 201-4.

AKIYAMA, M., TAKIZAWA, Y., SUZUKI, Y. & SHIMIZU, H. 2003. A novel homozygous mutation 371delA in TGM1 leads to a classic lamellar ichthyosis phenotype. *Br J Dermatol,* 148**,** 149-53.

ALLEN, D., WINTERS, E., KENNA, P. F., HUMPHRIES, P. & FARRAR, G. J. 2008. Reference gene selection for real-time rtPCR in human epidermal keratinocytes. *J Dermatol Sci,* 49**,** 217-25.

ALLIKMETS, R., GERRARD, B., HUTCHINSON, A. & DEAN, M. 1996. Characterization of the human ABC superfamily: isolation and mapping of 21 new genes using the expressed sequence tags database. *Hum Mol Genet,* 5**,** 1649-55.

ALPERIN, E. S. & SHAPIRO, L. J. 1997. Characterization of point mutations in patients with X-linked ichthyosis. Effects on the structure and function of the steroid sulfatase protein. *J Biol Chem,* 272**,** 20756-63.

ALTSCHUL, S. F., GISH, W., MILLER, W., MYERS, E. W. & LIPMAN, D. J. 1990. Basic local alignment search tool. *J Mol Biol,* 215**,** 403-10.

ANTON-LAMPRECHT, I. & HOFBAUER, M. 1972. Ultrastructural distinction of autosomal dominant ichthyosis vulgaris and X-linked recessive ichthyosis. *Humangenetik,* 15**,** 261-4.

ARICAN, O., ARAL, M., SASMAZ, S. & CIRAGIL, P. 2005. Serum levels of TNF-alpha, IFN-gamma, IL-6, IL-8, IL-12, IL-17, and IL-18 in patients with active psoriasis and correlation with disease severity. *Mediators Inflamm,* 2005**,** 273-9.

AUFENVENNE, K., RICE, R. H., HAUSSER, I., OJI, V., HENNIES, H. C., RIO, M. D., TRAUPE, H. & LARCHER, F. 2012. Long-term faithful recapitulation of transglutaminase 1-deficient lamellar ichthyosis in a skin-humanized mouse model, and insights from proteomic studies. *J Invest Dermatol,* 132**,** 1918-21.

BACKENDORF, C. & HOHL, D. 1992. A common origin for cornified envelope proteins? *Nat Genet,* 2**,** 91.

BALATO, A., SCHIATTARELLA, M., DI CAPRIO, R., LEMBO, S., MATTII, M., BALATO, N. & AYALA, F. 2014. Effects of adalimumab therapy in adult subjects with moderate-to-severe psoriasis on Th17 pathway. *J Eur Acad Dermatol Venereol,* 28**,** 1016-24.

BALOGH, A., PARAGH, G., JR., JUHASZ, A., KOBLING, T., TOROCSIK, D., MIKO, E., VARGA, V., EMRI, G., HORKAY, I., SCHOLTZ, B. & REMENYIK, E. 2008. Reference genes for quantitative real time PCR in UVB irradiated keratinocytes. *J Photochem Photobiol B,* 93**,** 133-9.

BAR, M., BAR, D. & LEHMANN, B. 2009. Selection and validation of candidate housekeeping genes for studies of human keratinocytes--review and recommendations. *J Invest Dermatol,* 129**,** 535-7.

BATHEJA, P., SONG, Y., WERTZ, P. & MICHNIAK-KOHN, B. 2009. Effects of growth conditions on the barrier properties of a human skin equivalent. *Pharm Res,* 26**,** 1689-700.

BEHNE, M., UCHIDA, Y., SEKI, T., DE MONTELLANO, P. O., ELIAS, P. M. & HOLLERAN, W. M. 2000. Omega-hydroxyceramides are required for corneocyte lipid envelope (CLE) formation and normal epidermal permeability barrier function. *J Invest Dermatol,* 114**,** 185-92.

BIEBER, T. 2008. Atopic dermatitis. *N Engl J Med,* 358**,** 1483-94.

BICIKOVA, M., HILL, M., RIPOVA, D., MOHR, P. & HAMPL, R. 2013. Determination of steroid metabolome as a possible tool for laboratory diagnosis of schizophrenia. *J Steroid Biochem Mol Biol,* 133**,** 77-83.

BIKLE, D. D., XIE, Z. & TU, C. L. 2012. Calcium regulation of keratinocyte differentiation. *Expert Rev Endocrinol Metab,* 7**,** 461-472.

BOEGLIN, W. E., KIM, R. B. & BRASH, A. R. 1998. A 12R-lipoxygenase in human skin: mechanistic evidence, molecular cloning, and expression. *Proc Natl Acad Sci U S A,* 95**,** 6744-9.

BOELSMA, E., VERHOEVEN, M. C. & PONEC, M. 1999. Reconstruction of a human skin equivalent using a spontaneously transformed keratinocyte cell line (HaCaT). *J Invest Dermatol,* 112**,** 489-98.

BORGONO, C. A., MICHAEL, I. P., KOMATSU, N., JAYAKUMAR, A., KAPADIA, R., CLAYMAN, G. L., SOTIROPOULOU, G. & DIAMANDIS, E. P. 2007. A potential role for multiple tissue kallikrein serine proteases in epidermal desquamation. *J Biol Chem,* 282**,** 3640-52.

BORKOWSKI, A. W., KUO, I. H., BERNARD, J. J., YOSHIDA, T., WILLIAMS, M. R., HUNG, N. J., YU, B. D., BECK, L. A. & GALLO, R. L. 2015. Toll-like receptor 3 activation is required for normal skin barrier repair following UV damage. *J Invest Dermatol,* 135**,** 569-78.

BORKOWSKI, A. W., PARK, K., UCHIDA, Y. & GALLO, R. L. 2013. Activation of TLR3 in keratinocytes increases expression of genes involved in formation of the epidermis, lipid accumulation, and epidermal organelles. *J Invest Dermatol,* 133**,** 2031-40.

BOROWIEC, A. S., DELCOURT, P., DEWAILLY, E. & BIDAUX, G. 2013. Optimal differentiation of in vitro keratinocytes requires multifactorial external control. *PLoS One,* 8**,** e77507.

BORST, P. & ELFERINK, R. O. 2002. Mammalian ABC transporters in health and disease. *Annu Rev Biochem,* 71**,** 537-92.

BRADSHAW, K. D. & CARR, B. R. 1986. Placental sulfatase deficiency: maternal and fetal expression of steroid sulfatase deficiency and X-linked ichthyosis. *Obstet Gynecol Surv,* 41**,** 401-13.

BRAFF, M. H., DI NARDO, A. & GALLO, R. L. 2005. Keratinocytes store the antimicrobial peptide cathelicidin in lamellar bodies. *J Invest Dermatol,* 124**,** 394-400.

BRASH, A. R. 1999. Lipoxygenases: occurrence, functions, catalysis, and acquisition of substrate. *J Biol Chem,* 274**,** 23679-82.

BRASH, A. R., BOEGLIN, W. E. & CHANG, M. S. 1997. Discovery of a second 15S-lipoxygenase in humans. *Proc Natl Acad Sci U S A,* 94**,** 6148-52.

BRASH, A. R., YU, Z., BOEGLIN, W. E. & SCHNEIDER, C. 2007. The hepoxilin connection in the epidermis. *FEBS J,* 274**,** 3494-502.

BRATTSAND, M., STEFANSSON, K., LUNDH, C., HAASUM, Y. & EGELRUD, T. 2005. A proteolytic cascade of kallikreins in the stratum corneum. *J Invest Dermatol,* 124**,** 198-203.

BRIGHTBILL, H. D., LIBRATY, D. H., KRUTZIK, S. R., YANG, R. B., BELISLE, J. T., BLEHARSKI, J. R., MAITLAND, M., NORGARD, M. V., PLEVY, S. E., SMALE, S. T., BRENNAN, P. J., BLOOM, B. R., GODOWSKI, P. J. & MODLIN, R. L. 1999. Host defense mechanisms triggered by microbial lipoproteins through toll-like receptors. *Science,* 285**,** 732-6.

BROWN, S. J., KROBOTH, K., SANDILANDS, A., CAMPBELL, L. E., POHLER, E., KEZIC, S., CORDELL, H. J., MCLEAN, W. H. & IRVINE, A. D. 2012. Intragenic copy number variation within filaggrin contributes to the risk of atopic dermatitis with a dose-dependent effect. *J Invest Dermatol,* 132**,** 98-104.

BROWN, S. J. & MCLEAN, W. H. 2012. One remarkable molecule: filaggrin. *J Invest Dermatol,* 132**,** 751-62.

BUONO, M. & COSMA, M. P. 2010. Sulfatase activities towards the regulation of cell metabolism and signaling in mammals. *Cell Mol Life Sci,* 67**,** 769-80.

BURNS D. A., COX, N., GRIFFITHS, C. E. 2010. *Rook's textbook of dermatology.*, Wiley-Blackwell.

BUSTIN, S. A., BENES, V., NOLAN, T. & PFAFFL, M. W. 2005. Quantitative real-time RT-PCR--a perspective. *J Mol Endocrinol,* 34**,** 597-601.

CALONJE, E. (2012). McKee's pathology of the skin with clinical correlations. Edinburgh, Elsevier/Saunders.

CANDI, E., SCHMIDT, R. & MELINO, G. 2005. The cornified envelope: a model of cell death in the skin. *Nat Rev Mol Cell Biol,* 6**,** 328-40.

CAUBET, C., JONCA, N., BRATTSAND, M., GUERRIN, M., BERNARD, D., SCHMIDT, R., EGELRUD, T., SIMON, M. & SERRE, G. 2004. Degradation of corneodesmosome proteins by two serine proteases of the kallikrein family, SCTE/KLK5/hK5 and SCCE/KLK7/hK7. *J Invest Dermatol,* 122**,** 1235-44.

CHAKRAVARTHY, M. V., LODHI, I. J., YIN, L., MALAPAKA, R. R., XU, H. E., TURK, J. & SEMENKOVICH, C. F. 2009. Identification of a physiologically relevant endogenous ligand for PPARalpha in liver. *Cell,* 138**,** 476-88.

CHAMCHEU, J. C., SIDDIQUI, I. A., SYED, D. N., ADHAMI, V. M., LIOVIC, M. & MUKHTAR, H. 2011. Keratin gene mutations in disorders of human skin and its appendages. *Arch Biochem Biophys,* 508**,** 123-37.

CHAN, A. & MAURO, T. 2011. Acidification in the epidermis and the role of secretory phospholipases. *Dermatoendocrinol,* 3**,** 84-90.

CHEN, H., COMMON, J. E., HAINES, R. L., BALAKRISHNAN, A., BROWN, S. J., GOH, C. S., CORDELL, H. J., SANDILANDS, A., CAMPBELL, L. E., KROBOTH, K., IRVINE, A. D., GOH, D. L., TANG, M. B., VAN BEVER, H. P., GIAM, Y. C., MCLEAN, W. H. & LANE, E. B. 2011. Wide spectrum of filaggrin-null mutations in atopic dermatitis highlights differences between Singaporean Chinese and European populations. *Br J Dermatol,* 165**,** 106-14.

CHEUNG, P. F., WONG, C. K., HO, A. W., HU, S., CHEN, D. P. & LAM, C. W. 2010. Activation of human eosinophils and epidermal keratinocytes by Th2 cytokine IL-31: implication for the immunopathogenesis of atopic dermatitis. *Int Immunol,* 22**,** 453-67.

CHOATE, K. A., MEDALIE, D. A., MORGAN, J. R. & KHAVARI, P. A. 1996. Corrective gene transfer in the human skin disorder lamellar ichthyosis. *Nat Med,* 2**,** 1263-7.

CHONG, B. F., MURPHY, J. E., KUPPER, T. S. & FUHLBRIGGE, R. C. 2004. E-selectin, thymus- and activation-regulated chemokine/CCL17, and intercellular adhesion molecule-1 are constitutively coexpressed in dermal microvessels: a foundation for a cutaneous immunosurveillance system. *J Immunol,* 172**,** 1575-81.

CHONG, H. C., TAN, M. J., PHILIPPE, V., TAN, S. H., TAN, C. K., KU, C. W., GOH, Y. Y., WAHLI, W., MICHALIK, L. & TAN, N. S. 2009. Regulation of epithelial-

mesenchymal IL-1 signaling by PPARbeta/delta is essential for skin homeostasis and wound healing. *J Cell Biol,* 184**,** 817-31.

COUTINHO, A., CARAMALHO, I., SEIXAS, E. & DEMENGEOT, J. 2005. Thymic commitment of regulatory T cells is a pathway of TCR-dependent selection that isolates repertoires undergoing positive or negative selection. *Curr Top Microbiol Immunol,* 293**,** 43-71.

CROFT, D., MUNDO, A. F., HAW, R., MILACIC, M., WEISER, J., WU, G., CAUDY, M., GARAPATI, P., GILLESPIE, M., KAMDAR, M. R., JASSAL, B., JUPE, S., MATTHEWS, L., MAY, B., PALATNIK, S., ROTHFELS, K., SHAMOVSKY, V., SONG, H., WILLIAMS, M., BIRNEY, E., HERMJAKOB, H., STEIN, L. & D'EUSTACHIO, P. 2014. The Reactome pathway knowledgebase. *Nucleic Acids Res,* 42**,** D472-7.

CUEVAS-COVARRUBIAS, S. A., DIAZ-ZAGOYA, J. C., RIVERA-VEGA, M. R., BEIRANA, A., CARRASCO, E., OROZCO, E. & KOFMAN-ALFARO, S. H. 1999. Higher prevalence of X-linked ichthyosis vs. ichthyosis vulgaris in Mexico. *Int J Dermatol,* 38**,** 555-6.

CULLEN, B. R. 2006. Enhancing and confirming the specificity of RNAi experiments. *Nat Methods,* 3**,** 677-81.

CUZICK, J., YANG, Z. H., FISHER, G., TIKISHVILI, E., STONE, S., LANCHBURY, J. S., CAMACHO, N., MERSON, S., BREWER, D., COOPER, C. S., CLARK, J., BERNEY, D. M., MOLLER, H., SCARDINO, P., SANGALE, Z. & TRANSATLANTIC PROSTATE, G. 2013. Prognostic value of PTEN loss in men with conservatively managed localised prostate cancer. *Br J Cancer,* 108**,** 2582-9.

DAHLQVIST, J., KLAR, J., HAUSSER, I., ANTON-LAMPRECHT, I., PIGG, M. H., GEDDE-DAHL, T., JR., GANEMO, A., VAHLQUIST, A. & DAHL, N. 2007. Congenital ichthyosis: mutations in ichthyin are associated with specific structural abnormalities in the granular layer of epidermis. *J Med Genet,* 44**,** 615-20.

DAHLQVIST, J., WESTERMARK, G. T., VAHLQUIST, A. & DAHL, N. 2012. Ichthyin/NIPAL4 localizes to keratins and desmosomes in epidermis and Ichthyin mutations affect epidermal lipid metabolism. *Arch Dermatol Res,* 304**,** 377-86.

DALE, B. A., HOLBROOK, K. A., FLECKMAN, P., KIMBALL, J. R., BRUMBAUGH, S. & SYBERT, V. P. 1990. Heterogeneity in harlequin ichthyosis, an inborn error of epidermal keratinization: variable morphology and structural protein expression and a defect in lamellar granules. *J Invest Dermatol,* 94**,** 6-18.

DANSO, M. O., VAN DRONGELEN, V., MULDER, A., VAN ESCH, J., SCOTT, H., VAN SMEDEN, J., EL GHALBZOURI, A. & BOUWSTRA, J. A. 2014. TNF-alpha and Th2 Cytokines Induce Atopic Dermatitis-Like Features on Epidermal Differentiation Proteins and Stratum Corneum Lipids in Human Skin Equivalents. *J Invest Dermatol*.

DAYNES, R. A. & JONES, D. C. 2002. Emerging roles of PPARs in inflammation and immunity. *Nat Rev Immunol,* 2**,** 748-59.

DEAN, M., HAMON, Y. & CHIMINI, G. 2001. The human ATP-binding cassette (ABC) transporter superfamily. *J Lipid Res,* 42**,** 1007-17.

DE JUANES, S., EPP, N., LATZKO, S., NEUMANN, M., FURSTENBERGER, G., HAUSSER, I., STARK, H. J. & KRIEG, P. 2009. Development of an ichthyosiform phenotype in Alox12b-deficient mouse skin transplants. *J Invest Dermatol,* 129**,** 1429-36.

DE KONING, H. D., SIMON, A., ZEEUWEN, P. L. & SCHALKWIJK, J. 2012. Pattern recognition receptors in immune disorders affecting the skin. *J Innate Immun,* 4**,** 225-40.

DE KONING, H. D., VAN DEN BOGAARD, E. H., BERGBOER, J. G., KAMSTEEG, M., VAN VLIJMEN-WILLEMS, I. M., HITOMI, K., HENRY, J., SIMON, M., TAKASHITA, N., ISHIDA-YAMAMOTO, A., SCHALKWIJK, J. & ZEEUWEN, P. L. 2012. Expression profile of cornified envelope structural proteins and keratinocyte differentiation-regulating proteins during skin barrier repair. *Br J Dermatol,* 166**,** 1245-54.

DENG, W., WANG, Y., LIU, Z., CHENG, H. & XUE, Y. 2014. HemI: a toolkit for illustrating heatmaps. *PLoS One,* 9**,** e111988.

DENNING, M. F., DLUGOSZ, A. A., WILLIAMS, E. K., SZALLASI, Z., BLUMBERG, P. M. & YUSPA, S. H. 1995. Specific protein kinase C isozymes mediate the induction of keratinocyte differentiation markers by calcium. *Cell Growth Differ,* 6**,** 149-57.

DESCARGUES, P., DERAISON, C., PROST, C., FRAITAG, S., MAZEREEUW-HAUTIER, J., D'ALESSIO, M., ISHIDA-YAMAMOTO, A., BODEMER, C., ZAMBRUNO, G. & HOVNANIAN, A. 2006. Corneodesmosomal cadherins are preferential targets of stratum corneum trypsin- and chymotrypsin-like hyperactivity in Netherton syndrome. *J Invest Dermatol,* 126**,** 1622-32.

DICKSON, M. A., HAHN, W. C., INO, Y., RONFARD, V., WU, J. Y., WEINBERG, R. A., LOUIS, D. N., LI, F. P. & RHEINWALD, J. G. 2000. Human keratinocytes that express hTERT and also bypass a p16(INK4a)-enforced mechanism that limits life span become immortal yet retain normal growth and differentiation characteristics. *Mol Cell Biol,* 20**,** 1436-47.

DOWNING, D. T. 1992. Lipid and protein structures in the permeability barrier of mammalian epidermis. *J Lipid Res,* 33**,** 301-13.

ECKERT, R. L., ADHIKARY, G., YOUNG, C. A., JANS, R., CRISH, J. F., XU, W. & RORKE, E. A. 2013. AP1 transcription factors in epidermal differentiation and skin cancer. *J Skin Cancer,* 2013**,** 537028.

ECKL, K. M., ALEF, T., TORRES, S. & HENNIES, H. C. 2011. Full-thickness human skin models for congenital ichthyosis and related keratinization disorders. *J Invest Dermatol,* 131**,** 1938-42.

ECKL, K. M., DE JUANES, S., KURTENBACH, J., NATEBUS, M., LUGASSY, J., OJI, V., TRAUPE, H., PREIL, M. L., MARTINEZ, F., SMOLLE, J., HAREL, A., KRIEG, P., SPRECHER, E. & HENNIES, H. C. 2009. Molecular analysis of 250 patients with autosomal recessive congenital ichthyosis: evidence for mutation hotspots in ALOXE3 and allelic heterogeneity in ALOX12B. *J Invest Dermatol,* 129**,** 1421-8.

ECKL, K. M., KRIEG, P., KUSTER, W., TRAUPE, H., ANDRE, F., WITTSTRUCK, N., FURSTENBERGER, G. & HENNIES, H. C. 2005. Mutation spectrum and functional analysis of epidermis-type lipoxygenases in patients with autosomal recessive congenital ichthyosis. *Hum Mutat,* 26**,** 351-61.

EDWARDS, A. D., DIEBOLD, S. S., SLACK, E. M., TOMIZAWA, H., HEMMI, H., KAISHO, T., AKIRA, S. & REIS E SOUSA, C. 2003. Toll-like receptor expression in murine DC subsets: lack of TLR7 expression by CD8 alpha+ DC correlates with unresponsiveness to imidazoquinolines. *Eur J Immunol,* 33**,** 827-33.

ELBASHIR, S. M., HARBORTH, J., LENDECKEL, W., YALCIN, A., WEBER, K. & TUSCHL, T. 2001a. Duplexes of 21-nucleotide RNAs mediate RNA interference in cultured mammalian cells. *Nature,* 411**,** 494-8.

ELBASHIR, S. M., LENDECKEL, W. & TUSCHL, T. 2001b. RNA interference is mediated by 21- and 22-nucleotide RNAs. *Genes Dev,* 15**,** 188-200.

ELIAS, P. M. 1983. Epidermal lipids, barrier function, and desquamation. *J Invest Dermatol,* 80 Suppl**,** 44s-49s.

ELIAS, P. M. 2010. Therapeutic Implications of a Barrier-based Pathogenesis of Atopic Dermatitis. *Ann Dermatol,* 22**,** 245-54.

ELIAS, P. M., CRUMRINE, D., RASSNER, U., HACHEM, J. P., MENON, G. K., MAN, W., CHOY, M. H., LEYPOLDT, L., FEINGOLD, K. R. & WILLIAMS, M. L. 2004. Basis for abnormal desquamation and permeability barrier dysfunction in RXLI. *J Invest Dermatol,* 122**,** 314-9.

ELIAS, P. M., WILLIAMS, M. L., CHOI, E. H. & FEINGOLD, K. R. 2014. Role of cholesterol sulfate in epidermal structure and function: lessons from X-linked ichthyosis. *Biochim Biophys Acta,* 1841**,** 353-61.

ELIAS, P. M., CULLANDER, C., MAURO, T., RASSNER, U., KOMUVES, L., BROWN, B. E. & MENON, G. K. 1998. The secretory granular cell: the outermost granular cell as a specialized secretory cell. *J Investig Dermatol Symp Proc,* 3**,** 87-100.

ELIAS, P. M. & MENON, G. K. 1991. Structural and lipid biochemical correlates of the epidermal permeability barrier. *Adv Lipid Res,* 24**,** 1-26.

ELIAS, P. M., CRUMRINE, D., RASSNER, U., HACHEM, J. P., MENON, G. K., MAN, W., CHOY, M. H., LEYPOLDT, L., FEINGOLD, K. R. & WILLIAMS, M. L. 2004. Basis for abnormal desquamation and permeability barrier dysfunction in RXLI. *J Invest Dermatol,* 122**,** 314-9.

ELIAS, P. M., SCHMUTH, M., UCHIDA, Y., RICE, R. H., BEHNE, M., CRUMRINE, D., FEINGOLD, K. R., HOLLERAN, W. M. & PHARM, D. 2002. Basis for the permeability barrier abnormality in lamellar ichthyosis. *Exp Dermatol,* 11**,** 248-56.

EPP, N., FURSTENBERGER, G., MULLER, K., DE JUANES, S., LEITGES, M., HAUSSER, I., THIEME, F., LIEBISCH, G., SCHMITZ, G. & KRIEG, P. 2007. 12R-lipoxygenase deficiency disrupts epidermal barrier function. *J Cell Biol,* 177**,** 173-82.

EPSTEIN, E. H., WILLIAMS, M. L. & ELIAS, P. M. 1984. The epidermal cholesterol sulfate cycle. *J Am Acad Dermatol,* 10**,** 866-8.

ERNST, M., INGLESE, M., WARING, P., CAMPBELL, I. K., BAO, S., CLAY, F. J., ALEXANDER, W. S., WICKS, I. P., TARLINTON, D. M., NOVAK, U., HEATH, J. K. & DUNN, A. R. 2001. Defective gp130-mediated signal transducer and activator of transcription (STAT) signaling results in degenerative joint disease, gastrointestinal ulceration, and failure of uterine implantation. *J Exp Med,* 194**,** 189-203.

ESPARZA-GORDILLO, J., SCHAARSCHMIDT, H., LIANG, L., COOKSON, W., BAUERFEIND, A., LEE-KIRSCH, M. A., NEMAT, K., HENDERSON, J., PATERNOSTER, L., HARPER, J. I., MANGOLD, E., NOTHEN, M. M., RUSCHENDORF, F., KERSCHER, T., MARENHOLZ, I., MATANOVIC, A., LAU, S., KEIL, T., BAUER, C. P., KUREK, M., CIECHANOWICZ, A., MACEK, M., FRANKE, A., KABESCH, M., HUBNER, N., ABECASIS, G., WEIDINGER, S., MOFFATT, M. & LEE, Y. A. 2013. A functional IL-6 receptor (IL6R) variant is a risk factor for persistent atopic dermatitis. *J Allergy Clin Immunol,* 132**,** 371-7.

ESPOSITO, C. & CAPUTO, I. 2005. Mammalian transglutaminases. Identification of substrates as a key to physiological function and physiopathological relevance. *FEBS J,* 272**,** 615-31.

EWALD, D.A., NODA, S., OLIVA, M., LITMAN, T., NAKAJIMA, S., LI, X., XU, H., WORKMAN, C.T., SCHEIPERS, P., SVITACHEVA, N. AND LABUDA, T., 2016. Major differences between human atopic dermatitis and murine models, as determined by using global transcriptomic profiling. *Journal of Allergy and Clinical Immunology*.

FABREGAT, A., SIDIROPOULOS, K., GARAPATI, P., GILLESPIE, M., HAUSMANN, K., HAW, R., JASSAL, B., JUPE, S., KORNINGER, F., MCKAY, S., MATTHEWS, L., MAY, B., MILACIC, M., ROTHFELS, K., SHAMOVSKY, V., WEBBER, M., WEISER, J., WILLIAMS, M., WU, G., STEIN, L., HERMJAKOB, H. &

D'EUSTACHIO, P. 2016. The Reactome pathway Knowledgebase. *Nucleic Acids Res,* 44**,** D481-7.

FEINGOLD, K. R. & JIANG, Y. J. 2011. The mechanisms by which lipids coordinately regulate the formation of the protein and lipid domains of the stratum corneum: Role of fatty acids, oxysterols, cholesterol sulfate and ceramides as signaling molecules. *Dermatoendocrinol,* 3**,** 113-8.

FALLON, P. G., SASAKI, T., SANDILANDS, A., CAMPBELL, L. E., SAUNDERS, S. P., MANGAN, N. E., CALLANAN, J. J., KAWASAKI, H., SHIOHAMA, A., KUBO, A., SUNDBERG, J. P., PRESLAND, R. B., FLECKMAN, P., SHIMIZU, N., KUDOH, J., IRVINE, A. D., AMAGAI, M. & MCLEAN, W. H. 2009. A homozygous frameshift mutation in the mouse Flg gene facilitates enhanced percutaneous allergen priming. *Nat Genet,* 41**,** 602-8.

FISCHER, J. 2009. Autosomal recessive congenital ichthyosis. *J Invest Dermatol,* 129**,** 1319-21.

FISCHER, C. L., BLANCHETTE, D. R., BROGDEN, K. A., DAWSON, D. V., DRAKE, D. R., HILL, J. R. & WERTZ, P. W. 2014. The roles of cutaneous lipids in host defense. *Biochim Biophys Acta,* 1841**,** 319-22.

FISCHER, J. & MEYER-HOFFERT, U. 2013. Regulation of kallikrein-related peptidases in the skin - from physiology to diseases to therapeutic options. *Thromb Haemost,* 110**,** 442-9.

FISCHER, H., ECKHART, L., MILDNER, M., JAEGER, K., BUCHBERGER, M., GHANNADAN, M. & TSCHACHLER, E. 2007. DNase1L2 degrades nuclear DNA during corneocyte formation. *J Invest Dermatol,* 127**,** 24-30.

FLECKMAN, P. 2003. Management of the ichthyoses. *Skin Therapy Lett,* 8**,** 3-7.

FLECKMAN, P. & BRUMBAUGH, S. 2002. Absence of the granular layer and keratohyalin define a morphologically distinct subset of individuals with ichthyosis vulgaris. *Exp Dermatol,* 11**,** 327-36.

FLORIN, L., KNEBEL, J., ZIGRINO, P., VONDERSTRASS, B., MAUCH, C., SCHORPP-KISTNER, M., SZABOWSKI, A. & ANGEL, P. 2006. Delayed wound healing and epidermal hyperproliferation in mice lacking JunB in the skin. *J Invest Dermatol,* 126**,** 902-11.

FLUHR, J. W., ELIAS, P. M., MAN, M. Q., HUPE, M., SELDEN, C., SUNDBERG, J. P., TSCHACHLER, E., ECKHART, L., MAURO, T. M. & FEINGOLD, K. R. 2010. Is the filaggrin-histidine-urocanic acid pathway essential for stratum corneum acidification? *J Invest Dermatol,* 130**,** 2141-4.

FOX, Z., PHILLIPS, A., COHEN, C., NEUHAUS, J., BAXTER, J., EMERY, S., HIRSCHEL, B., HULLSIEK, K. H., STEPHAN, C., LUNDGREN, J. & GROUP, S. S. 2008. Viral resuppression and detection of drug resistance following interruption of a suppressive non-nucleoside reverse transcriptase inhibitor-based regimen. *AIDS,* 22**,** 2279-89.

FREINKEL, R. K. & TRACZYK, T. N. 1985. Lipid composition and acid hydrolase content of lamellar granules of fetal rat epidermis. *J Invest Dermatol,* 85**,** 295-8.

FURUSE, M., HATA, M., FURUSE, K., YOSHIDA, Y., HARATAKE, A., SUGITANI, Y., NODA, T., KUBO, A. & TSUKITA, S. 2002. Claudin-based tight junctions are crucial for the mammalian epidermal barrier: a lesson from claudin-1-deficient mice. *J Cell Biol,* 156**,** 1099-111.

FUJISHIMA, S., WATANABE, H., KAWAGUCHI, M., SUZUKI, T., MATSUKURA, S., HOMMA, T., HOWELL, B. G., HIZAWA, N., MITSUYA, T., HUANG, S. K. & IIJIMA, M. 2010. Involvement of IL-17F via the induction of IL-6 in psoriasis. *Arch Dermatol Res,* 302**,** 499-505.

GAN, S. Q., MCBRIDE, O. W., IDLER, W. W., MARKOVA, N. & STEINERT, P. M. 1990. Organization, structure, and polymorphisms of the human profilaggrin gene. *Biochemistry,* 29**,** 9432-40.

GEILEN, C. C., WIEDER, T. & ORFANOS, C. E. 1997. Ceramide signalling: regulatory role in cell proliferation, differentiation and apoptosis in human epidermis. *Arch Dermatol Res,* 289**,** 559-66.

GENTLEMAN, R. C., CAREY, V. J., BATES, D. M., BOLSTAD, B., DETTLING, M., DUDOIT, S., ELLIS, B., GAUTIER, L., GE, Y., GENTRY, J., HORNIK, K., HOTHORN, T., HUBER, W., IACUS, S., IRIZARRY, R., LEISCH, F., LI, C., MAECHLER, M., ROSSINI, A. J., SAWITZKI, G., SMITH, C., SMYTH, G., TIERNEY, L., YANG, J. Y. & ZHANG, J. 2004. Bioconductor: open software development for computational biology and bioinformatics. *Genome Biol,* 5**,** R80.

GONZALEZ-HUERTA, L. M., MESSINA-BAAS, O. M., TORAL-LOPEZ, J., RIVERA-VEGA, M. R., KOFMAN-ALFARO, S. & CUEVAS-COVARRUBIAS, S. A. 2006. Point mutation in the STS gene in a severely affected patient with X-linked recessive ichthyosis. *Acta Derm Venereol,* 86**,** 78-9.

GOYTAIN, A., HINES, R. M. & QUAMME, G. A. 2008. Functional characterization of NIPA2, a selective Mg2+ transporter. *Am J Physiol Cell Physiol,* 295**,** C944-53.

GRALL, A., GUAGUERE, E., PLANCHAIS, S., GROND, S., BOURRAT, E., HAUSSER, I., HITTE, C., LE GALLO, M., DERBOIS, C., KIM, G. J., LAGOUTTE, L., DEGORCE-RUBIALES, F., RADNER, F. P., THOMAS, A., KURY, S., BENSIGNOR, E., FONTAINE, J., PIN, D., ZIMMERMANN, R., ZECHNER, R., LATHROP, M., GALIBERT, F., ANDRE, C. & FISCHER, J. 2012. PNPLA1 mutations cause autosomal recessive congenital ichthyosis in golden retriever dogs and humans. *Nat Genet,* 44**,** 140-7.

GRONE, A. 2002. Keratinocytes and cytokines. *Vet Immunol Immunopathol,* 88**,** 1-12.

GROSSMAN, R. M., KRUEGER, J., YOURISH, D., GRANELLI-PIPERNO, A., MURPHY, D. P., MAY, L. T., KUPPER, T. S., SEHGAL, P. B. & GOTTLIEB, A. B. 1989. Interleukin 6 is expressed in high levels in psoriatic skin and stimulates proliferation of cultured human keratinocytes. *Proc Natl Acad Sci U S A,* 86**,** 6367-71.

GRAHOVAC, M. & BUDIMCIC, D. 2009. Unrecognized dermatophyte infection in ichthyosis vulgaris. *Acta Dermatovenerol Croat,* 17**,** 127-30.

GRUBER, R., ELIAS, P. M., CRUMRINE, D., LIN, T. K., BRANDNER, J. M., HACHEM, J. P., PRESLAND, R. B., FLECKMAN, P., JANECKE, A. R., SANDILANDS, A., MCLEAN, W. H., FRITSCH, P. O., MILDNER, M., TSCHACHLER, E. & SCHMUTH, M. 2011. Filaggrin genotype in ichthyosis vulgaris predicts abnormalities in epidermal structure and function. *Am J Pathol,* 178**,** 2252-63.

GRUBER, R., JANECKE, A. R., FAUTH, C., UTERMANN, G., FRITSCH, P. O. & SCHMUTH, M. 2007. Filaggrin mutations p.R501X and c.2282del4 in ichthyosis vulgaris. *Eur J Hum Genet,* 15**,** 179-84.

GUILLOU, H., ZADRAVEC, D., MARTIN, P. G. & JACOBSSON, A. 2010. The key roles of elongases and desaturases in mammalian fatty acid metabolism: Insights from transgenic mice. *Prog Lipid Res,* 49**,** 186-99.

HAARMAN, B. C., RIEMERSMA-VAN DER LEK, R. F., NOLEN, W. A., MENDES, R., DREXHAGE, H. A. & BURGER, H. 2015. Feature-expression heat maps--a new visual method to explore complex associations between two variable sets. *J Biomed Inform,* 53**,** 156-61.

HAMMOND, S. M., BERNSTEIN, E., BEACH, D. & HANNON, G. J. 2000. An RNA-directed nuclease mediates post-transcriptional gene silencing in Drosophila cells. *Nature,* 404**,** 293-6.

HANEL, K. H., CORNELISSEN, C., LUSCHER, B. & BARON, J. M. 2013. Cytokines and the skin barrier. *Int J Mol Sci,* 14**,** 6720-45.
HANLEY, K., JIANG, Y., CRUMRINE, D., BASS, N. M., APPEL, R., ELIAS, P. M., WILLIAMS, M. L. & FEINGOLD, K. R. 1997. Activators of the nuclear hormone receptors PPARalpha and FXR accelerate the development of the fetal epidermal permeability barrier. *J Clin Invest,* 100**,** 705-12.
HANLEY, K., JIANG, Y., HE, S. S., FRIEDMAN, M., ELIAS, P. M., BIKLE, D. D., WILLIAMS, M. L. & FEINGOLD, K. R. 1998. Keratinocyte differentiation is stimulated by activators of the nuclear hormone receptor PPARalpha. *J Invest Dermatol,* 110**,** 368-75.
HANLEY, K., WOOD, L., NG, D. C., HE, S. S., LAU, P., MOSER, A., ELIAS, P. M., BIKLE, D. D., WILLIAMS, M. L. & FEINGOLD, K. R. 2001. Cholesterol sulfate stimulates involucrin transcription in keratinocytes by increasing Fra-1, Fra-2, and Jun D. *J Lipid Res,* 42**,** 390-8.
HARI, A., FLACH, T. L., SHI, Y. & MYDLARSKI, P. R. 2010. Toll-like receptors: role in dermatological disease. *Mediators Inflamm,* 2010**,** 437246.
HARDER, J. & SCHRODER, J. M. 2002. RNase 7, a novel innate immune defense antimicrobial protein of healthy human skin. *J Biol Chem,* 277**,** 46779-84.
HARTING, M., BRUNETTI-PIERRI, N., CHAN, C. S., KIRBY, J., DISHOP, M. K., RICHARD, G., SCAGLIA, F., YAN, A. C. & LEVY, M. L. 2008. Self-healing collodion membrane and mild nonbullous congenital ichthyosiform erythroderma due to 2 novel mutations in the ALOX12B gene. *Arch Dermatol,* 144**,** 351-6.
HEINRICH, P. C., BEHRMANN, I., HAAN, S., HERMANNS, H. M., MULLER-NEWEN, G. & SCHAPER, F. 2003. Principles of interleukin (IL)-6-type cytokine signalling and its regulation. *Biochem J,* 374**,** 1-20.
HEMMI, H., KAISHO, T., TAKEDA, K. & AKIRA, S. 2003. The roles of Toll-like receptor 9, MyD88, and DNA-dependent protein kinase catalytic subunit in the effects of two distinct CpG DNAs on dendritic cell subsets. *J Immunol,* 170**,** 3059-64.
HENNINGS, H., MICHAEL, D., CHENG, C., STEINERT, P., HOLBROOK, K. & YUSPA, S. H. 1980. Calcium regulation of growth and differentiation of mouse epidermal cells in culture. *Cell,* 19**,** 245-54.
HERMAN, M. L., FARASAT, S., STEINBACH, P. J., WEI, M. H., TOURE, O., FLECKMAN, P., BLAKE, P., BALE, S. J. & TORO, J. R. 2009. Transglutaminase-1 gene mutations in autosomal recessive congenital ichthyosis: summary of mutations (including 23 novel) and modeling of TGase-1. *Hum Mutat,* 30**,** 537-47.
HERNANDEZ-MARTIN, A., GONZALEZ-SARMIENTO, R. & DE UNAMUNO, P. 1999. X-linked ichthyosis: an update. *Br J Dermatol,* 141**,** 617-27.
HIRANO, T., ISHIHARA, K. & HIBI, M. 2000. Roles of STAT3 in mediating the cell growth, differentiation and survival signals relayed through the IL-6 family of cytokine receptors. *Oncogene,* 19**,** 2548-56.
HOFFJAN, S. AND STEMMLER, S., 2007. On the role of the epidermal differentiation complex in ichthyosis vulgaris, atopic dermatitis and psoriasis. *British journal of dermatology*, *157*(3), pp.441-449.
HOHL, D., HUBER, M. & FRENK, E. 1993. Analysis of the cornified cell envelope in lamellar ichthyosis. *Arch Dermatol,* 129**,** 618-24.
HOLLENSTEIN, K., FREI, D. C. & LOCHER, K. P. 2007. Structure of an ABC transporter in complex with its binding protein. *Nature,* 446**,** 213-6.
HOLLERAN, W. M., TAKAGI, Y. & UCHIDA, Y. 2006. Epidermal sphingolipids: metabolism, function, and roles in skin disorders. *FEBS Lett,* 580**,** 5456-66.

HONG, K. K., CHO, H. R., JU, W. C., CHO, Y. & KIM, N. I. 2007. A study on altered expression of serine palmitoyltransferase and ceramidase in psoriatic skin lesion. *J Korean Med Sci,* 22**,** 862-7.

HOPPE, T., WINGE, M. C., BRADLEY, M., NORDENSKJOLD, M., VAHLQUIST, A., BERNE, B. & TORMA, H. 2012. X-linked recessive ichthyosis: an impaired barrier function evokes limited gene responses before and after moisturizing treatments. *Br J Dermatol,* 167**,** 514-22.

HORIKOSHI, T., IGARASHI, S., UCHIWA, H., BRYSK, H. & BRYSK, M. M. 1999. Role of endogenous cathepsin D-like and chymotrypsin-like proteolysis in human epidermal desquamation. *Br J Dermatol,* 141**,** 453-9.

HORNEMANN, T., WEI, Y. & VON ECKARDSTEIN, A. 2007. Is the mammalian serine palmitoyltransferase a high-molecular-mass complex? *Biochem J,* 405**,** 157-64.

HUANG DA, W., SHERMAN, B. T. & LEMPICKI, R. A. 2009. Systematic and integrative analysis of large gene lists using DAVID bioinformatics resources. *Nat Protoc,* 4**,** 44-57.

HUBER, W., CAREY, V. J., GENTLEMAN, R., ANDERS, S., CARLSON, M., CARVALHO, B. S., BRAVO, H. C., DAVIS, S., GATTO, L., GIRKE, T., GOTTARDO, R., HAHNE, F., HANSEN, K. D., IRIZARRY, R. A., LAWRENCE, M., LOVE, M. I., MACDONALD, J., OBENCHAIN, V., OLES, A. K., PAGES, H., REYES, A., SHANNON, P., SMYTH, G. K., TENENBAUM, D., WALDRON, L. & MORGAN, M. 2015. Orchestrating high-throughput genomic analysis with Bioconductor. *Nat Methods,* 12**,** 115-21.

HUBER, M., RETTLER, I., BERNASCONI, K., FRENK, E., LAVRIJSEN, S. P., PONEC, M., BON, A., LAUTENSCHLAGER, S., SCHORDERET, D. F. & HOHL, D. 1995. Mutations of keratinocyte transglutaminase in lamellar ichthyosis. *Science,* 267**,** 525-8.

HENNINGS, H., MICHAEL, D., CHENG, C., STEINERT, P., HOLBROOK, K. & YUSPA, S. H. 1980. Calcium regulation of growth and differentiation of mouse epidermal cells in culture. *Cell,* 19**,** 245-54.

HUGGETT, J., DHEDA, K., BUSTIN, S. & ZUMLA, A. 2005. Real-time RT-PCR normalisation; strategies and considerations. *Genes Immun,* 6**,** 279-84.

HÜTTENHOFER, A., SCHATTNER, P., HALL, J., MATTICK, J.S., BRUMMELKAMP, T.R., BERNARDS, R. AND MARTIENSSEN, R.A., 2003. Whither RNAi. *Nat. Cell. Biol*, *5*, pp.489-490.

ICRE, G., WAHLI, W. & MICHALIK, L. 2006. Functions of the peroxisome proliferator-activated receptor (PPAR) alpha and beta in skin homeostasis, epithelial repair, and morphogenesis. *J Investig Dermatol Symp Proc,* 11**,** 30-5.

ILVES, T., TIITU, V., SUTTLE, M. M., SAARINEN, J. V. & HARVIMA, I. T. 2015. Epidermal Expression of Filaggrin/Profilaggrin Is Decreased in Atopic Dermatitis: Reverse Association With Mast Cell Tryptase and IL-6 but Not With Clinical Severity. *Dermatitis,* 26**,** 260-7.

IRVINE, A. D., MCLEAN, W. H. & LEUNG, D. Y. 2011. Filaggrin mutations associated with skin and allergic diseases. *N Engl J Med,* 365**,** 1315-27.

ISHII, K. J., SUZUKI, K., COBAN, C., TAKESHITA, F., ITOH, Y., MATOBA, H., KOHN, L. D. & KLINMAN, D. M. 2001. Genomic DNA released by dying cells induces the maturation of APCs. *J Immunol,* 167**,** 2602-7.

ISHIDA-YAMAMOTO, A., SIMON, M., KISHIBE, M., MIYAUCHI, Y., TAKAHASHI, H., YOSHIDA, S., O'BRIEN, T. J., SERRE, G. & IIZUKA, H. 2004. Epidermal lamellar granules transport different cargoes as distinct aggregates. *J Invest Dermatol,* 122**,** 1137-44.

ISHIKAWA, J., NARITA, H., KONDO, N., HOTTA, M., TAKAGI, Y., MASUKAWA, Y., KITAHARA, T., TAKEMA, Y., KOYANO, S., YAMAZAKI, S. & HATAMOCHI, A. 2010. Changes in the ceramide profile of atopic dermatitis patients. *J Invest Dermatol,* 130**,** 2511-4.

JAKOBSSON, A., WESTERBERG, R. & JACOBSSON, A. 2006. Fatty acid elongases in mammals: their regulation and roles in metabolism. *Prog Lipid Res,* 45**,** 237-49.

JANEWAY, C. A., JR. & MEDZHITOV, R. 2002. Innate immune recognition. *Annu Rev Immunol,* 20**,** 197-216.

JANSSENS, M., VAN SMEDEN, J., GOORIS, G. S., BRAS, W., PORTALE, G., CASPERS, P. J., VREEKEN, R. J., HANKEMEIER, T., KEZIC, S., WOLTERBEEK, R., LAVRIJSEN, A. P. & BOUWSTRA, J. A. 2012. Increase in short-chain ceramides correlates with an altered lipid organization and decreased barrier function in atopic eczema patients. *J Lipid Res,* 53**,** 2755-66.

JANSSENS, M., VAN SMEDEN, J., GOORIS, G. S., BRAS, W., PORTALE, G., CASPERS, P. J., VREEKEN, R. J., KEZIC, S., LAVRIJSEN, A. P. & BOUWSTRA, J. A. 2011. Lamellar lipid organization and ceramide composition in the stratum corneum of patients with atopic eczema. *J Invest Dermatol,* 131**,** 2136-8.

JENSEN, P.K., HERRMANN, F.H., HADLICH, J. AND BOLUND, L., 1989. Proliferation and differentiation of cultured epidermal cells from patients with X-linked ichthyosis and ichthyosis vulgaris. *Acta dermato-venereologica*, *70*(2), pp.99-104.

JENSEN, J.M.; PROKSCH, E.; ELIAS, P.M. 2005.Skin Barrier, New York, Marcel Dekker.

JETTEN, A. M., BRODY, A. R., DEAS, M. A., HOOK, G. E., REARICK, J. I. & THACHER, S. M. 1987. Retinoic acid and substratum regulate the differentiation of rabbit tracheal epithelial cells into squamous and secretory phenotype. Morphological and biochemical characterization. *Lab Invest,* 56**,** 654-64.

JETTEN, A. M., GEORGE, M. A., PETTIT, G. R., HERALD, C. L. & REARICK, J. I. 1989. Action of phorbol esters, bryostatins, and retinoic acid on cholesterol sulfate synthesis: relation to the multistep process of differentiation in human epidermal keratinocytes. *J Invest Dermatol,* 93**,** 108-15.

JIANG, Y. J., LU, B., KIM, P., PARAGH, G., SCHMITZ, G., ELIAS, P. M. & FEINGOLD, K. R. 2008. PPAR and LXR activators regulate ABCA12 expression in human keratinocytes. *J Invest Dermatol,* 128**,** 104-9.

JIANG, Y. J., UCHIDA, Y., LU, B., KIM, P., MAO, C., AKIYAMA, M., ELIAS, P. M., HOLLERAN, W. M., GRUNFELD, C. & FEINGOLD, K. R. 2009. Ceramide stimulates ABCA12 expression via peroxisome proliferator-activated receptor {delta} in human keratinocytes. *J Biol Chem,* 284**,** 18942-52.

JOBARD, F., LEFEVRE, C., KARADUMAN, A., BLANCHET-BARDON, C., EMRE, S., WEISSENBACH, J., OZGUC, M., LATHROP, M., PRUD'HOMME, J. F. & FISCHER, J. 2002. Lipoxygenase-3 (ALOXE3) and 12(R)-lipoxygenase (ALOX12B) are mutated in non-bullous congenital ichthyosiform erythroderma (NCIE) linked to chromosome 17p13.1. *Hum Mol Genet,* 11**,** 107-13.

JOHN, S., THIEBACH, L., FRIE, C., MOKKAPATI, S., BECHTEL, M., NISCHT, R., ROSSER-DAVIES, S., PAULSSON, M. & SMYTH, N. 2012. Epidermal transglutaminase (TGase 3) is required for proper hair development, but not the formation of the epidermal barrier. *PLoS One,* 7**,** e34252.

JONES, D. A., YAWALKAR, N., SUH, K. Y., SADAT, S., RICH, B. & KUPPER, T. S. 2004. Identification of autoantigens in psoriatic plaques using expression cloning. *J Invest Dermatol,* 123**,** 93-100.

JUNGERSTED, J. M., SCHEER, H., MEMPEL, M., BAURECHT, H., CIFUENTES, L., HOGH, J. K., HELLGREN, L. I., JEMEC, G. B., AGNER, T. & WEIDINGER, S. 2010. Stratum corneum lipids, skin barrier function and filaggrin mutations in patients with atopic eczema. *Allergy,* 65**,** 911-8.

KALININ, A. E., KAJAVA, A. V. & STEINERT, P. M. 2002. Epithelial barrier function: assembly and structural features of the cornified cell envelope. *Bioessays,* 24**,** 789-800.

KARIKO, K., NI, H., CAPODICI, J., LAMPHIER, M. & WEISSMAN, D. 2004. mRNA is an endogenous ligand for Toll-like receptor 3. *J Biol Chem,* 279**,** 12542-50.

KAWASAKI, H., NAGAO, K., KUBO, A., HATA, T., SHIMIZU, A., MIZUNO, H., YAMADA, T. & AMAGAI, M. 2012. Altered stratum corneum barrier and enhanced percutaneous immune responses in filaggrin-null mice. *J Allergy Clin Immunol,* 129**,** 1538-46 e6.

KELSELL, D. P., NORGETT, E. E., UNSWORTH, H., TEH, M. T., CULLUP, T., MEIN, C. A., DOPPING-HEPENSTAL, P. J., DALE, B. A., TADINI, G., FLECKMAN, P., STEPHENS, K. G., SYBERT, V. P., MALLORY, S. B., NORTH, B. V., WITT, D. R., SPRECHER, E., TAYLOR, A. E., ILCHYSHYN, A., KENNEDY, C. T., GOODYEAR, H., MOSS, C., PAIGE, D., HARPER, J. I., YOUNG, B. D., LEIGH, I. M., EADY, R. A. & O'TOOLE, E. A. 2005. Mutations in ABCA12 underlie the severe congenital skin disease harlequin ichthyosis. *Am J Hum Genet,* 76**,** 794-803.

KENT, L., EMERTON, J., BHADRAVATHI, V., WEISBLATT, E., PASCO, G., WILLATT, L. R., MCMAHON, R. & YATES, J. R. 2008. X-linked ichthyosis (steroid sulfatase deficiency) is associated with increased risk of attention deficit hyperactivity disorder, autism and social communication deficits. *J Med Genet,* 45**,** 519-24.

KEZIC, S., KEMPERMAN, P. M., KOSTER, E. S., DE JONGH, C. M., THIO, H. B., CAMPBELL, L. E., IRVINE, A. D., MCLEAN, W. H., PUPPELS, G. J. & CASPERS, P. J. 2008. Loss-of-function mutations in the filaggrin gene lead to reduced level of natural moisturizing factor in the stratum corneum. *J Invest Dermatol,* 128**,** 2117-9.

KIELTY, C. M., SHERRATT, M. J. & SHUTTLEWORTH, C. A. 2002. Elastic fibres. *J Cell Sci,* 115**,** 2817-28.

KIM, B. E., HOWELL, M. D., GUTTMAN-YASSKY, E., GILLEAUDEAU, P. M., CARDINALE, I. R., BOGUNIEWICZ, M., KRUEGER, J. G. & LEUNG, D. Y. 2011. TNF-alpha downregulates filaggrin and loricrin through c-Jun N-terminal kinase: role for TNF-alpha antagonists to improve skin barrier. *J Invest Dermatol,* 131**,** 1272-9.

KIM, I. G., MCBRIDE, O. W., WANG, M., KIM, S. Y., IDLER, W. W. & STEINERT, P. M. 1992. Structure and organization of the human transglutaminase 1 gene. *J Biol Chem,* 267**,** 7710-7.

KHAN, A. A., BETEL, D., MILLER, M. L., SANDER, C., LESLIE, C. S. & MARKS, D. S. 2009. Transfection of small RNAs globally perturbs gene regulation by endogenous microRNAs. *Nat Biotechnol,* 27**,** 549-55.

KHNYKIN, D., RONNEVIG, J., JOHNSSON, M., SITEK, J. C., BLAAS, H. G., HAUSSER, I., JOHANSEN, F. E. & JAHNSEN, F. L. 2012. Ichthyosis prematurity syndrome: clinical evaluation of 17 families with a rare disorder of lipid metabolism. *J Am Acad Dermatol,* 66**,** 606-16.

KOPPE, G., MARINKOVIC-ILSEN, A., RIJKEN, Y., DE GROOT, W. P. & JOBSIS, A. C. 1978. X-linked icthyosis. A sulphatase deficiency. *Arch Dis Child,* 53**,** 803-6.

KRIEG, P. & FURSTENBERGER, G. 2014. The role of lipoxygenases in epidermis. *Biochim Biophys Acta,* 1841**,** 390-400.

KRIEG, P., MARKS, F. & FURSTENBERGER, G. 2001. A gene cluster encoding human epidermis-type lipoxygenases at chromosome 17p13.1: cloning, physical mapping, and expression. *Genomics,* 73**,** 323-30.

KRIEG, P., ROSENBERGER, S., DE JUANES, S., LATZKO, S., HOU, J., DICK, A., KLOZ, U., VAN DER HOEVEN, F., HAUSSER, I., ESPOSITO, I., RAUH, M. & SCHNEIDER, H. 2013. Aloxe3 knockout mice reveal a function of epidermal lipoxygenase-3 as hepoxilin synthase and its pivotal role in barrier formation. *J Invest Dermatol,* 133**,** 172-80.

KRIEG, P., SIEBERT, M., KINZIG, A., BETTENHAUSEN, R., MARKS, F. & FURSTENBERGER, G. 1999. Murine 12(R)-lipoxygenase: functional expression, genomic structure and chromosomal localization. *FEBS Lett,* 446**,** 142-8.

KUBILUS, J., TARASCIO, A. J. & BADEN, H. P. 1979. Steroid-sulfatase deficiency in sex-linked ichthyosis. *Am J Hum Genet,* 31**,** 50-3.

KUCHLER, S., HENKES, D., ECKL, K. M., ACKERMANN, K., PLENDL, J., KORTING, H. C., HENNIES, H. C. & SCHAFER-KORTING, M. 2011. Hallmarks of atopic skin mimicked in vitro by means of a skin disease model based on FLG knock-down. *Altern Lab Anim,* 39**,** 471-80.

KUO, I. H., CARPENTER-MENDINI, A., YOSHIDA, T., MCGIRT, L. Y., IVANOV, A. I., BARNES, K. C., GALLO, R. L., BORKOWSKI, A. W., YAMASAKI, K., LEUNG, D. Y., GEORAS, S. N., DE BENEDETTO, A. & BECK, L. A. 2013a. Activation of epidermal toll-like receptor 2 enhances tight junction function: implications for atopic dermatitis and skin barrier repair. *J Invest Dermatol,* 133**,** 988-98.

KUO, I. H., YOSHIDA, T., DE BENEDETTO, A. & BECK, L. A. 2013b. The cutaneous innate immune response in patients with atopic dermatitis. *J Allergy Clin Immunol,* 131**,** 266-78.

KUPPER, T. S. & FUHLBRIGGE, R. C. 2004. Immune surveillance in the skin: mechanisms and clinical consequences. *Nat Rev Immunol,* 4**,** 211-22.

KURAMOTO, N., TAKIZAWA, T., MATSUKI, M., MORIOKA, H., ROBINSON, J. M. & YAMANISHI, K. 2002. Development of ichthyosiform skin compensates for defective permeability barrier function in mice lacking transglutaminase 1. *J Clin Invest,* 109**,** 243-50.

KYPRIOTOU, M., HUBER, M. & HOHL, D. 2012. The human epidermal differentiation complex: cornified envelope precursors, S100 proteins and the 'fused genes' family. *Exp Dermatol,* 21**,** 643-9.

LAIHO, E., IGNATIUS, J., MIKKOLA, H., YEE, V. C., TELLER, D. C., NIEMI, K. M., SAARIALHO-KERE, U., KERE, J. & PALOTIE, A. 1997. Transglutaminase 1 mutations in autosomal recessive congenital ichthyosis: private and recurrent mutations in an isolated population. *Am J Hum Genet,* 61**,** 529-38.

LAMB, R. & AMBLER, C. A. 2013. Keratinocytes propagated in serum-free, feeder-free culture conditions fail to form stratified epidermis in a reconstituted skin model. *PLoS One,* 8**,** e52494.

LANG, V. R., ENGLBRECHT, M., RECH, J., NUSSLEIN, H., MANGER, K., SCHUCH, F., TONY, H. P., FLECK, M., MANGER, B., SCHETT, G. & ZWERINA, J. 2012. Risk of infections in rheumatoid arthritis patients treated with tocilizumab. *Rheumatology (Oxford),* 51**,** 852-7.

LAMBROS, M. P., PARSA, C., MULAMALLA, H., ORLANDO, R., LAU, B., HUANG, Y., PON, D. & CHOW, M. 2011. Identifying cell and molecular stress after radiation in a three-dimensional (3-D) model of oral mucositis. *Biochem Biophys Res Commun,* 405**,** 102-6.

LAMPE, M. A., BURLINGAME, A. L., WHITNEY, J., WILLIAMS, M. L., BROWN, B. E., ROITMAN, E. & ELIAS, P. M. 1983. Human stratum corneum lipids: characterization and regional variations. *J Lipid Res,* 24**,** 120-30.

LARKIN, M. A., BLACKSHIELDS, G., BROWN, N. P., CHENNA, R., MCGETTIGAN, P. A., MCWILLIAM, H., VALENTIN, F., WALLACE, I. M., WILM, A., LOPEZ, R., THOMPSON, J. D., GIBSON, T. J. & HIGGINS, D. G. 2007. Clustal W and Clustal X version 2.0. *Bioinformatics,* 23**,** 2947-8.

LAZO, N. D., MEINE, J. G. & DOWNING, D. T. 1995. Lipids are covalently attached to rigid corneocyte protein envelopes existing predominantly as beta-sheets: a solid-state nuclear magnetic resonance study. *J Invest Dermatol,* 105**,** 296-300.

LAWLOR, F. 1988. Progress of a harlequin fetus to nonbullous ichthyosiform erythroderma. *Pediatrics,* 82**,** 870-3.

LEFEVRE, C., AUDEBERT, S., JOBARD, F., BOUADJAR, B., LAKHDAR, H., BOUGHDENE-STAMBOULI, O., BLANCHET-BARDON, C., HEILIG, R., FOGLIO, M., WEISSENBACH, J., LATHROP, M., PRUD'HOMME, J. F. & FISCHER, J. 2003. Mutations in the transporter ABCA12 are associated with lamellar ichthyosis type 2. *Hum Mol Genet,* 12**,** 2369-78.

LEFEVRE, C., BOUADJAR, B., FERRAND, V., TADINI, G., MEGARBANE, A., LATHROP, M., PRUD'HOMME, J. F. & FISCHER, J. 2006. Mutations in a new cytochrome P450 gene in lamellar ichthyosis type 3. *Hum Mol Genet,* 15**,** 767-76.

LEFEVRE, C., BOUADJAR, B., KARADUMAN, A., JOBARD, F., SAKER, S., OZGUC, M., LATHROP, M., PRUD'HOMME, J. F. & FISCHER, J. 2004. Mutations in ichthyin a new gene on chromosome 5q33 in a new form of autosomal recessive congenital ichthyosis. *Hum Mol Genet,* 13**,** 2473-82.

LEINONEN, P. T., HAGG, P. M., PELTONEN, S., JOUHILAHTI, E. M., MELKKO, J., KORKIAMAKI, T., OIKARINEN, A. & PELTONEN, J. 2009. Reevaluation of the normal epidermal calcium gradient, and analysis of calcium levels and ATP receptors in Hailey-Hailey and Darier epidermis. *J Invest Dermatol,* 129**,** 1379-87.

LENZ, L. S., MARX, J., CHAMULITRAT, W., KAISER, I., GRONE, H. J., LIEBISCH, G., SCHMITZ, G., ELSING, C., STRAUB, B. K., FULLEKRUG, J., STREMMEL, W. & HERRMANN, T. 2011. Adipocyte-specific inactivation of Acyl-CoA synthetase fatty acid transport protein 4 (Fatp4) in mice causes adipose hypertrophy and alterations in metabolism of complex lipids under high fat diet. *J Biol Chem,* 286**,** 35578-87.

LESUEUR, F., BOUADJAR, B., LEFEVRE, C., JOBARD, F., AUDEBERT, S., LAKHDAR, H., MARTIN, L., TADINI, G., KARADUMAN, A., EMRE, S., SAKER, S., LATHROP, M. & FISCHER, J. 2007. Novel mutations in ALOX12B in patients with autosomal recessive congenital ichthyosis and evidence for genetic heterogeneity on chromosome 17p13. *J Invest Dermatol,* 127**,** 829-34.

LEVY, D. E. & DARNELL, J. E., JR. 2002. Stats: transcriptional control and biological impact. *Nat Rev Mol Cell Biol,* 3**,** 651-62.

LI, H., LORIE, E. P., FISCHER, J., VAHLQUIST, A. & TORMA, H. 2012. The expression of epidermal lipoxygenases and transglutaminase-1 is perturbed by NIPAL4 mutations: indications of a common metabolic pathway essential for skin barrier homeostasis. *J Invest Dermatol,* 132**,** 2368-75.

LI, H., VAHLQUIST, A. & TORMA, H. 2013. Interactions between FATP4 and ichthyin in epidermal lipid processing may provide clues to the pathogenesis of autosomal recessive congenital ichthyosis. *J Dermatol Sci,* 69**,** 195-201.

LI, W., SANDHOFF, R., KONO, M., ZERFAS, P., HOFFMANN, V., DING, B. C., PROIA, R. L. & DENG, C. X. 2007. Depletion of ceramides with very long chain fatty acids

causes defective skin permeability barrier function, and neonatal lethality in ELOVL4 deficient mice. *Int J Biol Sci,* 3**,** 120-8.
LIAO, H., WATERS, A. J., GOUDIE, D. R., AITKEN, D. A., GRAHAM, G., SMITH, F. J., LEWIS-JONES, S. & MCLEAN, W. H. 2007. Filaggrin mutations are genetic modifying factors exacerbating X-linked ichthyosis. *J Invest Dermatol,* 127**,** 2795-8.
LIN, Q., FANG, D., FANG, J., REN, X., YANG, X., WEN, F. & SU, S. B. 2011. Impaired wound healing with defective expression of chemokines and recruitment of myeloid cells in TLR3-deficient mice. *J Immunol,* 186**,** 3710-7.
LO, Y. H., TORII, K., SAITO, C., FURUHASHI, T., MAEDA, A. & MORITA, A. 2010. Serum IL-22 correlates with psoriatic severity and serum IL-6 correlates with susceptibility to phototherapy. *J Dermatol Sci,* 58**,** 225-7.
LONG, S. A., WERTZ, P. W., STRAUSS, J. S. & DOWNING, D. T. 1985. Human stratum corneum polar lipids and desquamation. *Arch Dermatol Res,* 277**,** 284-7.
LORAND, L. & GRAHAM, R. M. 2003. Transglutaminases: crosslinking enzymes with pleiotropic functions. *Nat Rev Mol Cell Biol,* 4**,** 140-56.
LYNLEY, A. M. & DALE, B. A. 1983. The characterization of human epidermal filaggrin. A histidine-rich, keratin filament-aggregating protein. *Biochim Biophys Acta,* 744**,** 28-35.
MAN, M. Q., CHOI, E. H., SCHMUTH, M., CRUMRINE, D., UCHIDA, Y., ELIAS, P. M., HOLLERAN, W. M. & FEINGOLD, K. R. 2006. Basis for improved permeability barrier homeostasis induced by PPAR and LXR activators: liposensors stimulate lipid synthesis, lamellar body secretion, and post-secretory lipid processing. *J Invest Dermatol,* 126**,** 386-92.
MADISON, K. C. 2003. Barrier function of the skin: "la raison d'etre" of the epidermis. *J Invest Dermatol,* 121**,** 231-41.
MALONEY, M. E., WILLIAMS, M. L., EPSTEIN, E. H., JR., LAW, M. Y., FRITSCH, P. O. & ELIAS, P. M. 1984. Lipids in the pathogenesis of ichthyosis: topical cholesterol sulfate-induced scaling in hairless mice. *J Invest Dermatol,* 83**,** 252-6.
MANABE, M., SANCHEZ, M., SUN, T. T. & DALE, B. A. 1991. Interaction of filaggrin with keratin filaments during advanced stages of normal human epidermal differentiation and in ichthyosis vulgaris. *Differentiation,* 48**,** 43-50.
MANSBRIDGE, J. N. & KNAPP, A. M. 1993. Penetration of lucifer yellow into human skin: a lateral diffusion channel in the stratum corneum. *J Histochem Cytochem,* 41**,** 909-14.
MARKOVA, N. G., MAREKOV, L. N., CHIPEV, C. C., GAN, S. Q., IDLER, W. W. & STEINERT, P. M. 1993. Profilaggrin is a major epidermal calcium-binding protein. *Mol Cell Biol,* 13**,** 613-25.
MATSUKI, M., YAMASHITA, F., ISHIDA-YAMAMOTO, A., YAMADA, K., KINOSHITA, C., FUSHIKI, S., UEDA, E., MORISHIMA, Y., TABATA, K., YASUNO, H., HASHIDA, M., IIZUKA, H., IKAWA, M., OKABE, M., KONDOH, G., KINOSHITA, T., TAKEDA, J. & YAMANISHI, K. 1998. Defective stratum corneum and early neonatal death in mice lacking the gene for transglutaminase 1 (keratinocyte transglutaminase). *Proc Natl Acad Sci U S A,* 95**,** 1044-9.
METZKER, M. L. 2010. Sequencing technologies - the next generation. *Nat Rev Genet,* 11**,** 31-46.
MCGRATH, J. A. & UITTO, J. 2008. The filaggrin story: novel insights into skin-barrier function and disease. *Trends Mol Med,* 14**,** 20-7.
MCLEAN, W. H. 2016. Filaggrin failure - from ichthyosis vulgaris to atopic eczema and beyond. *Br J Dermatol,* 175 Suppl 2**,** 4-7.
MEDZHITOV, R. 2001. Toll-like receptors and innate immunity. *Nat Rev Immunol,* 1**,** 135-45.

MEGURO, S., ARAI, Y., MASUKAWA, Y., UIE, K. & TOKIMITSU, I. 2000. Relationship between covalently bound ceramides and transepidermal water loss (TEWL). *Arch Dermatol Res,* 292**,** 463-8.

MENON, G. K., CLEARY, G. W. & LANE, M. E. 2012. The structure and function of the stratum corneum. *Int J Pharm,* 435**,** 3-9.

MICHALIK, L. & WAHLI, W. 2007. Peroxisome proliferator-activated receptors (PPARs) in skin health, repair and disease. *Biochim Biophys Acta,* 1771**,** 991-8.

MICALLEF, L., BELAUBRE, F., PINON, A., JAYAT-VIGNOLES, C., DELAGE, C., CHARVERON, M. & SIMON, A. 2009. Effects of extracellular calcium on the growth-differentiation switch in immortalized keratinocyte HaCaT cells compared with normal human keratinocytes. *Exp Dermatol,* 18**,** 143-51.

MILDNER, M., BALLAUN, C., STICHENWIRTH, M., BAUER, R., GMEINER, R., BUCHBERGER, M., MLITZ, V. & TSCHACHLER, E. 2006. Gene silencing in a human organotypic skin model. *Biochem Biophys Res Commun,* 348**,** 76-82.

MILDNER, M., JIN, J., ECKHART, L., KEZIC, S., GRUBER, F., BARRESI, C., STREMNITZER, C., BUCHBERGER, M., MLITZ, V., BALLAUN, C., STERNICZKY, B., FODINGER, D. & TSCHACHLER, E. 2010. Knockdown of filaggrin impairs diffusion barrier function and increases UV sensitivity in a human skin model. *J Invest Dermatol,* 130**,** 2286-94.

MILNER, M. E., O'GUIN, W. M., HOLBROOK, K. A. & DALE, B. A. 1992. Abnormal lamellar granules in harlequin ichthyosis. *J Invest Dermatol,* 99**,** 824-9.

MILLER, L. S. 2008. Toll-like receptors in skin. *Adv Dermatol,* 24**,** 71-87.

MINNER, F. & POUMAY, Y. 2009. Candidate housekeeping genes require evaluation before their selection for studies of human epidermal keratinocytes. *J Invest Dermatol,* 129**,** 770-3.

MISCHKE, D., KORGE, B. P., MARENHOLZ, I., VOLZ, A. & ZIEGLER, A. 1996. Genes encoding structural proteins of epidermal cornification and S100 calcium-binding proteins form a gene complex ("epidermal differentiation complex") on human chromosome 1q21. *J Invest Dermatol,* 106**,** 989-92.

MIZUTANI, H., OHMOTO, Y., MIZUTANI, T., MURATA, M. & SHIMIZU, M. 1997. Role of increased production of monocytes TNF-alpha, IL-1beta and IL-6 in psoriasis: relation to focal infection, disease activity and responses to treatments. *J Dermatol Sci,* 14**,** 145-53.

MOAZED, D. 2009. Small RNAs in transcriptional gene silencing and genome defence. *Nature,* 457**,** 413-20.

MOHAMADZADEH, M., MULLER, M., HULTSCH, T., ENK, A., SALOGA, J. & KNOP, J. 1994. Enhanced expression of IL-8 in normal human keratinocytes and human keratinocyte cell line HaCaT in vitro after stimulation with contact sensitizers, tolerogens and irritants. *Exp Dermatol,* 3**,** 298-303.

MONIAGA, C. S., EGAWA, G., KAWASAKI, H., HARA-CHIKUMA, M., HONDA, T., TANIZAKI, H., NAKAJIMA, S., OTSUKA, A., MATSUOKA, H., KUBO, A., SAKABE, J., TOKURA, Y., MIYACHI, Y., AMAGAI, M. & KABASHIMA, K. 2010. Flaky tail mouse denotes human atopic dermatitis in the steady state and by topical application with Dermatophagoides pteronyssinus extract. *Am J Pathol,* 176**,** 2385-93.

MONIAGA, C. S., JEONG, S. K., EGAWA, G., NAKAJIMA, S., HARA-CHIKUMA, M., JEON, J. E., LEE, S. H., HIBINO, T., MIYACHI, Y. & KABASHIMA, K. 2013. Protease activity enhances production of thymic stromal lymphopoietin and basophil accumulation in flaky tail mice. *Am J Pathol,* 182**,** 841-51.

MONIAGA, C. S. & KABASHIMA, K. 2011. Filaggrin in atopic dermatitis: flaky tail mice as a novel model for developing drug targets in atopic dermatitis. *Inflamm Allergy Drug Targets,* 10**,** 477-85.

MORAN, J. L., QIU, H., TURBE-DOAN, A., YUN, Y., BOEGLIN, W. E., BRASH, A. R. & BEIER, D. R. 2007. A mouse mutation in the 12R-lipoxygenase, Alox12b, disrupts formation of the epidermal permeability barrier. *J Invest Dermatol,* 127**,** 1893-7.

MOSKOWITZ, D. G., FOWLER, A. J., HEYMAN, M. B., COHEN, S. P., CRUMRINE, D., ELIAS, P. M. & WILLIAMS, M. L. 2004. Pathophysiologic basis for growth failure in children with ichthyosis: an evaluation of cutaneous ultrastructure, epidermal permeability barrier function, and energy expenditure. *J Pediatr,* 145**,** 82-92.

MUELLER, J. W., GILLIGAN, L. C., IDKOWIAK, J., ARLT, W. & FOSTER, P. A. 2015. The Regulation of Steroid Action by Sulfation and Desulfation. *Endocr Rev,* 36**,** 526-63.

MULUGETA, S., GRAY, J. M., NOTARFRANCESCO, K. L., GONZALES, L. W., KOVAL, M., FEINSTEIN, S. I., BALLARD, P. L., FISHER, A. B. & SHUMAN, H. 2002. Identification of LBM180, a lamellar body limiting membrane protein of alveolar type II cells, as the ABC transporter protein ABCA3. *J Biol Chem,* 277**,** 22147-55.

MUNOZ-GARCIA, A., THOMAS, C. P., KEENEY, D. S., ZHENG, Y. & BRASH, A. R. 2014. The importance of the lipoxygenase-hepoxilin pathway in the mammalian epidermal barrier. *Biochim Biophys Acta,* 1841**,** 401-8.

NACHAT, R., MECHIN, M. C., TAKAHARA, H., CHAVANAS, S., CHARVERON, M., SERRE, G. & SIMON, M. 2005. Peptidylarginine deiminase isoforms 1-3 are expressed in the epidermis and involved in the deimination of K1 and filaggrin. *J Invest Dermatol,* 124**,** 384-93.

NAKA, T., NARAZAKI, M., HIRATA, M., MATSUMOTO, T., MINAMOTO, S., AONO, A., NISHIMOTO, N., KAJITA, T., TAGA, T., YOSHIZAKI, K., AKIRA, S. & KISHIMOTO, T. 1997. Structure and function of a new STAT-induced STAT inhibitor. *Nature,* 387**,** 924-9.

NAPOLI, C., LEMIEUX, C. & JORGENSEN, R. 1990. Introduction of a Chimeric Chalcone Synthase Gene into Petunia Results in Reversible Co-Suppression of Homologous Genes in trans. *Plant Cell,* 2**,** 279-289.

NATSUGA, K., AKIYAMA, M., KATO, N., SAKAI, K., SUGIYAMA-NAKAGIRI, Y., NISHIMURA, M., HATA, H., ABE, M., ARITA, K., TSUJI-ABE, Y., ONOZUKA, T., AOYAGI, S., KODAMA, K., UJIIE, H., TOMITA, Y. & SHIMIZU, H. 2007. Novel ABCA12 mutations identified in two cases of non-bullous congenital ichthyosiform erythroderma associated with multiple skin malignant neoplasia. *J Invest Dermatol,* 127**,** 2669-73.

NAWAZ, S., TARIQ, M., AHMAD, I., MALIK, N. A., BAIG, S. M., DAHL, N. & KLAR, J. 2012. Non-bullous congentital ichthyosiform erythroderma associated with homozygosity for a novel missense mutation in an ATP binding domain of ABCA12. *Eur J Dermatol,* 22**,** 178-81.

NEDOSZYTKO, B., SOKOLOWSKA-WOJDYLO, M., RUCKEMANN-DZIURDZINSKA, K., ROSZKIEWICZ, J. & NOWICKI, R. J. 2014. Chemokines and cytokines network in the pathogenesis of the inflammatory skin diseases: atopic dermatitis, psoriasis and skin mastocytosis. *Postepy Dermatol Alergol,* 31**,** 84-91.

NEMES, Z., MAREKOV, L. N., FESUS, L. & STEINERT, P. M. 1999. A novel function for transglutaminase 1: attachment of long-chain omega-hydroxyceramides to involucrin by ester bond formation. *Proc Natl Acad Sci U S A,* 96**,** 8402-7.

NEMES, Z. & STEINERT, P. M. 1999. Bricks and mortar of the epidermal barrier. *Exp Mol Med,* 31**,** 5-19.

NEUNER, P., URBANSKI, A., TRAUTINGER, F., MOLLER, A., KIRNBAUER, R., KAPP, A., SCHOPF, E., SCHWARZ, T. & LUGER, T. A. 1991. Increased IL-6 production by monocytes and keratinocytes in patients with psoriasis. *J Invest Dermatol,* 97**,** 27-33.

NICOLAS, L. B., PINOTEAU, W., PAPOT, S., ROUTIER, S., GUILLAUMET, G. & MORTAUD, S. 2001. Aggressive behavior induced by the steroid sulfatase inhibitor COUMATE and by DHEAS in CBA/H mice. *Brain Res,* 922**,** 216-22.

NOMURA, T., AKIYAMA, M., SANDILANDS, A., NEMOTO-HASEBE, I., SAKAI, K., NAGASAKI, A., PALMER, C. N., SMITH, F. J., MCLEAN, W. H. & SHIMIZU, H. 2009. Prevalent and rare mutations in the gene encoding filaggrin in Japanese patients with ichthyosis vulgaris and atopic dermatitis. *J Invest Dermatol,* 129**,** 1302-5.

NOMURA, T., SANDILANDS, A., AKIYAMA, M., LIAO, H., EVANS, A. T., SAKAI, K., OTA, M., SUGIURA, H., YAMAMOTO, K., SATO, H., PALMER, C. N., SMITH, F. J., MCLEAN, W. H. & SHIMIZU, H. 2007. Unique mutations in the filaggrin gene in Japanese patients with ichthyosis vulgaris and atopic dermatitis. *J Allergy Clin Immunol,* 119**,** 434-40.

OHNO, Y., NAKAMICHI, S., OHKUNI, A., KAMIYAMA, N., NAOE, A., TSUJIMURA, H., YOKOSE, U., SUGIURA, K., ISHIKAWA, J., AKIYAMA, M. & KIHARA, A. 2015. Essential role of the cytochrome P450 CYP4F22 in the production of acylceramide, the key lipid for skin permeability barrier formation. *Proc Natl Acad Sci U S A,* 112**,** 7707-12.

OHNO, Y., SUTO, S., YAMANAKA, M., MIZUTANI, Y., MITSUTAKE, S., IGARASHI, Y., SASSA, T. & KIHARA, A. 2010. ELOVL1 production of C24 acyl-CoAs is linked to C24 sphingolipid synthesis. *Proc Natl Acad Sci U S A,* 107**,** 18439-44.

OJI, V., HAUTIER, J. M., AHVAZI, B., HAUSSER, I., AUFENVENNE, K., WALKER, T., SELLER, N., STEIJLEN, P. M., KUSTER, W., HOVNANIAN, A., HENNIES, H. C. & TRAUPE, H. 2006. Bathing suit ichthyosis is caused by transglutaminase-1 deficiency: evidence for a temperature-sensitive phenotype. *Hum Mol Genet,* 15**,** 3083-97.

OJI, V., TADINI, G., AKIYAMA, M., BLANCHET BARDON, C., BODEMER, C., BOURRAT, E., COUDIERE, P., DIGIOVANNA, J. J., ELIAS, P., FISCHER, J., FLECKMAN, P., GINA, M., HARPER, J., HASHIMOTO, T., HAUSSER, I., HENNIES, H. C., HOHL, D., HOVNANIAN, A., ISHIDA-YAMAMOTO, A., JACYK, W. K., LEACHMAN, S., LEIGH, I., MAZEREEUW-HAUTIER, J., MILSTONE, L., MORICE-PICARD, F., PALLER, A. S., RICHARD, G., SCHMUTH, M., SHIMIZU, H., SPRECHER, E., VAN STEENSEL, M., TAIEB, A., TORO, J. R., VABRES, P., VAHLQUIST, A., WILLIAMS, M. & TRAUPE, H. Revised nomenclature and classification of inherited ichthyoses: results of the First Ichthyosis Consensus Conference in Soreze 2009. *J Am Acad Dermatol,* 63**,** 607-41.

O'REGAN, G. M., KEMPERMAN, P. M., SANDILANDS, A., CHEN, H., CAMPBELL, L. E., KROBOTH, K., WATSON, R., ROWLAND, M., PUPPELS, G. J., MCLEAN, W. H., CASPERS, P. J. & IRVINE, A. D. 2010. Raman profiles of the stratum corneum define 3 filaggrin genotype-determined atopic dermatitis endophenotypes. *J Allergy Clin Immunol,* 126**,** 574-80 e1.

OREN, A., GANZ, T., LIU, L. & MEERLOO, T. 2003. In human epidermis, beta-defensin 2 is packaged in lamellar bodies. *Exp Mol Pathol,* 74**,** 180-2.

OSAWA, R., AKIYAMA, M. & SHIMIZU, H. 2011. Filaggrin gene defects and the risk of developing allergic disorders. *Allergol Int,* 60**,** 1-9.

OSAWA, R., KONNO, S., AKIYAMA, M., NEMOTO-HASEBE, I., NOMURA, T., NOMURA, Y., ABE, R., SANDILANDS, A., MCLEAN, W. H., HIZAWA, N., NISHIMURA, M. & SHIMIZU, H. Japanese-specific filaggrin gene mutations in Japanese patients suffering from atopic eczema and asthma. *J Invest Dermatol,* 130**,** 2834-6.

O'SHAUGHNESSY, R. F., CHOUDHARY, I. & HARPER, J. I. 2010. Interleukin-1 alpha blockade prevents hyperkeratosis in an in vitro model of lamellar ichthyosis. *Hum Mol Genet,* 19**,** 2594-605.

OYOSHI, M. K., MURPHY, G. F. & GEHA, R. S. 2009. Filaggrin-deficient mice exhibit TH17-dominated skin inflammation and permissiveness to epicutaneous sensitization with protein antigen. *J Allergy Clin Immunol,* 124**,** 485-93, 493 e1.

PADDISON, P. J., CAUDY, A. A., BERNSTEIN, E., HANNON, G. J. & CONKLIN, D. S. 2002. Short hairpin RNAs (shRNAs) induce sequence-specific silencing in mammalian cells. *Genes Dev,* 16**,** 948-58.

PAIGE, D. G., MORSE-FISHER, N. & HARPER, J. I. 1994. Quantification of stratum corneum ceramides and lipid envelope ceramides in the hereditary ichthyoses. *Br J Dermatol,* 131**,** 23-7.

PALIOURAS, M. & DIAMANDIS, E. P. 2006. The kallikrein world: an update on the human tissue kallikreins. *Biol Chem,* 387**,** 643-52.

PALMER, C. N., IRVINE, A. D., TERRON-KWIATKOWSKI, A., ZHAO, Y., LIAO, H., LEE, S. P., GOUDIE, D. R., SANDILANDS, A., CAMPBELL, L. E., SMITH, F. J., O'REGAN, G. M., WATSON, R. M., CECIL, J. E., BALE, S. J., COMPTON, J. G., DIGIOVANNA, J. J., FLECKMAN, P., LEWIS-JONES, S., ARSECULERATNE, G., SERGEANT, A., MUNRO, C. S., EL HOUATE, B., MCELREAVEY, K., HALKJAER, L. B., BISGAARD, H., MUKHOPADHYAY, S. & MCLEAN, W. H. 2006. Common loss-of-function variants of the epidermal barrier protein filaggrin are a major predisposing factor for atopic dermatitis. *Nat Genet,* 38**,** 441-6.

PARK, Y. H., JANG, W. H., SEO, J. A., PARK, M., LEE, T. R., PARK, Y. H., KIM, D. K. & LIM, K. M. 2012. Decrease of ceramides with very long-chain fatty acids and downregulation of elongases in a murine atopic dermatitis model. *J Invest Dermatol,* 132**,** 476-9.

PARMENTIER, L., CLEPET, C., BOUGHDENE-STAMBOULI, O., LAKHDAR, H., BLANCHET-BARDON, C., DUBERTRET, L., WUNDERLE, E., PULCINI, F., FIZAMES, C. & WEISSENBACH, J. 1999. Lamellar ichthyosis: further narrowing, physical and expression mapping of the chromosome 2 candidate locus. *Eur J Hum Genet,* 7**,** 77-87.

PARMENTIER, L., LAKHDAR, H., BLANCHET-BARDON, C., MARCHAND, S., DUBERTRET, L. & WEISSENBACH, J. 1996. Mapping of a second locus for lamellar ichthyosis to chromosome 2q33-35. *Hum Mol Genet,* 5**,** 555-9.

PEELMAN, F., LABEUR, C., VANLOO, B., ROOSBEEK, S., DEVAUD, C., DUVERGER, N., DENEFLE, P., ROSIER, M., VANDEKERCKHOVE, J. & ROSSENEU, M. 2003. Characterization of the ABCA transporter subfamily: identification of prokaryotic and eukaryotic members, phylogeny and topology. *J Mol Biol,* 325**,** 259-74.

PENDARIES, V., MALAISSE, J., PELLERIN, L., LE LAMER, M., NACHAT, R., KEZIC, S., SCHMITT, A. M., PAUL, C., POUMAY, Y., SERRE, G. & SIMON, M. 2014. Knockdown of filaggrin in a three-dimensional reconstructed human epidermis impairs keratinocyte differentiation. *J Invest Dermatol,* 134**,** 2938-46.

PENNEYS, N.S., FULTON, J.E., WEINSTEIN, G.D. AND FROST, P., 1970. Location of proliferating cells in human epidermis. *Archives of dermatology*, *101*(3), pp.323-327.

PLAGER, D. A., LEONTOVICH, A. A., HENKE, S. A., DAVIS, M. D., MCEVOY, M. T., SCIALLIS, G. F., 2ND & PITTELKOW, M. R. 2007. Early cutaneous gene transcription changes in adult atopic dermatitis and potential clinical implications. *Exp Dermatol,* 16**,** 28-36.

PRESLAND, R. B., BOGGESS, D., LEWIS, S. P., HULL, C., FLECKMAN, P. & SUNDBERG, J. P. 2000. Loss of normal profilaggrin and filaggrin in flaky tail (ft/ft) mice: an animal model for the filaggrin-deficient skin disease ichthyosis vulgaris. *J Invest Dermatol,* 115**,** 1072-81.

PRESLAND, R. B., HAYDOCK, P. V., FLECKMAN, P., NIRUNSUKSIRI, W. & DALE, B. A. 1992. Characterization of the human epidermal profilaggrin gene. Genomic organization and identification of an S-100-like calcium binding domain at the amino terminus. *J Biol Chem,* 267**,** 23772-81.

PROKSCH, E., BRANDNER, J. M. & JENSEN, J. M. 2008. The skin: an indispensable barrier. *Exp Dermatol,* 17**,** 1063-72.

RABIONET, M., GORGAS, K. & SANDHOFF, R. 2014. Ceramide synthesis in the epidermis. *Biochim Biophys Acta,* 1841**,** 422-34.

RICE, R. H., CRUMRINE, D., UCHIDA, Y., GRUBER, R. & ELIAS, P. M. 2005. Structural changes in epidermal scale and appendages as indicators of defective TGM1 activity. *Arch Dermatol Res,* 297**,** 127-33.

RIVIER, M., CASTIEL, I., SAFONOVA, I., AILHAUD, G. & MICHEL, S. 2000. Peroxisome proliferator-activated receptor-alpha enhances lipid metabolism in a skin equivalent model. *J Invest Dermatol,* 114**,** 681-7.

RIVIER, M., SAFONOVA, I., LEBRUN, P., GRIFFITHS, C. E., AILHAUD, G. & MICHEL, S. 1998. Differential expression of peroxisome proliferator-activated receptor subtypes during the differentiation of human keratinocytes. *J Invest Dermatol,* 111**,** 1116-21.

RADNER, F. P., MARRAKCHI, S., KIRCHMEIER, P., KIM, G. J., RIBIERRE, F., KAMOUN, B., ABID, L., LEIPOLDT, M., TURKI, H., SCHEMPP, W., HEILIG, R., LATHROP, M. & FISCHER, J. 2013. Mutations in CERS3 cause autosomal recessive congenital ichthyosis in humans. *PLoS Genet,* 9**,** e1003536.

RAJPAR, S. F., CULLUP, T., KELSELL, D. P. & MOSS, C. 2006. A novel ABCA12 mutation underlying a case of Harlequin ichthyosis. *Br J Dermatol,* 155**,** 204-6.

RAJPOPAT, S., MOSS, C., MELLERIO, J., VAHLQUIST, A., GANEMO, A., HELLSTROM-PIGG, M., ILCHYSHYN, A., BURROWS, N., LESTRINGANT, G., TAYLOR, A., KENNEDY, C., PAIGE, D., HARPER, J., GLOVER, M., FLECKMAN, P., EVERMAN, D., FOUANI, M., KAYSERILI, H., PURVIS, D., HOBSON, E., CHU, C., MEIN, C., KELSELL, D. & O'TOOLE, E. 2011. Harlequin ichthyosis: a review of clinical and molecular findings in 45 cases. *Arch Dermatol,* 147**,** 681-6.

RANASINGHE, A. W., WERTZ, P. W., DOWNING, D. T. & MACKENZIE, I. C. 1986. Lipid composition of cohesive and desquamated corneocytes from mouse ear skin. *J Invest Dermatol,* 86**,** 187-90.

RAYMOND, A. A., GONZALEZ DE PEREDO, A., STELLA, A., ISHIDA-YAMAMOTO, A., BOUYSSIE, D., SERRE, G., MONSARRAT, B. & SIMON, M. 2008. Lamellar bodies of human epidermis: proteomics characterization by high throughput mass spectrometry and possible involvement of CLIP-170 in their trafficking/secretion. *Mol Cell Proteomics,* 7**,** 2151-75.

REARICK, J. I., ALBRO, P. W. & JETTEN, A. M. 1987. Increase in cholesterol sulfotransferase activity during in vitro squamous differentiation of rabbit tracheal epithelial cells and its inhibition by retinoic acid. *J Biol Chem,* 262**,** 13069-74.

REHFELD, S. J., PLACHY, W. Z., WILLIAMS, M. L. & ELIAS, P. M. 1988. Calorimetric and electron spin resonance examination of lipid phase transitions in human stratum corneum: molecular basis for normal cohesion and abnormal desquamation in recessive X-linked ichthyosis. *J Invest Dermatol,* 91**,** 499-505.

RHEINWALD, J. G. & GREEN, H. 1975. Serial cultivation of strains of human epidermal keratinocytes: the formation of keratinizing colonies from single cells. *Cell,* 6**,** 331-43.

RICE, R. H., CRUMRINE, D., UCHIDA, Y., GRUBER, R. & ELIAS, P. M. 2005. Structural changes in epidermal scale and appendages as indicators of defective TGM1 activity. *Arch Dermatol Res,* 297**,** 127-33.

ROBINSON, N. A., LAPIC, S., WELTER, J. F. & ECKERT, R. L. 1997. S100A11, S100A10, annexin I, desmosomal proteins, small proline-rich proteins, plasminogen activator inhibitor-2, and involucrin are components of the cornified envelope of cultured human epidermal keratinocytes. *J Biol Chem,* 272**,** 12035-46.

RODRIGUEZ-PAZOS, L., GINARTE, M., FACHAL, L., TORIBIO, J., CARRACEDO, A. & VEGA, A. Analysis of TGM1, ALOX12B, ALOXE3, NIPAL4 and CYP4F22 in autosomal recessive congenital ichthyosis from Galicia (NW Spain): evidence of founder effects. *Br J Dermatol,* 165**,** 906-11.

ROSIN, D. L. & OKUSA, M. D. 2011. Dangers within: DAMP responses to damage and cell death in kidney disease. *J Am Soc Nephrol,* 22**,** 416-25.

RUSSELL, L. J., DIGIOVANNA, J. J., ROGERS, G. R., STEINERT, P. M., HASHEM, N., COMPTON, J. G. & BALE, S. J. 1995. Mutations in the gene for transglutaminase 1 in autosomal recessive lamellar ichthyosis. *Nat Genet,* 9**,** 279-83.

SAKAI, K., AKIYAMA, M., SUGIYAMA-NAKAGIRI, Y., MCMILLAN, J. R., SAWAMURA, D. & SHIMIZU, H. 2007. Localization of ABCA12 from Golgi apparatus to lamellar granules in human upper epidermal keratinocytes. *Exp Dermatol,* 16**,** 920-6.

SAKAI, K., AKIYAMA, M., YANAGI, T., MCMILLAN, J. R., SUZUKI, T., TSUKAMOTO, K., SUGIYAMA, H., HATANO, Y., HAYASHITANI, M., TAKAMORI, K., NAKASHIMA, K. & SHIMIZU, H. 2009. ABCA12 is a major causative gene for non-bullous congenital ichthyosiform erythroderma. *J Invest Dermatol,* 129**,** 2306-9.

SARRI, C. A., ROUSSAKI-SCHULZE, A., VASILOPOULOS, Y., ZAFIRIOU, E., PATSATSI, A., STAMATIS, C., GIDAROKOSTA, P., SOTIRIADIS, D., SARAFIDOU, T. & MAMURIS, Z. 2016. Netherton Syndrome: A Genotype-Phenotype Review. *Mol Diagn Ther*.

SASAKI, T., SHIOHAMA, A. & AMAGAI, M. 2014. [Mouse models for spontaneous dermatitis due to impaired skin barrier formation]. *Nihon Rinsho Meneki Gakkai Kaishi,* 37**,** 160-5.

SASAKI, T., SHIOHAMA, A., KUBO, A., KAWASAKI, H., ISHIDA-YAMAMOTO, A., YAMADA, T., HACHIYA, T., SHIMIZU, A., OKANO, H., KUDOH, J. & AMAGAI, M. 2013. A homozygous nonsense mutation in the gene for Tmem79, a component for the lamellar granule secretory system, produces spontaneous eczema in an experimental model of atopic dermatitis. *J Allergy Clin Immunol,* 132**,** 1111-1120 e4.

SANDILANDS, A., SUTHERLAND, C., IRVINE, A. D. & MCLEAN, W. H. 2009. Filaggrin in the frontline: role in skin barrier function and disease. *J Cell Sci,* 122**,** 1285-94.

SANDILANDS, A., TERRON-KWIATKOWSKI, A., HULL, P. R., O'REGAN, G. M., CLAYTON, T. H., WATSON, R. M., CARRICK, T., EVANS, A. T., LIAO, H., ZHAO, Y., CAMPBELL, L. E., SCHMUTH, M., GRUBER, R., JANECKE, A. R.,

ELIAS, P. M., VAN STEENSEL, M. A., NAGTZAAM, I., VAN GEEL, M., STEIJLEN, P. M., MUNRO, C. S., BRADLEY, D. G., PALMER, C. N., SMITH, F. J., MCLEAN, W. H. & IRVINE, A. D. 2007. Comprehensive analysis of the gene encoding filaggrin uncovers prevalent and rare mutations in ichthyosis vulgaris and atopic eczema. *Nat Genet,* 39**,** 650-4.

SANDHOFF, R. 2010. Very long chain sphingolipids: tissue expression, function and synthesis. *FEBS Lett,* 584**,** 1907-13.

SASAKI, T., SHIOHAMA, A. & AMAGAI, M. 2014. [Mouse models for spontaneous dermatitis due to impaired skin barrier formation]. *Nihon Rinsho Meneki Gakkai Kaishi,* 37**,** 160-5.

SASAKI, T., SHIOHAMA, A., KUBO, A., KAWASAKI, H., ISHIDA-YAMAMOTO, A., YAMADA, T., HACHIYA, T., SHIMIZU, A., OKANO, H., KUDOH, J. & AMAGAI, M. 2013. A homozygous nonsense mutation in the gene for Tmem79, a component for the lamellar granule secretory system, produces spontaneous eczema in an experimental model of atopic dermatitis. *J Allergy Clin Immunol,* 132**,** 1111-1120 e4.

SAWADA, E., YOSHIDA, N., SUGIURA, A. & IMOKAWA, G. 2012. Th1 cytokines accentuate but Th2 cytokines attenuate ceramide production in the stratum corneum of human epidermal equivalents: an implication for the disrupted barrier mechanism in atopic dermatitis. *J Dermatol Sci,* 68**,** 25-35.

SCHARSCHMIDT, T. C., MAN, M. Q., HATANO, Y., CRUMRINE, D., GUNATHILAKE, R., SUNDBERG, J. P., SILVA, K. A., MAURO, T. M., HUPE, M., CHO, S., WU, Y., CELLI, A., SCHMUTH, M., FEINGOLD, K. R. & ELIAS, P. M. 2009. Filaggrin deficiency confers a paracellular barrier abnormality that reduces inflammatory thresholds to irritants and haptens. *J Allergy Clin Immunol,* 124**,** 496-506, 506 e1-6.

SCHMID-WENDTNER, M. H. & KORTING, H. C. 2006. The pH of the skin surface and its impact on the barrier function. *Skin Pharmacol Physiol,* 19**,** 296-302.

SCHEIBNER, K. A., LUTZ, M. A., BOODOO, S., FENTON, M. J., POWELL, J. D. & HORTON, M. R. 2006. Hyaluronan fragments act as an endogenous danger signal by engaging TLR2. *J Immunol,* 177**,** 1272-81.

SCHONTHALER, H. B., HUGGENBERGER, R., WCULEK, S. K., DETMAR, M. & WAGNER, E. F. 2009. Systemic anti-VEGF treatment strongly reduces skin inflammation in a mouse model of psoriasis. *Proc Natl Acad Sci U S A,* 106**,** 21264-9.

SCHMID-WENDTNER, M. H. & KORTING, H. C. 2006. The pH of the skin surface and its impact on the barrier function. *Skin Pharmacol Physiol,* 19**,** 296-302.

SCHNARE, M., BARTON, G. M., HOLT, A. C., TAKEDA, K., AKIRA, S. & MEDZHITOV, R. 2001. Toll-like receptors control activation of adaptive immune responses. *Nat Immunol,* 2**,** 947-50.

SCHUETTE, C. G., DOERING, T., KOLTER, T. & SANDHOFF, K. 1999. The glycosphingolipidoses-from disease to basic principles of metabolism. *Biol Chem,* 380**,** 759-66.

SCOTT, I. R., HARDING, C. R. & BARRETT, J. G. 1982. Histidine-rich protein of the keratohyalin granules. Source of the free amino acids, urocanic acid and pyrrolidone carboxylic acid in the stratum corneum. *Biochim Biophys Acta,* 719**,** 110-7.

SHAPIRO, L. J., WEISS, R., BUXMAN, M. M., VIDGOFF, J., DIMOND, R. L., ROLLER, J. A. & WELLS, R. S. 1978. Enzymatic basis of typical X-linked icthyosis. *Lancet,* 2**,** 756-7.

SHAW, J. L. & DIAMANDIS, E. P. 2007. Distribution of 15 human kallikreins in tissues and biological fluids. *Clin Chem,* 53**,** 1423-32.

SHWAYDER, T. 1999. Ichthyosis in a nutshell. *Pediatr Rev,* 20**,** 5-12.

SIDBURY, R., TOM, W. L., BERGMAN, J. N., COOPER, K. D., SILVERMAN, R. A., BERGER, T. G., CHAMLIN, S. L., COHEN, D. E., CORDORO, K. M., DAVIS, D. M., FELDMAN, S. R., HANIFIN, J. M., KROL, A., MARGOLIS, D. J., PALLER, A. S., SCHWARZENBERGER, K., SIMPSON, E. L., WILLIAMS, H. C., ELMETS, C. A., BLOCK, J., HARROD, C. G., SMITH BEGOLKA, W. & EICHENFIELD, L. F. 2014. Guidelines of care for the management of atopic dermatitis: Section 4. Prevention of disease flares and use of adjunctive therapies and approaches. *J Am Acad Dermatol,* 71**,** 1218-33.

SIMPSON, C. L., PATEL, D. M. & GREEN, K. J. 2011. Deconstructing the skin: cytoarchitectural determinants of epidermal morphogenesis. *Nat Rev Mol Cell Biol,* 12**,** 565-80.

SMITH, F. J., IRVINE, A. D., TERRON-KWIATKOWSKI, A., SANDILANDS, A., CAMPBELL, L. E., ZHAO, Y., LIAO, H., EVANS, A. T., GOUDIE, D. R., LEWIS-JONES, S., ARSECULERATNE, G., MUNRO, C. S., SERGEANT, A., O'REGAN, G., BALE, S. J., COMPTON, J. G., DIGIOVANNA, J. J., PRESLAND, R. B., FLECKMAN, P. & MCLEAN, W. H. 2006. Loss-of-function mutations in the gene encoding filaggrin cause ichthyosis vulgaris. *Nat Genet,* 38**,** 337-42.

SMYTH, I., HACKING, D. F., HILTON, A. A., MUKHAMEDOVA, N., MEIKLE, P. J., ELLIS, S., SATTERLEY, K., COLLINGE, J. E., DE GRAAF, C. A., BAHLO, M., SVIRIDOV, D., KILE, B. T. & HILTON, D. J. 2008. A mouse model of harlequin ichthyosis delineates a key role for Abca12 in lipid homeostasis. *PLoS Genet,* 4**,** e1000192.

SOBRAL, C. S., GRAGNANI, A., CAO, X., MORGAN, J. R. & FERREIRA, L. M. 2007. Human keratinocytes cultured on collagen matrix used as an experimental burn model. *J Burns Wounds,* 7**,** e6.STEINERT, P. M. & MAREKOV, L. N. 1995. The proteins elafin, filaggrin, keratin intermediate filaments, loricrin, and small proline-rich proteins 1 and 2 are isodipeptide cross-linked components of the human epidermal cornified cell envelope. *J Biol Chem,* 270**,** 17702-11.

SORRELL, J. M., BABER, M. A. & CAPLAN, A. I. 2007. A self-assembled fibroblast-endothelial cell co-culture system that supports in vitro vasculogenesis by both human umbilical vein endothelial cells and human dermal microvascular endothelial cells. *Cells Tissues Organs,* 186**,** 157-68.

SOUTO, L. R., REHDER, J., VASSALLO, J., CINTRA, M. L., KRAEMER, M. H. & PUZZI, M. B. 2006. Model for human skin reconstructed in vitro composed of associated dermis and epidermis. *Sao Paulo Med J,* 124**,** 71-6.

SPERGEL, J. M. 2010. From atopic dermatitis to asthma: the atopic march. *Ann Allergy Asthma Immunol,* 105**,** 99-106; quiz 107-9, 117.

STAMATI, K., PRIESTLEY, J. V., MUDERA, V. & CHEEMA, U. 2014. Laminin promotes vascular network formation in 3D in vitro collagen scaffolds by regulating VEGF uptake. *Exp Cell Res,* 327**,** 68-77.

STAUMONT-SALLE, D., ABBOUD, G., BRENUCHON, C., KANDA, A., ROUMIER, T., LAVOGIEZ, C., FLEURY, S., REMY, P., PAPIN, J. P., BERTRAND-MICHEL, J., TERCE, F., STAELS, B., DELAPORTE, E., CAPRON, M. & DOMBROWICZ, D. 2008. Peroxisome proliferator-activated receptor alpha regulates skin inflammation and humoral response in atopic dermatitis. *J Allergy Clin Immunol,* 121**,** 962-8 e6.

STARR, R., WILLSON, T. A., VINEY, E. M., MURRAY, L. J., RAYNER, J. R., JENKINS, B. J., GONDA, T. J., ALEXANDER, W. S., METCALF, D., NICOLA, N. A. & HILTON, D. J. 1997. A family of cytokine-inducible inhibitors of signalling. *Nature,* 387**,** 917-21.

STEGMEIER, F., HU, G., RICKLES, R. J., HANNON, G. J. & ELLEDGE, S. J. 2005. A lentiviral microRNA-based system for single-copy polymerase II-regulated RNA interference in mammalian cells. *Proc Natl Acad Sci U S A,* 102**,** 13212-7.

STROTT, C. A. & HIGASHI, Y. 2003. Cholesterol sulfate in human physiology: what's it all about? *J Lipid Res,* 44**,** 1268-78.

SUGAWARA, T., NOMURA, E. & HOSHI, N. 2006. Both N-terminal and C-terminal regions of steroid sulfatase are important for enzyme activity. *J Endocrinol,* 188**,** 365-74.

SUH, B. Y., JUNG, J. J., PARK, N., SEONG, C. H., IM, H. J., KWON, Y., KIM, D. & CHUN, Y. J. 2011. Induction of steroid sulfatase expression by tumor necrosis factor-alpha through phosphatidylinositol 3-kinase/Akt signaling pathway in PC-3 human prostate cancer cells. *Exp Mol Med,* 43**,** 646-52.

SUN, T. T., EICHNER, R., NELSON, W. G., TSENG, S. C., WEISS, R. A., JARVINEN, M. & WOODCOCK-MITCHELL, J. 1983. Keratin classes: molecular markers for different types of epithelial differentiation. *J Invest Dermatol,* 81**,** 109s-15s.

SWARTZENDRUBER, D. C., WERTZ, P. W., MADISON, K. C. & DOWNING, D. T. 1987. Evidence that the corneocyte has a chemically bound lipid envelope. *J Invest Dermatol,* 88**,** 709-13.

TABARA, H., SARKISSIAN, M., KELLY, W. G., FLEENOR, J., GRISHOK, A., TIMMONS, L., FIRE, A. & MELLO, C. C. 1999. The rde-1 gene, RNA interference, and transposon silencing in C. elegans. *Cell,* 99**,** 123-32.

TAKEDA, K., NOGUCHI, K., SHI, W., TANAKA, T., MATSUMOTO, M., YOSHIDA, N., KISHIMOTO, T. & AKIRA, S. 1997. Targeted disruption of the mouse Stat3 gene leads to early embryonic lethality. *Proc Natl Acad Sci U S A,* 94**,** 3801-4.

TAKEDA, K., KAISHO, T. & AKIRA, S. 2003. Toll-like receptors. *Annu Rev Immunol,* 21**,** 335-76.

TAKEUCHI, O., KAUFMANN, A., GROTE, K., KAWAI, T., HOSHINO, K., MORR, M., MUHLRADT, P. F. & AKIRA, S. 2000. Cutting edge: preferentially the R-stereoisomer of the mycoplasmal lipopeptide macrophage-activating lipopeptide-2 activates immune cells through a toll-like receptor 2- and MyD88-dependent signaling pathway. *J Immunol,* 164**,** 554-7.

THOMAS, A. C., CULLUP, T., NORGETT, E. E., HILL, T., BARTON, S., DALE, B. A., SPRECHER, E., SHERIDAN, E., TAYLOR, A. E., WILROY, R. S., DELOZIER, C., BURROWS, N., GOODYEAR, H., FLECKMAN, P., STEPHENS, K. G., MEHTA, L., WATSON, R. M., GRAHAM, R., WOLF, R., SLAVOTINEK, A., MARTIN, M., BOURN, D., MEIN, C. A., O'TOOLE, E. A. & KELSELL, D. P. 2006. ABCA12 is the major harlequin ichthyosis gene. *J Invest Dermatol,* 126**,** 2408-13.

THOMAS, A. C., SINCLAIR, C., MAHMUD, N., CULLUP, T., MELLERIO, J. E., HARPER, J., DALE, B. A., TURC-CAREL, C., HOHL, D., MCGRATH, J. A., VAHLQUIST, A., HELLSTROM-PIGG, M., GANEMO, A., METCALFE, K., MEIN, C. A., O'TOOLE, E. A. & KELSELL, D. P. 2008. Novel and recurring ABCA12 mutations associated with harlequin ichthyosis: implications for prenatal diagnosis. *Br J Dermatol,* 158**,** 611-3.

THOMAS, A. C., TATTERSALL, D., NORGETT, E. E., O'TOOLE, E. A. & KELSELL, D. P. 2009. Premature terminal differentiation and a reduction in specific proteases associated with loss of ABCA12 in Harlequin ichthyosis. *Am J Pathol,* 174**,** 970-8.

TOIVOLA, D. M., BOOR, P., ALAM, C. & STRNAD, P. 2015. Keratins in health and disease. *Curr Opin Cell Biol,* 32**,** 73-81.

TRAPNELL, C., ROBERTS, A., GOFF, L., PERTEA, G., KIM, D., KELLEY, D. R., PIMENTEL, H., SALZBERG, S. L., RINN, J. L. & PACHTER, L. 2012. Differential

gene and transcript expression analysis of RNA-seq experiments with TopHat and Cufflinks. *Nat Protoc,* 7**,** 562-78.

TRENT, S., DENNEHY, A., RICHARDSON, H., OJARIKRE, O. A., BURGOYNE, P. S., HUMBY, T. & DAVIES, W. 2012. Steroid sulfatase-deficient mice exhibit endophenotypes relevant to attention deficit hyperactivity disorder. *Psychoneuroendocrinology,* 37**,** 221-9.

UCHI, H., TERAO, H., KOGA, T. & FURUE, M. 2000. Cytokines and chemokines in the epidermis. *J Dermatol Sci,* 24 Suppl 1**,** S29-38.

UCHIYAMA, N., YAMAMOTO, A., KAMEDA, K., YAMAGUCHI, H. & ITO, M. 2000. The activity of fatty acid synthase of epidermal keratinocytes is regulated in the lower stratum spinousum and the stratum basale by local inflammation rather than by circulating hormones. *J Dermatol Sci,* 24**,** 134-41.

UMEMOTO, H., AKIYAMA, M., YANAGI, T., SAKAI, K., AOYAMA, Y., OIZUMI, A., SUGA, Y., KITAGAWA, Y. & SHIMIZU, H. 2011. New insight into genotype/phenotype correlations in ABCA12 mutations in harlequin ichthyosis. *J Dermatol Sci,* 61**,** 136-9.

VAN DRONGELEN, V., ALLOUL-RAMDHANI, M., DANSO, M. O., MIEREMET, A., MULDER, A., VAN SMEDEN, J., BOUWSTRA, J. A. & EL GHALBZOURI, A. 2013. Knock-down of filaggrin does not affect lipid organization and composition in stratum corneum of reconstructed human skin equivalents. *Exp Dermatol,* 22**,** 807-12.

VAN SMEDEN, J., JANSSENS, M., BOITEN, W. A., VAN DRONGELEN, V., FURIO, L., VREEKEN, R. J., HOVNANIAN, A. & BOUWSTRA, J. A. 2014a. Intercellular skin barrier lipid composition and organization in Netherton syndrome patients. *J Invest Dermatol,* 134**,** 1238-45.

VAHLQUIST, A., BYGUM, A., GANEMO, A., VIRTANEN, M., HELLSTROM-PIGG, M., STRAUSS, G., BRANDRUP, F. & FISCHER, J. 2010. Genotypic and clinical spectrum of self-improving collodion ichthyosis: ALOX12B, ALOXE3, and TGM1 mutations in Scandinavian patients. *J Invest Dermatol,* 130**,** 438-43.

VAN SMEDEN, J., JANSSENS, M., KAYE, E. C., CASPERS, P. J., LAVRIJSEN, A. P., VREEKEN, R. J. & BOUWSTRA, J. A. 2014b. The importance of free fatty acid chain length for the skin barrier function in atopic eczema patients. *Exp Dermatol,* 23**,** 45-52.

VAVROVA, K., HENKES, D., STRUVER, K., SOCHOROVA, M., SKOLOVA, B., WITTING, M. Y., FRIESS, W., SCHREML, S., MEIER, R. J., SCHAFER-KORTING, M., FLUHR, J. W. & KUCHLER, S. 2014. Filaggrin deficiency leads to impaired lipid profile and altered acidification pathways in a 3D skin construct. *J Invest Dermatol,* 134**,** 746-53.

WAJID, M., KURBAN, M., SHIMOMURA, Y. & CHRISTIANO, A. M. NIPAL4/ichthyin is expressed in the granular layer of human epidermis and mutated in two Pakistani families with autosomal recessive ichthyosis. *Dermatology,* 220**,** 8-14.

WAJID, M., KURBAN, M., SHIMOMURA, Y. & CHRISTIANO, A. M. 2010. NIPAL4/ichthyin is expressed in the granular layer of human epidermis and mutated in two Pakistani families with autosomal recessive ichthyosis. *Dermatology,* 220**,** 8-14.

WANG, X. P., SCHUNCK, M., KALLEN, K. J., NEUMANN, C., TRAUTWEIN, C., ROSE-JOHN, S. & PROKSCH, E. 2004. The interleukin-6 cytokine system regulates epidermal permeability barrier homeostasis. *J Invest Dermatol,* 123**,** 124-31.

WANG, Z., GERSTEIN, M. & SNYDER, M. 2009. RNA-Seq: a revolutionary tool for transcriptomics. *Nat Rev Genet,* 10**,** 57-63.

BRADSHAW, K. D. & CARR, B. R. 1986. Placental sulfatase deficiency: maternal and fetal expression of steroid sulfatase deficiency and X-linked ichthyosis. *Obstet Gynecol Surv,* 41**,** 401-13.

CROFT, D., MUNDO, A. F., HAW, R., MILACIC, M., WEISER, J., WU, G., CAUDY, M., GARAPATI, P., GILLESPIE, M., KAMDAR, M. R., JASSAL, B., JUPE, S., MATTHEWS, L., MAY, B., PALATNIK, S., ROTHFELS, K., SHAMOVSKY, V., SONG, H., WILLIAMS, M., BIRNEY, E., HERMJAKOB, H., STEIN, L. & D'EUSTACHIO, P. 2014. The Reactome pathway knowledgebase. *Nucleic Acids Res,* 42**,** D472-7.

METZKER, M. L. 2010. Sequencing technologies - the next generation. *Nat Rev Genet,* 11**,** 31-46.

TRAPNELL, C., ROBERTS, A., GOFF, L., PERTEA, G., KIM, D., KELLEY, D. R., PIMENTEL, H., SALZBERG, S. L., RINN, J. L. & PACHTER, L. 2012. Differential gene and transcript expression analysis of RNA-seq experiments with TopHat and Cufflinks. *Nat Protoc,* 7**,** 562-78.

WARDE-FARLEY, D., DONALDSON, S. L., COMES, O., ZUBERI, K., BADRAWI, R., CHAO, P., FRANZ, M., GROUIOS, C., KAZI, F., LOPES, C. T., MAITLAND, A., MOSTAFAVI, S., MONTOJO, J., SHAO, Q., WRIGHT, G., BADER, G. D. & MORRIS, Q. 2010. The GeneMANIA prediction server: biological network integration for gene prioritization and predicting gene function. *Nucleic Acids Res,* 38**,** W214-20.

WATKINS, P. A. & ELLIS, J. M. 2012. Peroxisomal acyl-CoA synthetases. *Biochim Biophys Acta,* 1822**,** 1411-20.

WEINSTEIN, J. N. 2008. Biochemistry. A postgenomic visual icon. *Science,* 319**,** 1772-3.

WELLS, R. S. 1966. Ichthyosis. *Br Med J,* 2**,** 1504-6.

WERTZ, P. W., SWARTZENDRUBER, D. C., KITKO, D. J., MADISON, K. C. & DOWNING, D. T. 1989. The role of the corneocyte lipid envelopes in cohesion of the stratum corneum. *J Invest Dermatol,* 93**,** 169-72.

WESTERGAARD, M., HENNINGSEN, J., SVENDSEN, M. L., JOHANSEN, C., JENSEN, U. B., SCHRODER, H. D., KRATCHMAROVA, I., BERGE, R. K., IVERSEN, L., BOLUND, L., KRAGBALLE, K. & KRISTIANSEN, K. 2001. Modulation of keratinocyte gene expression and differentiation by PPAR-selective ligands and tetradecylthioacetic acid. *J Invest Dermatol,* 116**,** 702-12.

WICKHAM, H. (2009). ggplot2: Elegant Graphics for Data Analysis. Springer. p. 5. ISBN 978-0-387-98140-6.

WILLIAMS, M. L. 1991. Lipids in normal and pathological desquamation. *Adv Lipid Res,* 24**,** 211-62.

WILLIAMS, M. L. 1992a. Epidermal lipids and scaling diseases of the skin. *Semin Dermatol,* 11**,** 169-75.

WILLIAMS, M. L. 1992b. Ichthyosis: mechanisms of disease. *Pediatr Dermatol,* 9**,** 365-8.

WILLIAMS, M. L. & ELIAS, P. M. 1981. Stratum corneum lipids in disorders of cornification: increased cholesterol sulfate content of stratum corneum in recessive x-linked ichthyosis. *J Clin Invest,* 68**,** 1404-10.

HUBER, M., RETTLER, I., BERNASCONI, K., FRENK, E., LAVRIJSEN, S. P., PONEC, M., BON, A., LAUTENSCHLAGER, S., SCHORDERET, D. F. & HOHL, D. 1995. Mutations of keratinocyte transglutaminase in lamellar ichthyosis. *Science,* 267**,** 525-8.

KIELTY, C. M., SHERRATT, M. J. & SHUTTLEWORTH, C. A. 2002. Elastic fibres. *J Cell Sci,* 115**,** 2817-28.

KRIEG, P. & FURSTENBERGER, G. 2014. The role of lipoxygenases in epidermis. *Biochim Biophys Acta,* 1841**,** 390-400.

MUELLER, J. W., GILLIGAN, L. C., IDKOWIAK, J., ARLT, W. & FOSTER, P. A. 2015. The Regulation of Steroid Action by Sulfation and Desulfation. *Endocr Rev,* 36**,** 526-63.

RUSSELL, L. J., DIGIOVANNA, J. J., ROGERS, G. R., STEINERT, P. M., HASHEM, N., COMPTON, J. G. & BALE, S. J. 1995. Mutations in the gene for transglutaminase 1 in autosomal recessive lamellar ichthyosis. *Nat Genet,* 9**,** 279-83.

SIMPSON, C. L., PATEL, D. M. & GREEN, K. J. 2011. Deconstructing the skin: cytoarchitectural determinants of epidermal morphogenesis. *Nat Rev Mol Cell Biol,* 12**,** 565-80.

SUGIURA, K., MURO, Y., FUTAMURA, K., MATSUMOTO, K., HASHIMOTO, N., NISHIZAWA, Y., NAGASAKA, T., SAITO, H., TOMITA, Y. AND USUKURA, J., 2009. The unfolded protein response is activated in differentiating epidermal keratinocytes. *Journal of Investigative Dermatology*, *129*(9), pp.2126-2135.

SUN, T. T., EICHNER, R., NELSON, W. G., TSENG, S. C., WEISS, R. A., JARVINEN, M. & WOODCOCK-MITCHELL, J. 1983. Keratin classes: molecular markers for different types of epithelial differentiation. *J Invest Dermatol,* 81**,** 109s-15s.

VAHLQUIST, A., BYGUM, A., GANEMO, A., VIRTANEN, M., HELLSTROM-PIGG, M., STRAUSS, G., BRANDRUP, F. & FISCHER, J. 2010. Genotypic and clinical spectrum of self-improving collodion ichthyosis: ALOX12B, ALOXE3, and TGM1 mutations in Scandinavian patients. *J Invest Dermatol,* 130**,** 438-43.

WILLIAMS, M. L. & ELIAS, P. M. 1985. Heterogeneity in autosomal recessive ichthyosis. Clinical and biochemical differentiation of lamellar ichthyosis and nonbullous congenital ichthyosiform erythroderma. *Arch Dermatol,* 121**,** 477-88.

WILLIAMS, M. L. & ELIAS, P. M. 1993. From basket weave to barrier. Unifying concepts for the pathogenesis of the disorders of cornification. *Arch Dermatol,* 129**,** 626-9.

WINGE, M. C., HOPPE, T., BERNE, B., VAHLQUIST, A., NORDENSKJOLD, M., BRADLEY, M. & TORMA, H. 2011. Filaggrin genotype determines functional and molecular alterations in skin of patients with atopic dermatitis and ichthyosis vulgaris. *PLoS One,* 6**,** e28254.

WONG, C. K., LEUNG, K. M., QIU, H. N., CHOW, J. Y., CHOI, A. O. & LAM, C. W. 2012. Activation of eosinophils interacting with dermal fibroblasts by pruritogenic cytokine IL-31 and alarmin IL-33: implications in atopic dermatitis. *PLoS One,* 7**,** e29815.

WOOD, L. C., ELIAS, P. M., SEQUEIRA-MARTIN, S. M., GRUNFELD, C. & FEINGOLD, K. R. 1994. Occlusion lowers cytokine mRNA levels in essential fatty acid-deficient and normal mouse epidermis, but not after acute barrier disruption. *J Invest Dermatol,* 103**,** 834-8.

WURM, S., ZHANG, J., GUINEA-VINIEGRA, J., GARCÍA, F., MUÑOZ, J., BAKIRI, L., EZHKOVA, E. AND WAGNER, E.F., 2015. Terminal epidermal differentiation is regulated by the interaction of Fra-2/AP-1 with Ezh2 and ERK1/2. *Genes & development*, *29*(2), pp.144-156.

YAMAMOTO, M., SATO, S., HEMMI, H., HOSHINO, K., KAISHO, T., SANJO, H., TAKEUCHI, O., SUGIYAMA, M., OKABE, M., TAKEDA, K. & AKIRA, S. 2003a. Role of adaptor TRIF in the MyD88-independent toll-like receptor signaling pathway. *Science,* 301**,** 640-3.

YAMAMOTO, M., SATO, S., HEMMI, H., UEMATSU, S., HOSHINO, K., KAISHO, T., TAKEUCHI, O., TAKEDA, K. & AKIRA, S. 2003b. TRAM is specifically involved

in the Toll-like receptor 4-mediated MyD88-independent signaling pathway. *Nat Immunol,* 4**,** 1144-50.

YAMANAKA, Y., AKIYAMA, M., SUGIYAMA-NAKAGIRI, Y., SAKAI, K., GOTO, M., MCMILLAN, J. R., OTA, M., SAWAMURA, D. & SHIMIZU, H. 2007. Expression of the keratinocyte lipid transporter ABCA12 in developing and reconstituted human epidermis. *Am J Pathol,* 171**,** 43-52.

YAMANISHI, K., INAZAWA, J., LIEW, F. M., NONOMURA, K., ARIYAMA, T., YASUNO, H., ABE, T., DOI, H., HIRANO, J. & FUKUSHIMA, S. 1992. Structure of the gene for human transglutaminase 1. *J Biol Chem,* 267**,** 17858-63.

YAMANO, G., FUNAHASHI, H., KAWANAMI, O., ZHAO, L. X., BAN, N., UCHIDA, Y., MOROHOSHI, T., OGAWA, J., SHIODA, S. & INAGAKI, N. 2001. ABCA3 is a lamellar body membrane protein in human lung alveolar type II cells. *FEBS Lett,* 508**,** 221-5.

YANAGI, T., AKIYAMA, M., NISHIHARA, H., MIYAMURA, Y., SAKAI, K., TANAKA, S. & SHIMIZU, H. 2011. AKT has an anti-apoptotic role in ABCA12-deficient keratinocytes. *J Invest Dermatol,* 131**,** 1942-5.

YANAGI, T., AKIYAMA, M., NISHIHARA, H., SAKAI, K., NISHIE, W., TANAKA, S. & SHIMIZU, H. 2008. Harlequin ichthyosis model mouse reveals alveolar collapse and severe fetal skin barrier defects. *Hum Mol Genet,* 17**,** 3075-83.

YANG, T., LIANG, D., KOCH, P. J., HOHL, D., KHERADMAND, F. & OVERBEEK, P. A. 2004. Epidermal detachment, desmosomal dissociation, and destabilization of corneodesmosin in Spink5-/- mice. *Genes Dev,* 18**,** 2354-8.

YU, Z., SCHNEIDER, C., BOEGLIN, W. E., MARNETT, L. J. & BRASH, A. R. 2003. The lipoxygenase gene ALOXE3 implicated in skin differentiation encodes a hydroperoxide isomerase. *Proc Natl Acad Sci U S A,* 100**,** 9162-7.

YUKI, T., YOSHIDA, H., AKAZAWA, Y., KOMIYA, A., SUGIYAMA, Y. & INOUE, S. 2011. Activation of TLR2 enhances tight junction barrier in epidermal keratinocytes. *J Immunol,* 187**,** 3230-7.

ZAMORE, P. D., TUSCHL, T., SHARP, P. A. & BARTEL, D. P. 2000. RNAi: double-stranded RNA directs the ATP-dependent cleavage of mRNA at 21 to 23 nucleotide intervals. *Cell,* 101**,** 25-33.

ZETTERSTEN, E., MAN, M. Q., SATO, J., DENDA, M., FARRELL, A., GHADIALLY, R., WILLIAMS, M. L., FEINGOLD, K. R. & ELIAS, P. M. 1998. Recessive x-linked ichthyosis: role of cholesterol-sulfate accumulation in the barrier abnormality. *J Invest Dermatol,* 111**,** 784-90.

ZHANG, H., GUO, Y., WANG, W., SHI, M., CHEN, X. & YAO, Z. 2011. Mutations in the filaggrin gene in Han Chinese patients with atopic dermatitis. *Allergy,* 66**,** 420-7.

ZHENG, Y., YIN, H., BOEGLIN, W. E., ELIAS, P. M., CRUMRINE, D., BEIER, D. R. & BRASH, A. R. 2011. Lipoxygenases mediate the effect of essential fatty acid in skin barrier formation: a proposed role in releasing omega-hydroxyceramide for construction of the corneocyte lipid envelope. *J Biol Chem,* 286**,** 24046-56.

ZUO, Y., ZHUANG, D. Z., HAN, R., ISAAC, G., TOBIN, J. J., MCKEE, M., WELTI, R., BRISSETTE, J. L., FITZGERALD, M. L. & FREEMAN, M. W. 2008. ABCA12 maintains the epidermal lipid permeability barrier by facilitating formation of ceramide linoleic esters. *J Biol Chem,* 283**,** 36624-35.

Appendices

1.1 List of the top twenty most down-regulated and up-regulated genes following each ichthyosis knockdown.

***STS* Knockdown**

Genes	log2FoldChange	p-value
EGR1	-3.13659516	2.77E-40
CXCL2	-2.625523507	3.02E-36
CSRNP1	-2.486409501	4.90E-28
MXD1	-2.378182062	1.95E-25
STS	-2.326989107	1.50E-23
UGCG	-2.256061764	7.36E-22
PTTG1	-2.236460179	8.64E-21
FOS	-2.176869043	7.29E-19
S100P	-2.119997068	8.24E-19
GLRX	-2.102568035	1.40E-17
QRFP	2.534510476	0.045116527
LINC00475	1.95865165	0.038651169
IL10RB-AS1	1.923746485	0.035437792
ANKUB1	1.845987226	0.03434547
ATP8B5P	1.82658206	0.033147429
C11orf85	1.6713127	0.02991356
SERPINA3	1.631787293	0.02868242
RNF224	1.612742671	0.024576875
C9orf84	1.586141844	0.0239599
GNG2	1.568269762	0.0205199

***FLG* Knockdown**

Gene	log2FoldChange	p-value
CNTN1	-3.722811366	5.41E-41
SLC1A3	-3.694306697	5.63E-35
TM4SF1	-3.569569903	7.83E-32
LMNB1	-3.563780925	3.83E-25
WFDC5	-3.498235445	1.47E-24
ZFP36L2	-3.31897206	1.55E-24
SLC39A2	-3.178334284	1.58E-23
CA2	-3.157168997	5.69E-23
SERPINB3	-3.066075787	7.71E-23
MLKL	-3.005266984	9.30E-23
ANKRD20A5P	4.119379676	0.009629861
TAC4	3.222839048	0.009552845
ZBTB20	2.990840502	0.009106532

NEU1	2.943962461	0.009055
FBXO39	2.810769202	0.008908187
AMH	2.806019735	0.008645296
EN2	2.762803279	0.008560863
KCNMA1	2.755662932	0.008437104
KLHL32	2.689702161	0.008406787
GOLGA8M	2.652082658	0.008292749

***ABCA12* Knockdown**

Gene	log2FoldChange	p-value
TNFRSF11B	-3.262374639	8.11E-07
MX2	-3.077488486	1.54E-20
IL7R	-2.737010076	3.47E-08
CCL2	-2.580335899	3.63E-10
RPSAP52	-2.487336996	1.40E-05
CLSTN2	-2.465467559	8.79E-20
IFIT1	-2.417825371	5.24E-10
OAS2	-2.407346905	1.02E-20
RSAD2	-2.259594746	7.08E-08
STC1	-2.119862431	0.000126778
VIP	2.676812773	0.001939983
ENDOU	2.619950415	3.65E-08
COL23A1	2.440437982	0.003164209
WNT1	2.312568832	0.003538192
EGFL6	2.300764418	0.000369775
AF131216.5	2.300504172	7.00E-05
CYP2D6	2.209047391	0.000462555
AF064858.6	2.16692109	0.000704831
MIR34C	2.119188862	0.009675273
CRB1	2.088379811	0.005023746

***TGM1* Knockdown**

Genes	log2FoldChange	p-value
AANAT	-2.79949805	0.003278747
ANKRD1	-2.769682308	0.007868913
PSG6	-2.633544666	0.001492824
LYPD2	-2.614205954	0.001236176
PADI1	-2.523012149	1.93E-06
MYCN	-2.51405814	0.008475865
PPP1R1B	-2.459253324	0.000284455
TICRR	-2.428793703	1.12E-13

IER3	-2.406660705	0.000404402
FOS	-2.314059119	1.86E-22
SHH	3.723202709	5.90E-07

***ICH* Knockdown**

Genes	log2FoldChange	p-value
NIPAL4	-3.216795734	5.64E-48
EGR1	-3.137258364	9.55E-44
FOS	-2.999518922	4.98E-41
TCF4	-2.802168449	1.20E-32
NFIB	-2.588661344	3.01E-32
LMNB1	-2.504270664	3.43E-28
CENPJ	-2.477199161	3.77E-26
KIF20B	-2.441856784	1.55E-25
PTTG1	-2.366780049	1.53E-24
KNTC1	-2.353831724	3.49E-23
SHH	3.505214354	2.99E-06
VIP	3.08968926	0.000213322
OLR1	2.758240021	3.00E-11
ASNSP1	2.619783444	0.001394379
SLC5A2	2.592642863	0.000414818
CEND1	2.579983511	0.002024604
AF131216.5	2.53198813	8.55E-06
CCK	2.423864811	7.84E-05
C1QL4	2.317633698	0.005626192
TBC1D29	2.283336876	0.003513647

***ALOX12B* Knockdown**

Gene	log2FoldChange	p-value
ABCG4	-1.206351542	0.001727122
ACTG2	-1.489615109	0.004631323
ALOX12B	-1.090237652	2.07E-08
ANKRD20A11P	-1.759532882	0.005914811
ANXA8L1	-1.539526985	0.000542176
ARHGAP19	-1.038402414	2.42E-21
ATAD2	-1.413821341	2.86E-15
ATAD5	-1.012589339	0.000768791
BARD1	-1.033412284	2.16E-08
BBOX1	-1.775978591	8.59E-09
CCK	2.625026792	2.41E-05
SLC5A2	2.554282964	0.000794129
VIP	2.528158454	0.005192918
TAL1	2.517034085	0.000545945

ADAM23	2.394489117	4.25E-05
CEND1	2.340324375	0.008276367
FBXO39	2.319330547	8.37E-06
CYP2D6	2.273013364	0.000448682
VNN1	2.222244443	4.36E-13
INHBB	2.117971461	1.58E-12

1.2 RNA quantity and quality for microarray analysis: nanodrop.

Name on tube	Conc (ng/ul)	Volume (ul)	260/280
C-1	553.4	10	2.05
C-2	559.1	10	2.06
C-3	581.1	10	2.03
NT-1	428.3	10	2.03
NT-2	470.9	10	1.95
NT-3	416.7	10	2.01
M-1	342.1	10	2.03
M-2	342.1	10	2.03
M-3	324	10	2.03
FLG-1	375.9	10	2.03
FLG-2	412.7	10	2.02
FLG-3	383.2	10	2.02
ABCA-1	270.7	15	2.03
ABCA-2	249	15	2.02
ABCA-3	268.3	15	2.02
TGM-1	446.7	10	2.03
TGM-2	418.7	10	2.02
TGM-3	354.2	10	2.01
ALOX-1	401.5	10	2.03
ALOX-2	379	10	2.04
ALOX-3	393.5	10	2.04
ICH-1	366.4	10	2.02
ICH-2	384.6	10	2.02
ICH-3	409.9	10	2.02
STS-1	356.9	10	2.03
STS-2	347.5	10	2.02
STS-3	395.7	10	2.04

C=control, M=mock, NT-non-targeting